Y. Tajima
T. Kuroki
T. Kanematsu
Editors

Hepatobiliary and Pancreatic Carcinogenesis in the Hamster

Springer

Hepatobiliary and Pancreatic Carcinogenesis in the Hamster

Yoshitsugu Tajima • Tamotsu Kuroki
Takashi Kanematsu
Editors

Hepatobiliary and Pancreatic Carcinogenesis in the Hamster

Springer

Editors
Yoshitsugu Tajima M.D., Ph.D.
Associate Professor
Department of Surgery
Nagasaki University
Graduate School of Biomedical Sciences
1-7-1 Sakamoto, Nagasaki 852-8501
Japan
ytajima@net.nagasaki-u.ac.jp

Tamotsu Kuroki M.D., Ph.D.
Assistant Professor
Department of Surgery
Nagasaki University
Graduate School of Biomedical Sciences
1-7-1 Sakamoto, Nagasaki 852-8501
Japan
tkuroki-gi@umin.ac.jp

Takashi Kanematsu M.D., Ph.D.
Professor
Department of Surgery
Nagasaki University
Graduate School of Biomedical Sciences
1-7-1 Sakamoto, Nagasaki 852-8501
Japan
kanematsu@nagasaki-u.ac.jp

ISBN: 978-4-431-87772-1 Springer Tokyo Berlin Heidelberg New York
e-ISBN: 978-4-431-87773-8
DOI: 10.1007/978-4-431-87773-8

Library of Congress Control Number: 2008938543

Springer is a part of Springer Science+Business Media
springer.com

Preface

Malignant neoplasms occurring in the biliary tract and pancreas remain a therapeutic challenge. The mechanism of carcinogenesis as well as the growth and spread of these tumors is still poorly understood, making the development of rational treatment strategies difficult. In order to improve the clinical results achieved by surgical or other medical treatment of such malignant tumors, the establishment of an experimental animal model is critical.

For this purpose, attempts were made to induce carcinoma experimentally in the biliary tree and finally an animal model using the hamster was established in 1994 at our laboratory. Because the tumor in this model mimicked the characteristics of human tumors, a series of experimental investigations were conducted to clarify the pathological characteristics of biliary carcinoma, the genetic alterations during biliary carcinogenesis, and the relationship between biliary inflammation and carcinogenesis. The chemopreventive effects on the occurrence of biliary carcinoma were also successfully examined. In addition, in vitro studies led to the establishment of transplantable biliary cancer cell lines and biliary epithelial cell lines by utilizing the hamster model.

This monograph represents the collective efforts in hepato-biliary and pancreatic disease research over the past 20 years. I hope that this monograph will be a source of useful knowledge for basic researchers as well as for clinicians involved in the care of patients with hepato-biliary and pancreatic neoplasms.

Takashi Kanematsu, M.D., Ph.D.
Professor and Chairman
Department of Surgery
Nagasaki University

Contents

Contributors

Adachi, Tomohiko, M.D., Ph.D.
Department of Surgery, Nagasaki University Graduate School of Biomedical Sciences, 1-7-1 Sakamoto, Nagasaki 852-8501, Japan

Asakawa, Takayuki, M.D., Ph.D.
Department of Surgery, National Hospital Organization Saga National Hospital, 1-20-1 Hinode, Saga 849-0923, Japan

Eto, Toshifumi, M.D., Ph.D.
Department of Surgery, Eto Hospital, 132-1 Onojima, Isahaya, Nagasaki 854-0031, Japan

Fukahori, Tomohiro, M.D., Ph.D.
Department of Surgery, Aino Memorial Hospital, 838-1 Aino, Unzen, Nagasaki 854-0301, Japan

Fukuda, Kenzo, M.D., Ph.D.
Department of Surgery, Medical Shimada Hospital, 217-1 Ogori, Ogori, Fukuoka 838-0141, Japan

Ikematsu, Yoshito, M.D., Ph.D.
Department of Surgery, Hamamatsu Medical Center, 328 Tomitsuka, Nakaku, Hamamatsu, Shizuoka 432-8580, Japan

Inoue, Keiji, M.D., Ph.D.
Department of Surgery, Nagasaki Municipal Hospital, 6-39 Shinchi, Nagasaki 850-8555, Japan

Kanematsu, Takashi, M.D., Ph.D.
Department of Surgery, Nagasaki University Graduate School of Biomedical Sciences, 1-7-1 Sakamoto, Nagasaki 852-8501, Japan

Kitajima, Tomoo, M.D., Ph.D.
Department of Surgery, Nagasaki Municipal Hospital, 6-39 Shinchi, Nagasaki 850-8555, Japan

Kitasato, Amane, M.D., Ph.D.
Department of Surgery, National Hospital Organization Nagasaki Medical Center, 2-1001-1 Kubara, Omura, Nagasaki 856-8562, Japan

Kosaka, Taiichiro, M.D.
Department of Surgery, Nagasaki University Graduate School of Biomedical Sciences, 1-7-1 Sakamoto, Nagasaki 852-8501, Japan

Kuroki, Tamotsu, M.D., Ph.D.
Department of Surgery, Nagasaki University Graduate School of Biomedical Sciences, 1-7-1 Sakamoto, Nagasaki 852-8501, Japan

Matsuo, Kei, M.D., Ph.D.
Department of Surgery, Nagasaki Municipal Hospital, 6-39 Shinchi, Nagasaki 850-8555, Japan

Matsuzaki, Sumihiro, M.D., Ph.D.
Department of Surgery, Dialand Matsuzaki Clinic, 4-1-12 Dialand, Nagasaki 850-0963, Japan

Mishima, Takehiro, M.D.
Department of Surgery, Nagasaki University Graduate School of Biomedical Sciences, 1-7-1 Sakamoto, Nagasaki 852-8501, Japan

Okada, Kazuya, M.D., Ph.D.
Department of Surgery, Nagasaki Kouseikai Hospital, 3-12 Hayama, Nagasaki 852-8053, Japan

Onizuka, Shinya, M.D., Ph.D.
Department of Surgery, National Hospital Organization Nagasaki Medical Center, 2-1001-1 Kubara, Omura, Nagasaki 856-8562, Japan

Sasaki, Makoto, M.D., Ph.D.
Department of Surgery, NTT West Nagasaki Hospital, 10-40 Oura, Nagasaki 850-0918, Japan

Shiku, Hiroshi, M.D., Ph.D.
Department of Cancer Vaccine and Immuno-Gene Therapy, Mie University Graduate School of Medicine, 2-174 Edobashi, Tsu, Mie 514-8507, Japan

Tajima, Yoshitsugu, M.D., Ph.D.
Department of Surgery, Nagasaki University Graduate School of Biomedical Sciences, 1-7-1 Sakamoto, Nagasaki 852-8501, Japan

Tomioka, Tsutomu, M.D., Ph.D.
Department of Surgery, Nagasaki Yurino Hospital, 1155-2 Motomura, Togitsu, Nishisonogi, Nagasaki 851-2103, Japan

Tsuneoka, Noritsugu, M.D., Ph.D.
Department of Surgery, Nagasaki University Graduate School of Biomedical Sciences, 1-7-1 Sakamoto, Nagasaki 852-8501, Japan

Tsunoda, Tsukasa, M.D., Ph.D.
Department of Surgery, Division of Gastroenterological Surgery, Kawasaki Medical School, 577 Matsushima, Kurashiki, Okayama 701-0192, Japan

Tsutsumi, Ryuji, M.D., Ph.D.
Department of Surgery, Nagasaki Prefectural Shimabara Hospital, 7895 Shimokawajiri, Shimabara, Nagasaki 855-0861, Japan

Yamanaka, Shizuo, M.D., Ph.D.
Department of Surgery, Narumidai Yamanaka Clinic, 1-28-5 Narumidai, Nagasaki 851-2215, Japan

Chapter 1
The Syrian Hamster as an Experimental Animal

Yoshitsugu Tajima

1.1 Introduction

The choice of an appropriate species and strain of laboratory animals is one of the scientist's major concerns. The Syrian hamster (*Mesocricetus auratus*) provides a unique tool for studying hepatobiliary and pancreatic carcinomas because the anatomical structure of its hepatobiliary and pancreatic duct system is similar to that of humans. Moreover, the tumors induced in the liver, biliary tract, and pancreas of hamsters with nitrosamines closely resemble those of humans. Biochemically, hamster bile is unsaturated under normal conditions and the bile acid composition is similar to human bile [1–4]. Pancreatic juice components in this species also resemble those of humans [5,6]. Therefore, the Syrian hamster may be an ideal animal model for investigating carcinogenic mechanisms in hepatobiliary and pancreatic tumors.

1.2 Taxonomic Classification of the Hamster

Hamsters are rodents belonging to the subfamily Cricetinae. The subfamily contains about 18 species, classified into six or seven genera [7,8]. The taxonomic classification of hamsters are as follows:

Kingdom: Animalia
Phylum: Chordata
Class: Mammalia
Order: Rodentia
Suborder: Myomorpha
Superfamily: Muroidea
Family: Cricetidae
Subfamily: Cricetinae

Y. Tajima et al. (eds.), *Hepatobiliary and Pancreatic Carcinogenesis in the Hamster*,
DOI: 10.1007/978-4-431-87773-8_1, © Springer 2009

- Genus *Allocricetulus*
  Species *A. curtatus* – Mongolian hamster
  Species *A. eversmanni* – Kazakh hamster, also called Eversmann's hamster
- Genus *Cansumys*
  Species *C. canus* – Gansu hamster
- Genus *Cricetulus*
  Species *C. alticola* – Ladak hamster
  Species *C. barabensis*, including "*C. pseudogriseus*" and "*C. obscurus*"–Chinese Striped hamster, also called Chinese hamster; Striped Dwarf hamster
  Species *C. griseus* – Chinese hamster
  Species *C. kamensis* – Tibetan hamster
  Species *C. longicaudatus* – Long-tailed hamster
  Species *C. migratorius* – Armenian hamster, also called Migratory Grey hamster; Grey hamster; Grey Dwarf hamster; Migratory hamster
  Species *C. sokolovi* – Sokolov's hamster
- Genus *Cricetus*
  Species *C. cricetus* – European hamster, also called Common hamster or Black-Bellied Field hamster
- Genus *Mesocricetus* – Golden hamsters
  Species *M. auratus* – Syrian hamster, also called the Golden hamster or Teddy Bear hamster
  Species *M. brandti* – Turkish hamster, also called Brandt's hamster; Azerbaijani hamster
  Species *M. newtoni* – Romanian hamster
  Species *M. raddei* – Ciscaucasian Hamster
- Genus *Phodopus* – Dwarf hamsters
  Species *P. campbelli* – Campbell's Russian Dwarf hamster
  Species *P. roborovskii* – Roborovski hamster, sometimes known as the Mongolian hamster, creating confusion with the *A. curtatus*
  Species *P. sungorus* – Winter White Russian Dwarf hamster
- Genus *Tscherskia*
  Species *T. triton* – Greater Long-tailed hamster, also called Korean hamster

1.3 Anatomy of the Liver

The liver of the Syrian hamster is composed of three major lobes and two minor caudal lobes [9]. The major lobes are the left lateral, middle, and right lateral lobes. In the hamster bile duct system, each major lobe of the liver provides a hepatic duct at the hepatic hilum and these ducts converge to form a common bile duct (Figure 1.1). The major intrahepatic bile duct gives rise to intermediate and first-order bile ductules, followed by several secondary and tertiary ductules with dichotomous branching (Figure 1.2). Histologically, a single row of cuboidal cells lines the intrahepatic bile ducts and ductules (Figure 1.3). Goblet cells are not normally observed.

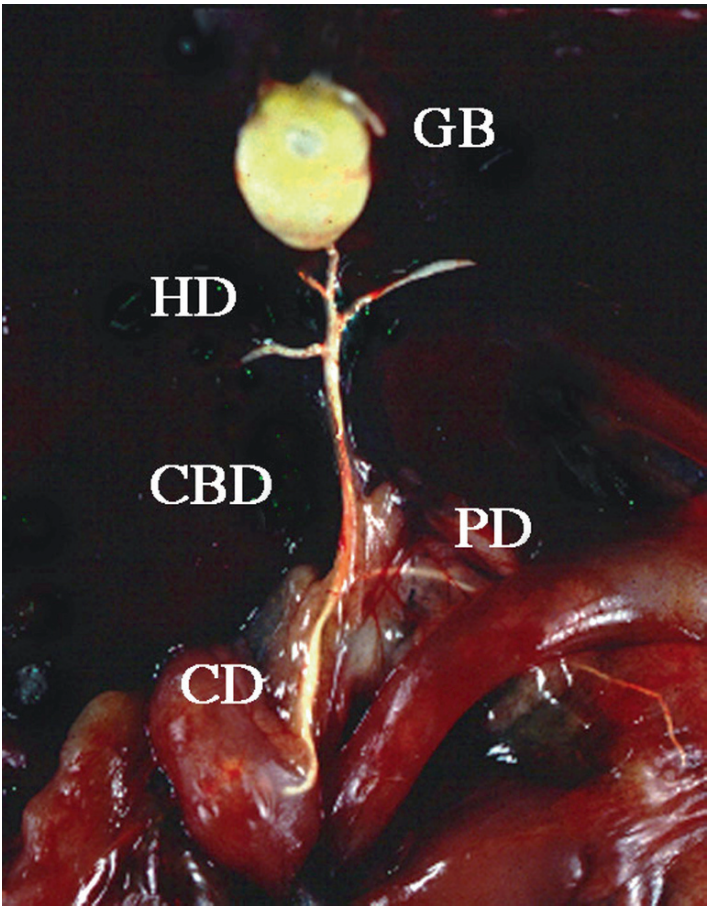

Fig. 1.1 Hepatobiliary and pancreatic duct system of the hamster. GB, gallbladder; HD, hepatic duct; CBD, common bile duct; CD, common duct; PD, pancreatic duct

1.4 Anatomy of the Gallbladder

Hamsters have a gallbladder, which is attached to the underside of the middle lobe of the liver. In a 7-week-old Syrian hamster, the gallbladder is about 6–8 mm long and about 4–5 mm in diameter. In the distended gallbladder, the mucosal layer is composed of cuboidal or columnar cells. In the undistended gallbladder, mucosal folds (Figure 1.4) are covered with tall columnar epithelial cells containing dark elongated nuclei (Figure 1.5). Mucinous glands in the gallbladder wall open onto the mucosal surface [10]. The gallbladder wall contains a loose muscle layer formed of smooth muscle bundles. The cystic duct leads from the gallbladder and then joins the common bile duct. A single row of cuboidal cells lines the cystic duct.

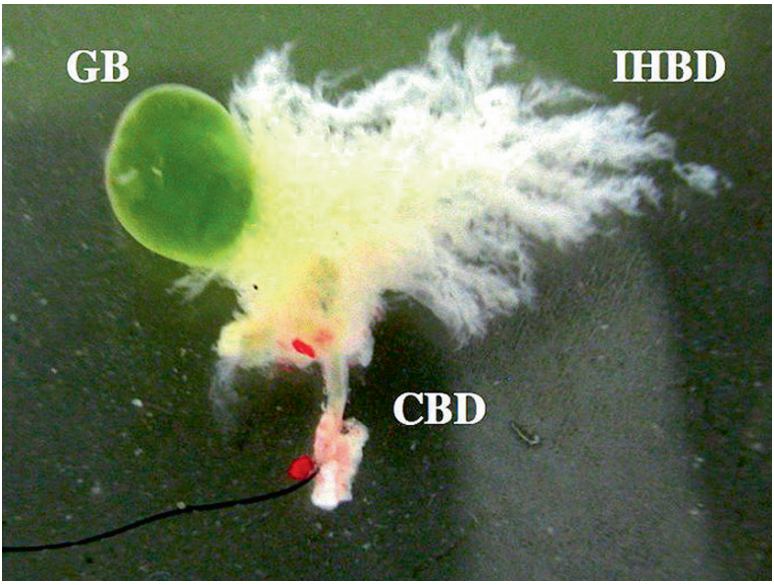

Fig. 1.2 Biliary tree of the hamster. GB, gallbladder; IHBD, intrahepatic bile duct; CBD, common bile duct

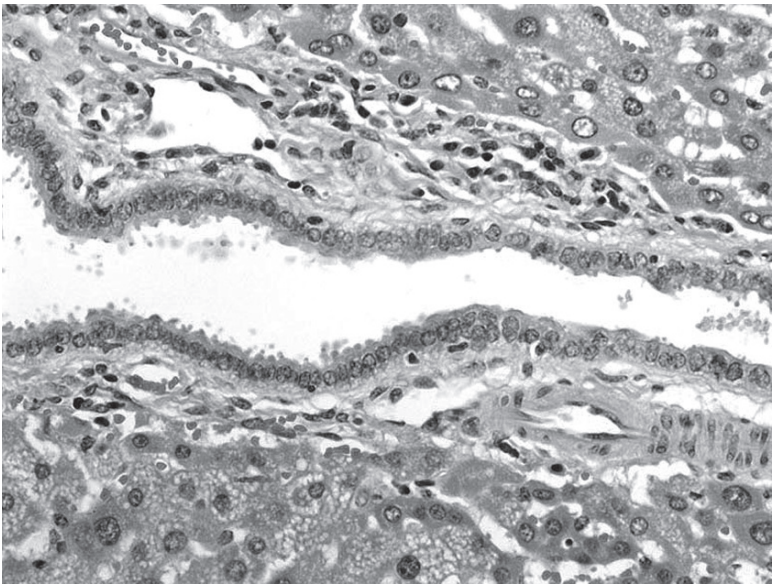

Fig. 1.3 Epithelial cells in the intrahepatic bile duct (H&E, ×100)

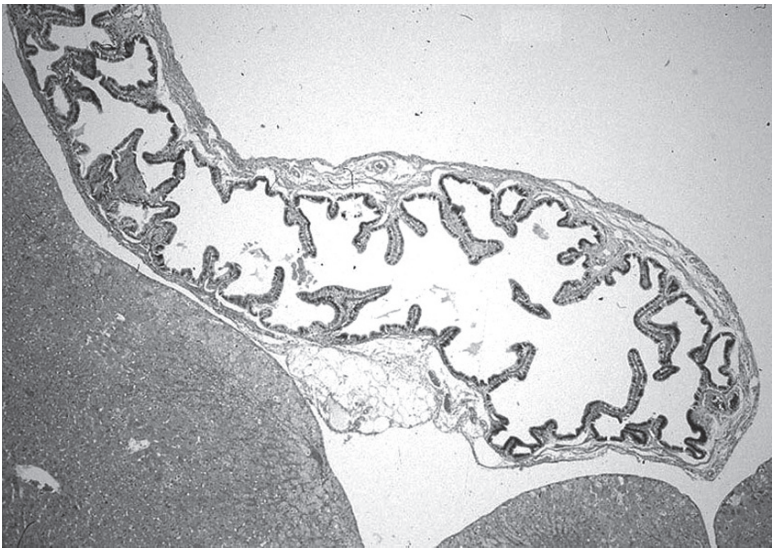

Fig. 1.4 The gallbladder of the hamster (H&E, ×5)

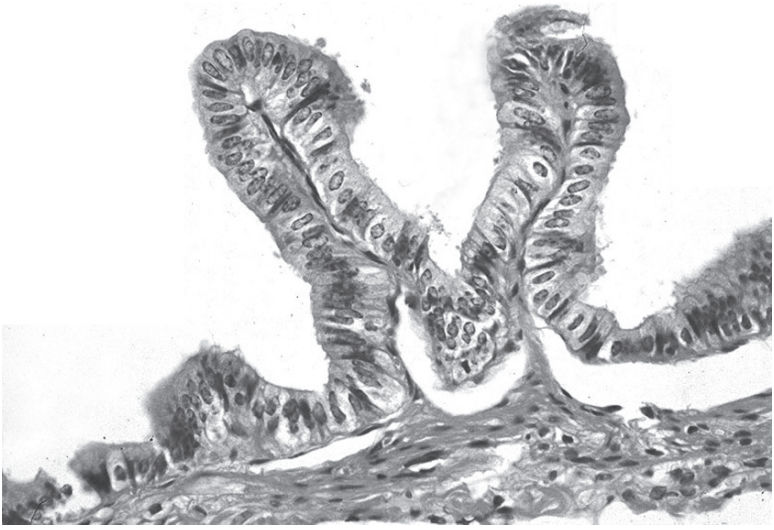

Fig. 1.5 Epithelial cells in the gallbladder (H&E, ×100)

Fig. 1.6 Epithelial cells in the common bile duct (H&E, ×20)

1.5 Anatomy of the Extrahepatic Bile Duct

The extrahepatic bile duct in hamsters is composed of three bile duct segments: the hepatic ducts, the common bile duct, and the common duct [11]. The common bile duct enters the head of the pancreas and opens into the duodenum on the dorsal side. In the head of the pancreas, two major pancreatic ducts enter the distal portion of the common bile duct. The short bile duct segment between the opening of the pancreatic ducts and duodenum is called the common duct. Several small ductules from the head of the pancreas enter directly into the common duct [12].

The common bile duct has the largest lumen and the thickest periductal connective tissue. The bile duct epithelium is lined throughout by a single row of low cuboidal or cylindric mucin-producing epithelial cells, organized on a basement membrane (Figure 1.6). Papillary projections of the mucosal epithelium are evident in the common duct merging into the duodenum.

1.6 Anatomy of the Pancreas

The pancreas consists of a head and three well-defined segments; namely, the duodenal, gastric, and splenic lobes, forming a λ-shaped organ. Each pancreatic lobe has one main duct and the duodenal duct enters the common bile duct directly.

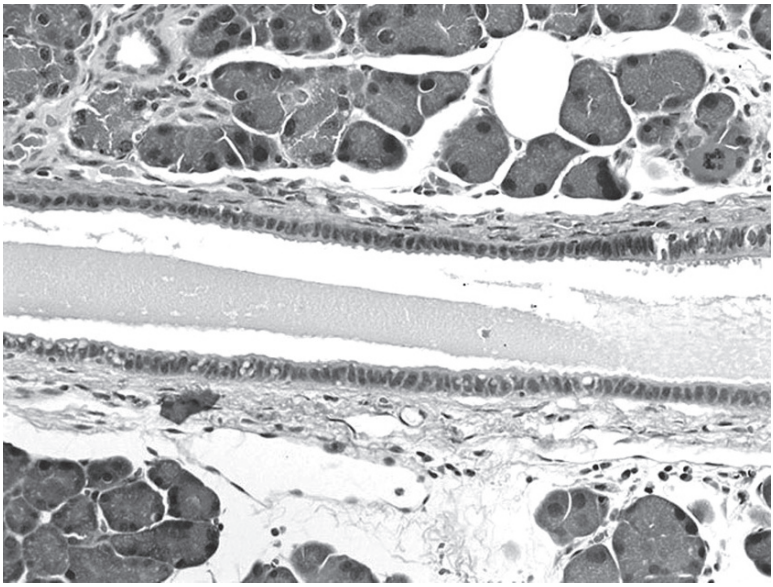

Fig. 1.7 Epithelial cells in the main pancreatic duct (H&E, ×60)

The gastric and splenic ducts form a common pancreatic duct, which opens into the common bile duct close to the duodenal duct to form a common duct [12,13]. A single row of low cuboidal cells lines the pancreatic ducts (Figure 1.7).

References

1. Andersen JM, Cook LR. Regulation of gallbladder cholesterol concentration in the hamster. Role of hepatic cholesterol level. Biochim Biophys Acta 1986 875(3):582–592
2. Reyes H, Kern F Jr. Effect of pregnancy on bile flow and biliary lipids in the hamster. Gastroenterology 1979 76(1):144–150.
3. Pearlman BJ, Bonorris GG, Phillips MJ, Chung A, Vimadalal S, Marks JW, Schoenfield LJ. Cholesterol gallstone formation and prevention by chenodeoxycholic and ursodeoxycholic acids. A new hamster model. Gastroenterology 1979 77(4):634–641.
4. Singhal AK, Finver-Sadowsky J, McSherry CK, Mosbach EH. Effect of cholesterol and bile acids on the regulation of cholesterol metabolism in hamster. Biochim Biophys Acta 1983 12;752(2):214–222.
5. Helgeson AS, Pour P, Lawson T, Grandjean CJ. Exocrine pancreatic secretion in the Syrian golden hamster *Mesocricetus auratus* – I. Basic values. Comp Biochem Physiol 1980 66A:214–222.
6. Rinderknecht H, Maset R, Collias K, Carmack C. Pancreatic secretory profiles of protein, digestive, and lysosomal enzymes in Syrian golden hamster. Effect of secretin and cholecystokinin. Dig Dis Sci 1983 28(6):518–525.
7. Lebedev VS, Ivanova NV, Pavlova NK, Poltoraus AB. Molecular phylogeny of the Palearctic hamsters. *In* Proceedings of the International Conference Devoted to the 90th Anniversary of Prof. I. M. Gromov on Systematics, Phylogeny and Paleontology of Small Mammals, eds. Averianov A, Abramson N (2003). 114–118, Russian Academy of Science, St. Petersburg.

8. Musser GG, Carleton MD. Superfamily Muroidea. *In* Mammal Species of the World a Taxonomic and Geographic Reference, eds. Wilson DE, Reeder DM (2005). Johns Hopkins University Press, Baltimore, MD.
9. Moore MA, Thamavit W, Bannasch P. Tumours of the liver. *In* Pathology of Tumours in Laboratory Animals – Tumours of the Hamster, eds. Turusov VS, Mohr U, 2nd Ed., Vol. 3, pp. 79–108 (1996). International Agency for Research on Cancer, Lyon.
10. Turusov VS, Gorin B. Tumours of the gallbladder. *In* Pathology of Tumours in Laboratory Animals – Tumours of the Hamster, eds. Turusov VS, Mohr U, 2nd Ed., Vol. 3, pp. 109–125 (1996). International Agency for Research on Cancer, Lyon.
11. Tajima Y, Kitajima T, Tsuneoka N, Fukuda K, Kuroki T, Ikematsu Y, Tomioka T, Kanematsu T. Developmental process of biliary carcinoma arising in pancreaticobiliary maljunction – Experimental studies using a hamster model. *In* Pancreaticobiliary Maljunction, eds. Koyanagi Y, Aoki T, 1st Ed., pp. 219–227 (2002). Igaku Tosho Shuppan, Tokyo.
12. Takahashi M, Pour P, Althoff J, Donnelly T. The pancreas of the Syrian hamster (*Mesocricetus auratus*). I Anatomical study. Lab Anim Sci 1977 27(3):336–342.
13. Pour PM, Tomioka T. Tumours of the pancreas. *In* Pathology of Tumours in Laboratory Animals – Tumours of the Hamster, eds. Turusov VS, Mohr U, 2nd Ed., Vol. 3, pp. 149–173 (1996). International Agency for Research on Cancer, Lyon.

Chapter 2
Surgical Instruments

Taiichiro Kosaka, Takehiro Mishima, and Tomohiko Adachi

To operate on hamsters, it is essential to own your own set of instruments (Figure 2.1). The surgical instruments should consist of the following:

Needle Holders
- A pair of microsurgical needle holders, without a lock (small and large)
- A non-microsurgical straight slender needle holder

Ring-Handled Scissors
- Straight, sharp/sharp ring-handled preparation scissors
- Curved, blunt/sharp ring-handled preparation scissors

Anatomical or Dissecting Forceps
- A pair of straight anatomical forceps (small and large)
- A pair of straight fine-toothed forceps

Artery Forceps
- Baby mosquito forceps

Additional Utilities
- Safety razors
- Cotton buds
- Paper clips
- Hairpins
- Towel clips
- An operating table
- A light source
- An instrument case

Microsurgical instruments are delicate and require careful handling and maintenance. The instruments should be held in a pencil grip, which provides optimal stability when performing microdissection and microsuturing. In principle, only your fingertips move while the rest of your hand rests on a stable object. We utilize some small tools, such as safety razors, paper clips, cotton buds, and hairpins, as substitutes for surgical instruments (Figure 2.2). A safety razor is suitable for shaving the hamster's thin hair and for making the skin incision. A paper clip can be used as a wound retractor by lengthening and transforming its unilateral extremity at right angles to each other, and coiling it around a pin (Figure 2.3). The unilateral extremity of the

Y. Tajima et al. (eds.), *Hepatobiliary and Pancreatic Carcinogenesis in the Hamster*,
DOI: 10.1007/978-4-431-87773-8_2, © Springer 2009

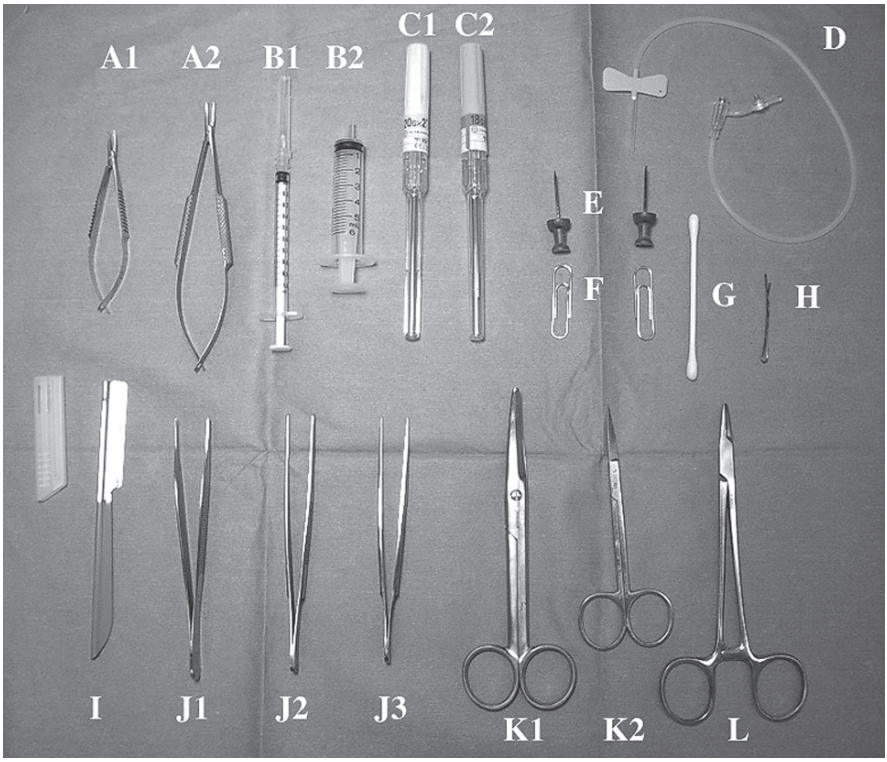

Fig. 2.1 The surgical instruments. A1 – small microsurgical needle holder, without a lock. A2 – large microsurgical needle holders, without a lock. B1 – 1 ml syringe. B2 – 5 ml syringe. C1 – 20G needle with an elastic sheath. C2 – 18G needle with an elastic sheath. D – 22G needle for blood sampling. E – pin. F – paper clip. G – cotton bud. H – hairpin. I – razor. J1 – straight fine toothed forceps. J2/J3 – straight anatomical forceps (small and large). K1 – curved, blunt/blunt ring-handled preparation scissors. K2 – straight, sharp/sharp ring-handled preparation scissors. L – non-microsurgical straight slender needle holder

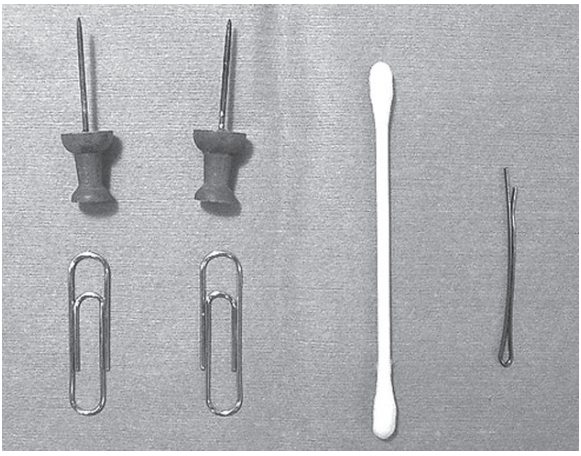

Fig. 2.2 The utilities for proceeding with surgery on hamsters

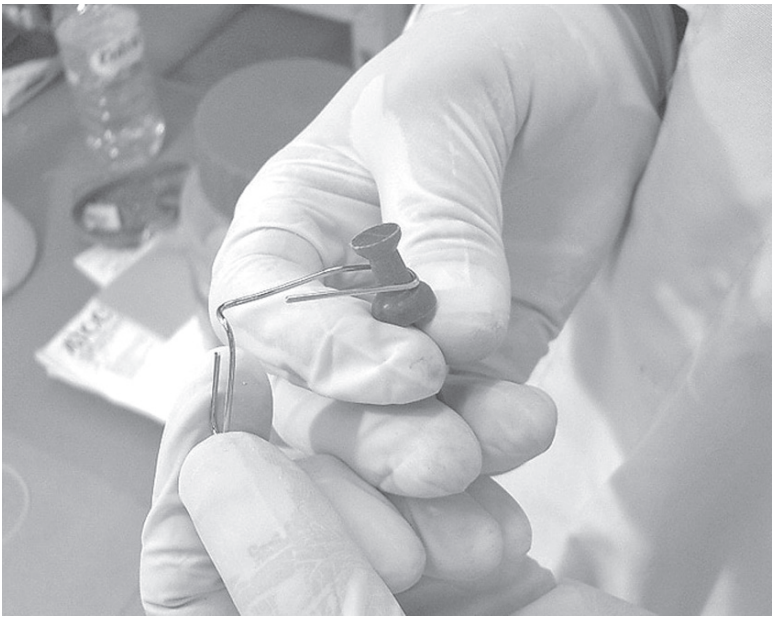

Fig. 2.3 The paper clip as a wound retractor

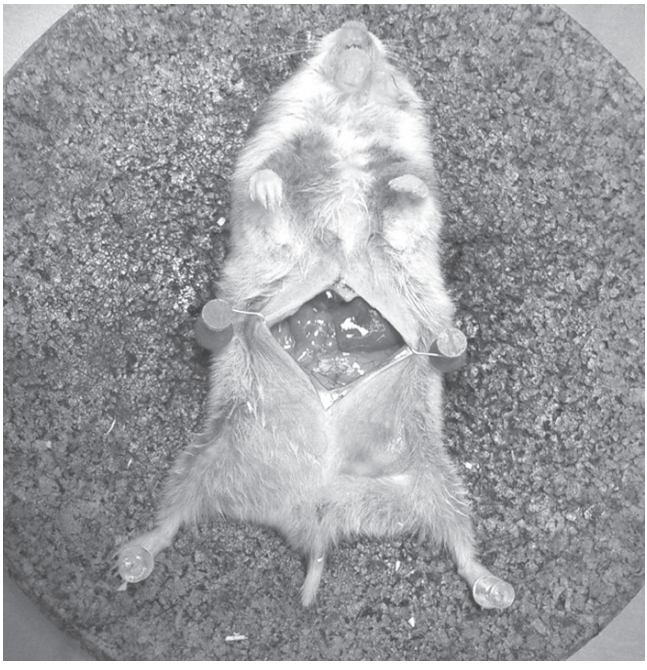

Fig. 2.4 Wound retraction with paper clips and pins

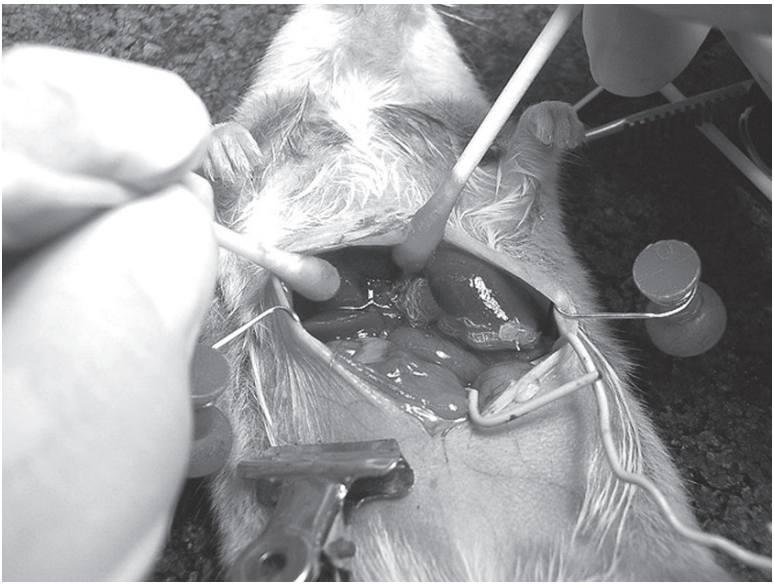

Fig. 2.5 The application of cotton buds in surgery on hamsters

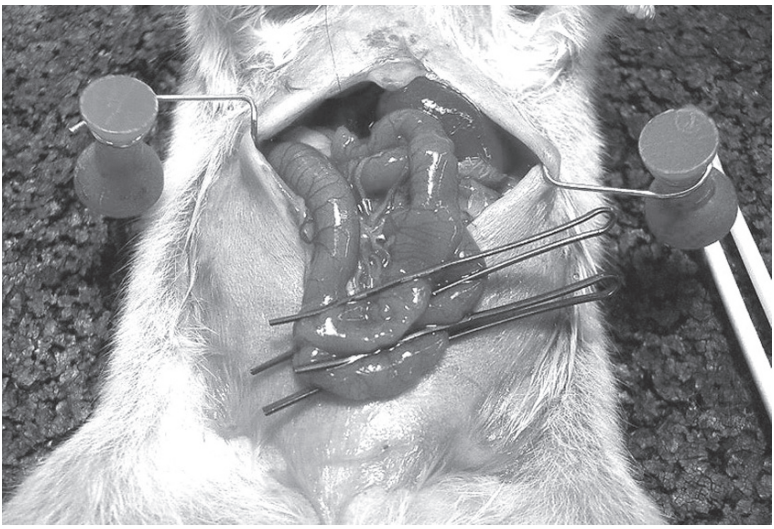

Fig. 2.6 Common hairpins are used as intestinal clamps

clip is used to hook and retract the abdominal wall, and the opposite side of the clip is then fixed to the operating board with a pin (Figure 2.4). This inexpensive tool is very easy to make and allows a good operative view. A cotton bud can be used as a surgical gauze ball for blunt dissection and to hold organs, or for hemostasis and the absorption of blood (Figure 2.5). A common hairpin can be used as an intestinal clamp (Figure 2.6). This is a very inexpensive instrument that acts as a gentle and effective clamp of the small intestine.

Chapter 3
Anesthesia of the Laboratory Hamster

Takehiro Mishima, Tomohiko Adachi, and Taiichiro Kosaka

3.1 Introduction

It is essential, ethically and legally, to reduce the perception of pain and minimize the discomfort felt by the animal subjected to experimental surgery. A range of anesthetic agents is available to obtain adequate analgesia, and the appropriate choice depends on the duration of the surgical procedure to be performed. In some cases, sedation, muscle relaxation, and inhibition of sympathetic or parasympathetic reflexes would be needed.

3.2 Preoperative Care

Hamsters are housed one per plastic cage lined with sawdust bedding. They are kept at 24 ± 2 °C in 50 ± 20% humidity with a 12 h alternate light and dark cycle. They are fed a standard pelleted diet and provided drinking water *ad libitum*. Unlike several other species, including dogs, cats, and pigs, which require pre-anesthetic fasting to reduce the risk of vomiting, fasting is not necessary in hamsters because they do not vomit. However, fasting for 8–12 h prior to surgery on the digestive systems is recommended, so that the stomach and the intestines are as empty as possible. The pre-anesthetic sedation of hamsters is not necessary.

3.3 General Anesthesia

The induction of anesthesia in hamsters is most conveniently achieved by inhalation anesthesia, using an anesthetic chamber made of transparent material, called an "ether jar" (Figure 3.1). It is common practice to anesthetize hamsters in a glass chamber containing cotton wool, wastepaper, or wood-shavings, moistened with liquid anesthetic, especially ether (diethyl-ether). Ether is inexpensive and allows for the easy handling of animals in the induction of anesthesia. It is important to remember that

Y. Tajima et al. (eds.), *Hepatobiliary and Pancreatic Carcinogenesis in the Hamster*,
DOI: 10.1007/978-4-431-87773-8_3, © Springer 2009

Fig. 3.1 The anesthetic chamber

Fig. 3.2 The intraperitoneal injection. A short 27G needle is pushed into the abdomen of a hamster. The animal is held firmly with its head tilted slightly downwards

direct contact with the vaporizing liquid is highly unpleasant for the animal as it freezes the skin and irritates the mucous membranes of the mouth and the respiratory tract.

Following the induction of anesthesia using ether, it is best to give pentobarbital as an intraperitoneal (i.p.) injection to achieve sufficient general anesthesia in hamsters (Figure 3.2). Pentobarbital (Nembutal®), at a dose of 50–60 mg/kg, i.p., will produce

profound analgesia and sufficient muscle relaxation without severe respiratory depression, to allow intra-abdominal surgery lasting 40–60 min. Endotracheal intubation and artificial respiration is not required. Hamsters generally recover 60–80 min after the injection of pentobarbital. Pentobarbital, at a dose of 30–60 mg/kg, i.p., is reported to result in high mortality as a result of severe respiratory depression in rats; however, in our experience, the mortality associated with the use of pentobarbital in hamsters is low, even at a dosage of 50–60 mg/kg, i.p.

3.4 Management During Anesthesia

Because the biliary surgery described in this handbook requires no longer than 40–50 min, no additional agents are needed to maintain the anesthesia after the i.p. injection of pentobarbital. Additional doses of pentobarbital can be given to prolong the anesthetic period. A subtle dose of pentobarbital should be added drop by drop, using a 1 ml syringe with a 27G needle. About 10 min of prolonged anesthesia can be induced by a drop of pentobarbital onto the peritoneal cavity. Overdose will induce respiratory depression and bad circulation.

Hamsters lose a lot of heat through their body surface and from the exposed abdominal organs during abdominal surgery, resulting in a rapid fall in temperature. Hypothermia often causes anesthetic death and delayed postoperative recovery of the animal. Hypovolemia is another frequent cause of death of this animal. Thus, we routinely moisten the intestines with warm (35 °C) saline or Ringer's solution (Figure 3.3) especially during prolonged abdominal surgery. The solution must be dripped constantly into the abdominal cavity.

Fig. 3.3 The water bath equipment

Fig. 3.4 The heating pad

3.5 Postoperative Care

To promote smooth recovery from the anesthesia, the room in which the animals recover must be warm (27–30 °C) and quiet. The temperature can be regulated by placing the hamster's cage on a heating pad (Figure 3.4), or by setting the desk lamp (incandescent lamp) on the cage.

3.6 Euthanasia

The animal must be killed humanely with minimal physical and mental suffering. We usually euthanize hamsters by exsanguination at the end of the experimental protocol. After inducing anesthesia, a blood sample is collected by puncturing the inferior vena cava. The hamster may die after losing 3–4 ml of blood. Other recommended methods of euthanasia are the administration of pentobarbital 100–150 mg/kg or leaving hamsters in a jar full of diethyl-ether gas.

Chapter 4
Fundamental Surgical Techniques

Tomohiko Adachi, Taiichiro Kosaka, and Takehiro Mishima

4.1 Introduction

This chapter delineates the fundamental techniques used for surgery in hamsters.

4.2 Shaving the Animal

After the induction of general anesthesia, the hamster is placed on its back on the operating board. The thin hairs on the hamster's abdomen are shaved off with a razor (Figure 4.1) after the area is sprayed with alcohol to moisten and disinfect the abdominal wall.

4.3 Opening the Abdominal Wall

After shaving, the animal is held in the supine position and secured to the operating table with pins (Figure 4.2). It should not be necessary to fix the limbs if adequate general anesthesia has been given. A midline skin incision is made from the level of the xiphoid process to below the navel using a razor (Figure 4.3). The abdominal muscles are lifted with forceps and a small incision is made to allow air to enter the peritoneal cavity (Figure 4.4). One side of the scissors is inserted into the abdominal cavity to lift up the abdominal wall and the abdomen is opened by making an incision over the linea alba towards the xiphoid cartilage. The "paper clip" wound retractors are effective for obtaining a wide operative view (Figure 4.5). A small piece of wet gauze can be used to fix the left lateral lobe of the liver (Figure 4.6) and the small intestine, and to moisten these organs.

Y. Tajima et al. (eds.), *Hepatobiliary and Pancreatic Carcinogenesis in the Hamster*,
DOI: 10.1007/978-4-431-87773-8_4, © Springer 2009

Fig. 4.1 Shaving the hamster

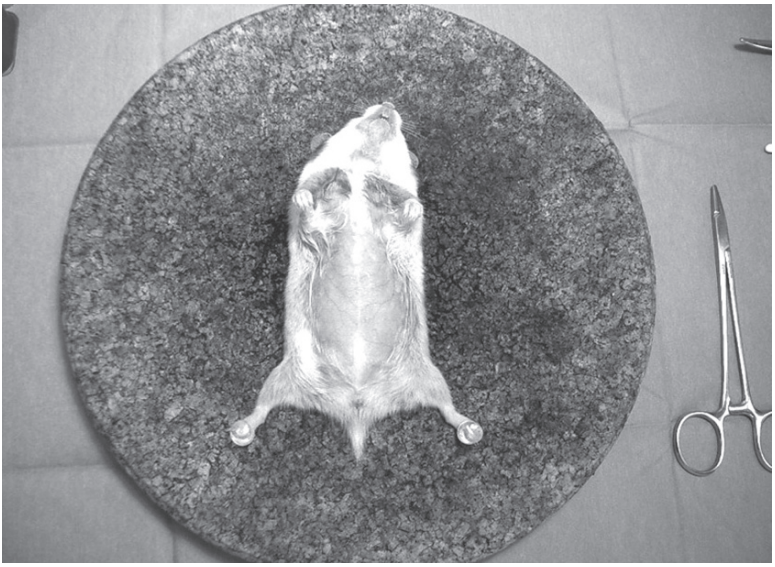

Fig. 4.2 Operating position. The hind legs are secured to the operating board with pins

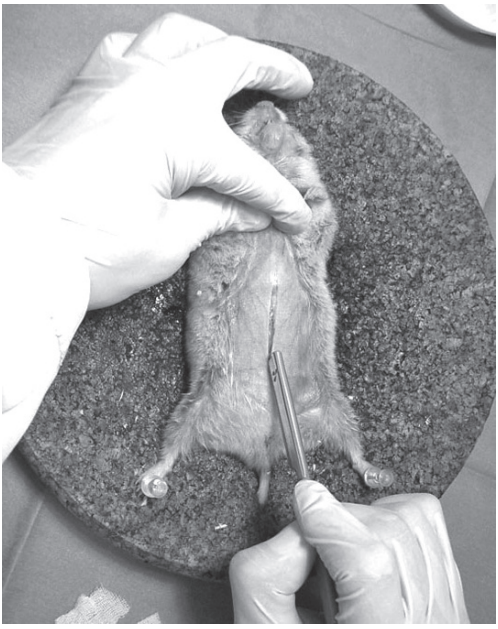

Fig. 4.3 Opening the abdominal cavity. A midline skin incision is made using a razor

Fig. 4.4 Opening the abdominal cavity. A small incision is made in the abdominal muscles to allow air to enter the peritoneal cavity

Fig. 4.5 Retraction of the abdominal wall using paper clips

Fig. 4.6 Fixation of the left lateral lobe of the liver using a small wet piece of gauze

4.4 Closure of the Abdominal Wall

The abdominal wall is closed in two layers: The first layer is the peritoneum and abdominal muscle, which is closed with a continuous absorbable 4–0 suture (Figure 4.7). Attention must be paid to the tension of the thread so as not to shorten the abdominal wall. The second layer is the skin, which is closed using the same technique with an absorbable 2–0 suture (Figure 4.8).

Fig. 4.7 Closure of the abdominal wall. The abdominal muscle is closed with a continuous absorbable 4–0 suture

Fig. 4.8 Closure of the abdominal wall. The skin is closed using the same technique with an absorbable 2–0 suture

4.5 Blood Sampling

Collecting peripheral blood from hamsters is difficult. To collect a large quantity of blood, a cardiac puncture can be performed. We usually take a blood sample from the inferior vena cava at the end of the experimental protocol. After a laparotomy, the inferior vena cava is exposed and a 22G needle with a 20 cm-long polyethylene tube is pushed into the vena cava (Figure 4.9). A 5 ml syringe is attached to the tube without changing the needle position (Figure 4.10), and blood can be withdrawn.

Fig. 4.9 Blood sampling. The inferior vena cava is exposed

Fig. 4.10 Blood sampling. A 22G needle with a 20 cm-long polyethylene tube is pushed into the vena cava and blood flows out immediately

Chapter 5
Hamster Models of Biliary Carcinoma

Yoshitsugu Tajima, Tomoo Kitajima, Tsutomu Tomioka, Toshifumi Eto, Keiji Inoue, Tomohiro Fukahori, Makoto Sasaki, and Tsukasa Tsunoda

A. Pancreaticobiliary Maljunction Model

5.1 Introduction

Pancreaticobiliary maljunction (PBM) is a congenital anomaly characterized by a union of the pancreatic and biliary ducts, located outside the duodenal wall [1]. This anomalous condition has recently been recognized as a high risk factor for the development of biliary carcinomas later in life [2,3]. Two-way regurgitation occurs in this disorder, as the reflux of pancreatic juice up to the biliary tree and/or of bile up to pancreatic duct, because the sphincter muscle of Oddi does not act functionally in this anomalous union. Therefore, patients with PBM are prone to the development of various pathological conditions of the biliary tract and pancreas, including cholangitis, pancreatitis, biliary and pancreatic calculi, and eventually biliary carcinoma [2–6].

Different animal models have been developed to investigate the pathogenesis of PBM, using dogs [7–9], cats [10], goats [11], lambs [12], and rats [13], and the important documented findings of these studies may contribute to clinical practice. Since the pathogenesis of PBM-related diseases is broad, a variety of species and preparatory methods have been studied. In particular, the association between PBM and biliary carcinogenesis has been investigated extensively; however, few animal experiments have successfully induced biliary carcinoma.

The most important pathophysiological condition in PBM is "pancreatic juice regurgitation into the biliary tract". We performed cholecystoduodenostomy with dissection of the extrahepatic bile duct in the distal end of the common duct (CDDB) in hamsters. Despite the reported difficulties, we induced carcinoma of the gallbladder and extrahepatic duct with marked dilatation of the extrahepatic bile duct in hamsters, by administering a carcinogenic agent, *N*-nitrosobis(2-oxopropyl) amine (BOP) [14]. In this hamster model, pancreatic juice regurgitates into the biliary tract, and then flows into the duodenum through the gallbladder. On the other hand, the duodenal contents flow readily into the biliary tract. The CDDB model is based on the following clinical data: the risk of PBM-related biliary carcinogenesis is extremely high in patients undergoing an internal bilioenterostomy such as cystoduodenostomy or cholecystoduodenostomy [15–17]; and biliary

Y. Tajima et al. (eds.), *Hepatobiliary and Pancreatic Carcinogenesis in the Hamster*,
DOI: 10.1007/978-4-431-87773-8_5, © Springer 2009

carcinoma develops in patients with a bilioenterostomy 15 years earlier than in those who have not been subjected to this procedure [17]. We explain our method for the successful induction of biliary carcinoma in hamsters, and describe the histopathological characteristics of the induced tumors.

5.2 Preparation of the Model

Under general anesthesia, 7-week-old female Syrian golden hamsters are subjected to cholecystoduodenostomy with dissection of the extrahepatic bile duct at the distal end of the common duct (CDDB) [14]. The schema of the completed surgical procedure of CDDB is illustrated in Figure 5.1. After anesthetization with sodium pentobarbital (50 mg/kg of body weight) an upper abdominal midline incision is made. First, the distal end of the common duct is doubly ligated with 6-0 nylon and dissected (Figures 5.2 and 5.3). The ligation of the common duct will cause distension of the gallbladder. Next, one 5 mm-long incision is made in the duodenal wall, approximately 10 mm distal to the pyloric ring of the stomach (Figure 5.4), and one

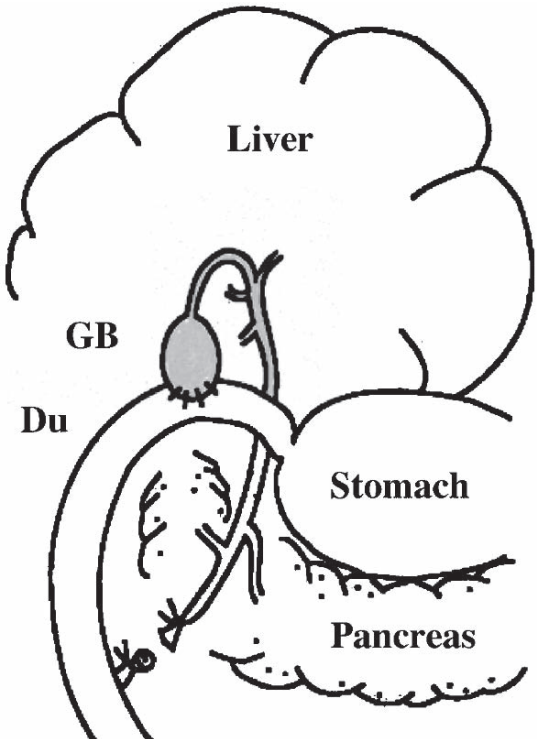

Fig. 5.1 Cholecystoduodenostomy with dissection of the distant common duct end (CDDB model) in the hamster. GB, gallbladder; Du, duodenum (modified from [14], with permission)

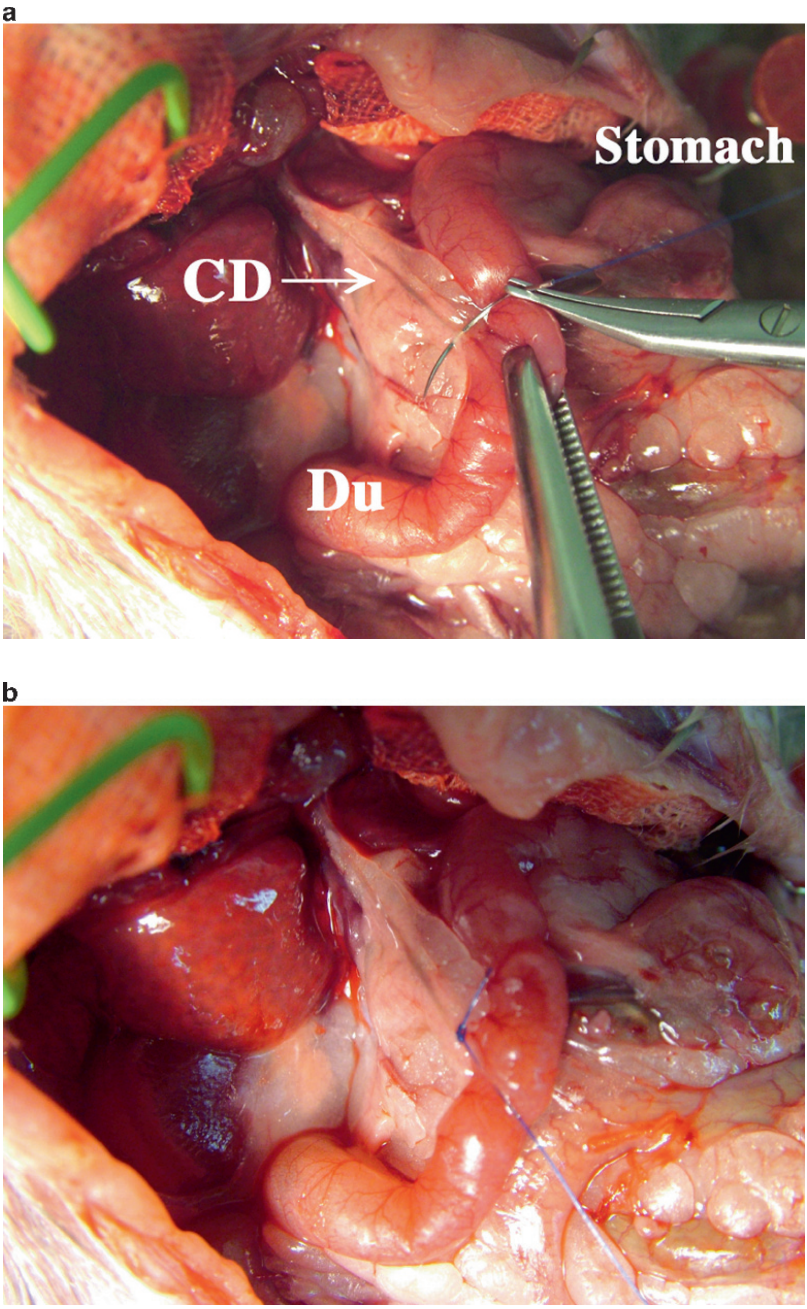

Fig. 5.2 **(a)** The duodenal wall is pulled up from opposite the opening of the common duct (CD) into the duodenum (Du), and then hooked onto the distal end of the common duct, using a needle. **(b)** The common duct is ligated

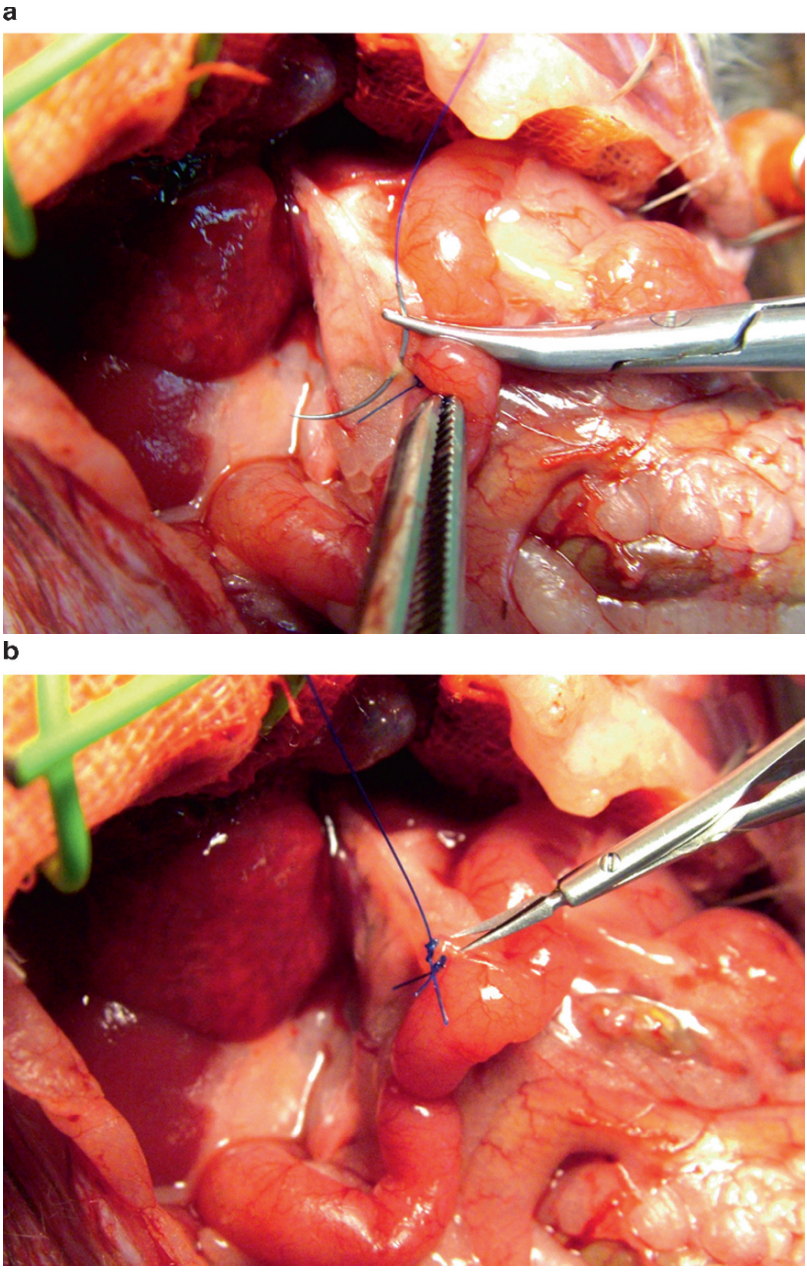

Fig. 5.3 The distal end of the common duct is doubly ligated **(a)**, and then dissected **(b)**

5 mm-long incision is made in the gallbladder fundus (Figure 5.5); then the cholecystoduodenostomy is done. The incision in the duodenal wall should be made in an avascular area to minimize blood loss. Anastomosis is performed using a running suture with 7-0 nylon. The first suture is placed in the right corner of the gallbladder,

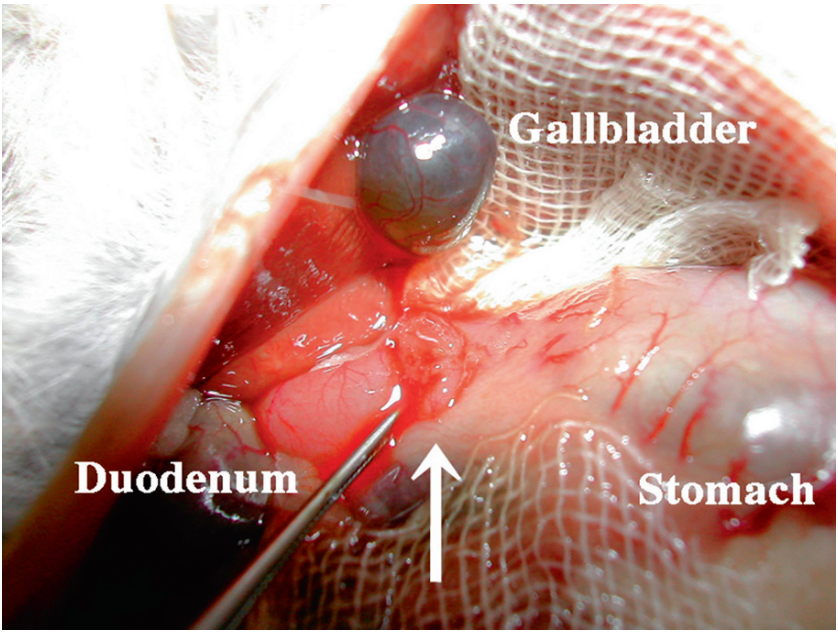

Fig. 5.4 A small incision is made in the duodenum (*arrow*)

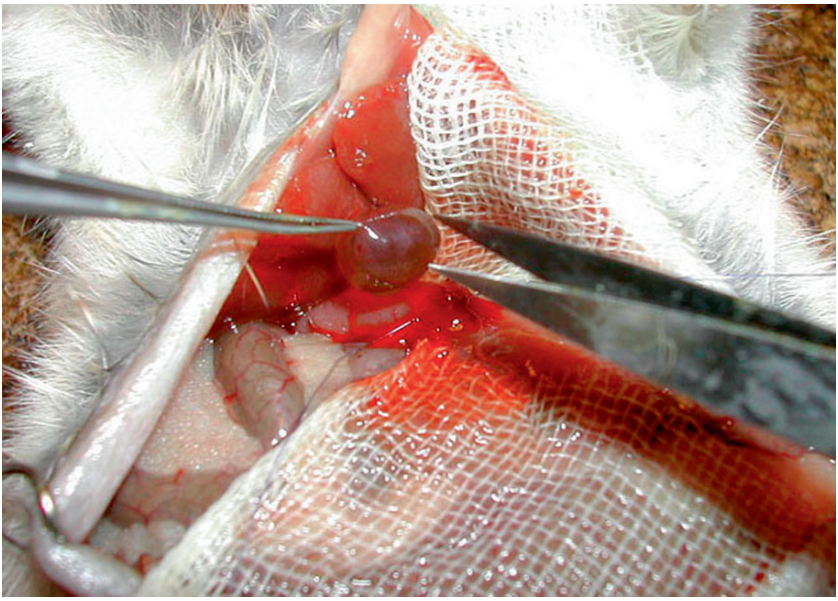

Fig. 5.5 A small incision is made in the fundus of the gallbladder

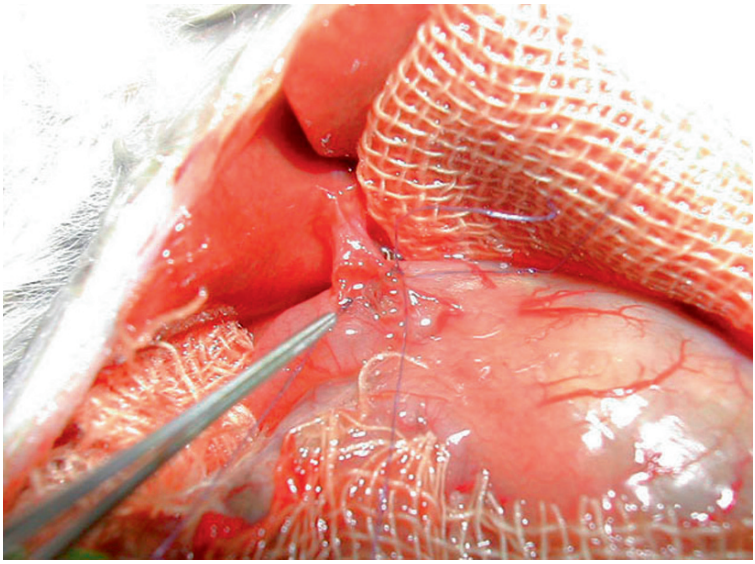

Fig. 5.6 A running suture is placed in the posterior wall for cholecystoduodenostomy

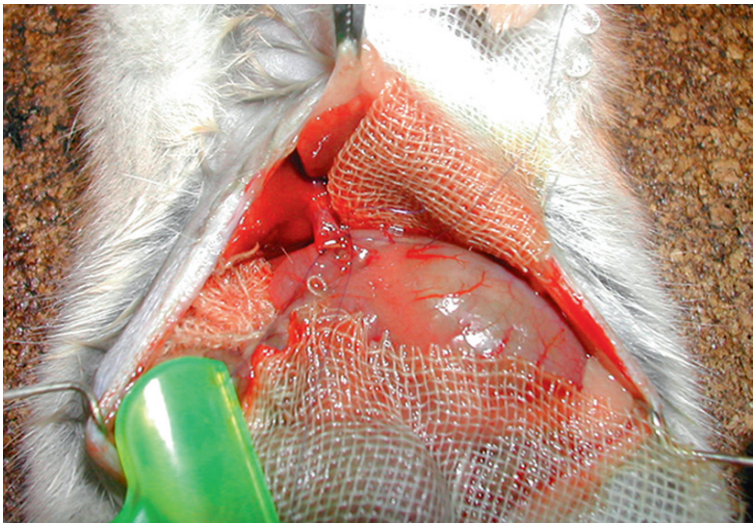

Fig. 5.7 The free end of the first suture is retracted with a small clip

from outside in, and the needle is then passed through the duodenal wall, from inside out. The right corner stitch is knotted and the needle is passed again through the duodenal wall, from outside in and a running suture is placed in the posterior wall, from inside out (Figure 5.6). To perform the anastomosis comfortably and correctly, there must be good exposure of the surgical area. During the cholecystoduodenostomy, we retract the free end of the first suture with a small clip (Figure 5.7). Finally,

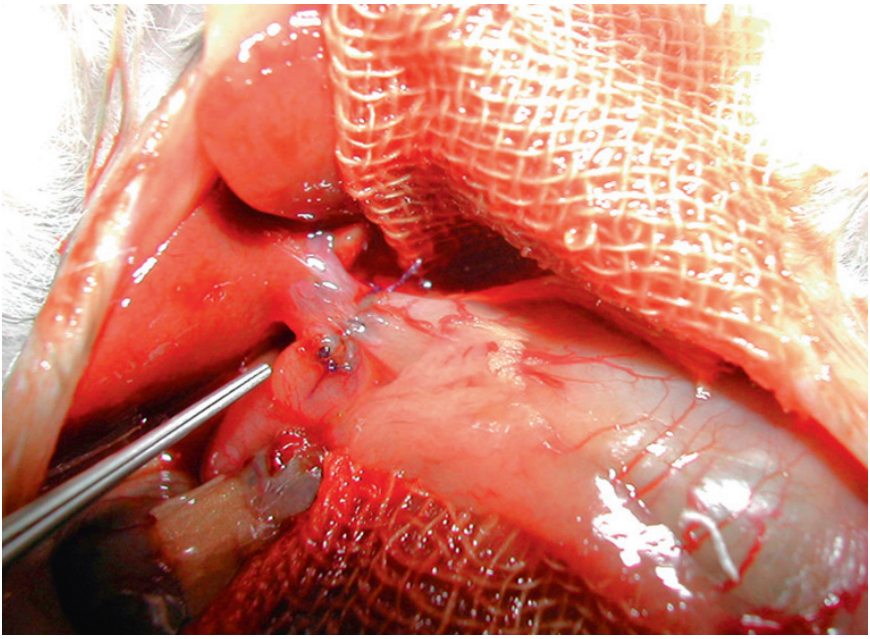

Fig. 5.8 The cholecystoduodenostomy is completed

the needle is inserted through the duodenal wall, from inside out, in the left corner. A second suture is placed in the left corner and knotted as in the right corner stitch. The needle end of the first suture and the free end of the second suture are knotted and then the free end of the second suture is retracted. Anterior wall closure is completed with a continuous running suture (Figure 5.8).

5.3 Histological Examination

After the animal is killed, the extrahepatic bile duct and gallbladder are removed en bloc with the liver, pancreatic head, and part of the duodenum, and fixed in 10% buffered formalin (Figure 5.9). Because pancreatic juice-related autolysis of the biliary epithelium is considerable in CDDB hamsters, the biliary system must be fixed in formalin solution immediately after extirpation.

The formalin-fixed specimen is usually cut into six blocks and embedded in paraffin. For pathological examination of the biliary tree, one slice is taken from each block; that is, one from the hepatic ducts, one from the common bile duct, one from the common duct, one from the gallbladder, and five from the liver (Figure 5.10). Histological sections are then stained with hematoxylin and eosin (H&E).

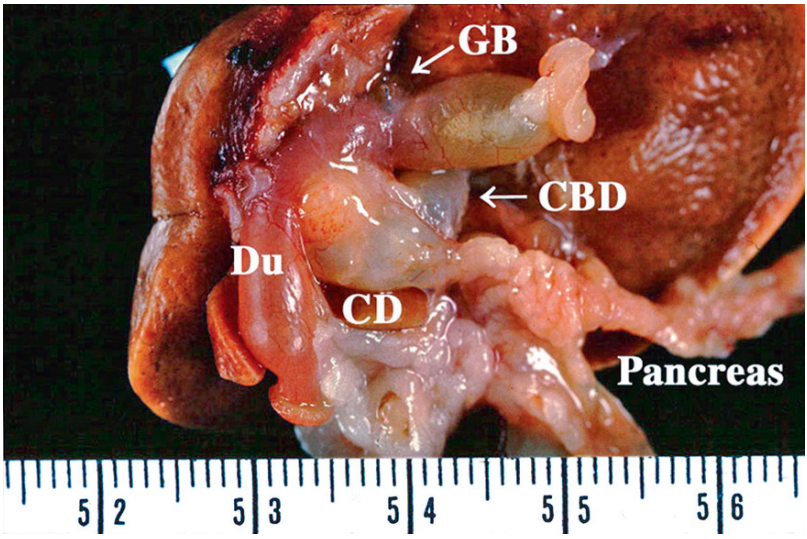

Fig. 5.9 The gallbladder and extrahepatic bile duct are extirpated as a mass with the liver, pancreas, and duodenum for pathological examination. GB, gallbladder; CBD, common bile duct; CD, common duct; Du, duodenum

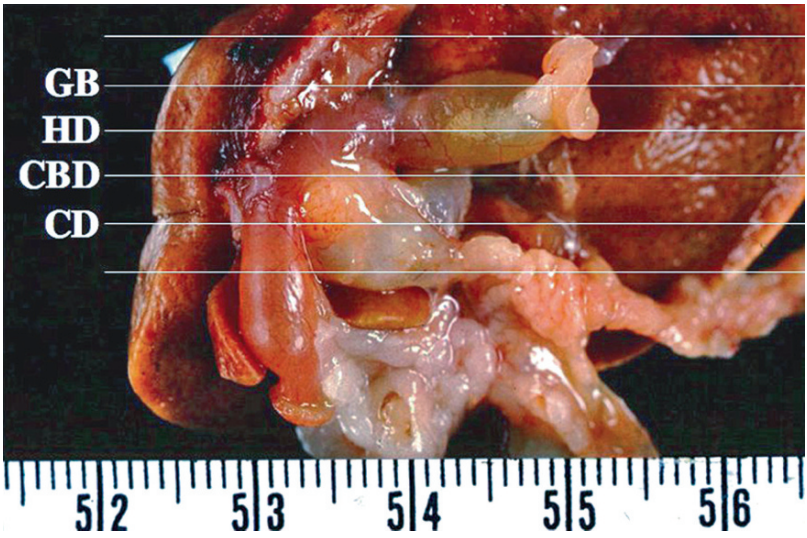

Fig. 5.10 Preparation of the surgical specimen for pathological examination. The white lines indicate the cutting planes of the specimen. GB, gallbladder; HD, hepatic duct; CBD, common bile duct; CD, common duct

5.4 Changes in the Biliary Tract

Morphologically, spindle or cystic dilatation is evident in the extrahepatic bile duct of hamsters after the CDDB procedure (Figure 5.11), although no changes are seen in the biliary tract during simple laparotomy. In the CDDB model, cholangiography can be done by injecting contrast medium into the duodenum (Figure 5.12).

Histologically, the normal gallbladder and extrahepatic bile duct are lined by a single row of low cuboidal or cylindric epithelial cells (Figures 5.13 and 5.14). In the CDDB model, hyperplastic changes in the gallbladder and bile duct epithelium are seen 2 weeks or more after preparation of the model, without the administration of carcinogens. After 3 weeks, atypical changes and metaplastic changes involving the goblet cells are seen, and after 4 weeks, exacerbation of the above changes is seen involving an extensive area of the biliary system (Figures 5.15–5.20).

Changes in biliary epithelial cell kinetics can be evaluated immunohistologically using the bromodeoxyuridine-labeling index (BrdU-LI) or the proliferating cell nuclear antigen-labeling index (PCNA-LI). About 4 weeks after simple laparotomy (SL), both the gallbladder epithelium and the extrahepatic bile duct epithelium have a BrdU-LI value of approximately 1%, which does not change during subsequent follow-up. However, in the CDDB model, the gallbladder epithelium and extrahepatic

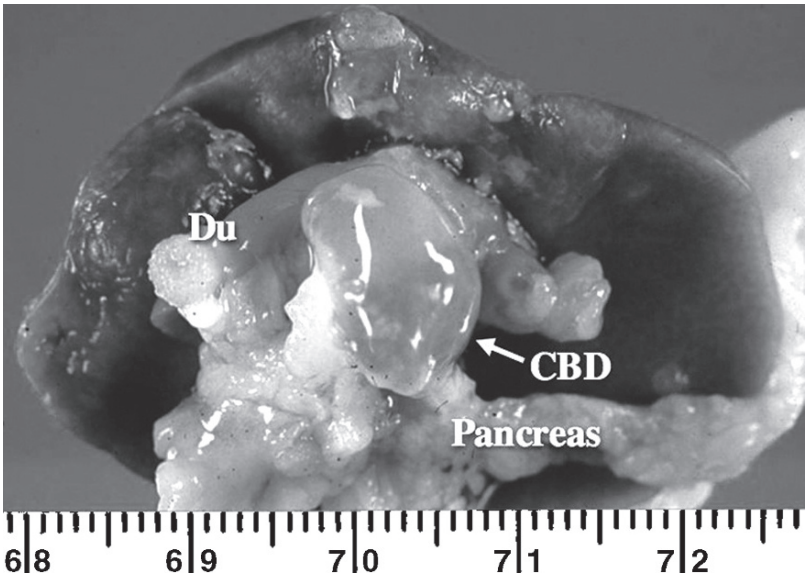

Fig. 5.11 Cystic dilatation of the extrahepatic bile duct, 16 weeks after preparation of the CDDB procedure. CBD, common bile duct; Du, duodenum

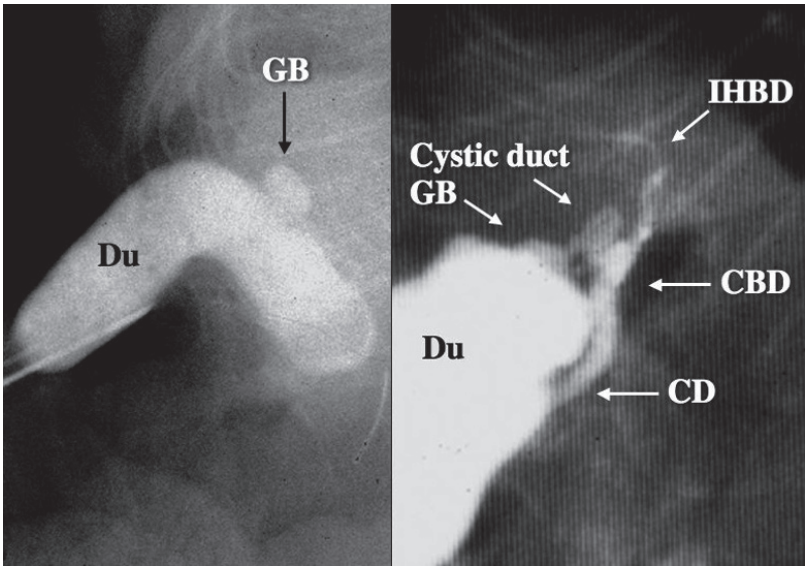

Fig. 5.12 Cholangiogram in a hamster, 7 days after preparation of the CDDB procedure. GB, gallbladder; IHBD, intrahepatic bile duct; CBD, common bile duct; CD, common duct; Du, duodenum

Fig. 5.13 Normal histologic pattern of the gallbladder epithelium (H&E, ×100)

Fig. 5.14 Normal histologic pattern of the extrahepatic bile duct epithelium (H&E, ×100)

Fig. 5.15 Papillary hyperplasia of the gallbladder epithelium, 4 weeks after preparation of the CDDB procedure (H&E, ×60)

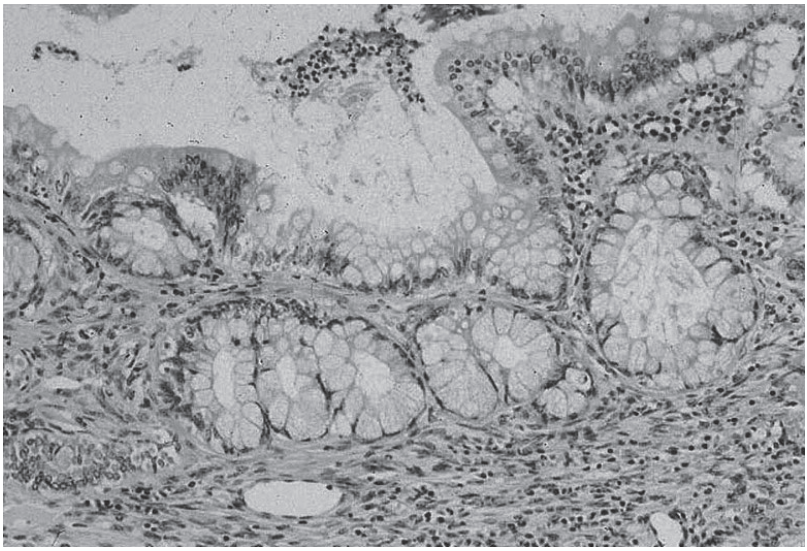

Fig. 5.16 Metaplastic changes showing goblet cell metaplasia of the gallbladder epithelium, 8 weeks after preparation of the CDDB procedure (H&E, ×200)

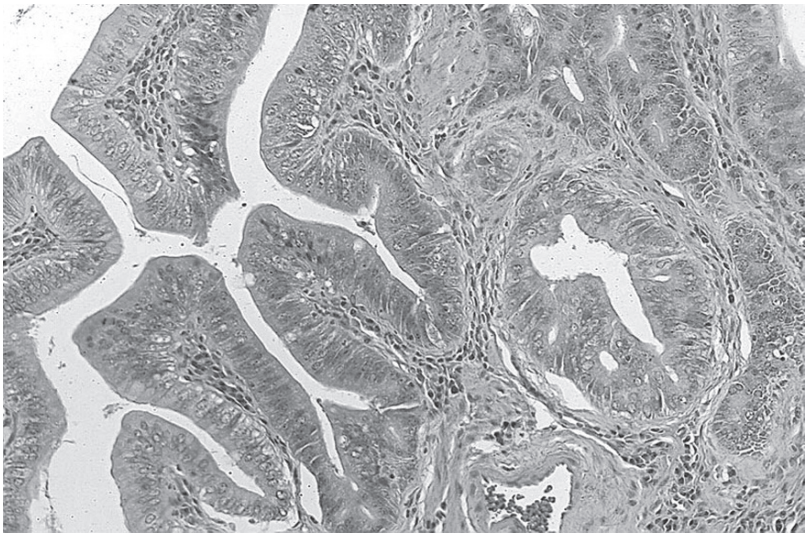

Fig. 5.17 Atypical epithelial foci with stratification, cell pleomorphism, and mitotic figures of the gallbladder epithelium, 12 weeks after preparation of the CDDB procedure (H&E, ×200)

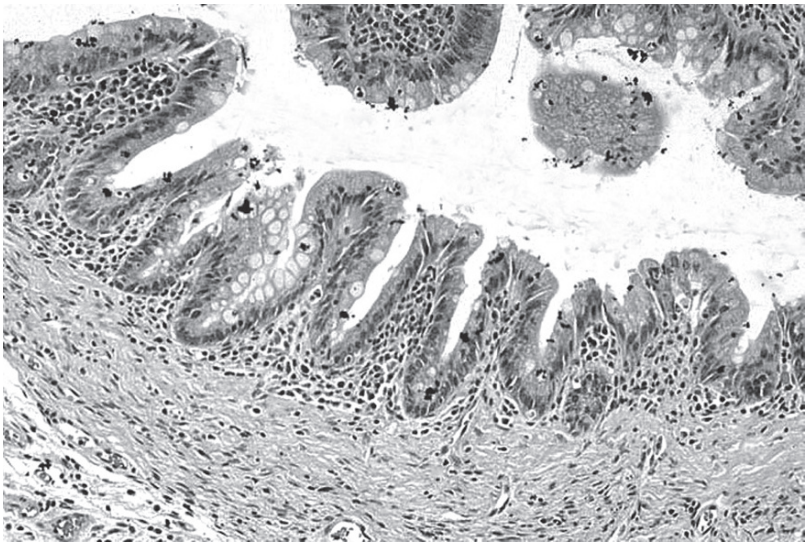

Fig. 5.18 Papillary hyperplasia of the extrahepatic bile duct epithelium, 8 weeks after preparation of the CDDB procedure (H&E, ×100)

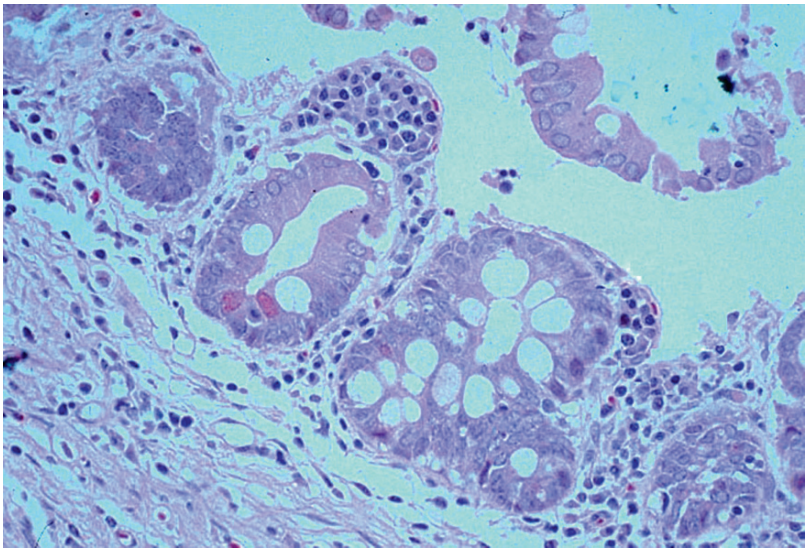

Fig. 5.19 Metaplastic changes showing goblet cell metaplasia of the extrahepatic bile duct epithelium, 12 weeks after preparation of the CDDB procedure (H&E, ×200)

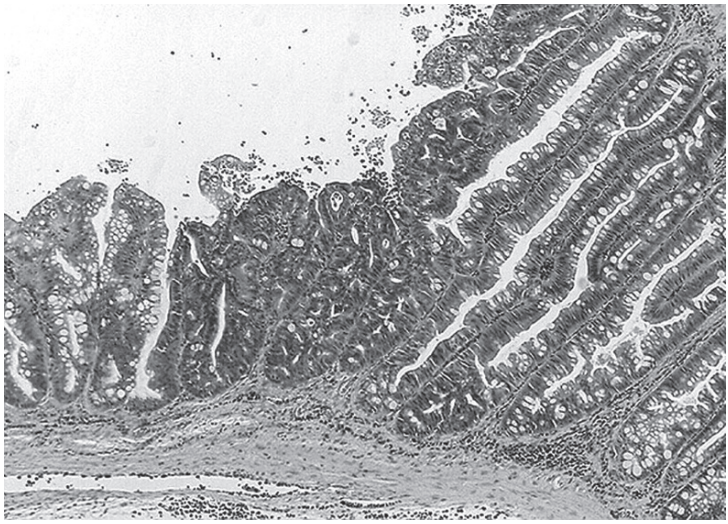

Fig. 5.20 Papillary hyperplasia with atypical epithelial foci, cell pleomorphism, and mitotic figures in the extrahepatic bile duct epithelium, 20 weeks after preparation of the CDDB procedure (H&E, ×80)

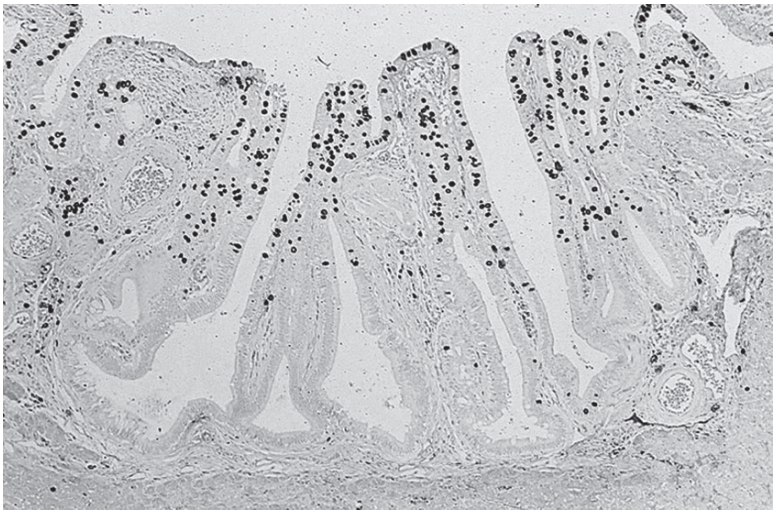

Fig. 5.21 Immunohistochemical staining of the gallbladder epithelium, 8 weeks after preparation of the CDDB procedure; done using BrdU and anti-BrdU monoclonal antibody (H&E, ×100)

bile duct epithelium have BrdU-LI values of 8.6% and 4.4% respectively, 4 weeks after surgery, suggesting an abnormal enhancement of biliary epithelial cell kinetics (Figures 5.21 and 5.22). Thereafter, the BrdU-LI values increase gradually, to 14% and 10%, respectively, 20 weeks after surgery (Table 5.1). In a hyperplastic epithelial region with cell atypia, the BrdU-LI value is remarkably high.

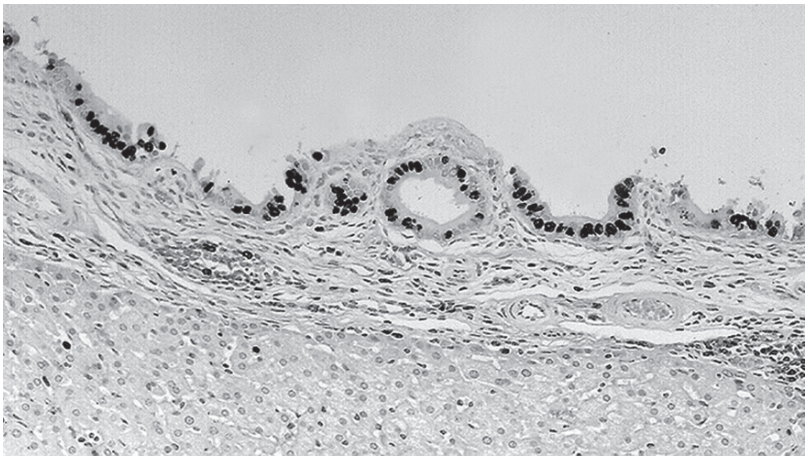

Fig. 5.22 Immunohistochemical staining of the extrahepatic bile duct epithelium, 8 weeks after preparation of the CDDB procedure; done using BrdU and anti-BrdU monoclonal antibody (H&E, ×120)

5.5 Induction of Biliary Carcinoma

It is known that the subcutaneous administration of BOP or BOP-related substances, such as *N*-nitrosobis(2-hydroxypropyl)amine (BHP), to hamsters induces pancreatic carcinoma and intrahepatic cholangiocarcinoma at a high incidence, and gallbladder carcinoma at a lower incidence, but it is extremely difficult to induce carcinoma in the extrahepatic bile duct. Conversely, the subcutaneous administration of BOP to the CDDB hamster model induces gallbladder carcinoma and extrahepatic bile duct carcinoma at a high incidence. The experimental protocol for the induction of biliary carcinoma and the results obtained [14] are summarized as follows:

First, 7–week-old female Syrian golden hamsters were subjected to the CDDB procedure; then, 4 weeks later, they were given weekly subcutaneous injections of BOP at a dose of 10 mg/kg body weight for 9 weeks. The animals were killed 12 (CDDB-1), 16 (CDDB-2), and 20 (CDDB-3) weeks after the initiation of BOP treatment. Marked dilatation of the extrahepatic bile duct was noted in almost all the hamsters in all of the CDDB groups (Table 5.2). Gallbladder carcinoma developed in 58% of the hamsters in group CDDB-1, 81% of those in group CDDB-2, and 82% of those in group CDDB-3 (Table 5.3), respectively. Extrahepatic bile duct carcinoma developed in 16% of the hamsters in group CDDB-1, 24% of those in group CDDB-2, and 41% of those in group CDDB-3 (Table 5.4), respectively. These incidences were significantly higher than those in sham-operated controls ($P < 0.01$).

The induced gallbladder carcinoma usually shows protruding papillary growth and the histology of papillary adenocarcinoma (Figure 5.23). Approximately half of the induced gallbladder carcinomas are early lesions. In early carcinoma, papillary hyperplasia with marked atypical epithelial foci is frequently observed in the

Table 5.1 BrdU labeling indices in the biliary epithelium of hamsters after cholecystoduodenostomy with dissection of the distal end of the common duct or simple laparotomy

Group	Operative procedure	Experimental period[a](wk)	Initial no. of hamsters	No. of hamsters killed	BrdU labeling index (%)[b]			
					Extrahepatic bile ducts[c]			
					HD	CBD	CD	Gallbaldder
1	CDDB	4	8	6	4.78 ± 2.43*	4.27 ± 2.29*	4.13 ± 2.54*	8.57 ± 3.95**
2	CDDB	8	9	6	6.49 ± 1.75***	6.12 ± 2.02***	6.11 ± 1.71***	7.77 ± 2.87***
3	CDDB	12	8	5	8.07 ± 2.16****	6.29 ± 1.14****	8.26 ± 2.93****	15.71 ± 2.67****
4	CDDB	16	8	6	9.47 ± 4.35*****	9.67 ± 5.38*****	6.36 ± 1.64*****	14.67 ± 4.85*****
5	CDDB	20	9	6	10.33 ± 3.41******	9.88 ± 4.16******	9.09 ± 2.59******	14.15 ± 5.20******
6	SL	4	5	5	0.63 ± 0.36	0.52 ± 0.21	0.75 ± 0.47	0.76 ± 0.32
7	SL	8	5	5	0.92 ± 0.52	0.70 ± 0.28	1.14 ± 0.65	0.59 ± 0.30
8	SL	12	5	5	1.12 ± 0.69	0.90 ± 0.41	1.34 ± 0.89	1.33 ± 1.25
9	SL	16	5	5	1.08 ± 0.62	0.94 ± 0.55	1.22 ± 0.70	1.05 ± 0.65
10	SL	20	5	5	1.36 ± 1.01	1.57 ± 1.31	1.15 ± 0.69	1.49 ± 1.20

*Significantly different from Group 6 ($P < 0.05$).
**Significantly different from Group 6 ($P < 0.01$).
***Significantly different from Group 7 ($P < 0.01$).
****Significantly different from Group 8 ($P < 0.01$).
*****Significantly different from Group 9 ($P < 0.01$).
******Significantly different from Group 10 ($P < 0.01$).
[a]Period from the operation to killing (wk, weeks).
[b]Mean ± SD.
[c]HD, hepatic ducts; CBD, common bile duct; CD, common duct. (modified from [14], with permission)

Table 5.2 Changes in number and body weight of hamsters during the experiment, and diameter of the common bile duct examined at autopsy

Group	Treatment	Experimental period[a] (wk)	Initial no. of hamsters	No.(%) of survivals at BOP initiation	No. (%) of hamsters killed	Average body weight (g)[b]			Average diameter of the common bile duct (mm)at autopsy[c]
						Initial	At BOP initiation	Final	
CDDB-1	CDDB + BOP	12	29	20(69)	19(66)	111 ± 5	131 ± 9*	167 ± 23*	4.60 ± 1.69*
CDDB-2	CDDB + BOP	16	36	25(69)	21(58)	110 ± 5	128 ± 11**	150 ± 14**	5.50 ± 1.37**
CDDB-3	CDDB + BOP	20	42	29(69)	22(52)	112 ± 5	133 ± 11***	143 ± 19***	5.31 ± 2.01***
SL-1	SL + BOP	12	20	20(100)	20(100)	111 ± 8	150 ± 7	185 ± 15	0.71 ± 0.14
SL-2	SL + BOP	16	20	20(100)	20(100)	110 ± 7	147 ± 10	187 ± 17	0.95 ± 0.86
SL-3	SL + BOP	20	20	20(100)	18(90)	110 ± 5	153 ± 8	178 ± 20	1.26 ± 1.63

*Significantly different from SL-1 ($P < 0.01$).
**Significantly different from SL-2 ($P < 0.01$).
***Significantly different from SL-3 ($P < 0.01$).
[a]Period from initial BOP treatment to killing (wk, weeks).
[b,c]Mean ± SD. (modified from [14], with permission)

Table 5.3 Gallbladder carcinomas induced in BOP-treated hamsters after cholecystoduodenostomy with dissection of the distal end of the common duct or simple laparotomy

Group	No. of hamsters killed	No. (%) of hamsters with		Total no. of carcinomas	Tumor shape		Histology[a]	
		Carcinoma	Invasive carcinoma		Papillary	Nodular	Tub	Pap
CDDB-1	19	11(58)[*]	4(21)[**]	11	11	0	0	11
CDDB-2	21	17(81)[***]	10(48)[***]	17	16	1	1	16
CDDB-3	22	18(82)[****]	10(45)[*****]	18	18	0	0	18
SL-1	20	0	0	0	0	0	0	0
SL-2	20	1(5)	0	1	1	0	0	1
SL-3	18	2(11)	1(6)	2	2	0	0	2

[*]Significantly different from SL-1 ($P < 0.01$).
[**]Significantly different from SL-1 ($P < 0.05$).
[***]Significantly different from SL-2 ($P < 0.01$).
[****]Significantly different from SL-3 ($P < 0.01$).
[*****]Significantly different from SL-3 ($P < 0.05$).
[a]Tub, tubular adenocarcinoma; Pap, papillary adenocarcinoma. (modified from [14], with permission)

Table 5.4 Extrahepatic bile duct carcinomas induced in BOP-treated hamsters after cholecystoduodenostomy with dissection of the distal end of the common duct or simple laparotomy

Group	No. of hamsters killed	No. (%) of hamsters with carcinoma	Total no. of carcinomas	Tumor location[a]			Tumor shape[b]		Histology[c]	
				HD	CBD	CD	Poly	Super	Tub	Pap
CDDB-1	19	3(16)	5	3	1	1	5	0	5	0
CDDB-2	21	5(24)	7	5	2	0	4	3	4	3
CDDB-3	22	9(41)[*]	12	7	3	2	7	5	7	5
SL-1	20	0	0	0	0	0	0	0	0	0
SL-2	20	1(5)	1	1	0	0	0	1	0	1
SL-3	18	0	0	0	0	0	0	0	0	0

[*]Significantly different from SL-3 ($P < 0.01$).
[a]HD, hepatic ducts; CBD, common bile duct; CD, common duct.
[b]Poly, polypoid type; Super, superficial type.
[c]Tub, tubular adenocarcinoma; Pap, papillary adenocarcinoma. (modified from [14], with permission)

peri-carcinomatous areas of the gallbladder (Figures 5.24 and 5.25). Advanced gallbladder carcinoma with hepatic or duodenal involvement (Figure 5.26) is detected in about half of the animals with induced gallbladder carcinoma, and shows the histology of papillary adenocarcinoma with papillary growth (Figure 5.27). However, at the site of infiltration, the histological type is tubular adenocarcinoma (Figure 5.28).

Most induced extrahepatic bile duct carcinoma lesions are early carcinomas, with cancer cells confined to the mucosal layer of the bile duct. In early carcinoma, hyperplastic epithelium with cell atypia is evident in the peri-carcinomatous areas of the extrahepatic bile duct. These early carcinomas show the following three different growth patterns: protruding type, consisting of polypoid and papillary tumors; superficial spreading type; and periductal glandular type. There are no depressed tumors. The polypoid type (Figures 5.29 and 5.30) comprises about

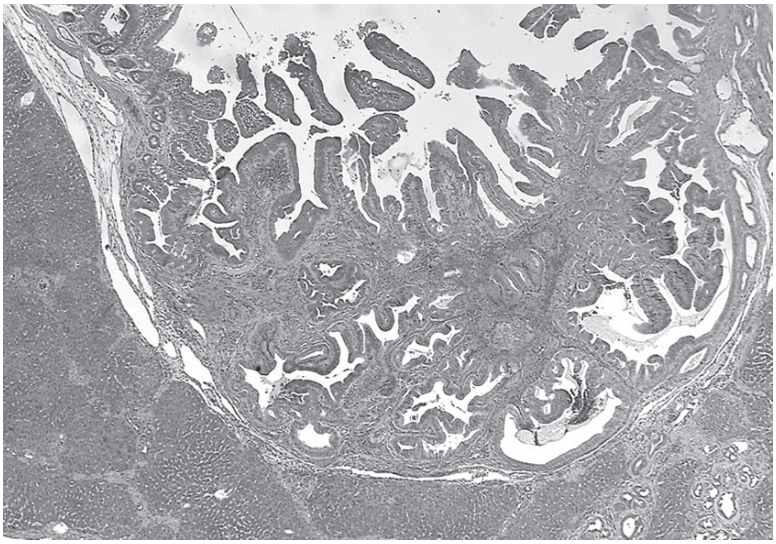

Fig. 5.23 Gallbladder carcinoma induced in a CDDB hamster (H&E, ×60)

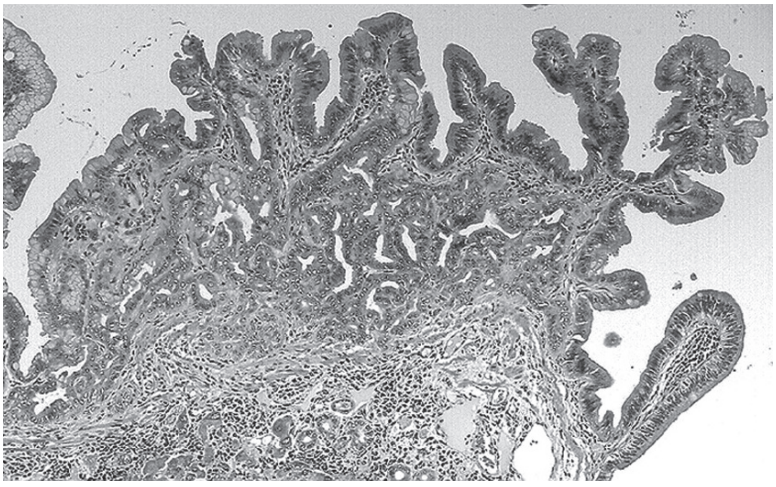

Fig. 5.24 Early gallbladder carcinoma induced in a CDDB hamster (H&E, ×120)

50%. This reflects that most human early bile duct carcinomas develop as protruding lesions composed mainly of polypoid tissue [18,19]. The papillary type (Figure 5.31) comprises about 25%, and atypical hyperplasia within the tumor mass is frequently noted in this type of carcinoma. The superficial spreading type (Figure 5.32) comprises about 15% and periductal glandular type carcinoma (Figure 5.33), derived from the periductal glands around the extrahepatic bile duct, comprises about 10%. The periductal glands are thought to be a possible source of

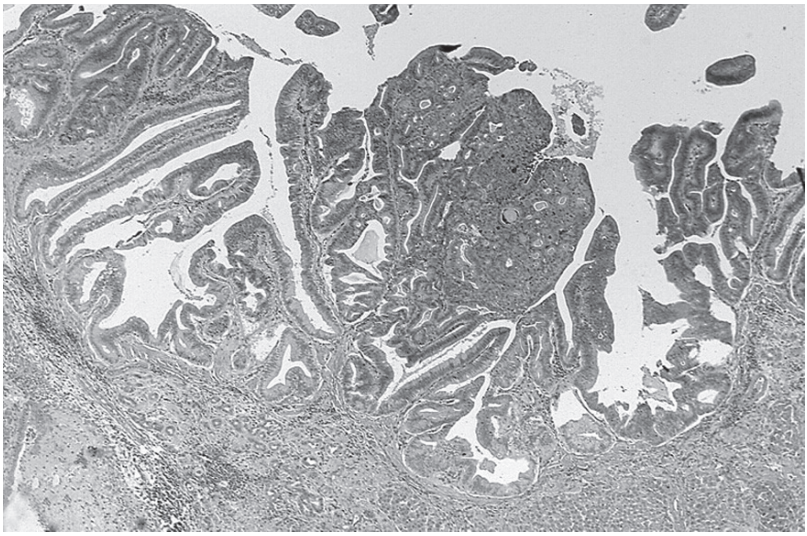

Fig. 5.25 Early gallbladder carcinoma induced in a CDDB hamster (H&E, ×100)

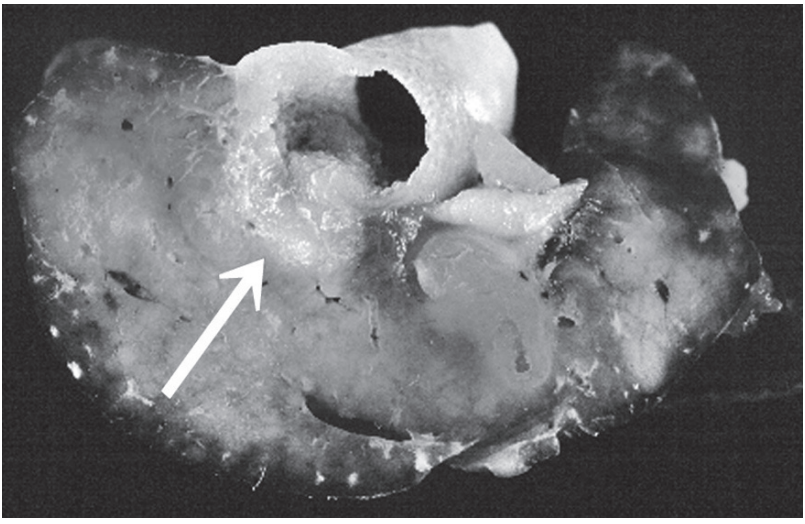

Fig. 5.26 Macroscopic appearance of an advanced gallbladder carcinoma with liver invasion (arrow)

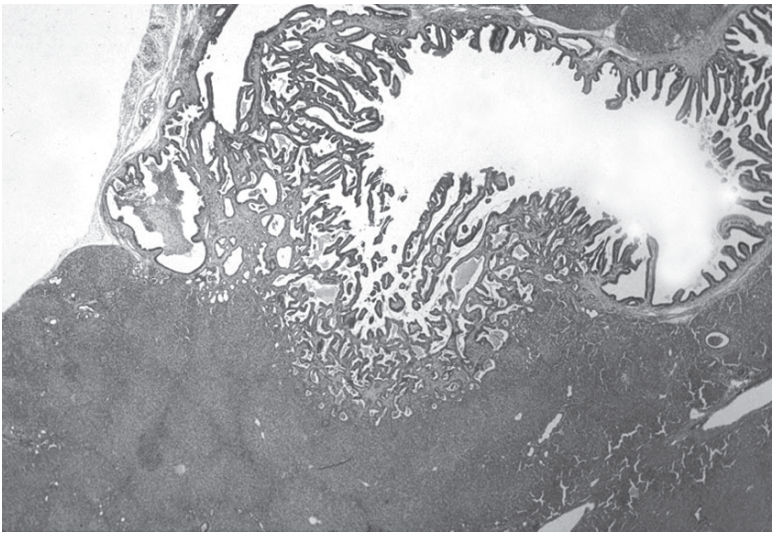

Fig. 5.27 Advanced gallbladder carcinoma induced in a CDDB hamster (H&E, ×40). There is evidence of invasion into the adjacent liver tissue

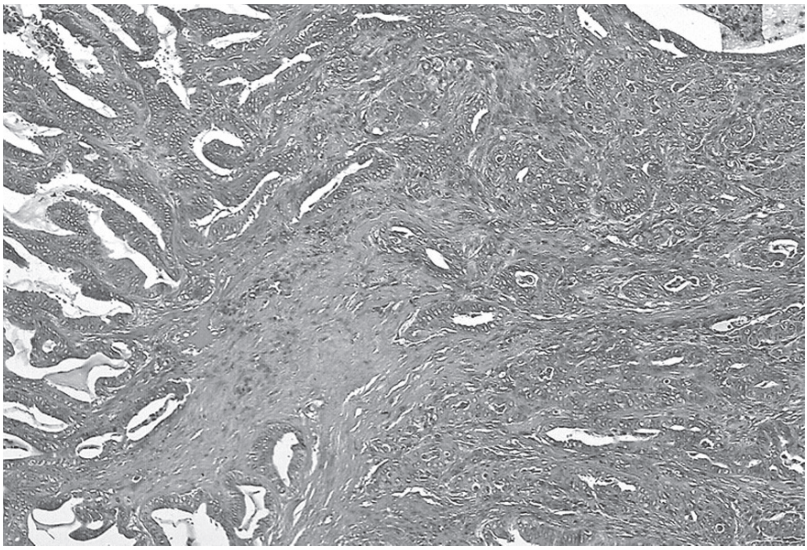

Fig. 5.28 Liver invasion of gallbladder carcinoma (H&E, ×200)

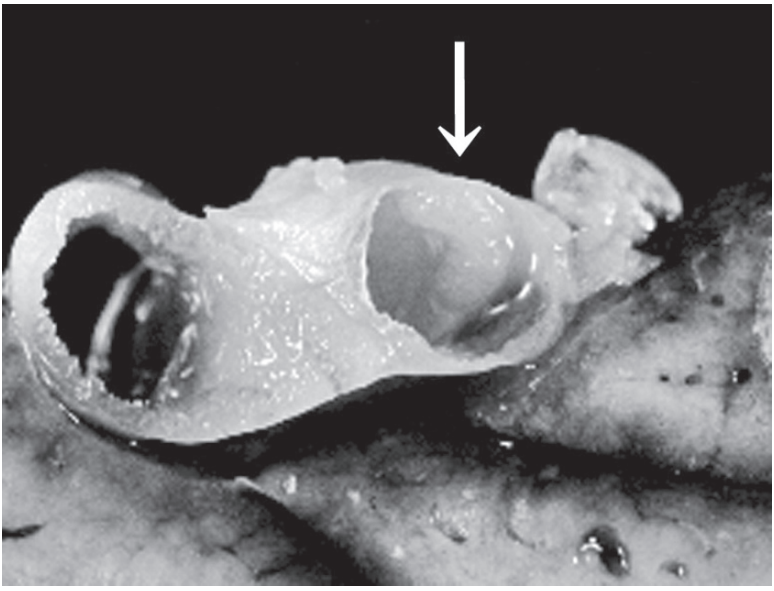

Fig. 5.29 Macroscopic view of a polypoid type carcinoma of the extrahepatic bile duct (*arrow*)

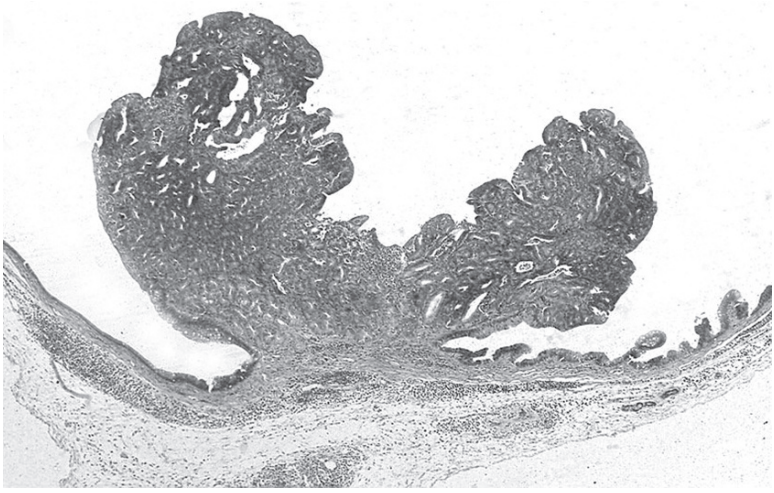

Fig. 5.30 A polypoid type carcinoma of the extrahepatic bile duct induced in a CDDB hamster. The tumor protrudes into the lumen of the markedly dilated bile duct (H&E, ×60)

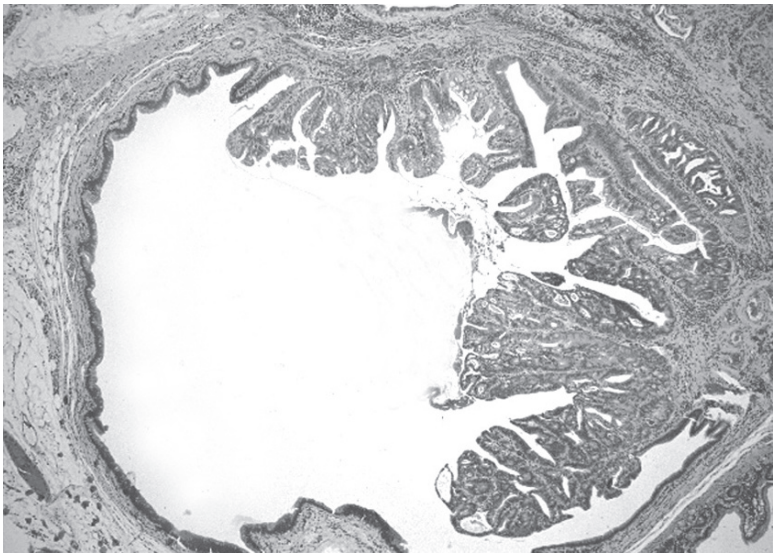

Fig. 5.31 A papillary type carcinoma of the extrahepatic bile duct induced in a CDDB hamster (H&E, ×80)

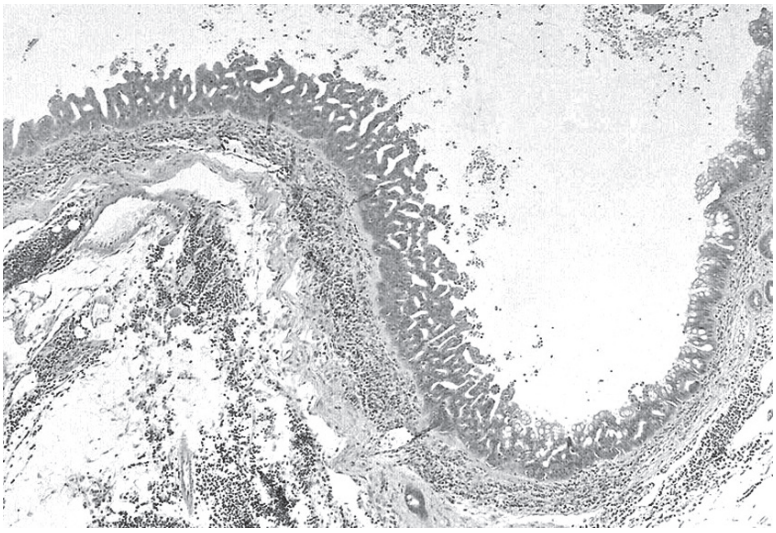

Fig. 5.32 A superficial spreading type carcinoma of the extrahepatic bile duct induced in a CDDB hamster (H&E, ×80)

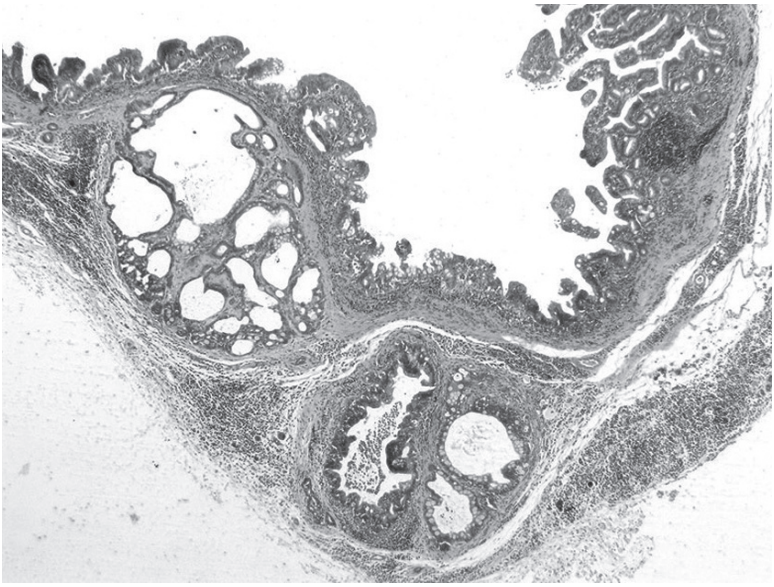

Fig. 5.33 A periductal glandular type carcinoma of the extrahepatic bile duct induced in a CDDB hamster (H&E, ×80)

intrahepatic bile duct carcinoma [20], and may also be a location for human extrahepatic bile duct carcinoma.

Tumorigenicity in the liver and pancreas is summarized in Table 5.5. Most livers from the CDDB group hamsters showed a high degree of tumor development from the bile ductule, in the form of cholangiocarcinomas and cholangiomas. The incidence of carcinoma and adenoma, and the average number of both carcinomas and adenomas per animal was significantly higher in the CDDB groups than in the corresponding SL groups.

Pancreatic tumors were induced frequently in hamsters in all the experimental groups. Most of these tumors were ductular adenocarcinomas. Neither the incidence of carcinoma nor the average number of carcinomas per animal differed significantly among the corresponding groups.

B. Biliary Reconstruction Models

5.6 Introduction

Reconstruction of the biliary system is a surgical technique used widely in the field of hepatobiliary and pancreatic surgery; however, biliary carcinomas can develop as a delayed complication of bilioenterostomy [21–25]. Moreover, high incidences

Table 5.5 Carcinomas of the liver and pancreas induced in BOP-treated hamsters after cholecystoduodenostomy with dissection of the distal end of the common duct or simple laparotomy

		Liver					Pancreas				
				Histology[a]					Histology[a]		
Group	No. of hamsters killed	No. (%) of hamsters with carcinoma	Average no. of carcinomas per animal	Tub	Pap	Others	No. (%) of hamsters with carcinoma	Average no. of carcinomas per animal	Tub	Pap	Others
CDDB-1	19	7(37)*	1.47**	24	2	2	10(53)	1.16	19	2	1
CDDB-2	21	16(76)***	2.71***	50	4	3	17(81)	2.00	35	3	4
CDDB-3	22	19(86)****	5.14****	104	5	4	18(82)	2.18	41	4	3
SL-1	20	0	0	0	0	0	9(45)	0.60	10	1	1
SL-2	20	4(20)	0.50	10	0	0	17(85)	1.80	27	5	4
SL-3	18	10(56)	2.11	36	1	1	16(89)	2.33	35	4	3

*Significantly different from SL-1 ($P < 0.01$).
**Significantly different from SL-1 ($P < 0.05$).
***Significantly different from SL-2 ($P < 0.01$).
****Significantly different from SL-3 ($P < 0.05$).
[a]Tub, tubular adenocarcinoma; pap, papillary adenocarcinoma. (modified from [14], with permission)

of secondary biliary carcinoma following biliary-enteric drainage for benign disease [26], transduodenal sphincteroplasty [27] or endoscopic sphincterotomy have been reported [28]. These therapeutic procedures induce reflux of the intestinal contents into the biliary tract because the papillary muscle of the ampulla of Vater is inactive. Reflux of the intestinal contents into the biliary system may lead to the development of biliary carcinoma. To clarify if bilioenterostomy plays a role in biliary carcinogenesis, we devised two models of bilioenterostomy in hamsters: choledochoduodenostomy and choledochojejunostomy, both of which closely resemble those performed clinically.

5.7 Preparation of the Model

Schemata of the completed surgical procedures of choledochoduodenostomy (CD model) and choledochojejunostomy (CJ model) are illustrated in Figures 5.34 and 5.35, respectively.

Using 7-week-old female Syrian golden hamsters under general anesthesia with sodium pentobarbital (50 mg/kg body weight) an upper abdominal midline incision is made and the distal end of the common bile duct is doubly ligated with 6-0 nylon and divided (Figures 5.36 and 5.37). At this point, the suture used for the ligation of the proximal bile duct must be left long. Following ligation of the cystic duct, the gallbladder is removed. In the CJ procedure, the jejunum is doubly ligated with 6-0 nylon and cut about 7 cm distal to the pyloric ring of the stomach (Figure 5.38). Roux-en-Y anastomosis is done about 4 cm anal of the jejunum and the intestinal anastomosis is done in a side-to-side manner. A common hairpin can be used as an intestinal clamp (Figure 5.39). The side-to-side anastomosis is performed using a

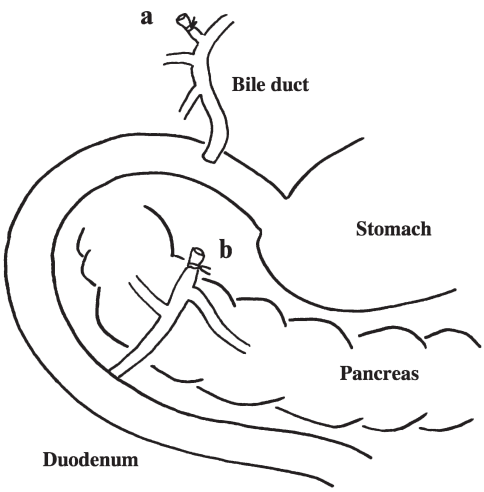

Fig. 5.34 Choledochoduodenostomy (CD model) in the hamster. Choledochoduodenostomy is done approximately 1 cm distal to the pyloric ring of the stomach. **(a)** The gallbladder is removed. **(b)** The bile duct is transected at the distal end of the common bile duct (modified from [29], with permission)

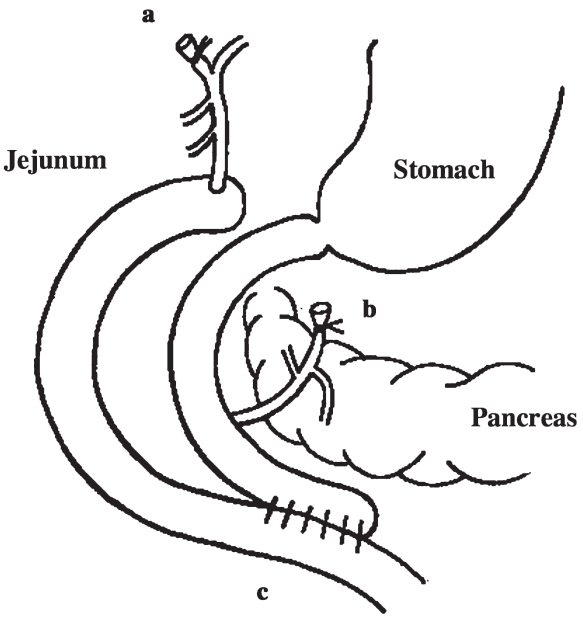

Fig. 5.35 Choledochojejunostomy with Roux-en-Y anastomosis (CJ model) in the hamster. The jejunal limb is 4 cm long. **(a)** The gallbladder is removed. **(b)** The bile duct is transected at the distal end of the common bile duct. (c) Side-to-side intestinal anastomosis (modified from [29], with permission)

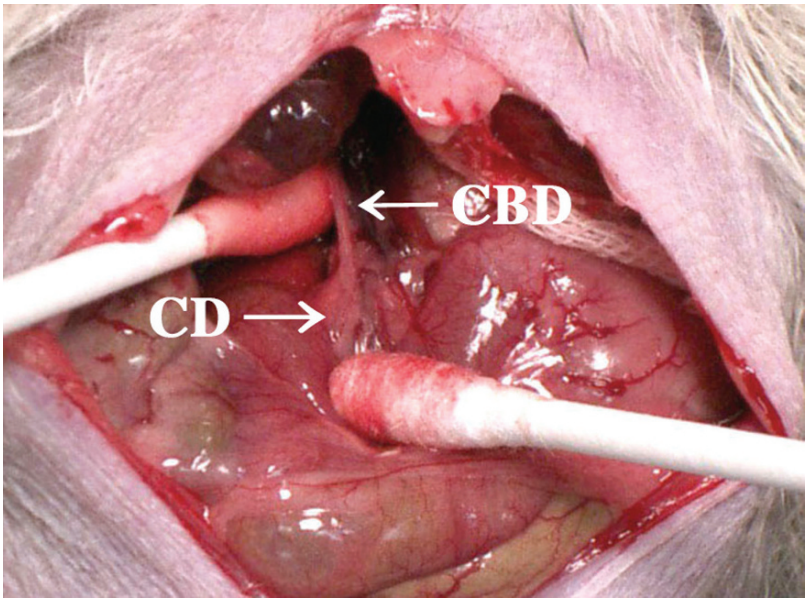

Fig. 5.36 The extrahepatic bile duct is exposed by using cotton buds. CBD, common bile duct; CD, common duct

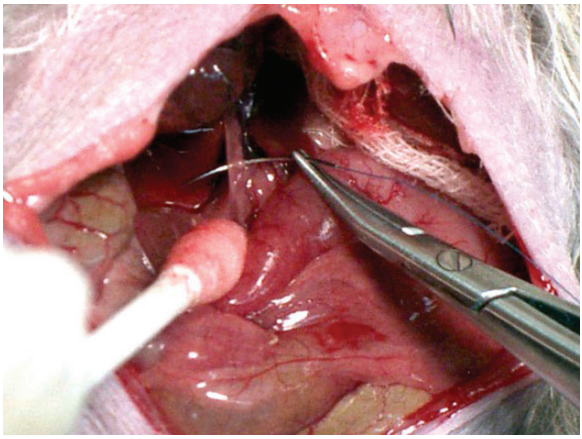

Fig. 5.37 The distal end of the common bile duct is hooked using a needle, and then ligated

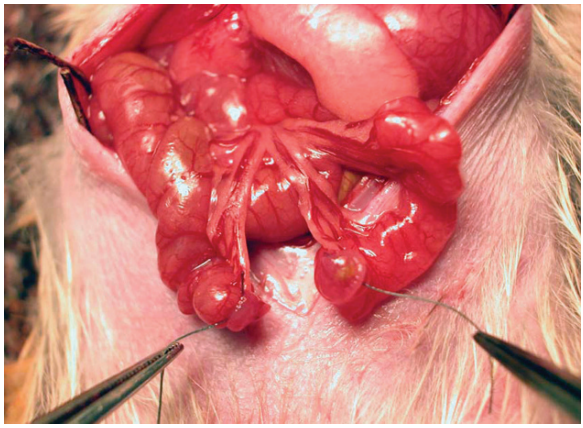

Fig. 5.38 The jejunum is cut about 7 cm distal to the pyloric ring of the stomach

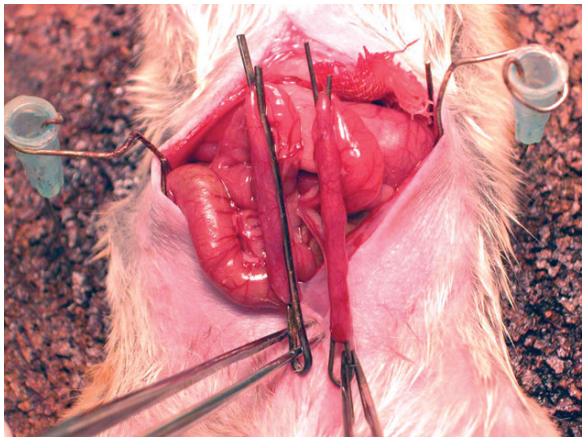

Fig. 5.39 A common hairpin is used as an intestinal clamp

running 7-0 nylon suture (Figures 5.40 and 5.41). Details of the choledochojejunostomy are illustrated in Figure 5.42. After making a purse string suture in the jejunal wall, approximately 5 mm distal to the stump of the jejunal limb (Figure 5.43), the jejunum is transfixed at the center of this suture using a 20G needle with an elastic sheath (Figures 5.42a and 5.44). The elastic sheath is left in place. Next, the suture used for the ligation of the proximal common bile duct is inserted into the elastic sheath (Figure 5.45) along with the tied common bile duct (Figures 5.42b and 5.46), so that the cut end of the bile duct protrudes through the needle hole after a removal of the elastic sheath (Figure 5.47). The common bile duct is then cut about half-way towards the tied end for bile drainage (Figures 5.42c and 5.48) and then pulled back

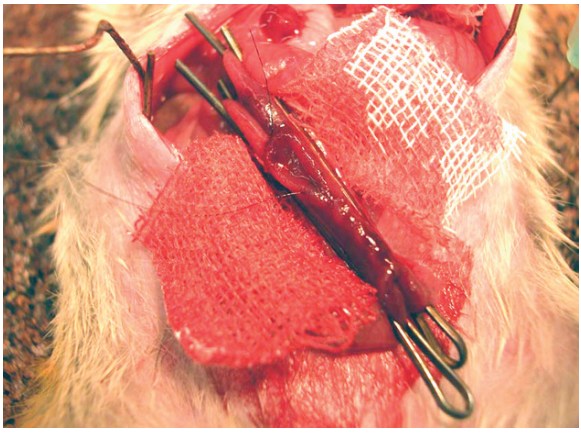

Fig. 5.40 Roux-en-Y anastomosis is done side-to-side using a running 7-0 nylon suture

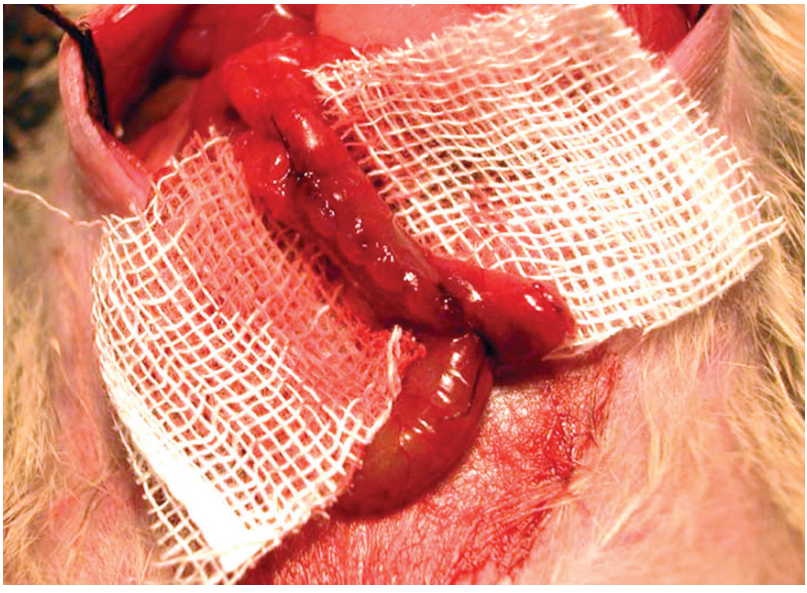

Fig. 5.41 The Roux-en Y anastomosis is completed

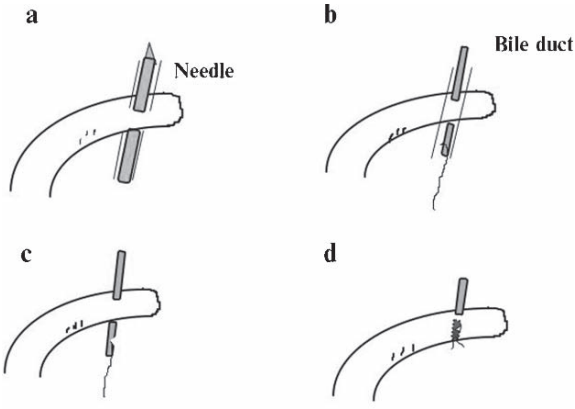

Fig. 5.42 Schemata of the surgical procedures of choledochojejunostomy in the hamster. (a) The jejunum is transfixed using a 20G needle with an elastic sheath. (b) The elastic sheath is left in place, and the suture is introduced into the elastic sheath with the tied common bile duct. (c) The common bile duct is cut about half-way towards the tied end for bile drainage. (d) The common bile duct is pulled back into the duodenum and fixed to the jejunal wall

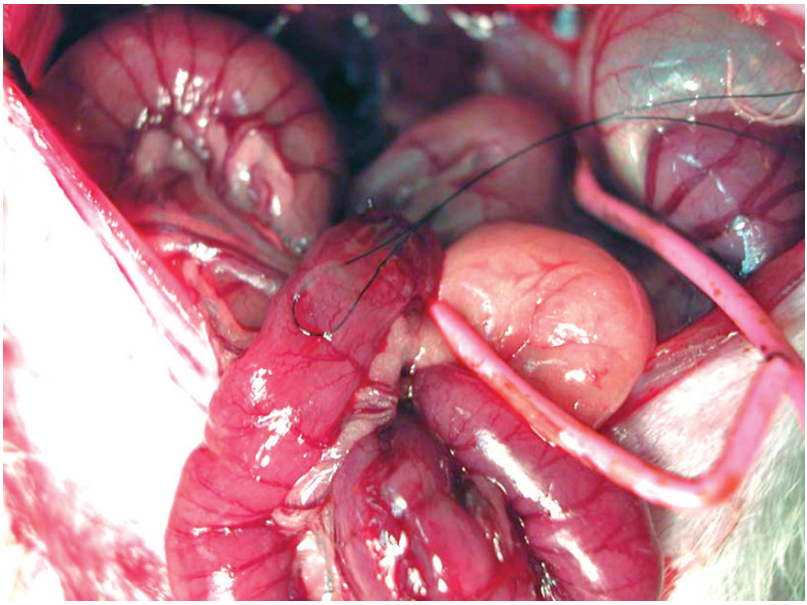

Fig. 5.43 A purse string suture is placed on the jejunal wall, approximately 5 mm distal to the tip of the jejunal limb

into the duodenum. The purse string suture is knotted to close the needle hole. Finally, the suture used for the bile duct ligation is knotted together with the purse string suture and fixed to the jejunal wall (Figures 5.42d and 5.49). In the CD procedure, choledoduodenostomy is performed in a similar manner to the CJ procedure after cholecystectomy.

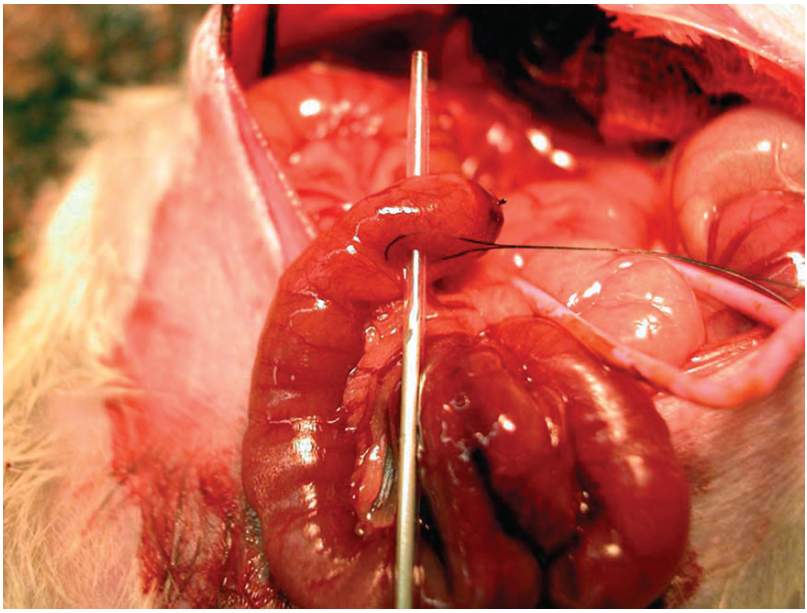

Fig. 5.44 The jejunum is transfixed at the center of the purse string suture, using a 20G needle with an elastic sheath. The elastic sheath is left in place (see Figure 5.42a)

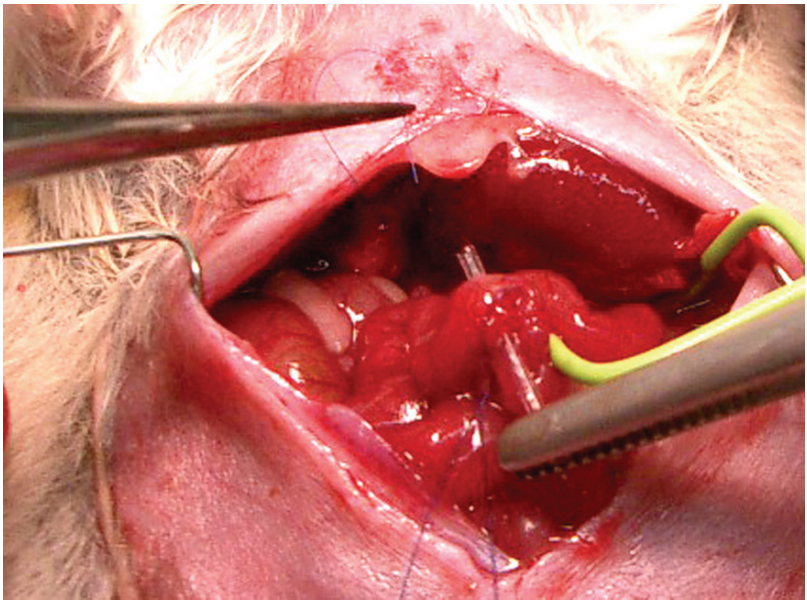

Fig. 5.45 The suture used to ligate the common bile duct is introduced through the elastic sheath

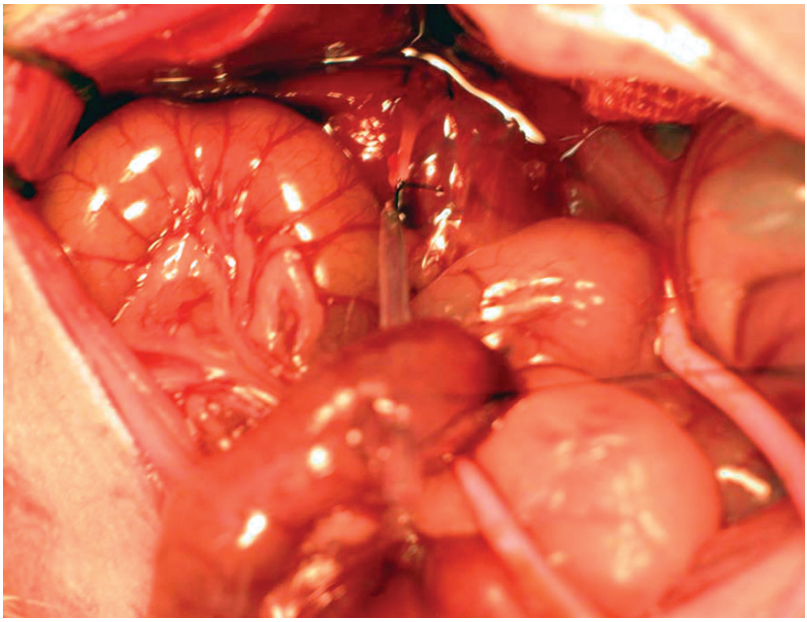

Fig. 5.46 The suture is pulled so that the tied common bile duct protrudes through into the elastic sheath (see Figure 5.42b)

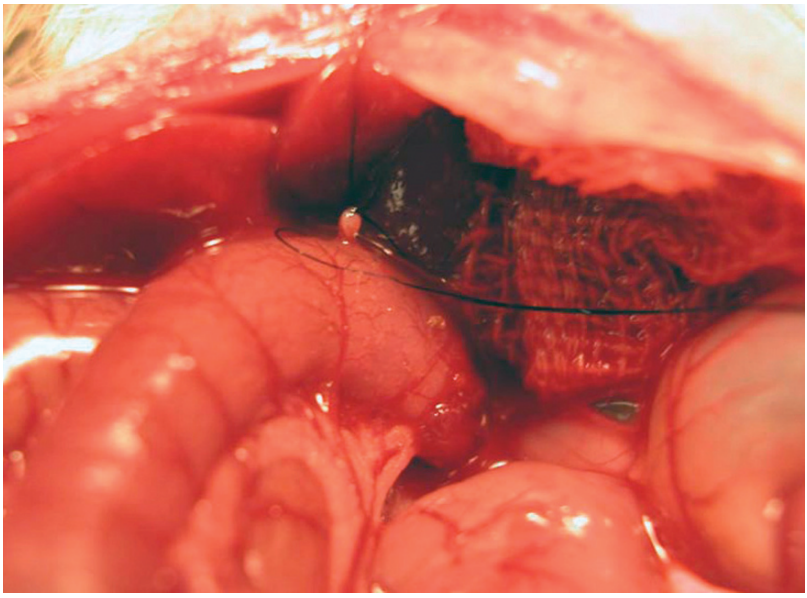

Fig. 5.47 The cut end of the common bile duct is pulled out through the needle hole

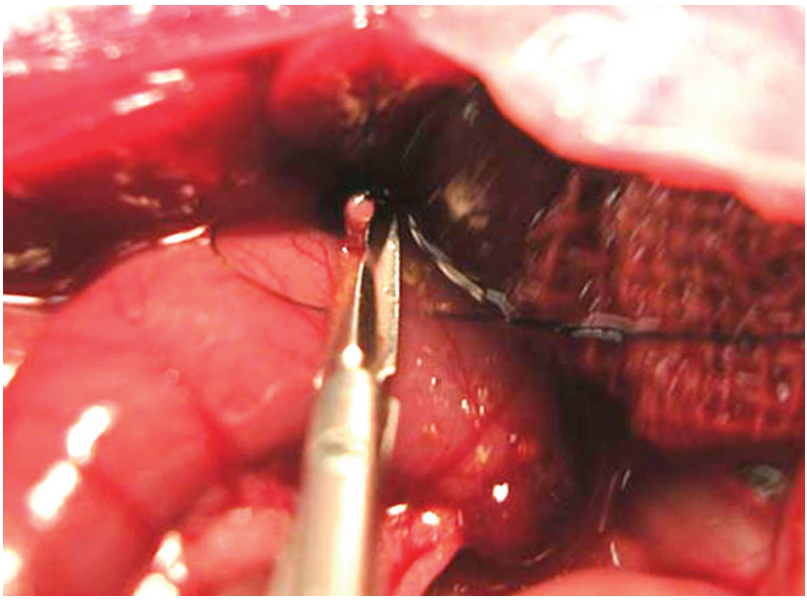

Fig. 5.48 The common bile duct is cut about half-way towards the tied end for bile drainage (see Figure 5.42c)

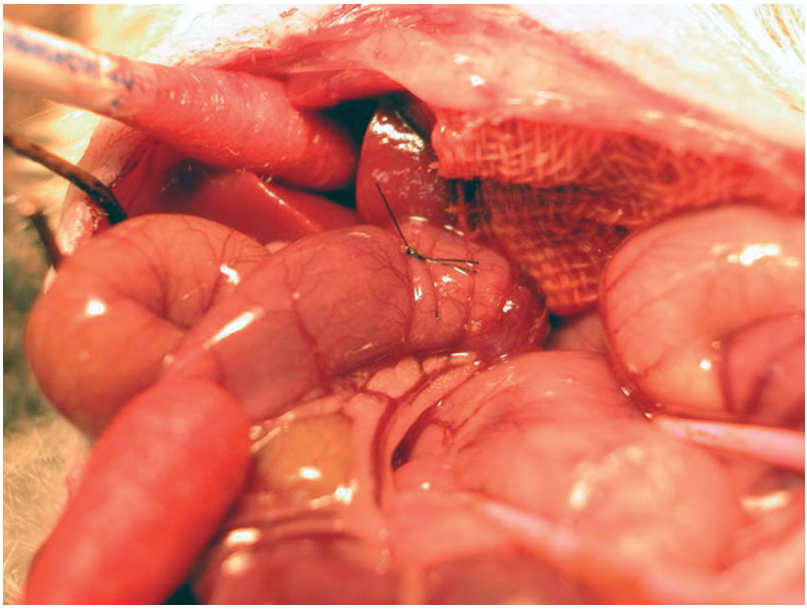

Fig. 5.49 The common bile duct is pulled back into the jejunum and the suture used for the common bile duct ligation is fixed to the jejunal wall (see Figure 5.42d)

5.8 Induction of Biliary Carcinoma

The experimental protocol for the induction of biliary carcinoma in bilioenterostomized hamsters and the results obtained [29] are as follows: First, 7-week-old female Syrian golden hamsters were subjected to simple laparotomy (SL), choledochoduodenostomy (CD) and choledochojejunostomy (CJ). Then, 4 weeks later, they were treated with weekly subcutaneous injections of BOP at a dose of 10 mg/kg body weight for 9 weeks. The animals were killed 20 weeks after surgery. Marked dilatation of the extrahepatic bile duct was noted in almost all the hamsters in the CD and CJ groups. Carcinoma of the intrahepatic bile duct developed in 40% of hamsters in the SL group, 41% of those in the CD group, and 50% of those in the CJ group. However, numerous bile duct carcinomas were found in the bilioenterostomized animals, especially in the CJ group (Table 5.6). Carcinoma of the extrahepatic bile duct developed in 5% of the hamsters in the CD group and 8% of those in the CJ group. No extrahepatic bile duct carcinoma was seen in the SL group hamsters.

Epithelial neoplasms and associated lesions arising in the hamster liver are divided into two broad categories depending on the cell of origin: hepatocellular or cholangiocellular. However, liver tumors of hepatocellular origin rarely develop in response to BOP insult in hamsters. Tumors of cholangiocellular origin, such as the intrahepatic cholangiocarcinomas induced by BOP in hamsters are classified grossly into four histological types: tubular adenocarcinoma, papillary adenocarcinoma, mucinous cystadenocarcinoma, and others. Tubular adenocarcinoma is the most common, accounting for about 70% of intrahepatic cholangiocarcinomas (Figures 5.50 and 5.51), followed by papillary adenocarcinoma (Figures 5.52 and 5.53) and mucinous cystadenocarcinoma (Figures 5.54 and 5.55), accounting for about 20% and 5%, respectively. There are three different patterns of growth of these tumors: mass-forming, periductal infiltrating, and intraductal. The mass-forming growth pattern, seen in about 50% of tumors, is characterized by a distinct, localized round mass in the liver parenchyma (Figure 5.56). The periductal infiltrating growth pattern, seen in about 40% of tumors, is characterized by diffuse tumor infiltration along the long axis of the portal tract (Figure 5.57). The intraductal growth pattern, seen in only about 10% of tumors, is characterized by papillary (Figure 5.58) or polypoid (Figure 5.59) growth within the dilated bile duct lumen, with occasional superficial spread (Figure 5.60) or periductal gland involvement (Figures 5.61 and 5.62).

Table 5.6 The incidence and number of carcinomas induced in hamsters after bilioenterostomy

Groups	No. of hamsters	Average body weight (g)	No. (%) of hamsters with carcinoma of		Total no. of carcinomas	Average no. of carcinomas per CBA
			IHBD	EHBD		
SL	20	202.5	8(40.0)	0	16	2.00
CD	22	180.5	9(40.9)	1(4.5)	56	6.22
CJ	26	171.0	13(50.0)	2(14.5)	189	14.53*

IHBD, intrahepatic bile duct; EHBD, extrahepatic bile duct; CBA, carcinoma-bearing animal.
*Significantly different from SL ($P < 0.01$) and CD ($P < 0.05$). (modified from [29], with permission)

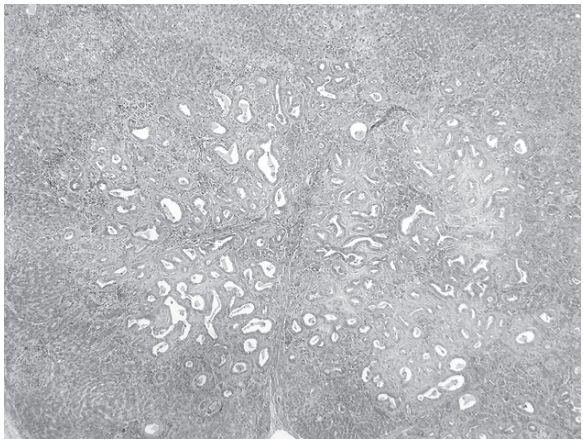

Fig. 5.50 Intrahepatic cholangiocarcinoma: tubular adenocarcinoma

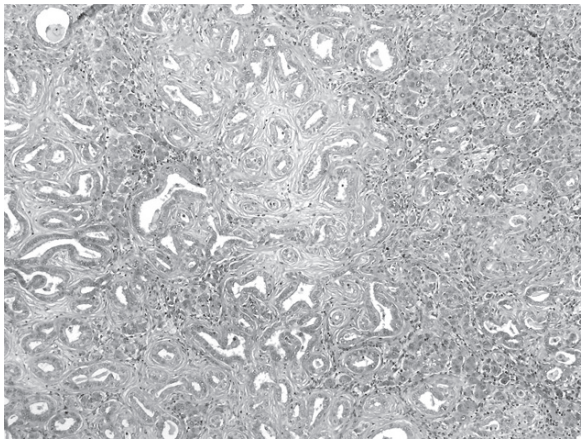

Fig. 5.51 Microscopic appearance of tubular adenocarcinoma

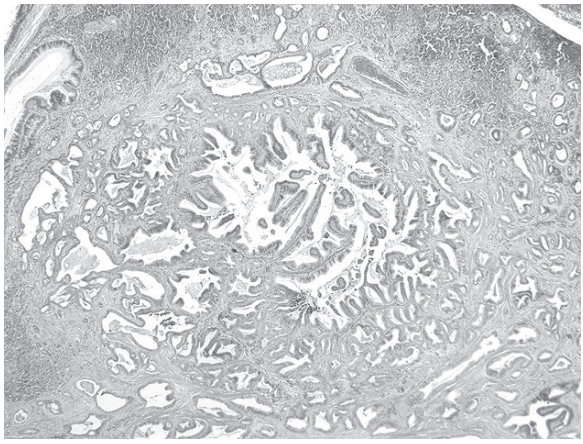

Fig. 5.52 Intrahepatic cholangiocarcinoma: papillary adenocarcinoma

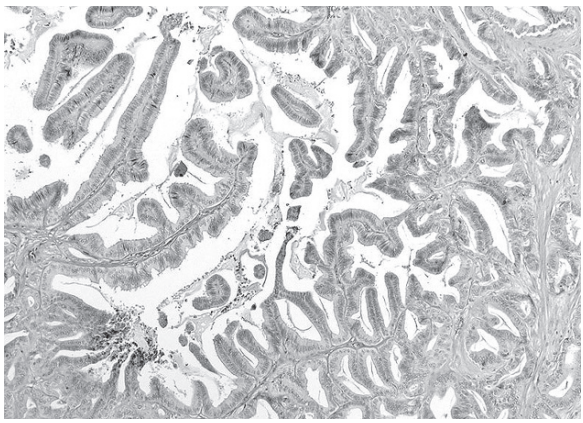

Fig. 5.53 Microscopic appearance of papillary adenocarcinoma

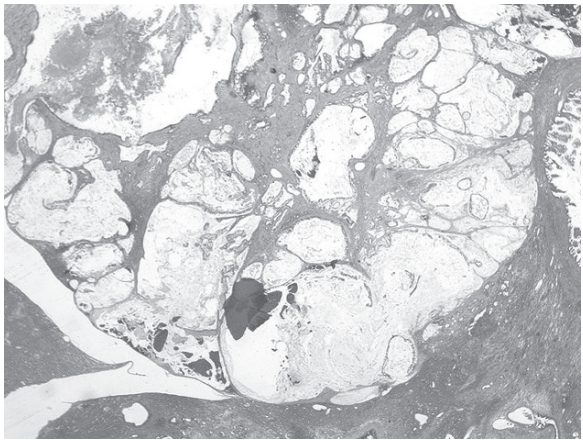

Fig. 5.54 Intrahepatic cholangiocarcinoma: mucinous cystadenocarcinoma

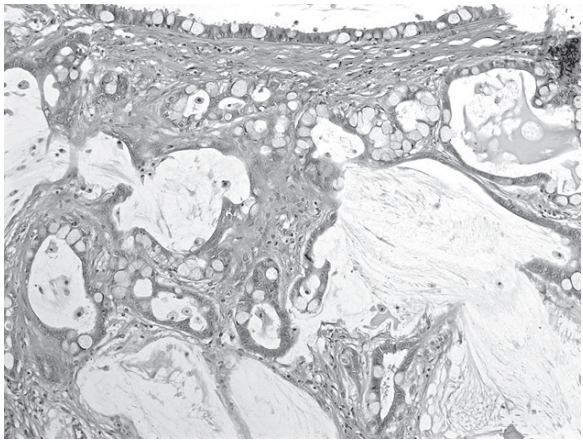

Fig. 5.55 Microscopic appearance of mucinous cystadenocarcinoma

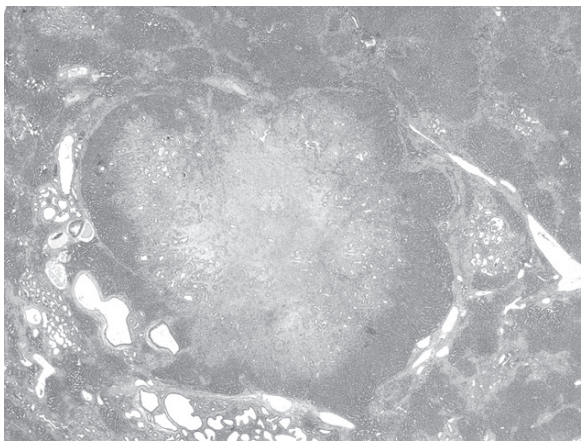

Fig. 5.56 The mass-forming growth pattern of intrahepatic cholangiocarcinoma

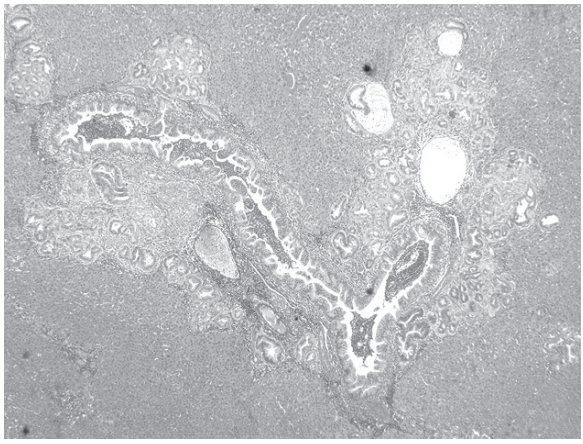

Fig. 5.57 The periductal infiltrating growth pattern of intrahepatic cholangiocarcinoma

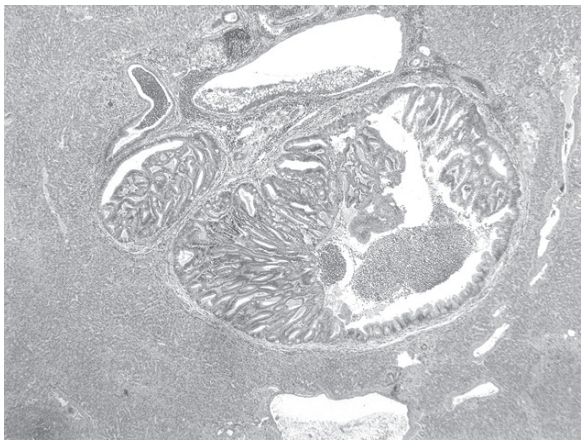

Fig. 5.58 The intraductal growth pattern of intrahepatic cholangiocarcinoma, with papillary growth

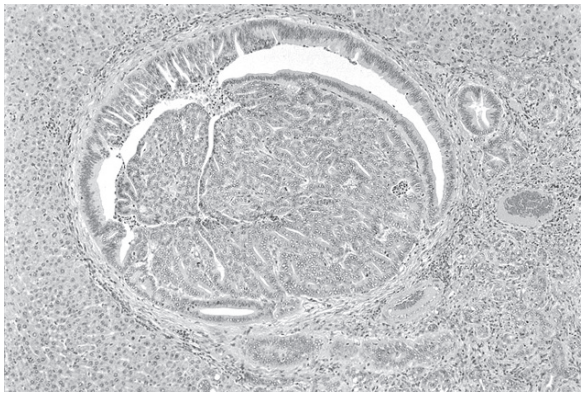

Fig. 5.59 The intraductal growth pattern of intrahepatic cholangiocarcinoma, with polypoid growth

Fig. 5.60 The intraductal growth pattern of intrahepatic cholangiocarcinoma, with superficial spread

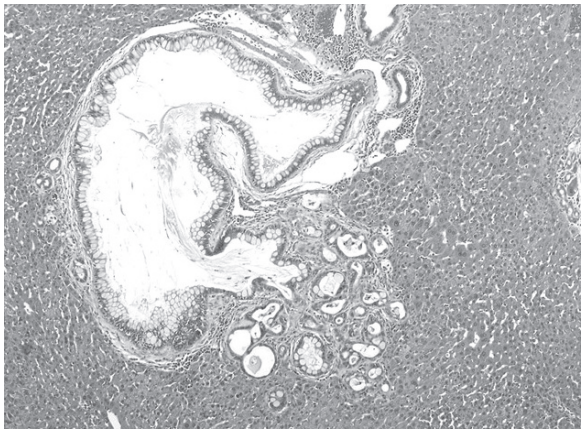

Fig. 5.61 The intraductal growth pattern of intrahepatic cholangiocarcinoma, with periductal glandular involvement

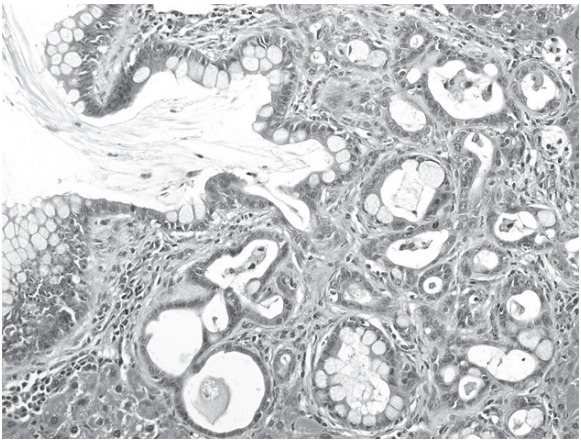

Fig. 5.62 Microscopic appearance of cholangiocarcinoma with periductal glandular involvement

References

1. The Japanese Study Group on Pancreaticobiliary Maljunction (JSPBM), The Committee of JSPBM for Diagnostic Criteria. Diagnostic criteria of pancreaticobiliary maljunction. J Hepatobiliary Pancreat Surg 1994 1:219–221.
2. Matsumoto Y, Fujii H, Itakura J, Matsuda M, Nobukawa B, Suda K. Recent advances in pancreaticobiliary maljunction. J Hepatobiliary Pancreat Surg 2002 9:45–54.
3. Kimura Y, Nishikawa N, Okita K, Furuhata T, Mizuguchi T, Nobuoka T, Nishimori H, Zenbutsu H, Satoh M, Katsuramaki T, Hirata K. Biliary tract malignancy and chronic inflammation from the perspective of pancreaticobiliary maljunction. Oncology 2005 69 Suppl 1:41–45.
4. Tashiro S, Imaizumi T, Ohkawa H, Okada A, Katoh T, Kawaharada Y, Shimada H, Takamatsu H, Miyake H, Todani T; Committee for Registration of the Japanese Study Group on Pancreaticobiliary Maljunction. Pancreaticobiliary maljunction: retrospective and nationwide survey in Japan. J Hepatobiliary Pancreat Surg 2003 10:345–351.
5. Matsumoto Y, Fujii H, Itakura J, Matsuda M, Yang Y, Nobukawa B, Suda K. Pancreaticobiliary maljunction: pathophysiological and clinical aspects and the impact on biliary carcinogenesis. Langenbecks Arch Surg 2003 388:122–131.
6. Tsuchida A, Itoi T, Aoki T, Koyanagi Y. Carcinogenetic process in gallbladder mucosa with pancreaticobiliary maljunction. Oncol Rep 2003 10:1693–1699.
7. Kato T, Hebiguchi T, Matsuda K, Yoshino H. Action of pancreatic juice on the bile duct: pathogenesis of congenital choledochal cyst. J Pediatr Surg 1981 16:146–151.
8. Miyano T, Tokumaru T, Suzuki F, Suda K. Adenoma and stone formation of the biliary tract in puppies that had choledochopancreatic anastomosis. J Pediatr Surg 1989 24:539–542.
9. Qian D, Kinouchi T, Kunitomo K, Kataoka K, Matin MA, Akimoto S, Komi N, Ohnishi Y. Mutagenicity of the bile of dogs with an experimental model of an anomalous arrangement of the pancreaticobiliary duct. Carcinogenesis 1993 14:743–747.
10. Kaneko K, Ando H, Umeda T, Murahashi O, Hiraiwa K, Niimi N, Hossain M, Ito T. A new model for pancreaticobiliary maljunction without bile duct dilatation: demonstration of cell proliferation in the gallbladder epithelium. J Surg Res 1996 60:115–121.
11. Toyosaka A, Nose K, Tomimoto Y. A goat model of dilatation of the common bile duct. Surg Res Comm 1994 16:35–46.
12. Spitz L. Experimental production of cystic dilatation of the common bile duct in neonatal lambs. J Pediatr Surg 1977 12:39–42.

13. Nakamura T, Okada A, Higaki J, Tojo H, Okamoto M. Pancreaticobiliary maljunction-associated pancreatitis: an experimental study on the activation of pancreatic phospholipase A2. World J Surg 1996 20:543–550.
14. Tajima Y, Eto T, Tsunoda T, Tomioka T, Inoue K, Fukahori T, Kanematsu T. Induction of extrahepatic biliary carcinoma by *N*-nitrosobis(2-oxopropyl)amine in hamsters given cholecystoduodenostomy with dissection of the common duct. Jpn J Cancer Res 1994 85:780–788.
15. Flanigan PD. Biliary cysts. Ann Surg 1975 182(5):635–643.
16. Tsuchiya R, Harada N, Ito T, Furukawa M, Yoshihiro I. Malignant tumors in choledochal cysts. Ann Surg 1977 186(1):22–28.
17. Todani T, Watanabe Y, Toki A, Urushihara N. Carcinoma related to choledochal cysts with internal drainage operations. Surg Gynecol Obstet 1987 164:61–64.
18. Tsunoda T, Eto T, Koga M, Tomioka T, Motoshima K, Yamaguchi T, Izawa K, Tsuchiya R. Early carcinoma of the extrahepatic bile duct. Jpn J Surg 1989 19(6):691–698.
19. Kozuka S, Tsubone M, Hachisuka K. Evolution of carcinoma in the extrahepatic bile ducts. Cancer 1984 54(1):65–72.
20. Terada T, Nakanuma Y. Pathological observations of intrahepatic peribiliary glands in 1,000 consecutive autopsy livers. III. Survey of necroinflammation and cystic dilatation. Hepatology 1990 12:1229–1233.
21. Coyle KA, Bradley EL 3rd. Cholangiocarcinoma developing after simple excision of a type II choledochal cyst. South Med J 1992 85(5):540–544.
22. Watanabe Y, Toki A, Todani T. Bile duct cancer developed after cyst excision for choledochal cyst. J Hepatobiliary Pancreat Surg 1999 6(3):207–212.
23. Strong RW. Late bile duct cancer complicating biliary-enteric anastomosis for benign disease. Am J Surg 1999 177(6):472–474.
24. Tsuchida A, Kasuya K, Endo M, Saito H, Inoue K, Nagae I, Aoki T, Koyanagi Y. High risk of bile duct carcinogenesis after primary resection of a congenital biliary dilatation. Oncol Rep 2003 10:1183–1187.
25. Goto N, Yasuda I, Uematsu T, Kanemura N, Takao S, Ando K, Kato T, Osada S, Takao H, Saji S, Shimokawa K, Moriwaki H. Intrahepatic cholangiocarcinoma arising 10 years after the excision of congenital extrahepatic biliary dilation. J Gastroenterol 2001 36:856–862.
26. Tocchi A, Mazzoni G, Liotta G, Lepre L, Cassini D, Miccini M. Late development of bile duct cancer in patients who had biliary-enteric drainage for benign disease: a follow-up study of more than 1,000 patients. Ann Surg 2001 234(2):210–214.
27. Hakamada K, Sasaki M, Endoh M, Itoh T, Morita T, Konn M. Late development of bile duct cancer after sphincteroplasty: a ten- to twenty-two-year follow-up study. Surgery 1997 121(5):488–492.
28. Tanaka M, Takahata S, Konomi H, Matsunaga H, Yokohata K, Takeda T, Utsunomiya N, Ikeda S. Long-term consequence of endoscopic sphincterotomy for bile duct stones. Gastrointest Endosc 1998 48(5):465–469.
29. Kitajima T, Tajima Y, Onizuka S, Matsuzaki S, Matsuo K, Kanematsu T. Linkage of persistent cholangitis after bilioenterostomy with biliary carcinogenesis in hamsters. J Exp Clin Cancer Res 2000 19(4):453–458.

Chapter 6
Biliary Carcinomas Induced in the Hamster

Yoshitsugu Tajima, Shizuo Yamanaka, Sumihiro Matsuzaki, Toshifumi Eto, Kazuya Okada, Hiroshi Shiku, Tsutomu Tomioka, Tsukasa Tsunoda, and Takashi Kanematsu

A. Morphological Characteristics and Pathogenesis of Induced Biliary Carcinoma

6.1 Summary

Syrian hamsters were subjected to cholecystoduodenostomy with dissection of the common duct, and given *N*-nitrosobis(2-oxopropyl)amine (BOP). We then investigated the histomorphological characteristics of the adenomas and early carcinomas induced in the extrahepatic bile duct. The tumors that developed in the extrahepatic bile duct included 10 adenomas and 55 early carcinomas in 56 of the 156 hamsters killed. All the adenomas were polypoid in shape, whereas the early carcinomas, which were restricted to the mucosal layer of the bile duct, showed the following three different growth patterns: protruding in 41 (75%), 27 of which were polypoid and 14, papillary; superficial spreading in 9 (16%); and periductal glandular in 5 (9%). There were no depressed tumors. Carcinomas coexisting with or in adenoma were evident in 12 (22%) tumors, 11 of which were polypoid. Atypical papillary hyperplasia was seen within the tumor mass in 22 early carcinomas (40%) and was particularly prominent in papillary type tumors. These findings support the concept of an adenoma–carcinoma sequence in most polypoid tumors of the extrahepatic bile duct. Atypical papillary hyperplasia might also be premalignant, and these precursor lesions could reflect the growth patterns of tumors, at least in the early stage of tumorigenesis.

6.2 Introduction

It is well known that most early gastric carcinomas have a slightly depressed gross shape, whereas early carcinomas of the colon and rectum are usually polypoid. Based on the clinicopathological features, at least two different concepts of colorectal carcinogenesis have been proposed: the adenoma–carcinoma sequence for early

Y. Tajima et al. (eds.), *Hepatobiliary and Pancreatic Carcinogenesis in the Hamster*,
DOI: 10.1007/978-4-431-87773-8_6, © Springer 2009

polypoid carcinomas [1,2] and the de novo pathway for flat or depressed early carcinomas [3–5]. In conjunction with this, early carcinomas of the extrahepatic bile duct remain a diagnostic challenge despite recent advances in imaging modalities, and little is known about early neoplastic changes in the bile duct.

In this chapter, we describe the histopathological characteristics of adenomas and early carcinomas of the extrahepatic bile duct induced in hamsters, with special reference to their histogenesis and growth patterns. Clarifying the growth form of early carcinomas and the precursor changes in the bile duct may contribute to a better understanding of this highly malignant tumor [6].

6.3 Experimental Protocol

We used two hundred and twenty-one 7-week-old female Syrian golden hamsters (SLC, Inc., Shizuoka, Japan) for these experiments. The average weight of each animal at the beginning of the experiments was 110 g. The animals were housed one per cage with sawdust bedding under standard laboratory conditions in the Laboratory Animal Center for Biochemical Research at Nagasaki University Graduate School of Biomedical Sciences. They were given a standard pellet diet and allowed water *ad libitum* during the experiment. All experiments were performed following the Guidelines for Animal Experimentation of Nagasaki University Graduate School of Biomedical Sciences.

The extrahepatic bile duct tumors were induced in the hamsters according to the experimental protocol described in Chapter 5. Briefly, the hamsters were subjected to cholecystoduodenostomy with dissection of the extrahepatic bile duct at the distal end of the common duct. The procedure was tolerated by 173 of the animals: the other 48 died of liver abscess or peritonitis, or both, a few days after surgery. These 173 hamsters were given weekly subcutaneous injections of *N*-nitrosobis(2-oxopropyl) amine (BOP) at a dose of 10 mg/kg body weight for 9 consecutive weeks. BOP administration was started 4 weeks after surgery. Five hamsters died of BOP toxicity and 12 died of carcinomas of the liver or pancreas before being killed. Finally, 156 hamsters were successively killed for pathological examination at 2-week intervals from 12 to 20 weeks after the initial administration of BOP, with 24, 26, 33, 38, and 35 hamsters killed at 12, 14, 16, 18, and 20 weeks, respectively. The extrahepatic bile duct was removed *en bloc* with the liver, gallbladder, pancreas and part of the duodenum, and all organs were fixed in 10% buffered formalin. The extrahepatic bile duct was cut into three blocks and embedded so that each section contained the hepatic ducts, common bile duct, and common duct. All sections were then cut and stained with hematoxylin and eosin (H&E).

Lesions induced in the extrahepatic bile duct were classified in accordance with the WHO classification of tumors in hamsters [7,8]. In general, adenoma and carcinoma were defined as lesions that showed signs of expansive growth. Unlike adenomas, carcinomas showed signs of malignancy, such as nuclear atypia, mitotic activity, disruption of epithelial cell polarity, and invasion. Hyperplastic epithelium

with marked papillary proliferation, pseudostratification, and hyperchromatism of the nuclei was considered to indicate atypical hyperplasia.

We used proliferating cell nuclear antigen (PCNA) to evaluate cell kinetic activity of the normal biliary epithelium, hyperplastic epithelium with or without atypia, adenomas, and carcinomas. Tissue sections were cut at 4 μm thickness, mounted on glass slides coated with 5-aminoprophyltriethoxy saline, and dewaxed in xylene. The sections were microwave heated for 5 min in phosphate-buffered saline (PBS) at 500 W. After blocking endogenous peroxidase, the sections were incubated with mouse monoclonal antibodies against PCNA (clone-PC 10; DAKO, Kyoto, Japan) at a dilution of 1:100. The cell nuclei were counterstained with hematoxylin. The proportion of labeled nuclei (labeling index; LI) was calculated by counting the labeled nuclei in >1,000 epithelial cells in a lesion. The Mann–Whitney *U*-test was used for statistical analysis of the PCNA-LI and differences of $p < 0.05$ were considered significant.

6.4 Incidence, Location and Histologic Findings of Induced Tumors

The incidence and number of tumors induced in the extrahepatic bile duct increased, depending on the observation period after the administration of BOP (Table 6.1). A total of 69 tumor nodules arose from the extrahepatic bile duct in 56 hamsters. The tumor nodules were located mainly in the hepatic ducts and the common bile duct. Of the 69 tumors, 59 were diagnosed histologically as carcinoma and 10, as adenoma. Papillary carcinoma was found in 36 tumors and tubular carcinoma in 23. Furthermore, 55 of the 59 carcinomas were found, to a limited extent, within the mucosal layer of the bile duct. Four of the adenomas were of the papillary type and six, of the tubular type. Pancreatic carcinomas developed in 118 (76%) hamsters. The majority of these tumors were ductular adenocarcinoma. Gallbladder carcinomas and intrahepatic cholangiocarcinomas developed in 114 (73%) and 107 (69%) hamsters, respectively. The growth pattern of the gallbladder carcinomas was papillary, and they were diagnosed as papillary adenocarcinoma. Half of the gallbladder carcinomas invaded the liver.

6.5 Gross Shape of Adenoma and Early Carcinoma of the Bile Duct

All the adenomas were polypoid and protruded into the lumen of the bile duct (Figures 6.1 and 6.2). The 55 early bile duct carcinomas were divided into three types according to the gross shape of the tumors (Table 6.2).

1. Protruding, divided into two subtypes: pedunculated or sessile polypoid type, seen in 27 lesions (Figure 6.3); and papillary type, growing into the lumen of the bile duct with marked papillary projections, seen in 14 lesions (Figures 6.4 and 6.5).

Table 6.1 Incidence and pathological findings of tumors induced in the extrahepatic bile duct by *N*-nitrosobis(2-oxopropyl)amine in hamsters

Experimental[a] periods (weeks)	No. of hamsters[b] examined	No. (%) of hamsters with EHBD tumor	No. of EHBD tumors	Tumor locatio			Histology		Major histology type			
									Carcinoma		Adenoma	
				HD	CBD	C	Carcinoma	Adenom	Pap	Tub	Pap	Tub
12	24	5(21)	6	4	1	1	5	1	3	2	0	1
14	26	7(27)	8	4	2	2	7	1	5	2	1	0
16	33	11(33)	13	6	5	2	11	2	7	4	1	1
18	38	17(45)	22	12	8	2	19	3	11	8	1	2
20	35	16(46)	20	11	7	2	17	3	10	7	1	2
Total	156	56(36)	69	37	23	9	59	10	36	23	4	6

EHBD, extrahepatic bile duct; HD, hepatic ducts; CBD, common bile duct; CD, common duct; Pap, papillary; Tub, tubular.

[a]Periods from the start of *N*-nitrosobis(2-oxopropyl)amine treatment to killing of the hamsters.

[b]All the hamsters were subjected to cholecystoduodenostomy with dissection of the distal end of the common duct. (modified from [6], with permission)

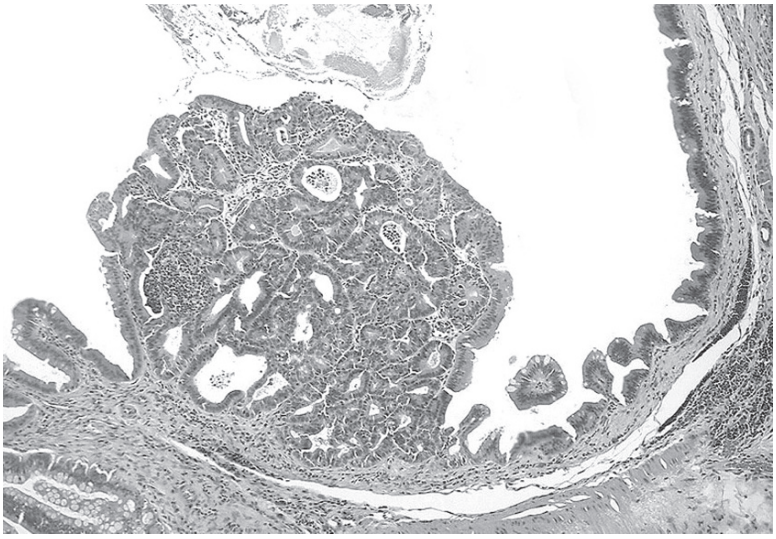

Fig. 6.1 A polypoid type adenoma in the common bile duct, with simple glandular proliferation. The individual glands are separated from each other by a broad stroma (H&E, ×60) (modified from [6], with permission)

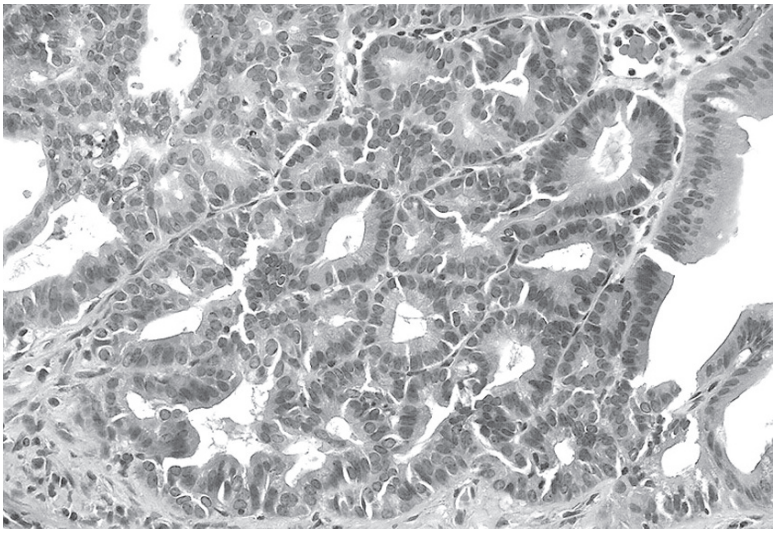

Fig. 6.2 High magnification of the polypoid type adenoma in Figure 6.1 (H&E, ×200)

2. Superficial, spreading along the bile duct wall with slight elevation of the cancerous mucosa, seen in nine lesions (Figures 6.6 and 6.7).
3. Periductal glandular, developing from the periductal glands of the bile duct with expansive growth within the bile duct wall, seen in five lesions (Figures 6.8 and 6.9).

Table 6.2 Gross shape of early carcinomas of the extrahepatic bile duct and coexisting non-cancerous component within the tumor mass induced in hamsters (modified from [6], with permission)

Gross shape of the tumors	Major histologic type			No. of coexisting non-cancerous components within the tumor mass	
	No. of lesions	Papillary	Tubular	Adenoma	Hyperplasia
Protruding	**41**	**23**	**18**	**11**	**18**
Polypoid	27	9	18	11	6
Papillary	14	14	0	0	12
Superficial spreading	**9**	**9**	**0**	**0**	**0**
Periductal glandular	**5**	**1**	**4**	**1**	**4**
Total	**55**	**33**	**22**	**12**	**22**

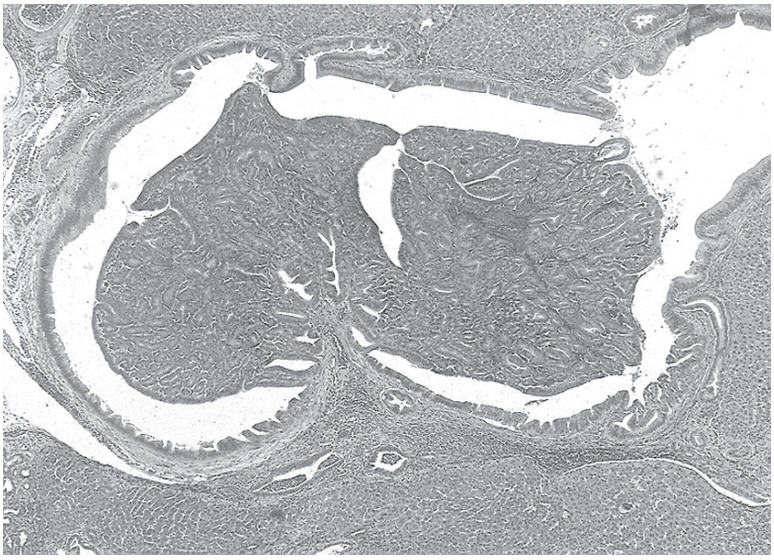

Fig. 6.3 A polypoid type carcinoma arising in the hepatic duct. The tumor protrudes into the lumen of the bile duct with a stalk (H&E, ×20) ([6], with permission)

The early bile duct carcinomas were thus classified predominantly as the protruding type, according to their gross shape. There were no ulcerated or depressed tumors.

6.6 Coexistence of Non-malignant Lesions

The coexistence of non-cancerous components within the tumor mass was also investigated in the 55 early bile duct carcinomas (Table 6.2). Adenomatous components were found in 11 (41%) of the 27 polypoid type carcinomas (Figures 6.10–

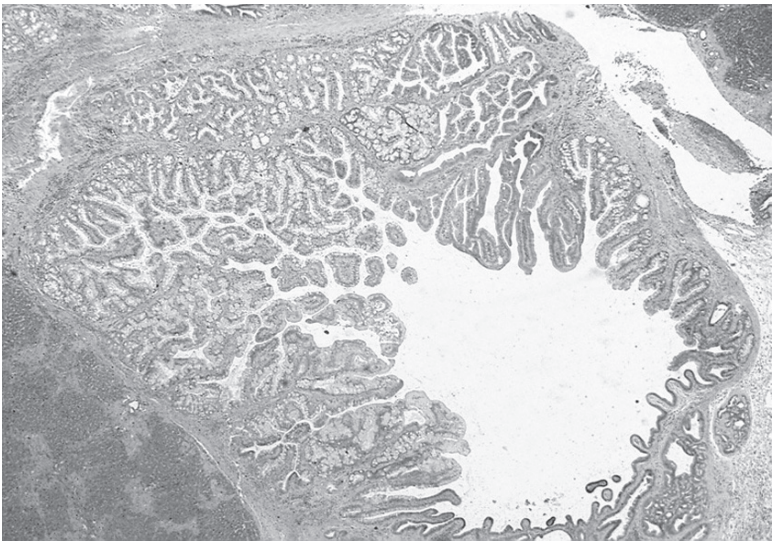

Fig. 6.4 A papillary type carcinoma in the common bile duct. The tumor is growing into the lumen of the bile duct with marked papillary projections (H&E, ×10) ([6], with permission)

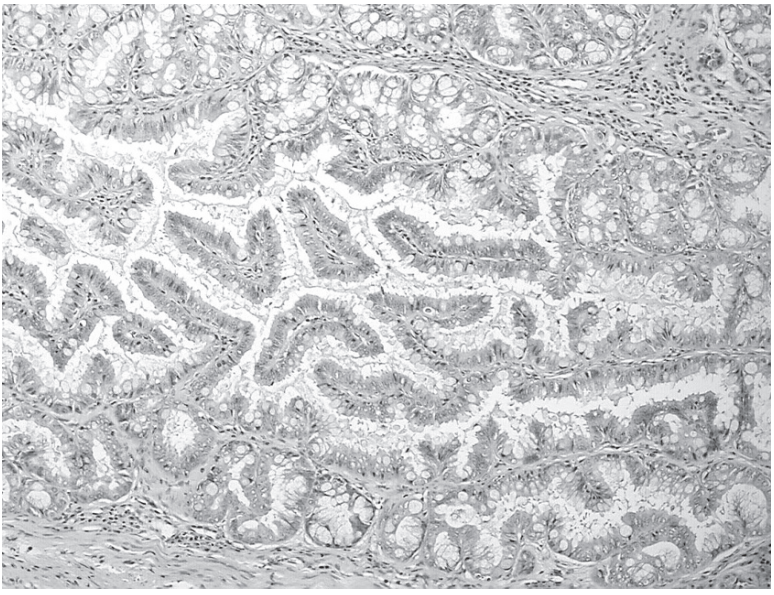

Fig. 6.5 High magnification of the papillary type carcinoma in Figure 6.4 (H&E, ×60)

6.12), including two carcinomas within adenoma (Figures 6.13–6.15). Papillary hyperplasia with degrees of atypia was also observed in six polypoid carcinomas. There was no evidence of adenomatous or hyperplastic changes in the remaining

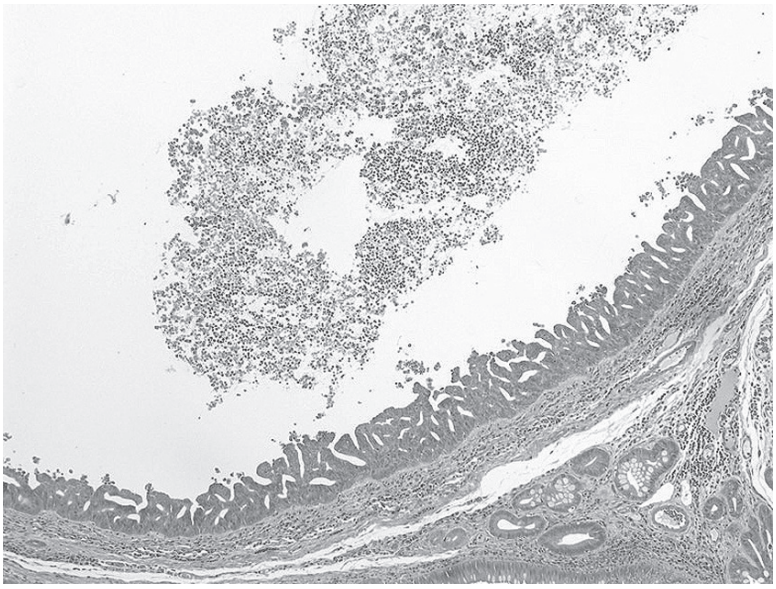

Fig. 6.6 A superficial spreading type carcinoma in the common bile duct. The cancer cells spread superficially along the mucosal layer of the bile duct. The cancer cell proliferation lacks a connective tissue stalk (H&E, ×40)

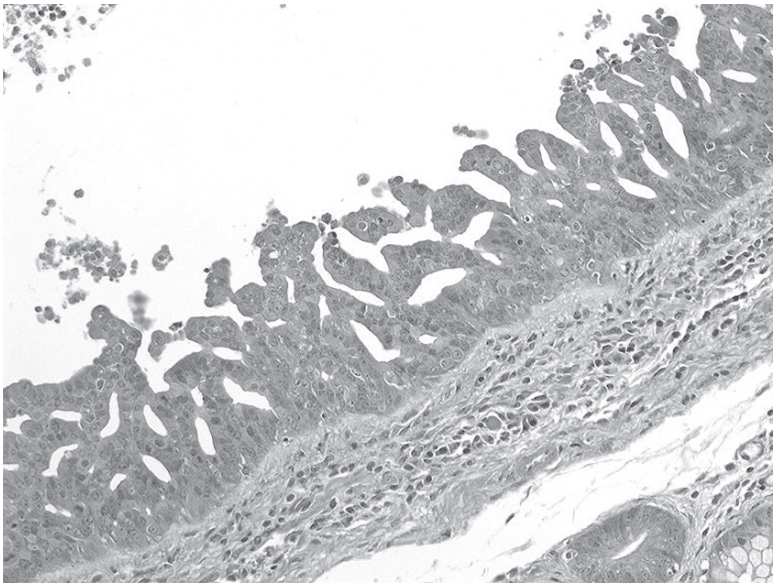

Fig. 6.7 High magnification of the superficial spreading type carcinoma in Figure 6.6 (H&E, ×200)

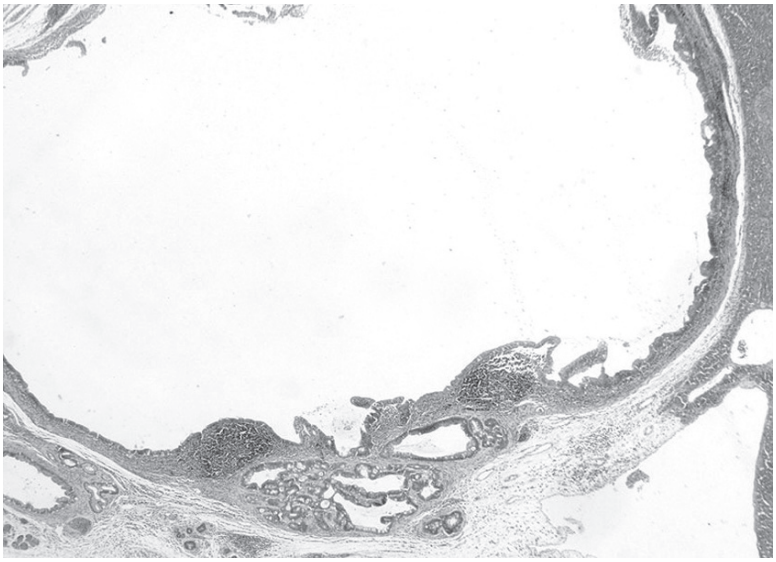

Fig. 6.8 A periductal glandular type carcinoma in the common bile duct. The tumor is growing expansively within the bile duct wall (H&E, ×20)

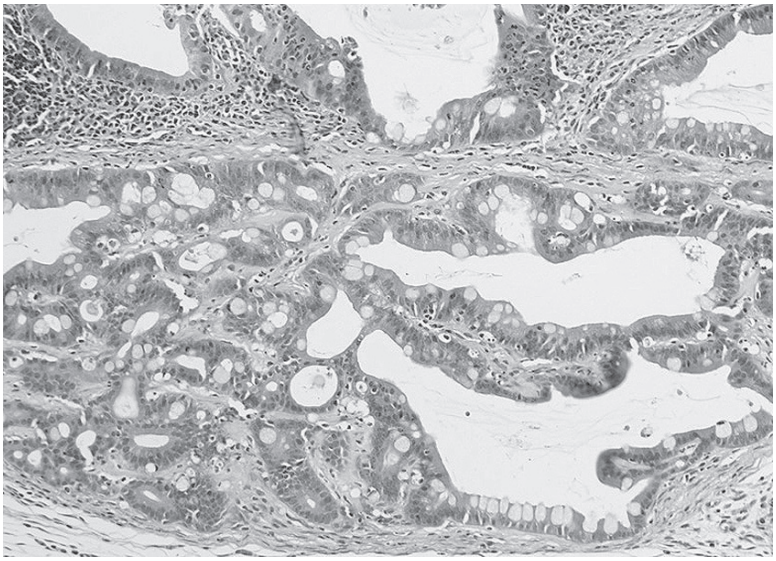

Fig. 6.9 High magnification of the periductal glandular type carcinoma in Figure 6.8 (H&E, ×120)

polypoid carcinomas. Hyperplastic epithelium with marked papillary proliferation, pseudostratification, and hyperchromatism of the nuclei were observed within the tumor mass in 12 (86%) of the 14 papillary type carcinomas (Figures 6.16–6.18).

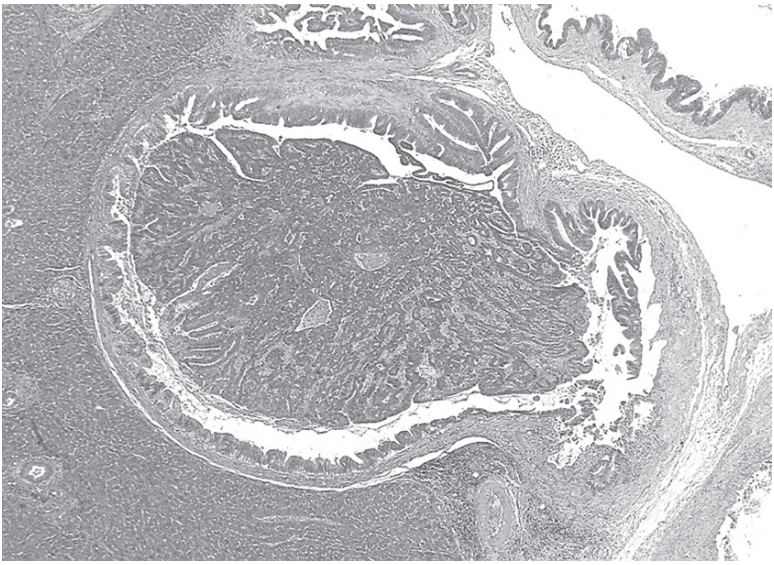

Fig. 6.10 A polypoid type carcinoma with adenomatous residue in the hepatic duct (H&E, ×20)

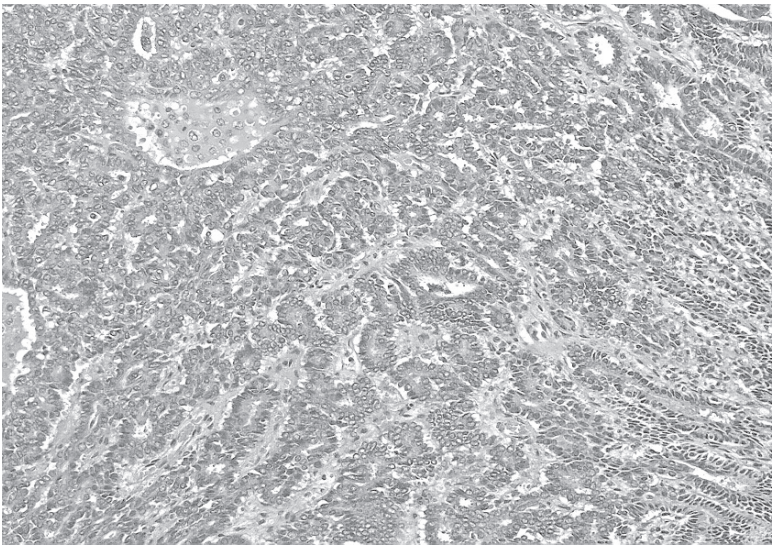

Fig. 6.11 High magnification of the carcinoma in Figure 6.10, showing well differentiated tubular adenocarcinoma (H&E, ×100)

No adenomatous component or hyperplastic epithelium was seen within the tumor mass in the superficial spreading type carcinomas, although atypical hyperplasia with a serrate proliferation of the epithelium was observed in the border zone between the cancerous and non-cancerous mucosa. An adenomatous component

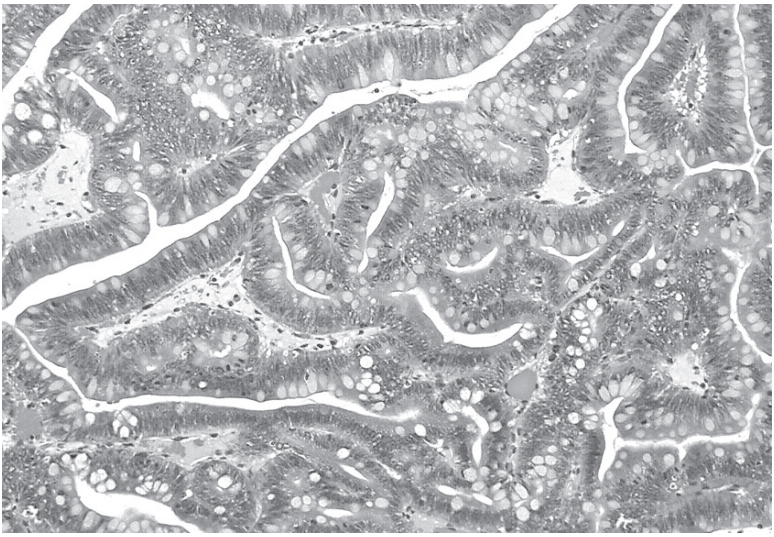

Fig. 6.12 High magnification of the adenomatous component at the tip of the tumor in Figure 6.10. Note the simple glandular proliferation with a broad stroma. The nuclei are arranged regularly, close to the basement membrane with abundant goblet cell metaplasia (H&E, ×120)

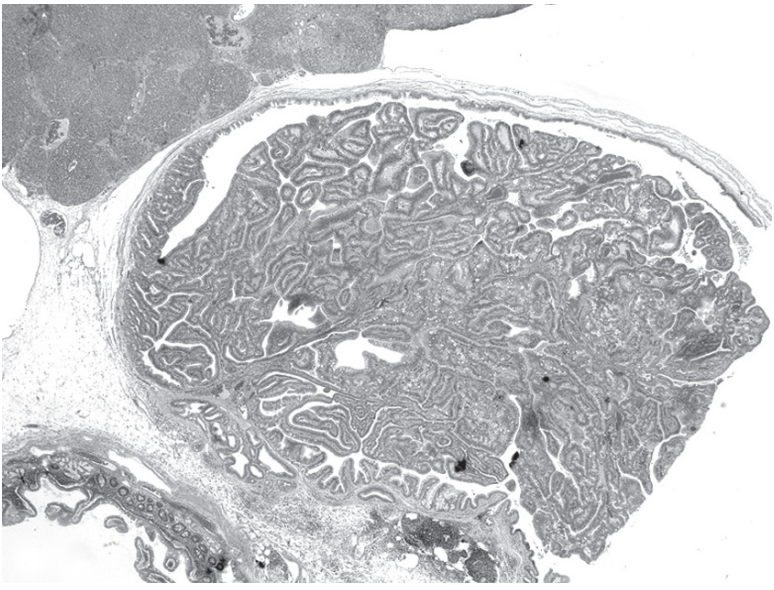

Fig. 6.13 Carcinoma in adenoma in the common duct (H&E, ×10)

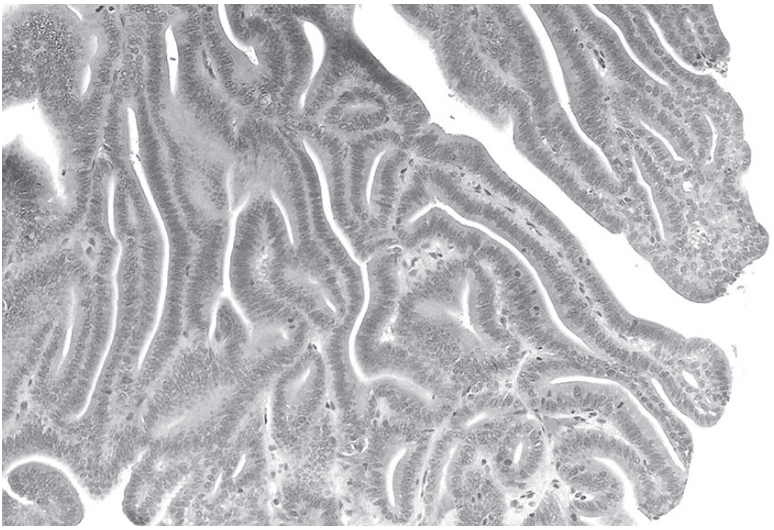

Fig. 6.14 High magnification of the adenoma in Figure 6.13 (H&E, ×120)

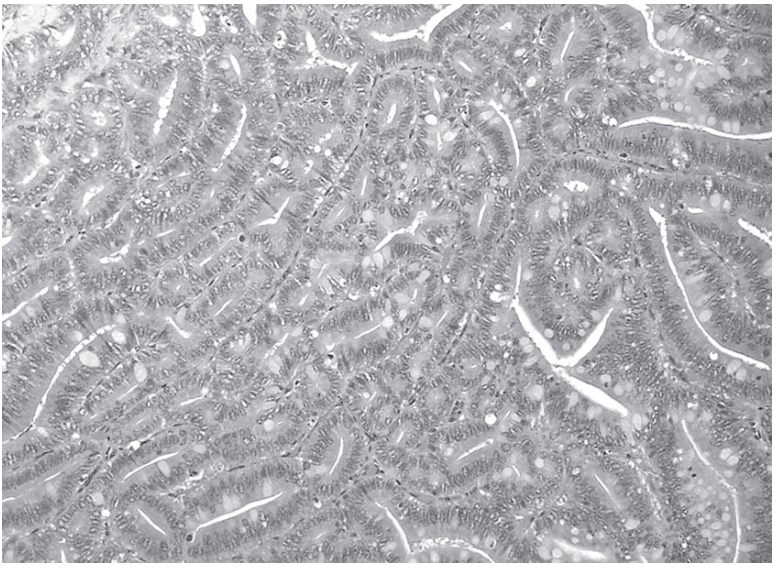

Fig. 6.15 High magnification of the carcinomatous foci in the tumor in Figure 6.13, showing mild cellular pleomorphism and nuclear hyperchromasia with back-to-back glandular structures (H&E, ×120) (modified from [6], with permission)

was found in one of the periductal glandular type carcinomas and hyperplastic epithelium was found in four. In summary, adenomatous components and atypical papillary hyperplasia were found in 12 (22%) and 22 (40%), respectively, of the 55 early carcinomas of the extrahepatic bile duct.

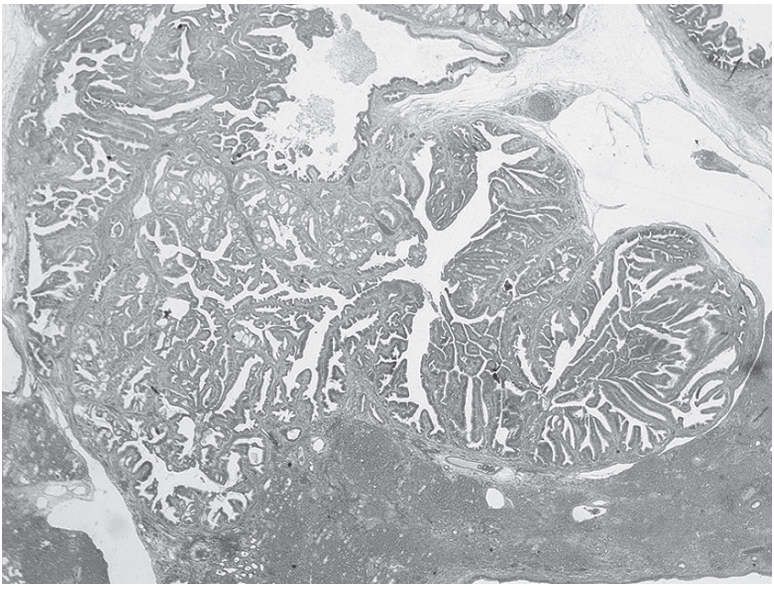

Fig. 6.16 A papillary type carcinoma with hyperplastic epithelium in a tumor in the common duct (H&E, ×10)

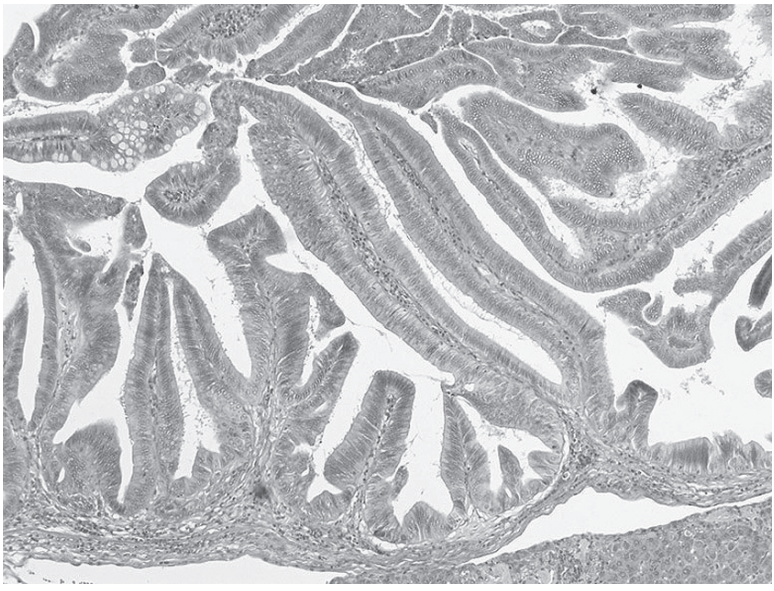

Fig. 6.17 High magnification of the papillary hyperplasia in the tumor in Figure 6.16. The nuclei are close to the basement membrane (H&E, ×100)

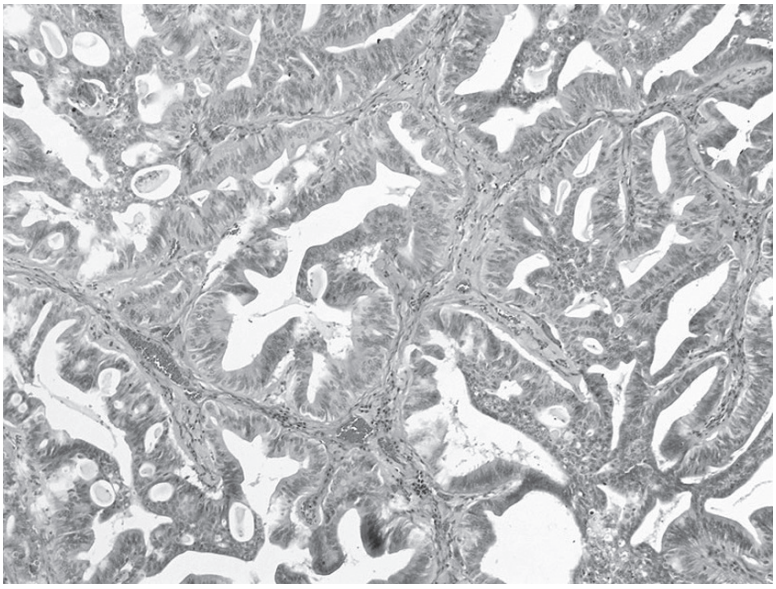

Fig. 6.18 High magnification of the papillary carcinoma (H&E, ×100)

Table 6.3 Cell kinetic activity of lesions induced in the extrahepatic bile duct by *N*-nitrosobis(2-oxopropyl)amine in hamsters

Lesions	No. of lesions examined	Average of PCNA-LI (%)[a]
Normal biliary epithelium	27	6.7 ± 2.4
Hyperplasia without atypia	51	19.9 ± 6.9[*]
Hyperplasia with atypia	82	32.9 ± 12.6[*,**]
Adenoma	10	42.9 ± 5.7[*,**,***]
Carcinoma	59	50.1 ± 11.4[*,**,***,****]

PCNA-LI, proliferating cell nuclear antigen labeling index.

[*]Significantly different from normal biliary epithelium ($P < 0.01$).

[**]Significantly different from hyperplasia without atypia ($P < 0.01$).

[***]Significantly different from hyperplasia with atypia ($P < 0.01$).

[****]Significantly different from adenoma ($P < 0.05$).

[a]Mean ± SD. (modified from [6], with permission)

6.7 Cell Kinetic Studies

Cell kinetic activity of the biliary epithelium during biliary carcinogenesis was investigated in 56 hamsters with extrahepatic bile duct tumors, and the results are summarized in Table 6.3. Carcinomas and adenomas had extremely high proliferation activity. Hyperplastic epithelium with atypia also possessed high potential for proliferation.

6.8 Comments

The adenoma–carcinoma sequence is well recognized in tumors throughout the gastrointestinal tract, especially in the ampulla of Vater [9–10], small intestine [11], colon, and rectum. In the biliary system, the adenoma–carcinoma sequence is found most often in the gallbladder [12,13]. Although several investigators have reported cancerous foci in adenoma in the intra- and extrahepatic bile duct [14–16], the histogenesis of these bile duct carcinomas is still a subject of debate. In the present study, adenomatous residue, including carcinoma in adenoma, was found in 12 (22%) of 55 early carcinomas of the extrahepatic bile duct. The coexistence of an adenomatous component within a tumor mass was particularly prominent in the polypoid type carcinomas, seen in 11 (41%) of 27 cases. The high percentage of adenomatous residue in the tumor mass found in this study justifies the application of the adenoma–carcinoma sequence to some tumors of the extrahepatic bile duct, particularly polypoid type carcinomas.

Yamanaka et al. [17] and Majima et al. [18] investigated genetic changes in the biliary epithelium during biliary carcinogenesis using our experimental hamster model, and detected frequent K-*ras* point mutations in the hyperplastic mucosal epithelium of the bile duct and in induced biliary carcinomas. In the present study, cell kinetic analysis revealed that hyperplastic epithelium with atypia possessed a high potential for proliferation. The fact that papillary hyperplastic lesions with atypia were found within the tumor mass in about 40% of the early bile duct carcinomas in hamsters suggests that these lesions might be premalignant. This speculation is in line with recent molecular biological findings of gastroenterological carcinogenesis [19–26].

Morphologically, most of the early carcinomas of the extrahepatic bile duct induced in hamsters in this study exhibited either a polypoid or papillary growth protruding into the lumen of the bile duct. There were no ulcerated or depressed carcinomas. All the adenomas were polypoid in gross shape. In humans, early extrahepatic bile duct carcinoma confined within the mucosal or fibromucosal layer is either polypoid or papillary in shape [27–29], whereas advanced carcinoma is generally ulcerated [28]. The carcinomas examined in the present study were restricted to within the mucosal layer of the bile duct without invasion into the deeper layers. These findings suggest that early carcinomas of the extrahepatic bile duct tend to exhibit a protrusive growth. The possible precursors, such as adenoma and papillary hyperplastic lesions, may reflect the growth patterns of these tumors, at least in the early stage of tumorigenesis.

Another interesting finding of this study was the presence of periductal glandular type carcinoma in the extrahepatic bile duct. The presence of periductal glands around the intra- and extrahepatic bile ducts is well documented [30,31]. Terada and Nakamura [32] suggested that the intrahepatic periductal glands are a possible source of intrahepatic bile duct carcinoma, and our findings indicate that the periductal glands may be one of the original sites of extrahepatic bile duct carcinoma.

In summary, we confirmed morphologically, the adenoma–carcinoma sequence in tumors of the extrahepatic bile duct, particularly in polypoid type carcinomas, in hamsters. Papillary hyperplastic lesions with atypia might also be involved in the histogenesis of bile duct carcinoma. In reflection, it may be assumed that the bile duct epithelium possesses a similar biological potential for carcinogenesis to that of the colon and rectum, rather than to that of the stomach.

B. Genetic Alterations During Biliary Carcinogenesis

6.9 Summary

Inbred female hamsters were given a subcutaneous injection of *N*-nitrosobis (2-oxopropyl)amine (BOP) after dissection of the extrahepatic bile duct at the distal end of the common duct and cholecystoduodenostomy (CDDB) or simple laparotomy (SL). Neoplastic lesions arising from the intrahepatic bile duct were examined histologically, and K-*ras* mutations were investigated. Mutations of K-*ras* codon 12 were evident in 12% of the tubular hyperplasias, 19% of the tubular adenocarcinomas, 15% of the papillary hyperplasias, and 36% of the papillary adenocarcinomas. K-*ras* mutations were more frequent in papillary adenocarcinomas arising from a large bile duct than in tubular adenocarcinomas arising from ductule or ductular proliferation. K-*ras* mutations were present even in hyperplasia, but they increased in the presence of carcinoma. Genetic changes in carcinoma of the intrahepatic bile duct varied according to the sites of the duct and the histological type. Some of the hyperplastic lesions in the intrahepatic bile duct revealed K-*ras* gene mutations. This suggests that K-*ras* gene mutation is an early event in the carcinogenic process. In carcinoma of the intrahepatic bile duct, lesions arising from a large bile duct in the hepatic hilum tended to exhibit a higher frequency of K-*ras* gene mutation than tubular lesions arising from a ductule or ductal proliferation.

6.10 Introduction

Recent analyses of the genes involved in malignant tumors have increased our understanding of gene-related carcinogenesis [33–37]. The activation of a promotor gene and the loss of a suppressor gene, such as *p53*, were observed early during the development of adenocarcinoma from an adenoma [38,39]. In human bile duct carcinoma, Levi et al. [40] reported frequent Kirsten-*ras* (K-*ras*) mutations with a sensitive polymerase chain reaction (PCR), whereas other investigators reported a low frequency of these mutations [41–44]. Thus, the relationship between K-*ras* mutation and carcinogenesis of the intrahepatic bile duct remains unclear.

To clarify the gene-related carcinogenesis of the intrahepatic bile duct carcinoma, we investigated mutation in the K-*ras* gene in various early hyperplastic and neoplastic lesions induced in hamsters, according to the original sites of the lesions. The experimental protocol and the results obtained [17] are herein described.

6.11 Experimental Protocol

Under sodium pentobarbital anesthesia, 50 mg/kg body weight, hamsters were subjected to cholecystoduodenostomy with dissection of the extrahepatic bile duct at the distal end of the common duct (CDDB). Control hamsters were subjected to simple laparotomy (SL). The 61 hamsters that tolerated the procedure were given subcutaneous injections of BOP 10 mg/kg, once a week, starting 4 weeks after surgery, and continuing for 9 weeks. Then, 20, 21, and 20 hamsters were killed 12 (CDDB-1), 16 (CDDB-2), and 20 (CDDB-3) weeks, respectively, after the BOP injections were started. The 63 control hamsters were given the same BOP treatment. Then 20, 22, and 21 hamsters were killed after the same observation periods (SL-1, SL-2, and SL-3).

The liver was immediately removed, fixed in 10% neutral formalin, then cut into five blocks and embedded in paraffin. Sections were stained with hematoxylin-eosin and examined histologically. The intrahepatic bile duct carcinomas were classified into four subtypes according to the original sites, as follows [45]: duct-infiltrating type, developing from ductal proliferation in medium to large bile ducts; mass-forming type, developing from ductules as a scirrhous lesion; intraductal growth type, developing as a papillary elevated lesion in the biliary lumen in the large bile duct near the hepatic hilum; and periductal type, developing from the periductal gland in the biliary wall (see Chapter 5).

Slides were soaked in xylene and ethanol to remove the paraffin from the surface of the samples. Histologically identified neoplastic lesions were marked and these areas were scraped from the slides. The fragments were incubated in buffer (50 mM Tris, 1 mM-EDTA, 0.1% sodium dodecyl sulfate (SDS), 200 mg/ml proteinase K) for 12–24 h at 37 °C and phenol-chloroform was used to purify the genomic DNA.

Mutations in exon 1 of the hamster K-*ras* gene were investigated using the following primers specific for the codon 12 and 13 regions of the human K-*ras* gene [34,44]: sense primer 58-GGCCTGCTGAAAATGACTGA-38 and antisense primer 58-GTCCTGCACCAGTAATATGC-38. These primers encompassed 162 bp and were synthesized by a DNA synthesizer (model 380B; Applied Biosystems, Foster City, California). The 58-end of these primers was labeled with [g-32P]ATP and T4 polynucleotide kinase. Thirty-five cycles of polymerase chain reaction (PCR) were programmed as 1 min at 94 °C, 55 °C, and 72 °C, respectively. We mixed 2 ml of PCR product with 5 ml of 0.1% SDS containing 10 mM EDTA, 7 ml 95% formamide, 20 mM EDTA, and 0.05% bromophenol blue. This mixture was heated at 90 °C for 3 min, then applied to a 6% polyacrylamide

gel containing 5% glycerol, and electrophoresed at 1,800 V for 90–120 min under a cooling fan in a room at 4 °C.

Sequencing primers were end labeled with [g-32P]ATP and T4 polynucleotide kinase. The DNA fragment obtained with PCR was extracted from the band in the polyacrylamide gel and directly sequenced using a DNA cycle sequencing kit (Takara, Kyoto, Japan). The amplificated reaction mixture was resolved by electrophoresis in 8% acrylamide sequence gel containing 7 mol/l urea.

6.12 Genetic Mutations

The intrahepatic bile ducts of hamsters in the CDDB groups showed marked ductal proliferation with cholangitis (Figure 6.19a) and a high degree of carcinoma development. Cancer was confirmed in 15 (75%) of the 20 animals killed 12 weeks after the BOP injections were started (CDDB-1), 18 (86%) of the 21 animals killed 16 weeks after (CDDB-2) and 16 (80%) of the 20 animals killed 20 weeks after (CDDB-3) (Table 6.4). There was only one hamster with no cancer or hyperplasia when killed 12 weeks after the BOP injection was started. The histological type of cancer was tubular adenocarcinoma (Figure 6.19c) in 129 (77%) of 167 lesions, and papillary adenocarcinoma in 20 (12%) lesions (Figures 6.19f, g). The papillary adenocarcinomas all seemed to be of the intraductal growth type. The tubular adenocarcinomas consisted of scirrhous lesions from the peripheral bile duct (Figure 6.19b), as well as lesions advancing from ductal proliferation in the large to medium bile ducts. However, differentiation was difficult in advanced cancers and only three early scirrhous lesions were identified among all the tubular adenocarcinomas. In addition, we found four cystadenocarcinomas and two mucinous carcinomas (Figure 6.19h). The incidence of carcinoma and the average number of carcinomas per animal were significantly higher in the CDDB groups than in the corresponding SL groups (Table 6.4). In the CDDB groups, hyperplastic lesions were observed in all the hamsters, except for one of those killed 12 weeks after the BOP injection was started (Table 6.5). The histological type was tubular hyperplasia in 267 (67%) of the 401 hyperplastic lesions and papillary hyperplasia in 134 (33%) lesions (Figures 6.19d, e). The incidence of hyperplasia and the average number of hyperplasia lesions per animal were significantly higher in the CDDB-1 group than in the SL-1 group, although hyperplastic lesions were also common in the SL-2 and SL-3 groups.

K-*ras* exon 1 in the neoplastic lesions arising from the intrahepatic bile duct was analyzed by PCR-SSCP, using the normal bile duct from hamsters not treated with BOP, as a negative control. An abnormal band or shift was observed in 5 (19%) of 26 tubular adenocarcinomas and 5 (36%) of 14 papillary adenocarcinomas (Figure 6.20a). An abnormal band or shift was also observed in 3 (12%) of 26 tubular hyperplasias, the early lesion of tubular adenocarcinoma (Figure 6.20b), and in 2 (16%) of 13 papillary hyperplasias, the early lesion of papillary adenocarcinoma. Although the number of lesions was small, no mutation was

Table 6.4 Intrahepatic bile duct carcinomas induced in hamsters after cholecystoduodenostomy with dissection of the distal end of the common duct or simple laparotomy

Group	No. of hamsters analyzed	No. (%) of hamsters with carcinoma	Average no. of carcinomas per animal	Total no. of carcinomas	Histology			
					Tub	Pap	Peri	Others
CDDB-1	20	15(75)*	2.00*	40	31	5	1	3
CDDB-2	21	18(86)**	2.24**	47	33	7	1	6
CDDB-3	20	16(80)***	4.00****	80	65	8	1	6
SL-1	20	2(10)	0.10	2	2	0	0	0
SL-2	22	4(18)	0.36	8	8	0	0	0
SL-3	21	9(43)	1.33	28	26	2	0	0

CDDB, cholecystoduodenostomy with dissection of the extrahepatic bile duct on the distal end of the common duct; SL, simple laparotomy; Tub, tubular adenocarcinoma; Pap, papillary adenocarcinoma; Peri, adenocarcinoma arising from periductal gland.

*Significantly different from SL-1 ($P < 0.01$).

**Significantly different from SL-2 ($P < 0.01$).

***Significantly different from SL-3 ($P < 0.05$).

****Significantly different from SL-3 ($P < 0.01$). (modified from [17], with permission)

Table 6.5 Hyperplastic lesions in the intrahepatic bile duct of hamsters after cholecystoduodenostomy with dissection of the distal end of the common duct or simple laparotomy

Group	No. of hamsters analyzed	No. (%) of hamsters with hyperplasia	Average no. of hyperplasias per animal	Total no. of hyperplasias	Histology	
					Tub	Pap
CDDB-1	20	19(95)*	6.05**	121	77	44
CDDB-2	21	21(100)	6.76	142	93	49
CDDB-3	20	20(100)	6.90	138	97	41
SL-1	20	10(50)	2.10	42	28	14
SL-2	22	18(82)	4.09	90	66	24
SL-3	21	21(100)	6.00	126	81	45

CDDB, cholecystoduodenostomy with dissection of the extrahepatic bile duct on the distal end of the common duct; SL, simple laparotomy; Tub, tubular hyperplasia; Pap, papillary hyperplasia.

*Significantly different from SL-1 ($P < 0.05$).

**Significantly different from SL-2 ($P < 0.01$). (modified from [17], with permission)

detected in cystadenocarcinoma or tubular adenocarcinoma arising from the periductal gland (Table 6.6). There were too few small scirrhous lesions arising from peripheral ducts for a valid analysis of K-*ras* gene mutations. The direct sequencing method led to the detection of a base substitution from GGT (Gly) to TGT (Val) in codon 12 in one tubular adenocarcinoma (Figure 6.21, panel 2) and one papillary adenocarcinoma lesion. In the other lesions, the base substitution was from GGT (Gly) to GAT (Asp) in codon 12 (Figure 6.21, panels 3 and 4). Mutation in codon 13 was not observed in any lesion. Histologically, normal parts

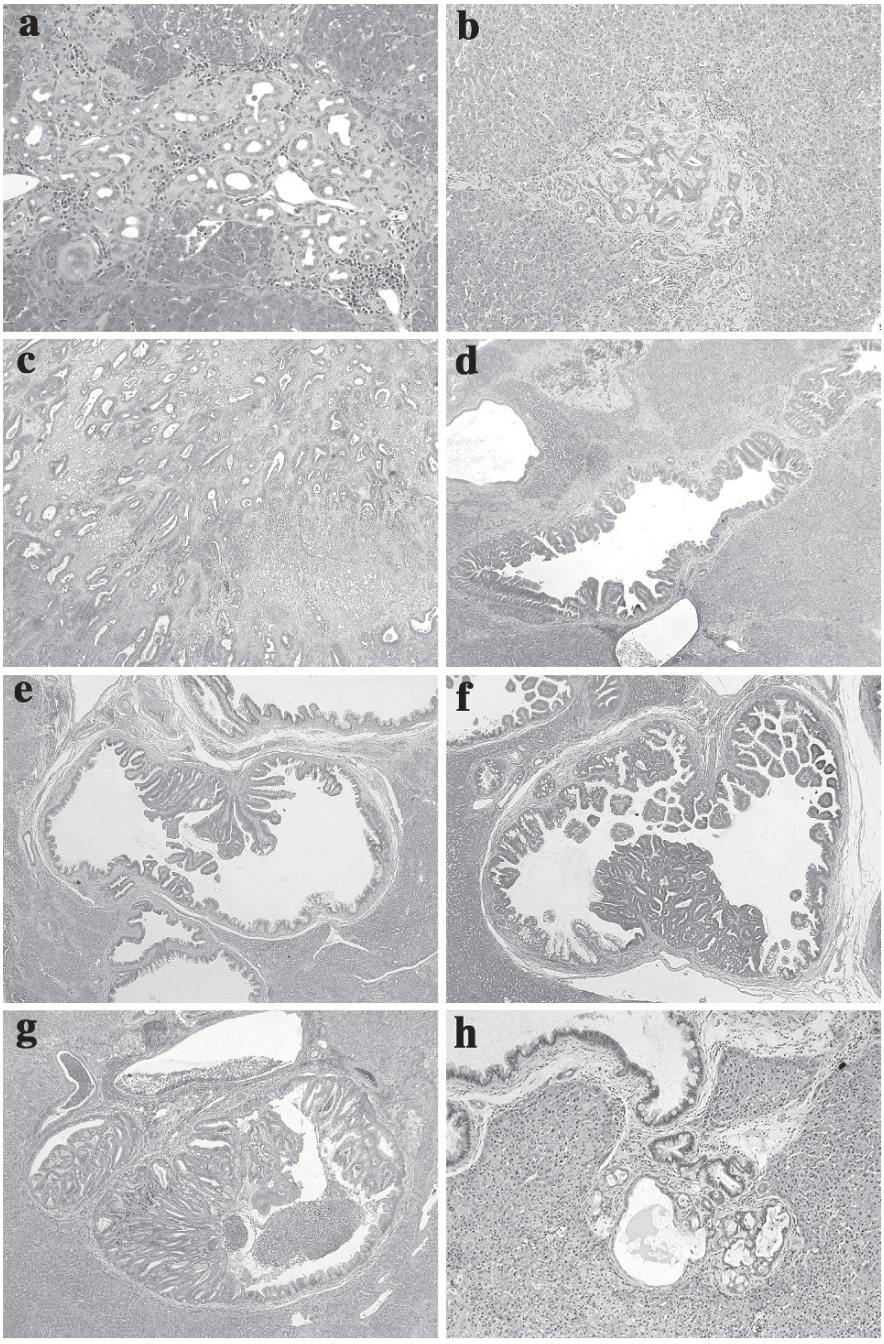

Fig. 6.19 Photomicrographs of intrahepatic bile duct lesions in hamsters. (a) Ductal proliferation with cholangitis around the bile duct (H&E, ×120). (b) Adenocarcinoma that developed suddenly as a round tumor from a ductule (H&E, ×100). (c) Advanced tubular adenocarcinoma (H&E, ×20).

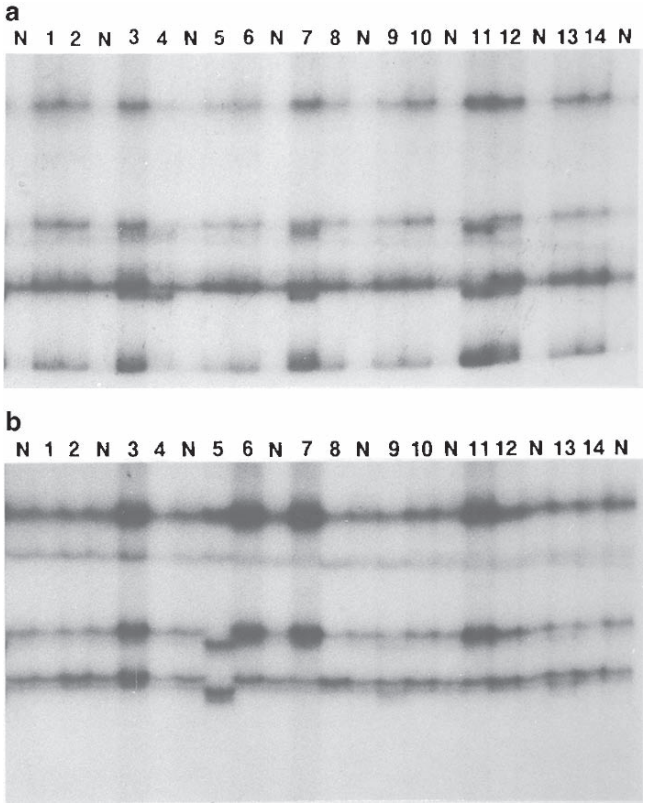

Fig. 6.20 Single-strand conformation polymorphism analysis of polymerase chain reaction-amplified Kirsten-*ras* exon 1 from intrahepatic bile duct lesions in hamsters. (a) Papillary adenocarcinoma of the intrahepatic bile duct. Lanes 3, 4, 7, 11, 12, shifted bands in addition to normal ones (N). (b) Tubular hyperplasia of the intrahepatic bile duct. Lanes 5, 9, 13, shifted bands in addition to normal ones (N) ([17], with permission)

of the bile duct from hamsters administered BOP were also examined, but no mutation was detected in codon 12 or codon 13. The frequencies of K-*ras* mutation of papillary adenocarcinoma were significantly different from that of the normal duct from BOP-treated hamsters ($P < 0.05$, the chi-square test) (Table 6.6).

Fig. 6.19 (d) Papillary hyperplasia surrounded by irregular lumen (H&E, ×20). (e) Papillary hyperplasia developing as papillary elevated lesions from the biliary lumen (H&E, ×20). (f) Papillary adenocarcinoma developing from a large duct near the hepatic hilum (H&E, ×40). (g) Papillary adenocarcinoma developing from a peripheral duct (H&E, ×40). (h) Mucinous carcinoma that may have developed from a periductal gland in the biliary wall (H&E, ×100)

Table 6.6 Analysis of Kirasten-*ras* codon 12 in intrahepatic bile duct lesions in Syrian golden hamsters

Histology	No. of samples analyzed	No. (%) of mutations detected (%)	Substitutions	
			GGT > GAT	GGT > TGT
Normal duct from *N*-nitrosobis(2-oxopropyl)amine (BOP)-treated hamsters	13	0	–	–
Tubular hyperplasia	26	3(12)	3	–
Tubular adenocarcinoma	26	5(19)	4	1
Papillary hyperplasia	13	2(15)	2	–
Papillary adenocarcinoma	14	5(36)*	4	1
Cystadenocarcinoma	2	0	–	–
Tubular adenocarcinoma arising from periductal gland	1	0	–	–

*Significantly different from normal duct. ($P < 0.05$). (modified from [17], with permission)

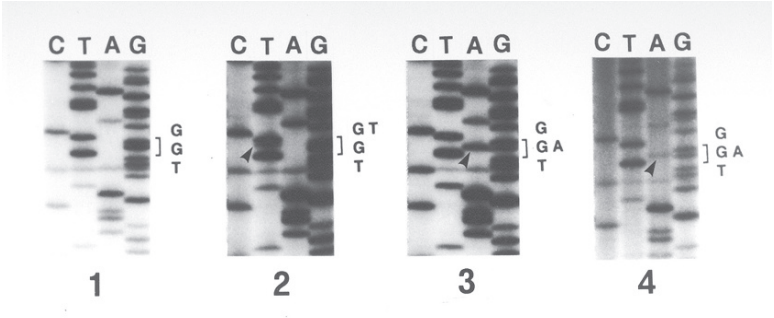

Fig. 6.21 Direct sequencing of the Kirsten-*ras* gene around codon 12 of the intrahepatic bile duct lesions in hamsters. Neoplastic and preneoplastic lesions revealed shifted bands in polymerase chain reaction–single-strand conformation polymorphism analysis. 1: Normal bile duct tissue in the hamster. 2: Tubular adenocarcinoma of the intrahepatic bile duct. 3: Papillary adenocarcinoma of the intrahepatic bile duct. 4: Papillary hyperplasia of the intrahepatic bile duct. Arrowheads show the point-mutated nucleotide. Point mutations from GGT to TGT (2) and to GAT (3 and 4) were observed ([17], with permission)

6.13 Comments

BOP is a potent carcinogen in the pancreas of the hamster, and BOP-induced carcinoma resembles carcinoma in humans [46,47]. BOP-induced intrahepatic bile duct carcinoma has made it possible to observe various early stage lesions, which are difficult to observe in humans. According to our classification [45], the duct-infiltrating type and the mass-forming type are common in human intrahepatic bile duct carcinoma, and we classified them histologically as tubular adenocarcinomas.

In the present study, we mainly analyzed K-*ras* mutations of ductal proliferation and advanced-stage tubular adenocarcinomas. Yamamoto [30] from our laboratory reported that there was evidence of hyperplasia and hypertrophic changes in the periductal glands of patients with intrahepatic stones. Nakanuma et al. [48] reported proliferation and inflammation of periductal glands. Although K-*ras* mutation was not detected in carcinomas arising from the periductal gland in the present study, these reports suggest the possibility of intrahepatic bile duct carcinoma developing in the periductal gland in humans.

A 25% frequency of K-*ras* gene mutation in intrahepatic bile duct carcinoma induced by *N*-nitrosobis(2-hydroxypropyl)amine (BHP) in the hamster was reported [49]. However, the K-*ras* gene mutation in carcinoma of the bile duct in humans was reported to be uncommon [40–43]. At first, we expected that the BOP-induced intrahepatic bile duct carcinomas would exhibit a similar incidence and pattern of K-*ras* mutation to the pancreatic cancers [50–52] if BOP changed the same part of the gene level in the bile and pancreatic duct. However, the incidence of K-*ras* mutations was not as high in the intrahepatic bile duct carcinomas as in the pancreatic cancers. The incidence of K-*ras* mutation in intrahepatic bile duct carcinoma and pancreatic carcinoma in hamsters is similar to that in humans.

Our study also revealed that K-*ras* gene mutations were already present in part of the tubular and papillary hyperplasia lesions; thus, K-*ras* gene mutation is an early event in the carcinogenic process. In carcinoma of the intrahepatic bile duct, papillary lesions arising from relatively large bile ducts in the hepatic hilum tended to exhibit a higher frequency of K-*ras* gene mutation than tubular lesions, which developed in ductules and bile ducts. Motojima et al. [43] from our laboratory reported that K-*ras* gene mutation in carcinoma of the distal part of the extrahepatic bile duct in humans was more frequent than that that of the proximal part, which is consistent with the results of this study.

Other investigators have reported that a base substitution in codon 12 from GGT (Gly) to GAT (Asp) accounts for most mutations in pancreatic carcinomas and intrahepatic bile duct carcinomas of hamsters and humans [53–56]. In the present study, base substitutions from GGT (Gly) to TGT (Val), a change occasionally observed in cancers and cell lines of humans [43,53,55,57], was detected in one papillary adenocarcinoma and one tubular adenocarcinoma. In other lesions, including hyperplastic ones, base substitution was from GGT (Gly) to GAT (Asp), similar to findings in pancreatic carcinoma in Syrian hamsters [49,52,56]. The regurgitation of pancreatic juice into the biliary tract, accompanying the anomalous arrangement of the pancreaticobiliary ductal union is thought to contribute to the development of biliary carcinoma [58]. In addition to BOP, the regurgitation of pancreatic juice and duodenal fluid is considered to accelerate K-*ras* gene mutation in our hamster model. Both histologically and genetically, our model is useful to investigate the early phenomena in the development of bile duct carcinoma in humans.

In summary, some of the hyperplastic lesions in the intrahepatic bile duct revealed K-*ras* gene mutation. This suggests that K-*ras* gene mutation is an early event in the carcinogenic process. In carcinoma of the intrahepatic bile duct, a lesion arising from a large bile duct of the hepatic hilum tended to exhibit a higher

frequency of K-*ras* gene mutation than a tubular lesion arising from a ductule or ductal proliferation.

References

1. Morson B. The polyp-cancer sequence in the large bowel. Proc. R. Soc. Med. 1974 67:451–457.
2. Muto T, Bussey HJ, Morson BC. The evolution of cancer of the colon and rectum. Cancer 1975 36:2251–2270.
3. Kuramoto S, Oohara T. Minute cancers arising de novo in the human large intestine. Cancer 1988 61:829–834.
4. Shimoda T, Ikegami M, Fujisaki J, Matsui T, Aizawa S, Ishikawa E. Early colorectal carcinoma with special reference to its development de novo. Cancer 1989 64:1138–1146.
5. Kudo S. Endoscopic mucosal resection of flat and depressed types of early colorectal cancer. Endoscopy 1993 25:455–461.
6. Tajima Y, Tomioka T, Ikematsu Y, Yamanaka S, Kuroki T, Kitajima T, Fukuda K, Tsuneoka N, Kitazato A, Adachi T, Kanematsu T. Experimental Study on Pathogenesis and Histomorphology of Early Carcinoma of the Extrahepatic Bile Duct in the Syrian Hamster. J Exp Clin Cancer Res 2005 24(3): 475–482.
7. Moore MA, Thamavit W, Bannasch P. Tumours of the liver. In Pathology of tumours in laboratory animals, eds. Turusov V.S and Mohr U, 2nd Ed., Vol. 3 – Tumours of the hamster. Lyon: International Agency for Research on Cancer 1996:79–108.
8. Turusov VS, Gorin B. Tumours of the gallbladder. In Pathology of tumours in laboratory animals, eds. Turusov VS and Mohr U, 2nd Ed., Vol. 3 – Tumours of the hamster. Lyon: International Agency for Research on Cancer 1996:109–126.
9. Wittekind C, Tannapfel A. Adenoma of the papilla and ampulla–premalignant lesions? Langenbecks Arch. Surg. 2001 386:172–175.
10. Kaiser A, Jurowich C, Schonekas H, Gebhar dt C, Wunsch PH. The adenoma-carcinoma sequence applies to epithelial tumours of the papilla of Vater. Z. Gastroenterol. 2002 40:913–920.
11. Scott-Coombes DM, Williamson RCN. Surgical treatment of primary duodenal carcinoma: a personal series. Br. J. Surg. 1994 81:1472–1474.
12. Sato H, Mizushima M, Ito J, Doi K. Sessile adenoma of the gallbladder. Reappraisal of its importance as a precancerous lesions. Arch. Pathol. Lab. Med. 1985 109:65–69.
13. Nakajo S, Yamamoto M, Tahara E. Morphometrical analysis of gall-bladder adenoma and adenocarcinoma with reference to histogenesis and adenoma-carcinoma sequence. Virchows Arch. A Pathol. Anat. Histopathol. 1990 417:49–56.
14. Callea F, Sergi C, Fabbretti G, Brisigotti M, Cozzutto C, Medicina D. Precancerous lesions of the biliary tree. J. Surg. Oncol. Suppl. 1993 (3):131–133.
15. Lee SS, Kim MH, Lee SK, Jang SJ, Song MH, Kim KP, Kim HJ, Seo DW, Song DE, Yu E, Lee SG, Min YI. Clinicopathologic review of 58 patients with biliary papillomatosis. Cancer 2004 100:783–793.
16. Shimonishi T, Sasaki M, Nakanuma Y. Precancerous lesions of intrahepatic cholangiocarcinoma. J. Hepatobiliary Pancreat. Surg. 2000 7:542–550.
17. Yamanaka S, Tomioka T, Tajima Y, Okada K, Shiku H, Kanematsu T. K-ras gene mutations in intrahepatic bile duct tumors of Syrian golden hamsters. J. Surg. Oncol. 1997 66:97–103.
18. Majima T, Tsujiuchi T, Tsutsumi M, Tsunoda T, Konishi Y. Mutations of K-ras but not p53 genes in biliary duct and pancreatic duct carcinomas induced in hamsters by cholecystoduodenostomy with dissection of the common duct followed by *N*-nitrosobis(2-oxopropyl) amine. Cancer Lett. 1997 118:47–53.
19. Cern WL, Mangold KA, Scarpelli DG. K-ras mutation is an early event in pancreatic duct carcinogenesis in the Syrian golden hamster. Cancer Res. 1992 52:4507–4513.

20. Day JD, Digiuseppe JA, Yeo C, Lai-Goldman M, Anderson SM, Goodman SN, Kern SE, Hruban RH. Immunohistochemical evaluation of HER-2/neu expression in pancreatic adenocarcinoma and pancreatic intraepithelial neoplasms. Hum. Pathol. 1996 27:119–124.
21. Fearon ER, Vogelstein B. A genetic model for colorectal tumorigenesis. Cell 1990 61:759–767.
22. Kuroki T, Fujiwara Y, Tsuchiya E, Nakamori S, Imaoka S, Kanematsu T, Nakamura Y. Accumulation of genetic changes during development and progression of hepatocellular carcinoma: loss of heterozygosity on chromosome arm Ip occurs at an early stage of hepatocarcinogenesis. Genes, Chromosomes Cancer 1995 13:163–167.
23. Tanno S, Obara T, Fujii T, Mizukami Y, Shudo R, Nishino N, Ura H, Klein-Szanto AJ, Kohgo Y. Proliferative potential and K-ras mutation in epithelial hyperplasia of the gallbladder in patients with anomalous pancreaticobiliary ductal union. Cancer 1998 83:267–275.
24. Matsumoto Y, Fujii H, Itakura J, Matsuda M, Yang Y, Nobukawa B, Suda K. Pancreaticobiliary maljunction: pathophysiological and clinical aspects and the impact on biliary carcinogenesis. Langenbecks Arch. Surg. 2003 388:122–131.
25. Yao T, Kajiwara M, Kuroiwa S, Iwashita A, Oya M, Kabashima A, Tsuneyoshi M. Malignant transformation of gastric hyperplastic polyps: alteration of phenotypes, proliferative activity, and p53 expression. Hum. Pathol. 2002 33:1016–1022.
26. Jass JR, Iino H, Ruszkiewicz A, Painter D, Solomon MJ, Koorey DJ, Cohn D, Furlong KL, Walsh MD, Palazzo J, Edmonston TB, Fishel R, Young J, Leggett BA. Neoplastic progression occurs through mutator pathways in hyperplastic polyposis of the colorectum. Gut 2000 47:43–49.
27. Tsunoda T, Eto T, Koga M, Tomioka T, Motoshima K, Yamaguchi T, Izawa K, Tsuchiya R. Early carcinoma of the extrahepatic bile duct. Jpn. J. Surg. 1989 19:691–698.
28. Kozuka S, Tsubone M, Hachisuka K. Evolution of carcinoma in the extrahepatic bile ducts. Cancer 1984 54:65–72.
29. Mizumoto R, Ogura Y, Kusuda T. Definition and diagnosis of early cancer of the biliary tract. Hepatogastroenterology 1993 12:163–170.
30. Yamamoto K. Intrahepatic periductal glands and their significances in primary intrahepatic lithiasis. Jpn. J. Surg. 1982 12:163–170.
31. Terada T, Nakanuma Y, Ohta G. Glandular elements around the intrahepatic bile ducts in man; their morphology and distribution in normal livers. Liver 1987 7:1–8.
32. Terada T, Nakanuma Y. Pathological observations of intrahepatic peribiliary glands in 1,000 consecutive autopsy livers. II. A possible source of cholangiocarcinoma. Hepatology 1990 12:92–97.
33. Kumar R, Sukumar S, Barbacid M. Activation of *ras* oncogenes preceding the onset of neoplasia. Science 1990 248:1101–1104.
34. Scarpa A, Zamboni G, Achille A, Capelli P, Bogina G, Iacono C, Serio G, Accolla RS. *ras*-family gene mutations in neoplasia of the ampulla of Vater. Int. J. Cancer 1994 59:39–42.
35. Nakanuma Y, Harada K, Ishikawa A, Zen Y, Sasaki M. Anatomic and molecular pathology of intrahepatic cholangiocarcinoma. J. Hepatobiliary Pancreat. Surg. 2003 10:265–281.
36. Kuroki T, Tajima Y, Matsuo K, Kanematsu T. Genetic alterations in gallbladder carcinoma. Surg. Today 2005 35:101–105.
37. Cowgill SM, Muscarella P. The genetics of pancreatic cancer. Am. J. Surg. 2003 186:279–286.
38. Forrester K, Almoguera C, Han K, Grizzle WE, Perucho M. Detection of high incidence of K-*ras* oncogenes during human colon tumorigenesis. Nature 1987 327:298–303.
39. Vogelstein B, Fearon ER, Hamilton SR, Kern SE, Preisinger AC, Leppert M, Nakamura Y, White R, Smits AM, Bos JL. Genetic alterations during colorectal-tumor development. N Engl. J. Med. 1988 319:525–532.
40. Levi S, Urbano-Ispizua A, Gill R, Thomas DM, Gilbertson J, Foster C, Marshall CJ. Multiple K-*ras* codon 12 mutations in cholangiocarcinomas demonstrated with a sensitive polymerase chain reaction technique. Cancer Res. 1991 51:3497–3502.
41. Tada M, Omata M, Ohto M. Analysis of *ras* gene mutations in human hepatic malignant tumors by polymerase chain reaction and direct sequencing. Cancer Res. 1990 50:1121–1124.

42. Tada M, Yokosuka O, Omata M, Ohto M, Isono K. Analysis of *ras* gene mutations in biliary and pancreatic tumors by polymerase chain reaction and direct sequencing. Cancer 1990 66:930–935.
43. Motojima K, Tsunoda T, Kanematsu T, Nagata Y, Urano T, Shiku H. Distinguishing pancreatic carcinoma from other periampullary carcinomas by analysis of mutations in the Kirsten-*ras* oncogene. Ann. Surg. 1991 214:657–662.
44. Tsuda H, Satarug S, Bhudhisawasdi V, Kihana T, Sugimura T, Hirohashi S. Cholangiocarcinomas in Japanese and Thai patients: difference in etiology and incidence of point mutation of the c-Ki-*ras* proto-oncogene. Mol. Carcinog. 1992 6:266–269.
45. Tomioka T, Tajima Y, Ikematsu Y, Eto T, Tsunoda T, Kanematsu T. The early lesions and invasive patterns of the intrahepatic bile duct carcinoma – comparable study of the hamster and the human lesions. In the Thirty-sixth World Congress of Surgery meeting program, Aug 27–Sept 2, 1995, Lisbon, Portugal, 1995:156 (abst PP39).
46. Pour P, Althoff J, Kruger FW, Mohr U. A potent pancreatic carcinogen in Syrian golden hamsters: *N*-nitrosobis(2-oxopropyl)amine. J. Natl. Cancer Inst. 1977 58:1449–1453.
47. Konishi Y, Mizumoto K, Kitazawa S, Tsujiuchi T, Tsutsumi M, Kamano T. Early ductal lesions of pancreatic carcinogenesis in animals and humans. Int. J. Pancreatol. 1990 7:83–89.
48. Nakanuma Y, Yamaguchi K, Ohta G, Terada T. Pathologic features of hepatolithiasis in Japan. Hum. Pathol. 1988 19:1181–1186.
49. Tsutsumi M, Murakami Y, Kondoh S, Tsujiuchi T, Hohnoki K, Horiguchi K, Noguchi O, Kobayashi E, Okita S, Sekiya T. Comparison of K-*ras* oncogene activation in pancreatic duct carcinomas and cholangiocarcinomas induced in hamsters by *N*-nitrosobis(2-hydroxypropyl) amine. Jpn. J. Cancer Res. 1993 84:956–960.
50. Cerny WL, Mangold KA, Scarpelli DG. Activation of K-*ras* in transplantable pancreatic ductal adenocarcinomas of Syrian golden hamsters. Carcinogenesis 1990 11:2075–2079.
51. van Kranen HJ, Vermeulen E, Schoren L, Bax J, Woutersen RA, van Iersel P, van Kreijl CF, Scherer E. Activation of c-K-*ras* is frequent in pancreatic carcinomas of Syrian hamsters, but is absent in pancreatic tumors of rats. Carcinogenesis 1991 12:1477–1482.
52. Ushijima T, Tsutsumi M, Sakai R, Ishizaka Y, Takaku F, Konishi Y, Takahashi M, Sugimura T, Nagao M. Ki-*ras* activation in pancreatic carcinomas of Syrian hamsters induced by *N*-nitrosobis(2-hydroxopropyl)amine. Jpn. J. Cancer Res. 1991 82:965–968.
53. Smit VT, Boot AJ, Smits AM, Fleuren GJ, Cornelisse CJ, Bos JL. KRAS codon 12 mutations occur very frequently in pancreatic adenocarcinomas. Nucleic Acids Res. 1988 16:7773–7782.
54. Grünewald K, Lyons J, Fröhlich A, Feichtinger H, Weger RA, Schwab G, Janssen JW, Bartram CR. High frequency of Ki-*ras* codon 12 mutations in pancreatic adenocarcinomas. Int. J. Cancer 1989 43:1037–1041.
55. Nagata Y, Abe M, Motoshima K, Nakayama E, Shiku H. Frequent glycine-to-aspartic acid mutations at codon 12 of c-Ki-*ras* gene in human pancreatic cancer in Japanese. Jpn. J. Cancer Res. 1990 81:135–140.
56. Tsutsumi M, Kondoh S, Noguchi O, Horiguchi K, Kobayashi E, Okita S, Ohashi K, Honoki K, Tsujiuchi T, Konishi Y. K-*ras* gene mutation in early ductal lesions induced in a rapid production model for pancreatic carcinomas in Syrian hamsters. Jpn. J. Cancer Res. 1993 84:1101–1105.
57. Berrozpe G, Schaeffer J, Peinado MA, Real FX, Perucho M. Comparative analysis of mutations in the *p53* and K-*ras* genes in pancreatic cancer. Int. J. Cancer 1994 58:185–191.
58. Kinoshita H, Nagata E, Hirohashi K, Sakai K, Kobayashi Y. Carcinoma of the gallbladder with an anomalous connection between the choledocus and the pancreatic duct: report of 10 cases and review of the literature in Japan. Cancer 1984 54:762–769.

Chapter 7
Biliary Inflammation and Biliary Carcinogenesis

Tomoo Kitajima, Yoshitsugu Tajima, Kei Matsuo, Tamotsu Kuroki, Shinya Onizuka, Yoshito Ikematsu, Sumihiro Matsuzaki, and Takashi Kanematsu

7.1 Summary

Biliary carcinoma has been reported as a late complication of bilioenterostomy. The present study was designed to find out if bilioenterostomy promotes biliary carcinogenesis, and to clarify the relationship between biliary inflammation and biliary carcinogenesis in hamsters. Syrian hamsters were subjected to simple laparotomy (SL), choledochoduodenostomy (CD), or choledochojejunostomy (CJ). All hamsters received subcutaneous injections of the chemical carcinogen, *N*-nitrosobis(2-oxopropyl)amine (BOP), and were killed 20 weeks after surgery. Neoplastic lesions in the biliary tree were examined histologically, and the presence and degree of cholangitis was evaluated with special reference to the biliary carcinogenesis. The incidence of bile duct carcinoma did not differ significantly among the three groups. However, numerous bile duct carcinomas were recognized in the bilioenterostomized animals, especially in the CJ group. Moreover, there was a significant correlation between biliary carcinogenesis and the presence of cholangitis in the CD and CJ groups, but not in the SL control group. Severe cholangitis was evident in the CJ group, and the number of biliary carcinomas was well correlated with the degree of cholangitis. These findings suggest that the risk of carcinoma in the biliary tract is increased when cholangitis persists after biliary reconstruction.

7.2 Introduction

Reconstruction of the biliary system is performed widely in the field of hepatobiliary pancreatic surgery. The most common problem after reconstruction of the biliary system is reflux of intestinal juice into the biliary tract, which results from inactivity of the papillary muscle of the ampulla of Vater. Reflux cholangitis [1–3], biliary stones [3,4] and liver abscess [2] are well-known complications after biliary reconstruction. Moreover, biliary carcinomas have recently been reported as a late complication after bilioenterostomy [5–7]. The malignant potential of the

Y. Tajima et al. (eds.), *Hepatobiliary and Pancreatic Carcinogenesis in the Hamster*,
DOI: 10.1007/978-4-431-87773-8_7, © Springer 2009

choledochal cyst, which causes the regurgitation of pancreatic juice into the biliary tract and is considered a factor promoting the development of biliary carcinoma, is thought to be accelerated by enteric internal drainage [8–10]. According to one report, eight cases of primary bile duct cancer were found among 108 patients, 10 to 22 years after sphincteroplasty [11].

Biliary carcinogenesis under conditions of biliary reconstruction has not been evaluated sufficiently. Therefore, this study aimed to clarify whether biliary reconstruction plays a role in biliary carcinogenesis in hamsters. We prepared two types of bilioenterostomy in hamsters: choledochoduodenostomy (CD) and choledochojejunostomy (CJ), to closely resemble the clinical situation. In this chapter, we discuss the possible factors relating to biliary carcinogenesis after bilioenterostomy.

7.3 Experimental Protocol

Seven-week-old female Syrian golden hamsters (SLC Inc., Shizuoka, Japan) were used. The animals were housed three per plastic cage on sawdust bedding, kept at 24 ± 2 °C in 50 ± 20% humidity with a 12 h alternating light and dark cycle. They were fed a CE-2 pelleted diet (Clea Japan Inc., Tokyo, Japan) and provided drinking water *ad libitum*. Animals were checked daily and weighed weekly during the experiment.

The hamsters were subjected to CD or CJ, according to the procedures described in Chapter 5. The control hamsters underwent simple laparotomy alone (SL). All animals were given weekly subcutaneous injections of *N*-nitrosobis(2-oxopropyl) amine (BOP) (Nakarai Tesque, Kyoto, Japan) at a dose of 10 mg/kg body weight in 0.9% saline [12,13]. Injections started 4 weeks after the surgery and continued for 9 weeks. All the animals were killed 20 weeks after the procedure.

The maximum diameter of the extrahepatic bile duct was measured. Bile in the biliary duct and blood samples from the vena cava were collected in ice-chilled tubes containing heparin, and then centrifuged (3,000 rpm) for 10 min. The levels of total bilirubin (T-Bil), alkaline phosphatase (ALP), glutamic–oxaloacetic transaminase (GOT), glutamic–pyruvic transaminase (GPT), lactate dehydrogenase (LDH), total bile acids (TBA), and amylase and phospholipase A2 (PLA2) in the bile were then measured.

The liver, biliary system and pancreas were removed en bloc. After fixation in 10% neutral formalin, the specimen was cut into five blocks and embedded in paraffin. Histological sections were stained with hematoxylin and eosin, and then examined by a pathologist unaware of the experimental details. The number of histologically verified carcinomas was counted. The diagnosis of carcinoma was based on disruption of the polarity of the epithelial cells and evidence of an invasive event.

To analyze the relationship between cholangitis and biliary carcinogenesis, the grade of cholangitis was scored according to the infiltration of inflammatory cells as follows:

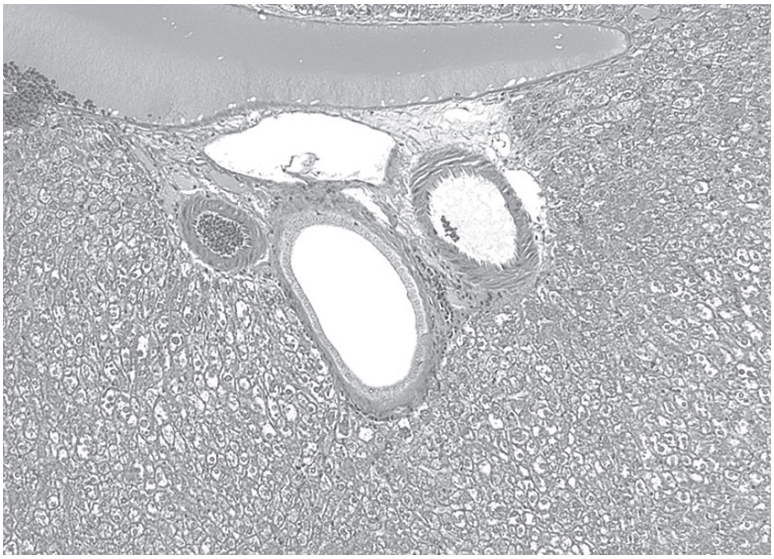

Fig. 7.1 Cholangitis grade 0: there are no inflammatory cells around the bile duct (H&E, ×60)

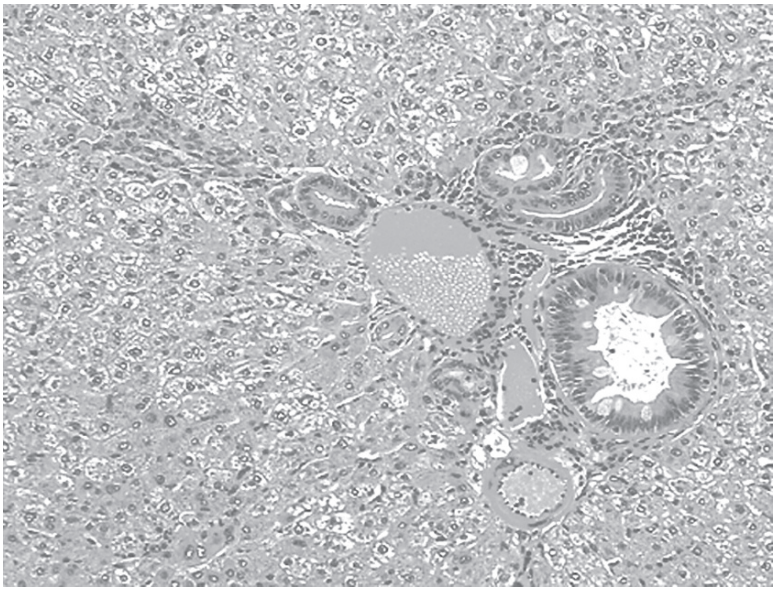

Fig. 7.2 Cholangitis grade 1: there is mild invasion of inflammatory cells around the bile duct and some proliferation (H&E, ×100)

grade 0, no cholangitis (Figure 7.1); grade 1, mild invasion of inflammatory cells around the bile duct (Figure 7.2); grade 2, severe invasion of inflammatory cells around the bile duct (Figure 7.3); and grade 3, abscess formation in the liver (Figure 7.4).

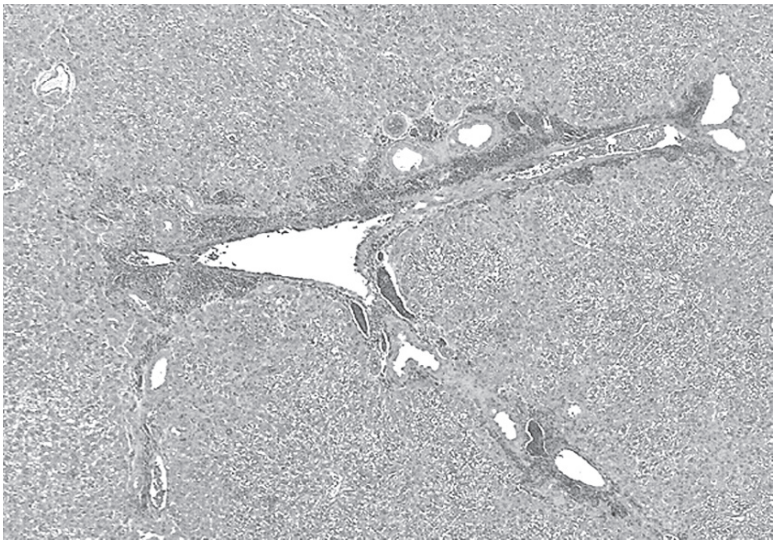

Fig. 7.3 Cholangitis grade 2: there is severe invasion of inflammatory cells around the bile duct and severe proliferation (H&E, ×40)

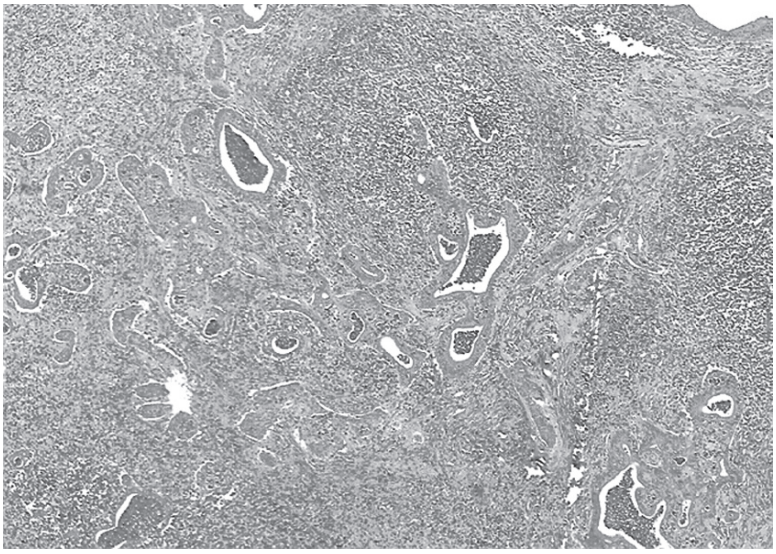

Fig. 7.4 Cholangitis grade 3: there is abscess formation in the liver (H&E, ×40)

The incidence of tumor formation and cholangitis were analyzed statistically using the chi-square test and Fisher's exact test. Student's *t* test and the Mann–Whitney test were also used to compare body weight, diameter of the extrahepatic bile duct,

number of tumors per animal, and laboratory data on serum and bile juice in the treatment groups and controls.

7.4 Morphological and Physiological Changes in the Hepatobiliary System

Table 7.1 summarizes the morphological and physiological changes seen in the hepatobiliary system after bilioenterostomy. Marked dilatation of the extrahepatic bile duct was seen in almost all of the hamsters in the CD and CJ groups. There were significant differences in the average diameter of the extrahepatic bile duct between the CD and SL groups, and between the CJ and SL groups. The serum levels of GOT, GPT, and LDH did not differ among the three groups, but the levels of T-Bil, ALP, and TBA were significantly higher in the CJ group than in the CD and SL groups. Amylase and PLA2 levels in the bile did not differ between the CD and CJ groups.

7.5 Development of Biliary Carcinoma

Carcinoma of the intrahepatic bile duct developed in 40.0%, 40.9%, and 50.0% of hamsters in the SL group, CD group, and CJ group, respectively. Carcinoma of the extrahepatic bile duct developed in 0%, 4.5%, and 7.7% of hamsters in the SL group, CD group, and CJ group, respectively. No significant difference was noted in the incidence of intra- and extrahepatic bile duct carcinoma among the three groups; however, numerous carcinomas developed in the bilioenterostomized animals, and the number of carcinomas per tumor-bearing animal was much greater in the CJ group than in the CD and SL groups (Table 7.2).

7.6 Cholangitis and Biliary Carcinogenesis

Cholangitis was observed in 25.0%, 31.8%, and 65.4% of hamsters in the SL group, CD group, and CJ group, respectively (Table 7.3). In the CD group, biliary carcinoma developed in all of the hamsters with cholangitis, but in only 2 of the 15 hamsters without cholangitis. In the CJ group, biliary carcinoma developed in 12 of the 17 hamsters with cholangitis. There was a significant correlation between the presence of cholangitis and biliary carcinogenesis in the CD and CJ groups, but not in the SL group. Grade 2–3 cholangitis was observed in 15.0%, 27.3%, and 61.5% of hamsters in the SL group, CD group, and CJ group, respectively (Figure 7.5). The average number of carcinomas found in hamsters with cholangitis of grade 2 or 3 was 6.3 and 10.3, respectively, in the CD group, and 10.3 and 12.3,

Table 7.1 Morphological and physiological changes in hepatobiliary system of hamsters after bilioenterostomy

Groups	No. of hamsters	Average diameter of the extrahepatic bile duct (mm)[a]	Serum[a]					Bile[a]	
			GOT (IU/l)	LDH (IU/l)	T-Bil (mg/dl)	ALP (IU/l)	TBA (μmol/l)	Amylase (IU/l)	PLA2 (ng/dl)
SL	20	0.63 ± 0.19	165.4 ± 90.7	934.9 ± 478.9	0.48 ± 0.24	13.4 ± 2.35	31.5 ± 31.5	–	–
CD	22	3.50 ± 1.37*	185.8 ± 188.3	906.8 ± 500.4	0.50 ± 0.35	11.9 ± 2.50	48.2 ± 59.8	3007.1 ± 2244.8	163.5 ± 54.4
CJ	26	3.75 ± 2.04**	154.7 ± 126.7	1226.9 ± 810.1	2.03 ± 2.70***	18.8 ± 11.21****	83.6 ± 60.0*****	1521.3 ± 378.4	249.7 ± 69.5

GOT, glutamic-oxaloacetic transaminase; LDH, lactate dehydrogenase; T-Bil, total bilirubin; ALP, alkaline phosphatase; TBA, total bile acids; PLA2, phospholipase A2.

*,**Significantly different from SL ($P < 0.01$).

***Significantly different from SL ($P < 0.01$) and CD ($P < 0.01$).

****Significantly different from SL ($P < 0.05$) and CD ($P < 0.01$).

*****Significantly different from SL ($P < 0.01$) and CD ($P < 0.05$).

[a]Mean ± SD. (modified from [24], with permission)

Table 7.2 Incidence and number of carcinomas induced in hamsters after bilioenterostomy

Groups	No. of hamsters	Average body weight (g)	No. (%) of hamsters with carcinoma of		Total no. of carcinomas	Average no. of carcinomas per CBA
			IHBD	EHBD		
SL	20	202.5	8(40.0)	0	16	2.00
CD	22	180.5	9(40.9)	1(4.5)	56	6.22
CJ	26	171.0	13(50.0)	2(7.7)	189	14.53*

IHBD, intrahepatic bile duct; EHBD, extrahepatic bile duct; CBA, carcinoma-bearing animal.

*Significantly different from SL ($P < 0.01$) and CD ($P < 0.05$). (modified from [24], with permission)

Table 7.3 Relationship of cholangitis and biliary carcinogenesis in hamsters

Groups	No. of hamsters	No. (%) of hamsters		Occurrence rate (%) of biliary carcinoma in hamsters	
		With cholangitis	Without cholangitis	With cholangitis	Without cholangitis
SL	20	5(25.0)	15(75.0)	2/5(40.0)	6/15(40.0)
CD	22	7(31.8)	15(68.2)	7/7(100)*	2/15(13.3)*
CJ	26	17(65.4)	9(34.6)	12/17(70.6)**	1/9(11.1)**

*Correlation between the presence of cholangitis and biliary carcinogenesis is significant ($P = 0.0002$).

**Correlation between the presence of cholangitis and biliary carcinogenesis is significant ($P = 0.0058$). (modified from [24], with permission)

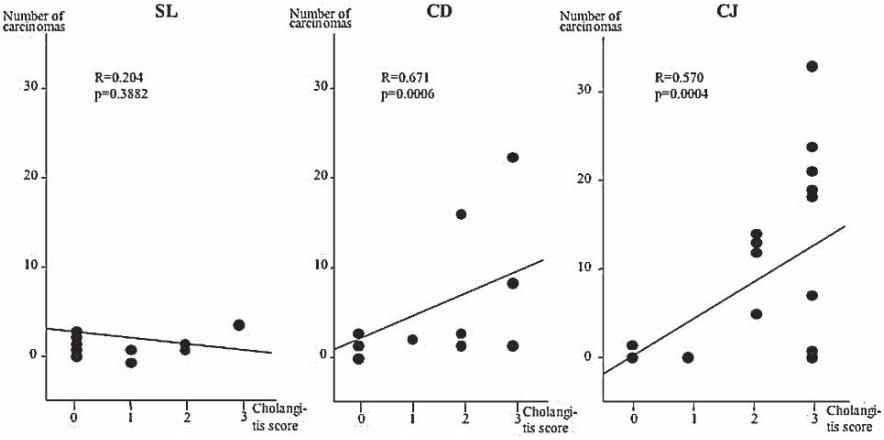

Fig. 7.5 Correlation between the cholangitis score and the number of carcinomas per tumor-bearing animal ([24], with permission)

respectively, in the CJ group. The number of biliary carcinomas was positively correlated with the degree of cholangitis in the CD and CJ groups, but not in the SL group.

7.7 Comments

Bilioenterostomy is a widely performed surgical procedure; however, it inevitably leads to the reflux of intestinal juice into the biliary tract. A previous study in our laboratory revealed an increased carcinogenic risk from intestinal juice regurgitating into the biliary tract after cholecystoduodenostomy or cholecystoileostomy in hamsters [14], and it became apparent that cholecystoduodenostomy enhanced the incidence of both intra- and extrahepatic bile duct carcinoma, whereas cholecystoileostomy promoted intrahepatic bile duct carcinoma. In the present study, there was no significant difference in the incidence of intra- and extrahepatic bile duct carcinoma after bilioenterostomy among the three groups. However, there was a significant correlation between the incidence of biliary carcinogenesis and the presence of cholangitis in the CD and CJ groups, but not in the SL group.

It is also noteworthy that numerous biliary carcinomas were found in the bilioenterostomized groups, especially in the CJ group, and that the number of biliary carcinomas correlated positively with the degree of cholangitis in both these groups. Moreover, bile stasis was clearly evident in the CJ group and the CD group, but not in the SL group. Bile stasis probably accelerates the progress of cholangitis, increasing the likelihood of carcinogenesis in the biliary tract. Although there is no conclusive evidence, mechanical irritation by cholelithiasis [15], bile stasis, and bacterial infection [16] has been considered a causative factor in the development of biliary carcinoma. The present results show clearly that the development of biliary carcinoma after bilioenterostomy is dependent on the presence and degree of associated cholangitis.

Cytokines are produced by a wide variety of cells, including macrophages, endothelial cells, hepatocytes, and fibroblasts, under inflammatory conditions [17,18]. Interleukin 6 is thought to promote an acute inflammatory response [19,20] and its serum levels are elevated in malignant tumors [21–23]. We surmised that some cytokines related to cholangitis play a role in biliary carcinogenesis and the multiplication of bile duct carcinoma after biliary reconstruction.

In conclusion, our findings provide evidence that although bilioenterostomy itself does not influence the development of biliary carcinoma, it promotes the reflux of intestinal juice into the biliary tract and induces bile stasis and cholangitis, which are associated with an increased incidence of carcinoma. Thus, when biliary inflammation is treated by bilioenterostomy, a high risk of multicentric biliary carcinogenesis might be created in the biliary tree.

References

1. Tocchi A, Costa G, Lepre L, Liotta G, Mazzoni G, Sita A. The long-term outcome of hepaticojejunostomy in the treatment of benign bile duct strictures. Ann Surg 1996 224:162–167.
2. Rothlin MA, Lopfe M, Schlumpf R, Largiader F. Long-term results of hepaticojejunostomy for benign lesions of the bile ducts. Am J Surg 1998 175:22–26.

3. Saing H, Han H, Chan KL, Lam W, Chan FL, Cheng W, Tam PK. Early and late results of excision of choledochal cysts. J Pediatr Surg 1997 32:1563–1566.
4. Sakaguchi T, Suzuki S, Suzuki A, Fukumoto K, Jindo O, Ota S, Inaba K, Kikuyama M, Nakamura S, Konno H. Late postoperative complications in patients with pancreaticobiliary maljunction. Hepatogastroenterology 2007 54:585–589.
5. Coyle KA, Bradley EL III. Cholangiocarcinoma developing after simple excision of a type II choledochal cyst. South Med J 1992 85:540–544.
6. Watanabe Y, Toki A, Todani T. Bile duct cancer developed after cyst excision for choledochal cyst. J Hep Bil Pancr Surg 1999 6:207–212.
7. Strong RW. Late bile duct cancer complicating biliary-enteric anastomosis for benign disease. Am J Surg 1999 177:472–474.
8. Tsuchiya R, Harada N, Ito T, Furukawa M, Yoshihiro I. Malignant tumors in choledochal cyst. Ann Surg 1977 186: 22–28.
9. Todani T, Watanabe Y, Toki A, Urushihara N. Carcinoma related to choledocal cysts with internal drainage operations. Surg Gynecol Obstet 1987 164: 61–64.
10. Funabiki T, Matsubara T, Ochiai M, Marugami Y, Sakurai Y, Hasegawa S, Imazu H. Biliary carcinogenesis in pancreaticobilialy maljunction. J Hep Bil Pancr Surg 1997 4: 405–411.
11. Hakamada K. Sasaki M. Endoh M. Itoh T. Morita T. Konn M. Late development of bile duct cancer after sphincteroplasty: a ten- to twenty-two-year follow-up study. Surgery 1997 121:488–492.
12. Pour P, Althoff J, Kruger FW, Mohr U. A potent pancreatic carcinogen in Syrian hamsters: *N*-nitrosobis(2-oxopropyl)amine. J Natl Cancer Inst 1977 58:1449–1453.
13. Tajima Y, Eto T, Tsunoda T, Tomioka T, Inoue K, Fukahori T, Kanematsu T. Induction of extrahepatic biliary carcinoma by *N*-nitrosobis(2-oxopropyl)amine in hamsters given cholecystoduodenostomy with dissection of the common duct. Jpn J Cancer Res 1994 85(8):780–788.
14. Ikematsu Y, Tomioka T, Yamanaka S, Tajima Y, Tsunoda T, Kanematsu T. Bilioenterostomy enhances biliary carcinogenesis in hamsters. Carcinogenesis 1996 17:1505–1509.
15. Ahrens W, Timmer A, Vyberg M, Fletcher T, Guénel P, Merler E, Merletti F, Morales M, Olsson H, Olsen J, Hardell L, Kaerlev L, Raverdy N, Lynge E. Risk factors for extrahepatic biliary tract carcinoma in men: medical conditions and lifestyle: results from a European multicentre case-control study. Eur J Gastroenterol Hepatol 2007 19:615–617.
16. Sharma V, Chauhan VS, Nath G, Kumar A, Shukla VK. Role of bile bacteria in gallbladder carcinoma. Hepatogastroenterology 2007 54:1622–1625.
17. Yudkin JS, Kumari M, Humphries SE, Mohamed-Ali V. Inflammation, obesity, stress and coronary heart disease: is interleukin-6 the link? Atherosclerosis 1999 1:209–214.
18. Matsumoto K, Fujii H, Michalopoulos G, Fung JJ, Demetris AJ. Human biliary epithelial cells secrete and respond to cytokines and hepatocyte growth factors *in vitro*: IL-6, HGF, and EGF promote DNA synthesis *in vitro*. Hepatology 1994 20:376–382.
19. Kopf M, Baumann H, Freer G, Freudenberg M, Lamers M, Kishimoto T, Zinkernagel R, Bluethmann H, Köhler G. Impaired immune and acute-phase responses in interleukin-6-deficient mice. Nature 1994 368:339–342.
20. Lotz M. Interleukin-6. Cancer Invest 1993 11:732–742.
21. Goydos JS, Brumfield AM, Frezza E, Booth A, Lotze MT, Carty SE. Marked elevation of serum interleukin-6 in patients with cholangiocarcinoma: validation of utility as a clinical marker. Ann Surg 1998 227:398–404
22. Heikkilä K, Ebrahim S, Lawlor DA. Systematic review of the association between circulating interleukin-6 (IL-6) and cancer. Eur J Cancer 2008 44:937–945.
23. Porta C, De Amici M, Quaglini S, Paglino C, Tagliani F, Boncimino A, Moratti R, Corazza GR. Circulating interleukin-6 as a tumor marker for hepatocellular carcinoma. Ann Oncol 2008 19:353–358.
24. Kitajima T, Tajima Y, Onizuka S, Matsuzaki S, Matsuo K, Kanemastu T. Linkage of persistent cholangitis after bilioenterostomy with biliary carcinogenesis in hamsters. J Exp Clin Cancer Res 2000 19:453–458.

Chapter 8
Spontaneous Biliary Carcinogenesis

Tomoo Kitajima, Sumihiro Matsuzaki, Tamotsu Kuroki, Kenzo Fukuda, Yoshitsugu Tajima, and Takashi Kanematsu

8.1 Summary

Biliary carcinomas arising in patients who have undergone bilioenterostomy is a clinical concern. Thus, we investigated if bilioenterostomy influences biliary carcinogenesis in hamsters. Syrian hamsters were divided into three groups according to the operative procedure: simple laparotomy (SL), choledochoduodenostomy (CD), and choledochojejunostomy (CJ). The animals were given no chemical carcinogens during the experiments and five to six hamsters in each group were killed every 20 weeks for up to 120 weeks after surgery. There were 37, 32, and 38 hamsters in the SL, CD, and CJ groups, respectively. Cholangiocarcinomas developed in 5.4%, 15.6%, and 23.7% of hamsters in the SL group, the CD group, and the CJ group, respectively. The incidence of biliary carcinoma was significantly higher in the bilioenterostomy groups, especially the CJ group ($P < 0.05$), than in the SL group. Tumor latency periods after surgery were 20 to 40 weeks shorter in the bilioenterostomy groups than in the SL group. Persistent cholangitis and bile stasis were observed in the bilioenterostomy groups, and there was a significant correlation between cholangitis and biliary carcinogenesis in the CD group. The proliferative cell nuclear antigen (PCNA) labeling index of the biliary epithelium was elevated in the bilioenterostomy groups. Thus, we conclude that persistent cholangitis after bilioenterostomy accelerates biliary carcinogenesis by activating the biliary epithelial cell kinetics.

8.2 Introduction

Biliary carcinoma may develop after operations such as complete excision of the extrahepatic bile duct followed by biliary reconstruction for congenital cystic dilatation of the common bile duct [1,2] or bilio-enteric anastomosis for iatrogenic bile duct injury [3]. This results in a poor prognosis. Moreover, extremely high incidences of secondary biliary carcinoma have been reported in patients who have undergone biliary-enteric drainage for benign disease [4], transduodenal sphincteroplasty [5], or endoscopic sphincterotomy [6]. Biliary reconstruction, enteric internal drainage,

Y. Tajima et al. (eds.), *Hepatobiliary and Pancreatic Carcinogenesis in the Hamster*,
DOI: 10.1007/978-4-431-87773-8_8, © Springer 2009

and sphincteroplasty induce the reflux of intestinal juice into the biliary tract because the papillary muscle of the ampulla of Vater becomes inactive. The reflux of intestinal contents into the biliary system may influence the development of biliary carcinogenesis; however, the etiology of secondary biliary carcinoma is not well understood.

Many investigators have attempted to induce carcinomas in the biliary tree of laboratory animals to clarify the mechanism of biliary carcinogenesis [7–9]. However, almost all of these investigators used chemicals to induce biliary carcinomas, whereas there have been few reports of spontaneous experimental biliary carcinoma. Our study was designed to clarify whether bilioenterostomy plays a role in biliary carcinogenesis in hamsters, without any loading of chemical carcinogens. We used the Syrian golden hamster because the anatomical structure of its pancreaticobiliary ductal system and the bile acid composition and pancreatic juice components are similar to those of humans [10–12].

8.3 Experimental Protocol

Seven-week-old female Syrian golden hamsters (SLC, Shizuoka, Japan) were used. The animals were housed one per plastic cage on sawdust bedding, kept at 24 ± 2 °C in 50 ± 20% humidity with a 12 h alternating light and dark cycle. They were fed a CE-2 pelleted diet (Clea Japan, Tokyo, Japan) and provided with drinking water *ad libitum*. The animals were checked daily and weighed weekly during the experiment. All experiments were conducted according to the Guidelines for Animal Experimentation of Nagasaki University.

We performed two types of bilioenterostomy closely resembling those used in the clinical situation: choledochoduodenostomy (CD) and choledochojejunostomy (CJ). The hamsters were anesthetized with sodium pentobarbital, 50 mg/kg body weight. Through an upper-abdominal midline incision, the distal end of the common bile duct was excised and the gallbladder was removed. Then, CD was performed in the duodenal wall, 10 mm distal to the pyloric ring of the stomach. CJ was achieved using about 4 cm of the jejunum for Roux-en-Y anastomosis [13, 14]. The details of the surgical techniques are described in Chapter 5. The control hamsters were subjected to simple laparotomy only (SL).

To evaluate morphological and physiological changes in the hepatobiliary system of hamsters after bilioenterostomy, five or six hamsters from each group were killed at 20-week intervals, from 20 to 120 weeks after surgery. The maximum diameter of the extrahepatic bile duct was measured and bile from the biliary duct and blood samples from the vena cava were collected in ice-chilled tubes containing heparin, and then centrifuged (3,000 rpm) for 10 min. The serum levels of total bilirubin (T-Bil), glutamic–oxaloacetic transaminase (GOT), total bile acids (TBA) and amylase in the bile were measured.

The liver, biliary system, and pancreas were removed *en bloc* and specimens were fixed in 10% neutral formalin, then cut into five blocks and embedded in

paraffin. Histological sections were stained with hematoxylin and eosin (H&E), and then examined by a pathologist without prior knowledge of the treatments. The biliary neoplasms were diagnosed according to standard criteria [15].

To evaluate the relationship between cholangitis and biliary carcinogenesis, the grade of cholangitis was scored in accordance with the infiltration of inflammatory cells: grade 0, no cholangitis; grade 1, mild invasion of inflammatory cells around the bile duct; grade 2, severe invasion of inflammatory cells around the bile duct; and grade 3, abscess formation in the liver (see Chapter 7).

We used anti-PCNA/horseradish peroxidase (Dako, Japan) to detect proliferative cell nuclear antigen (PCNA) in the specimens after treatment with a household microwave oven. The proportion of labeled nuclei (labeling index, LI) was measured by counting the labeled nuclei in >1,000 non-neoplastic epithelial cells of the intrahepatic and extrahepatic bile ducts.

The incidence of tumor development and the appearance of cholangitis were analyzed statistically using the χ^2 and Fisher's exact tests. Student's *t* and the Mann–Whitney tests were also used to compare body weight, diameter of the extrahepatic bile duct, number of tumors per animal, and laboratory data on serum and bile juice in the treatment groups and controls.

8.4 Morphological and Physiological Changes in the Hepatobiliary System

Table 8.1 summarizes the morphological and physiological changes in the hepatobiliary system of hamsters after bilioenterostomy. The number of hamsters examined was 37, 32, and 38 in the SL, CD, and CJ groups, respectively. Almost all the hamsters

Table 8.1 Morphological and physiological changes in the hepatobiliary system of hamsters after bilioenterostomy

Groups	No. of hamsters examined	Average diameter[a] of the extrahepatic bile duct (mm)	Serum[a]		Bile[a]	
			GOT (IU/l)	T-Bil (mg/dl)	TBA (μmol/l)	Amylase (IU/l)
SL	37	0.6 ± 0.2	103.0 ± 77.8	0.34 ± 0.13	22.0 ± 24.4	–
CD	32	3.4 ± 1.5[*]	128.6 ± 125.1	0.58 ± 1.12	38.4 ± 38.2[**]	7,162.0 ± 18,803
CJ	38	3.3 ± 1.6[*]	194.1 ± 202.4	0.57 ± 0.50[*]	48.8 ± 57.0[**]	4,486.6 ± 10,924

GOT, glutamic-oxaloacetic transaminase; T-Bil, total bilirubin; TBA, total bile acids.

[*]Significantly different from SL ($P < 0.01$).

[**]Significantly different from SL ($P < 0.05$).

[a]Mean ± SD. (modified from [28], with permission)

Table 8.2 The incidence and number of tumors developed in hamsters after bilioenterostomy

		IHBD				
		No. (%) of hamsters with		Average (total) no. of		EHBD
Groups	No. of hamsters examined	Adenoma	Carcinoma	Adenoma per ABA	Carcinoma per CBA	No. (%) of hamsters with carcinoma
SL	37	7(18.9)	2(5.4)	1.71(12)	1.0(2)	0
CD	32	9(28.1)	5(15.6)	2.66(24)**	3.6(18)	2(6.2)
CJ	38	9(23.7)	9(23.7)*	2.88(26)	1.4(13)	1(2.6)

IHB, intrahepatic bile duct; EHBD, extrahepatic bile duct; ABA, adenoma-bearing animal; CBA, carcinoma-bearing animal.

*Significantly different from SL ($P < 0.05$).

**Significantly different from SL ($P < 0.01$). (modified from [28], with permission)

in the CD and CJ groups had marked dilatation of the extrahepatic bile duct, and there were significant differences in the average diameters of the extrahepatic bile ducts between the bilioenterostomized groups and the SL group. The serum levels of GOT, T-Bil, and TBA did not differ among the three groups. The amylase activities in bile in the CD and CJ animals were high, although the differences among the groups were not significant.

8.5 Spontaneous Biliary Carcinogenesis

Spontaneous biliary neoplasms were observed in all three groups (Table 8.2). Representative cases of cholangioadenoma and cholangiocarcinoma are shown in Figures 8.1 and 8.2. The incidences of adenoma were 18.9%, 28.1%, and 23.7% in hamsters in the SL group, CD group, and CJ group, respectively, without significant differences among the three groups. However, numerous biliary adenomas developed in the bilioenterostomized animals. The number of adenomas per tumor-bearing animal was significantly higher in the CD group than in the SL group ($P < 0.01$). Cholangiocarcinomas developed in 5.4%, 15.6%, and 23.7% of hamsters in the SL group, CD group, and CJ group, respectively. The rate of cholangiocarcinoma in the CJ group was about four times higher than that in the SL group ($P < 0.05$). Carcinoma of the extrahepatic bile duct developed in two hamsters in the CD group and one hamster in the CJ group (Figure 8.3), but not in any of those in the SL group. The latencies of the biliary tumors after bilioenterostomy are shown in Figure 8.4. Cholangioadenomas were detected 40, 60, and 80 weeks after the procedure in the CJ, CD, and SL groups, respectively, whereas cholangiocarcinomas were detected 60, 60, and 80 weeks after the procedure in the CJ, CD and SL groups, respectively.

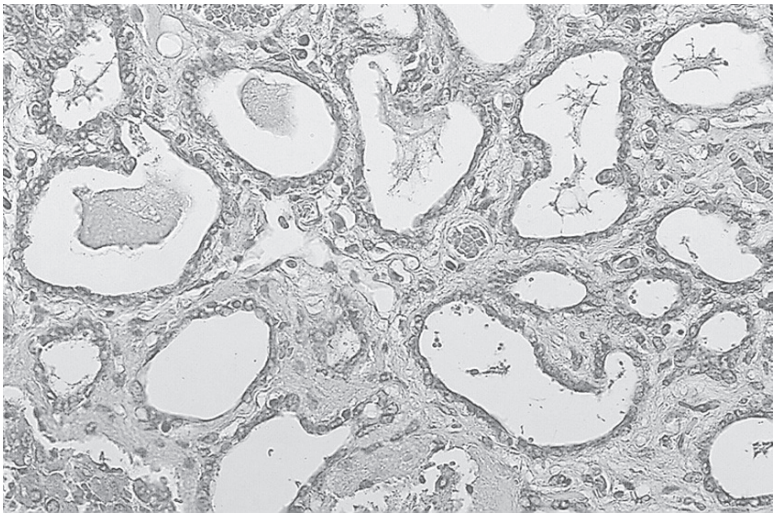

Fig. 8.1 Intrahepatic cholangioadenoma in a hamster 59 weeks after choledochoduodenostomy (CD) (H&E, ×200) ([28], with permission)

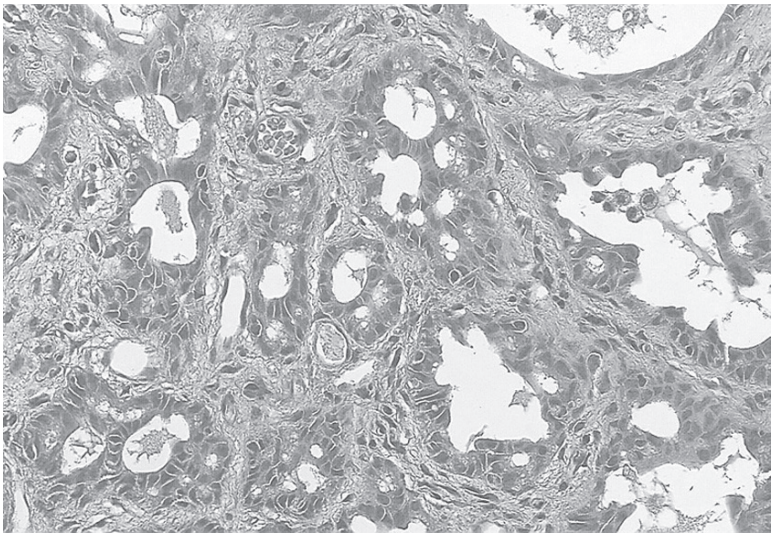

Fig. 8.2 Intrahepatic cholangiocarcinoma in a hamster 83 weeks after CD (H&E, ×200) ([28], with permission)

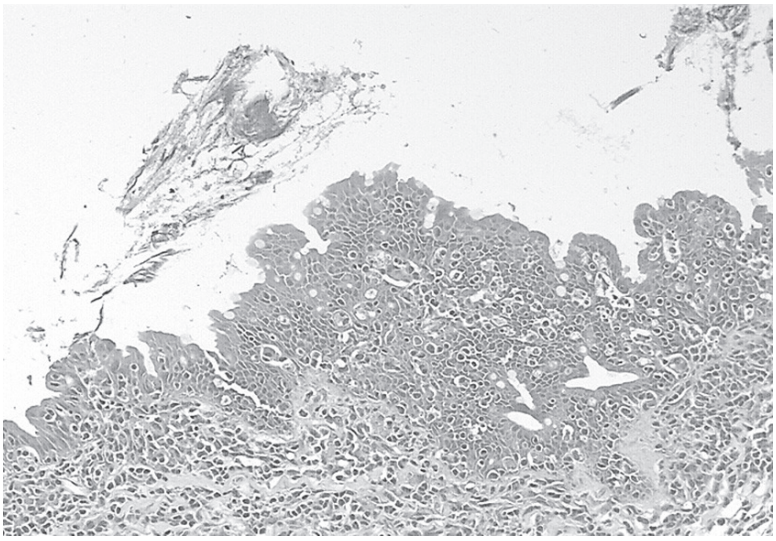

Fig. 8.3 Extrahepatic bile duct carcinoma in a hamster 70 weeks after choledochojejunostomy (CJ) (H&E, ×100) ([28], with permission)

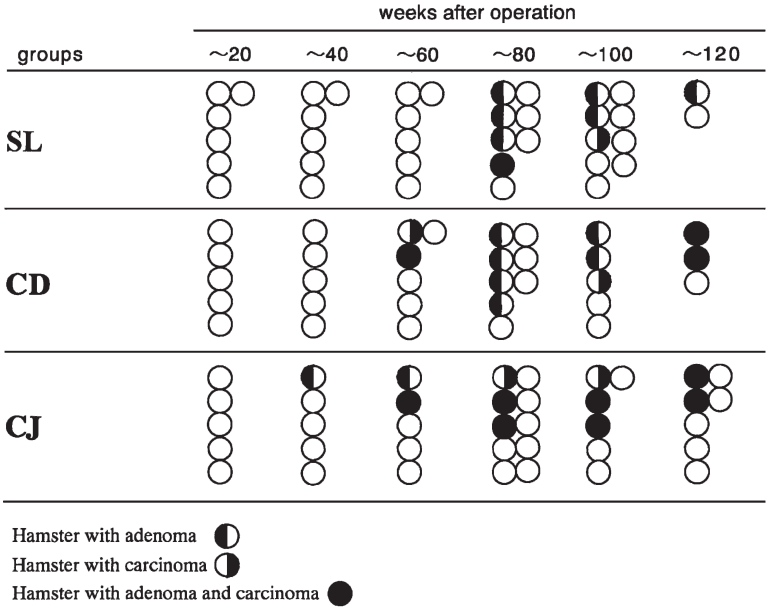

Fig. 8.4 Tumor latency periods after bilioenterostomy in hamsters ([28], with permission)

8.6 Cholangitis and Biliary Carcinogenesis

Cholangitis was observed in 54.1%, 81.2%, and 86.8% of hamsters in the SL group, CD group, and CJ group, respectively. Grade 2 or 3 cholangitis was observed only in the bilioenterostomized animals, and the cholangitis scores of the CD and CJ groups were significantly higher than that of the SL group. In the CD group, biliary carcinoma developed in all except one of the hamsters with grade 2 or 3 cholangitis, and there was a significant correlation between the presence of cholangitis and biliary carcinogenesis (Figure 8.5). There was no such correlation in the SL or CJ groups.

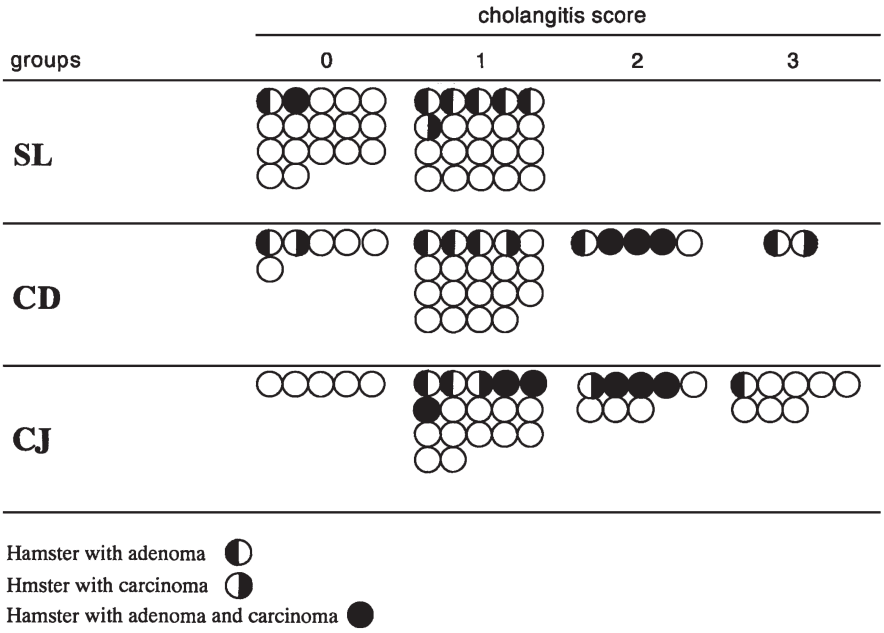

Fig. 8.5 Correlation between biliary carcinogenesis and cholangitis ([28], with permission)

Table 8.3 PCNA labeling index in the biliary epithelium in hamsters after bilioenterostomy

Groups	No. of examined Hamsters	IHBD (%)[a]		EHBD (%)[a]
		Center	Periphery	
SL	25	0.2 ± 0.3	0.2 ± 0.2	0.3 ± 0.6
CD	27	0.8 ± 1.6	0.7 ± 1.3	3.5 ± 8.4
CJ	26	2.3 ± 4.9*	1.1 ± 1.9*	4.3 ± 6.6*

IHBD, intrahepatic bile duct; EHBD, extrahepatic bile duct.

*Significantly different from SL ($P < 0.05$).

[a]Mean ± SD. ([28], with permission)

8.7 PCNA Labeling Indices

PCNA labeling indices (LIs) of the biliary epithelia are summarized in Table 8.3. The PCNA LIs in the enterostomized groups were higher than that in the SL group. There was a significant increase in the LIs in the intrahepatic and extrahepatic bile ducts of the CJ animals.

8.8 Comments

Spontaneous biliary tumors in Syrian hamsters were reported by Pour et al. [16], who described the development of cholangiocarcinoma in 3 of 118 female hamsters (2.5%) over a mean observation period of 71 weeks. In the present study, spontaneous cholangiocarcinomas developed in 2 of the 37 control hamsters (5.4%). The higher incidence of spontaneous cholangiocarcinomas than in the study by Pour et al. may be attributed to the longer observation period. However, extremely high incidences of spontaneous cholangiocarcinomas were observed in the bilioenterostomized hamsters; at 15.6% and 23.7% in the CD group and CJ group, respectively. Extrahepatic bile duct carcinomas were also observed in the enterostomized groups. Previously, we reported the enhancement of biliary carcinogenesis in hamsters induced by cholecystoduodenostomy or cholecystoileostomy in combination with a chemical carcinogen [7,8,14,17]; however, the present study showed the potent biliary carcinogenicity of bilioenterostomy alone in hamsters, without the use of chemical carcinogens.

According to clinical studies, bile duct cancer developed in 55 of 1,003 patients 11 to 19 years after a biliary-enteric anastomosis [4] and in 8 of 108 patients a mean 17 years after sphincteroplasty [5]. In the present study, spontaneous biliary neoplasms were found 80 weeks after surgery in the SL group, but after only 40 weeks in the bilioentrostomized hamsters, demonstrating a difference in the latency period of tumor development between the groups. This was also interesting because hamsters have a short life span of 100 to 150 weeks. Thus, bilioenterostomy accelerated spontaneous biliary carcinogenesis in hamsters. Mechanical irritation by cholelithiasis [18,19], chronic intrahepatic cholangitis with hepatolithiasis [20], bile stasis and bacterial infection [21] are all thought to be causal factors in the development of biliary carcinoma. Tocchi et al. [4] reported cholestasis and cholangitis in the clinical histories of 72% of patients with cholangiocarcinoma after biliary-enteric anastomosis. In the present study, cholangitis and bile stasis were found in the bilioenterostomized hamsters and there was a significant correlation between the development of biliary carcinoma and the presence of cholangitis in the CD group. No such correlation was noted in the CJ group, although the incidence of biliary carcinoma and the grade of cholangitis were higher in the CJ group than in the CD group. In the CJ group, eight hamsters had grade 3 cholangitis with a liver abscess, but no cholangiocarcinoma. Thus, the cholangitis appeared to affect biliary carcinogenesis by its ‘persistency’

rather than its 'severity'. Moreover, according to previous studies, non-tumorous biliary epithelium in the intrahepatic and extrahepatic bile ducts of bilioenterostomized hamsters contained higher than normal levels of PCNA, a 36 kDa intranuculear protein used in immunohistochemical studies of epithelial cell proliferation [22,23]. PCNA expression in the biliary epithelium may indicate increased proliferative activity in the epithelial cells and aggressive behavior of biliary carcinomas [24–27]. In the bilioenterostomized hamsters, PCNA LIs were elevated at the periphery and in the center of the intrahepatic bile duct and most of the biliary carcinomas originated from the peripheral ductules in the biliary tree. These findings indicate that bile stasis accelerates the progression and persistency of peripheral cholangitis, increasing cell kinetic activity of the biliary epithelium and eventually, cholangiocarcinoma.

In conclusion, spontaneous biliary carcinomas develop at an extremely high incidence in hamsters subjected to bilioenterostomy in association with persistent chronic cholangitis. Thus, a high risk of biliary carcinogenesis may be created in the biliary tree when biliary inflammation is induced by bilioenterostomy.

References

1. Coyle KA, Bradley EL, III. Cholangiocarcinoma developing after simple excision of a type II choledochal cyst. South Med. J. 1992 85:540–544.
2. Watanabe Y, Toki A, Todani T. Bile duct cancer developed after cyst excision for choledochal cyst. J. Hepatobiliary Pancreat. Surg. 1999 6:207–212.
3. Strong RW. Late bile duct cancer complicating biliary-enteric anastomosis for benign disease. Am. J. Surg. 1999 177:472–474.
4. Tocchi A, Mazzoni G, Liotta G, Lepre L, Cassini D, Miccini M. Late development of bile duct cancer in patients who had biliary-enteric drainage for benign disease: a follow-up study of more than 1,000 patients. Ann. Surg. 2001 234:210–214.
5. Hakamada K, Sasaki M, Endoh M, Itoh T, Morita T, Konn M. Late development of bile duct cancer after sphincteroplasty: a ten- to twenty-two-year follow-up study. Surgery 1997 121, 488–492.
6. Tanaka M, Takahata S, Konomi H, Matsunaga H, Yokohata K, Takeda T, Utsunomia N, Ikeda S. Long-term consequence of endoscopic sphincterotomy for bile duct stones. Gastrointest. Endosc. 1998 48:465–469.
7. Tajima Y, Eto T, Tsunoda T, Tomioka T, Inoue K, Fukahori T, Kanematsu T. Induction of extrahepatic biliary carcinoma by *N*-nitrosobis(2-oxopropyl)amine in hamsters given cholecystoduodenostomy with dissection of the common duct. Jpn. J. Cancer Res. 1994 85:780–788.
8. Ikematsu Y, Tomioka T, Tajima Y, Tsunoda T, Kanematsu T. Cholecystokinin promotes biliary carcinogenesis in hamster model. World J. Surg. 1995 19:847–851.
9. Ogura Y, Matsuda S, Usui M, Hanamura N, Kawarada Y. Effect of pancreatic juice reflux into biliary tract on *N*-nitrosobis(2-oxopropyl)amine (BOP)-induced biliary carcinogenesis in Syrian hamsters. Dig. Dis. Sci. 1999 44:79–86.
10. Takahashi M, Pour P, Althoff J, Donnelly T. The pancreas of the Syrian hamster (Mesocricetus auratus). Lab. Anim. Sci. 1977 27:336–342.
11. Singhal AK, Sadowsky JF, McSherry CK, Mosbach E.H. Effect of cholesterol and bile acids on the regulation of cholesterol mechanism in hamster. Biochim. Biophys. Acta 1983 752:214–222.

12. Rinderknecht H, Maset R, Collias K, Carmack C. Pancreatic secretory profiles of protein, digestive, and lysosomal enzymes in Syrian golden hamster. Effect of secretin and cholecystokinin. Dig. Dis. Sci. 1983 28:518–525.
13. Lee S, Chalters AC, Chandler JG, Orloff MJ. A technique for orthotopic liver transplantation in the rat. Transplantation 1973 16:664–669.
14. Kitajima T, Tajima Y, Onizuka S, Matsuzaki S, Matsuo K, Kanemastu T. Linkage of persistent cholangitis after bilioenterostomy with biliary carcinogenesis in hamsters. J. Exp. Clin. Cancer Res. 2000 19:453–458.
15. Turusov V, Mohr U (Eds.). Pathology of tumors in laboratory animals: tumours of the liver. Volume III—tumors of the hamster. (1996) International Agency for Research on Cancer, Lyon, 79–108.
16. Pour P, Mohr U, Cardesa A, Althoff J, Kmoch N. Spontaneous tumors and common diseases in two colonies of Syrian hamsters. II. Respiratory tract and digestive system. J. Natl. Cancer Inst. 1977 56:937–948.
17. Ikematsu Y, Tomioka T, Yamanaka S, Tajima Y, Tsunoda T, Kanematsu T. Bilioenterostomy enhances biliary carcinogenesis in hamsters. Carcinogenesis 1996 17:1505–1509.
18. Ohta T, Nagakawa T, Ueda N, Nakamura T, Akiyama T, Ueno K, Miyazaki I. Mucosal dysplasia of the liver and the intraductal variant of peripheral cholangiocarcinoma in hepatolithiasis. Cancer 1999 68:2217–2223.
19. Sheen-Chen SM, Chou FF, Eng HL. Intrahepatic cholangiocarcinoma in hepatolithiasis: a frequently overlooked disease. J. Surg. Oncol. 1991 47:131–135.
20. Falchuk KR, Lesser PB, Galdabini JJ, Isselbacher KJ. Cholangiocarcinoma as related to chronic intrahepatic cholangitis and hepatolithiasis. Case report and review of the literature. Am. J. Gastroenterol. 1976 66:57–61.
21. Chijiiwa K, Ichimiya H, Kuroki S, Koga A, Nakamura F. Late development of cholangiocarcinoma after the treatment of hepatolithiasis. Surg. Gynecol. Obstet. 1993 177:279–282.
22. Miyachi K, Fritzler MJ, Ten EM. Autoantibodies to a nuclear antigen in proliferating cells. J. Immunol. 1978 121:2228–2234.
23. Hall PA, Levinson DA, Woods AL. Proliferating cell nuclear antigen (PCNA) immunolocalization in paraffin sections: an index of cell proliferation with evidence of deregulated expression in some neoplasms. J. Pathol. 1990 162:285–294.
24. Soon Lee C. Difference in cell proliferation and prognostic significance of proliferating cell nuclear antigen and Ki-67 antigen immunoreactivity in in situ and invasive carcinoma of the extrahepatic biliary tract. Cancer 1996 78:1881–1887.
25. Nishida T, Nakao K, Hamaji M, Nakahara M, Tsujimoto M. Prognostic significance of proliferative cell nuclear antigen in carcinoma of the extrahepatic bile duct. World J. Surg. 1997 21:634–639.
26. Fujii H, Yang Y, Tang R, Kunimoto K, Itakura J, Mogaki M, Matsuda M, Suda K, Nobukawa B, Matsumoto Y. Epithelial cell proliferation activity of the biliary ductal system with congenital biliary malformations. J. Hepatobiliary Pancreat. Surg. 1999 6:294–302.
27. Jung YS, Lee KJ, Kim H, Kim WH, Kim IG, Yoo BM, Kim JH, Kim MW. Risk factor for extrahepatic bile duct cancer in patients with anomalous pancreaticobiliary duct union. Hepatogastroenterology 2004 51:946–949.
28. Kitajima T, Tajima Y, Matsuzaki S, Kuroki T, Fukuda K, Kanematsu T. Acceleration of spontaneous biliary carcinogenesis in hamsters by bilioenterostomy. Carcinogenesis 2003 24:133–137.

Chapter 9
Modification of Biliary Carcinogenesis

Yoshito Ikematsu, Tsutomu Tomioka, Tsukasa Tsunoda, Yoshitsugu Tajima, and Takashi Kanematsu

A. Cholecystokinin and Cholecystokinin-Receptor Antagonist

9.1 Summary

Cholecystokinin (CCK) exerts a trophic action on the gastrointestinal tract and on the pancreaticobiliary system. We evaluated the effects of CCK on biliary carcinogenesis in hamsters. Hamsters treated with *N*-nitrosobis(2-oxopropyl)amine (BOP) were divided into the following four groups: group 1, given a subcutaneous injection of hydrolyzed gelatin, a solvent of CCK; groups 2 and 3, given CCK 2.5 and 25 μg/kg, respectively; and group 4, given loxiglumide, a CCK receptor antagonist. CCK significantly exacerbated the carcinogenetic effect of BOP in the intra- and extrahepatic bile ducts, but not in the gallbladder or pancreas. Loxiglumide exerted an inhibitory effect on carcinogenesis in the intrahepatic bile duct.

9.2 Introduction

Biliary cancer sometimes develops in patients with congenital choledochal dilatation or biliary tract lithiasis [1]. Furthermore, proliferative changes can occur in the epithelium when the gallbladder contains stones [2]. Cholecystokinin (CCK) exerts a trophic action on the gastrointestinal tract and on the pancreas [3]. Lamote et al. [4] reported that CCK octapeptide (CCK-8) and caerulein (a CCK analogue) exerted a proliferative effect on the murine gallbladder epithelium. Another study found that CCK promoted azacerine-induced carcinoma of the pancreas in rats [5]. Conversely, a CCK receptor antagonist, lorglumide, was found to inhibit the growth of putative preneoplastic foci in this rat model [6]. However, the mechanism of how CCK influences carcinogenesis of the biliary system remains unclear [7]. In this study, we examined the effects of CCK, and of the CCK receptor antagonist, loxiglumide, on biliary carcinogenesis using our hamster model of biliary carcinoma [8].

Y. Tajima et al. (eds.), *Hepatobiliary and Pancreatic Carcinogenesis in the Hamster*,
DOI: 10.1007/978-4-431-87773-8_9, © Springer 2009

9.3 Experimental Protocol

Non-inbred 7-week-old female Syrian golden hamsters (SLC, Inc., Shizuoka, Japan) were used. To produce biliary carcinoma in hamsters, we performed cholecystoduodenostomy with dissection of the extrahepatic bile duct on the distal end of the common duct (CDDB) under sodium pentobarbital anesthesia, 50 mg/kg body weight, i.p., as detailed in Chapter 5. The 95 (68%) animals that had tolerated the procedure up until postoperative day 7 were included in the experiment. All of the 45 (32%) other hamsters died of biliary peritonitis within 7 days of the operation. Each animal was housed individually in a plastic cage with sawdust bedding in an alternating 12 h light and dark cycle in an air-conditioned room kept at 24 ± 2 °C in 50 ± 20% humidity. The hamsters were fed a CE-2 pelleted diet consisting of fat 4.4% and protein 24.8% (Clea Japan, Inc., Tokyo, Japan) and given access to drinking water *ad libitum*. The animals were checked daily and weighed weekly during the experiment.

CCK-8, purchased from Peninsula Laboratories Inc., CA, was dissolved in 16% hydrolyzed gelatin at a dose of 2.5 or 25 μg/kg body weight [9]. Loxiglumide (D,L,-4-[3,4-dichloro-benzoylamino]-5-[N-3-methoxy-propyl-pentyl-amino]-5-oxo-pentanoic acid; MW 461.38), a proglumide derivative [10] kindly provided by Tokyo Tanabe Co. (Tokyo, Japan), was dissolved in distilled water and brought to pH 9 by NaOH to produce a 0.5% solution. BOP was purchased from Nakarai Tesque, Kyoto, Japan.

The 95 animals that tolerated the surgery were divided into the following four groups: group 1, given 16% hydrolyzed gelatin, a solvent of CCK-8, subcutaneously, as a control (n = 27); group 2, given CCK-8 2.5 μg/kg body weight + gelatin (n = 20); group 3, given CCK-8 25 μg/kg body weight + gelatin (n = 25); and group IV, given loxiglumide 50 mg/kg body weight (n = 23). The chemicals were administered subcutaneously once daily for 3 consecutive days a week during the 15-week experimental period. During the first 9 weeks, BOP was also given weekly at a dose of 10 mg/kg body weight in 0.9% NaCl solution subcutaneously.

During postoperative week 16, all hamsters were fasted overnight and given a final injection 30 min prior to exsanguination, to assay CCK bioactivity. At necropsy, the maximum diameter of the common bile duct was measured and then the liver, duodenum, biliary system and pancreas were removed *en bloc*. To secure the extrahepatic bile duct, the gastric and splenic lobes of the pancreas were excised and carefully trimmed of all adherent fat, mesentery and lymph nodes. The pancreas was wet weighed before fixation in 10% buffered neutral formalin and being spread out on a piece of paper to ensure a maximal transectional area for subsequent sectioning. A portion of the liver, the area of anastomosis including the duodenum, the common bile duct, and the head and the duodenal segment of the pancreas were embedded *en bloc* and cut in step sections, with five sections per animal. Histological sections were stained with hematoxylin and eosin, and examined by light microscopy. Pancreaticobiliary neoplastic lesions were counted by anatomic location in the representative sections. A diagnosis of carcinoma was based on the disruption of polarity of the epithelial cells, evidence of invasion, and cytoplasmic or nuclear atypia.

Blood samples were collected in ice-chilled tubes containing heparin and left in an ice-bath until centrifugation (3,000 rpm) at 4 °C for 10 min. Plasma was stored

at −80 °C until extraction and the concentration of CCK on Sep Pac C18 cartridges (Waters Ass., Milford, MA). CCK levels in the plasma were measured by bioassay using dispersed acini, as described elsewhere [11,12].

The incidence of tumor production was analyzed statistically using the chi-square test with continuity correction. One factor ANOVA was also used to compare percent increments in body weight, diameter of the common bile duct, and plasma CCK bioactivity.

9.4 Carcinoma in the Biliary System and the Pancreas

Table 9.1 shows the incidence of carcinoma in the intra- and extrahepatic bile ducts, gallbladder, and pancreas in the four groups. The incidence of carcinoma was significantly higher in the intra- and extrahepatic bile ducts of the group 3 animals (given BOP followed by 25 μg/kg CCK-8) than in the group 1 animals. BOP carcinogenicity was significantly lower only in the intrahepatic bile duct of the group 4 animals (treated with BOP and then loxiglumide). Although CCK-8 25 μg/kg significantly enhanced the carcinogenetic effect of BOP in the intra- and extrahepatic bile ducts, a one-tenth dose of 2.5 μg/kg CCK-8 had no effect on BOP carcinogenicity in either the biliary system or the pancreas.

Histologically, most of the lesions in the intrahepatic bile duct and all the polypoid lesions were tubular adenocarcinoma, whereas all of the superficial lesions in the extrahepatic bile duct were papillary adenocarcinoma. The major tumors of the gallbladder were confirmed histologically to be papillary adenocarcinoma. Pancreatic carcinomas were induced frequently in hamsters in all the experimental groups. Almost all the lesions were tubular adenocarcinoma.

9.5 Pathological and Biochemical Studies

The body weight of hamsters increased significantly in the three groups treated with CCK-8 or loxiglumide (Table 9.2). The mean diameter of the common bile duct was significantly increased in the group 3 hamsters (given CCK-8 25 μg/kg) and the group 4 hamsters (given loxiglumide) than in the group 1 hamsters. Plasma CCK levels were significantly higher in groups 2 and 3 ($p < 0.01$), but significantly lower in group 4 ($p < 0.05$).

9.6 Comments

CCK-8 enhanced carcinogenesis in the intra- and extrahepatic bile duct of hamsters, although the administration of CCK did not change the incidence of carcinoma in the gallbladder and pancreas. Since CCK has a trophic effect on pancreatic acinar cells [13], most of the literature on the effects of CCK on pancreas cancer is

Table 9.1 Incidence of carcinoma induced in the hamster biliary system and pancreas

		No. (%) of hamsters with carcinoma			
Group	No. of hamsters	Intrahepatic bile duct	Extrahepatic Bile duct	Gallbladder	Pancreas
I (Control)	27	15(56)	4(15)	11(41)	21(78)
II (CCK-8 2.5 μg/kg)	20	14(70)	7(35)	11(55)	16(80)
III (CCK-8 25 μg/kg)	25	22(88)*	11(44)*	15(60)	25(100)
IV (Loxiglumide 50 mg/kg)	23	4(17)*	2(9)	5(22)	19(83)

*$p < 0.05$ vs. Group I. (modified from [30], with permission)

Table 9.2 Pathological and biochemical findings

				Pancreatic weight		
Group	No. of hamsters	Body weight increment[a] (%)	Diameter of CBD (mm)	Absolute (g)	Relative (g/kg)	CCK bioactivity (pM)
I (Control)	27	24 ± 2	4.9 ± 0.5	0.59 ± 0.08	4.81 ± 0.74	2.6 ± 0.3
II (CCK-8 2.5 μg/kg)	20	53 ± 6*	4.7 ± 0.6	0.71 ± 0.05	5.01 ± 0.41	4.4 ± 0.4*
III (CCK-8 25 μg/kg)	25	54 ± 4*	6.1 ± 0.3****,*****	0.76 ± 0.05****	5.55 ± 0.36	41.3 ± 6.9*,**
IV (Loxiglumide 50 mg/kg)	23	38 ± 3*,**,***	6.2 ± 0.4****,*****	0.56 ± 0.03***	3.95±0.21	1.6 ± 0.2**,***,****

Expressed as mean ± SE.CBD; common bile duct.

$^{*}p < 0.01$ vs. Group I.

$^{**}p < 0.01$ vs. Group II.

$^{***}p < 0.01$ vs. Group III.

$^{****}p < 0.05$ vs. Group I.

$^{*****}p < 0.05$ vs. Group II.

[a]{(Final body weight) − (Initial body weight)}/(Initial body weight) × 100. (modified from [30], with permission)

based on the rat-azacerine model [5,6]. However, because pancreatic carcinoma that arises in the hamster-nitrosamine model is of duct or ductular cell origin, the effect of CCK is unclear [14–17]. In our study, the incidence of pancreatic carcinoma, although high (78%) in the control group, was not affected by CCK-8 or loxiglumide. Conversely, the absolute and relative pancreatic weight was influenced by the occurrence of pancreatic carcinoma itself.

Experimental biliary carcinogenesis with CCK has been reported [7]. In rats and hamsters, a slightly supraphysiological concentration of plasma CCK occurred after a subcutaneous injection of 2.5 μg/kg CCK-8, compared with the dietary administration of corn oil [13]. Thus, an injected dose of 25 μg/kg CCK-8 was assumed to induce a pharmacologically high plasma concentration of CCK-8. The known enhancing effect of CCK on the gallbladder epithelial cells seems also to apply to the intrahepatic duct cells [4]. These proliferated cells show an increased susceptibility to the effect of carcinogens [18,19].

In the CDDB model, the epithelium of the biliary tract was inflamed by the activated pancreatic juice and the proliferated cells were more susceptible to the tumorigenic effects of carcinogens [8,18]. The biliary carcinoma in this model, which is similar to that in humans, could be induced at a high rate within 12 weeks, whereas no intrahepatic carcinoma was observed in the absence of surgery [8], Biliary neoplasms can arise in humans with congenital choledochal cysts accompanied by a relapsing cholangitis [19,20]. The pharmacological effect of CCK added to the CDDB model enhanced the BOP carcinogenicity of the intra- and extrahepatic bile duct epithelia.

Hepatocytes metabolize BOP into the active form and this is transported through the intrahepatic bile duct epithelium, much like the relationship between islet and ductular cells in the pancreas [15]. Therefore, a high concentration of activated carcinogens would affect the intrahepatic bile duct directly in conjunction with CCK-8. It is still unclear why the carcinogenesis of the extrahepatic bile duct and gallbladder was not affected by exogenous CCK-8; however, it may be because the carcinogenesis of cholangiocarcinoma and extrahepatic bile duct carcinoma is different, as suggested by analyses of *ras* gene mutation [21].

Loxiglumide inhibits the effect of CCK on gallbladder contraction and pancreatic secretion in humans [22,23]. Although CCK was extracted and concentrated on Sep Pac C18 cartridges, the presence of loxiglumide in the plasma samples might have interfered with the CCK bioassay in group 4 [11,24]. A recent study found that the growth of human pancreatic cancer lines was inhibited by loxiglumide [25]. In our study, loxiglumide inhibited the development of intrahepatic bile duct carcinoma, but it was uncertain whether this inhibitory effect of loxiglumide was dependent on decreased levels of CCK or on the direct action of the chemical itself.

In conclusion, CCK seems to play an important role in carcinogenesis of the intra- and extrahepatic bile duct. Loxiglumide, a CCK antagonist, has an inhibitory effect on BOP carcinogenesis in the intrahepatic biliary system of hamsters.

B. Cholecystoduodenostomy and Cholecystoileostomy

9.7 Summary

To find out if the type of bilioenterostomy influences biliary carcinogenesis, Syrian hamsters were divided into the following three groups: simple laparotomy (control group), cholecystoduodenostomy with dissection of the extrahepatic bile duct on the distal end of the common duct (CDDB group), and cholecystoileostomy with dissection of the extrahepatic bile duct on the distal end of the common duct (CIDB group). Following these procedures, all hamsters received *N*-nitrosobis(2-oxopropyl)amine. The diameter of the extrahepatic bile duct and plasma levels of cholecystokinin (CCK) were measured and the number of neoplastic lesions was counted microscopically. We used the proliferative cell nuclear antigen to evaluate the proliferative effect of the procedures on the biliary epithelium. In the CDDB group, the extrahepatic bile duct was

significantly dilated, and the carcinogenicity of the gallbladder and extrahepatic bile ducts was enhanced. In the CIDB group, the CCK bioactivity was stimulated and the carcinogenicity of the intrahepatic biliary duct, but not the gallbladder or extrahepatic bile duct, was more enhanced than in the CDDB group. Proliferation of the biliary duct epithelium was enhanced in both the CDDB and CIDB groups. Cholecystoduodenostomy enhanced intra- and extrahepatic bile duct carcinoma, whereas cholecystoileostomy promoted only the intrahepatic bile duct carcinoma. Thus, some components of the intestinal juice seem to play a role in the promotion of biliary tract carcinoma.

9.8 Introduction

Pancreaticobiliary maljunction (PBM) and congenital choledochal dilatation are often associated with cancers of the gallbladder or extrahepatic bile duct, but not intrahepatic bile duct carcinoma [26–29]. It is not yet known if intrahepatic and extrahepatic biliary carcinoma have the same etiology. We addressed this question using a new model of biliary carcinoma induction with *N*-nitrosobis(2-oxopropyl)amine (BOP) in the hamster subjected to bilioenterostomy [8]. In this model, dilated common bile ducts comparable to human congenital choledochal dilatation developed in all hamsters. Exogenous cholecystokinin (CCK) has been shown to enhance intrahepatic biliary carcinogenesis [30]. However, it is still unclear whether the reflux of duodenal juice is an important factor in dilatation of the common bile duct and biliary carcinogenesis. In this study, we evaluated the effects of duodenal or ileal juice reflux into the biliary tract caused by cholecystoduodenostomy or cholecystoileostomy, respectively.

9.9 Experimental Protocol

Outbred 7-week-old female Syrian golden hamsters (SLC, Inc., Shizuoka, Japan) were housed individually in plastic cages on sawdust bedding. They were kept at 24 ± 2 °C in 50 ± 20% humidity, with a 12 h alternate light and dark cycle. They were fed a CE-2 pelleted diet (fat 4.4% and protein 24.8%, Clea Japan, Inc., Tokyo, Japan) and provided drinking water *ad libitum*. Animals were checked daily and weighed weekly during the experiment.

Animals were randomly divided into the following three groups: simple laparotomy (control group), cholecystoduodenostomy with dissection of the extrahepatic bile duct on the distal end of the common duct below the opening of the pancreatic duct (CDDB group: Figure 9.1), and cholecystoileostomy with dissection of the extrahepatic bile duct on the distal end of the common duct as described (CIDB group: Figure 9.2). Ninety-two of the 110 hamsters tolerated the procedures up until postoperative day 7: 30 from the control group, 32 from the CDDB group, and 30 from the CIDB group. Eighteen of these hamsters died early of biliary peritonitis. We killed 27 of the surviving animals (control, n = 10; CDDB, n = 10; CIDB, n = 7) on day 14 of

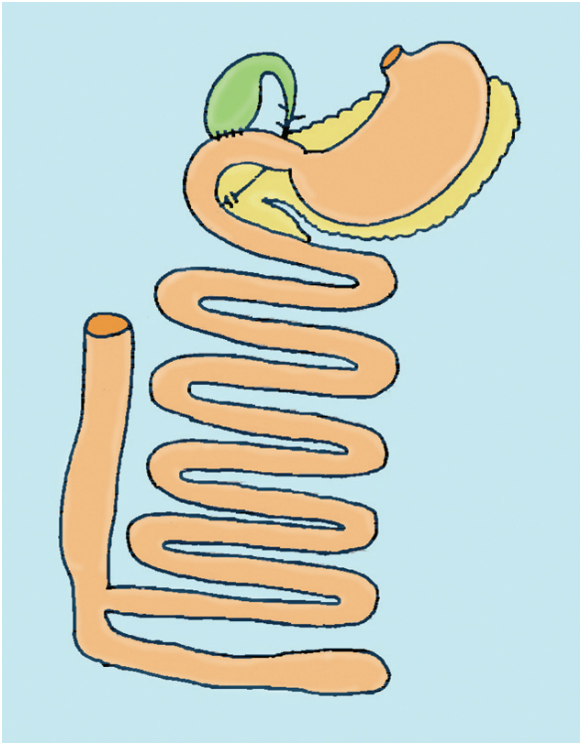

Fig. 9.1 Cholecystoduodenostomy with dissection of the extrahepatic bile duct at the distal end of the common duct (CDDB procedure) (modified from [38], with permission)

the experiment for CCK bioassay (2-week study) and gave the remaining 65 (control, n = 20; CDDB, n = 22; CIDB, n = 23) BOP (Nakarai Tesque, Kyoto, Japan) 10 mg/kg body in 0.9% NaCl solution, subcutaneously, weekly for 9 weeks. All these animals were killed on postoperative week 16 (16-week study).

All hamsters were fasted overnight, killed by exsanguination, and the liver, duodenum, biliary system and pancreas were removed *en bloc*. After measuring the maximum diameter of the extrahepatic bile duct, the pancreas was spread out on a piece of paper to ensure a maximal transectional area for subsequent sectioning. Portions of the liver, an area of anastomosis including duodenum, the common bile duct, and the duodenal segment of the pancreas were embedded *en bloc* and cut in step sections (five sections per animal). Histological sections were stained with hematoxylin and eosin, and examined by light microscopy. The number of pancreaticobiliary neoplastic lesions in each anatomic location was counted in the representative sections.

Blood samples from the vena cava were collected in ice-chilled tubes containing heparin and centrifuged (3,000 rpm) at 4 °C for 10 min. The total bilirubin level was measured. Plasma was stored at −80 °C until CCK was extracted and concentrated in Sep Pak C18 cartridges (Waters Ass., Milford, MA). Plasma CCK levels were measured by dispersed acini, as described elsewhere [11,12]. Proliferative cell nuclear antigen

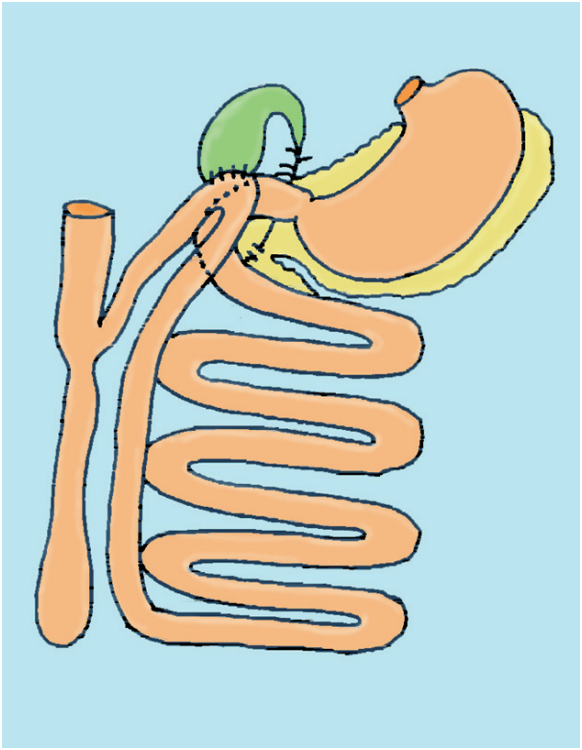

Fig. 9.2 Cholecystoileostomy with dissection of the extrahepatic bile duct at the distal end of the common duct (CIDB procedure) (modified from [38], with permission)

(PCNA) was demonstrated in the 16-week study specimens by anti-PCNA/horseradish peroxidase (DAKO, Denmark) after household microwave treatment. Labeled nuclei in more than 1,000 non-neoplastic epithelial cells of the intra- and extrahepatic bile ducts, the gallbladder, and the pancreatic ducts were counted in every ten sections and the percentages of labeled nuclei (labeling index, L.I.) were calculated.

The tumor incidence was analyzed by the chi-square test with continuity correction. Student's *t* test was also used to compare the diameter of the common bile duct, the total bilirubin level, CCK bioactivity, and PCNA labeling indices.

9.10 Diameter of the Extrahepatic Bile Duct and the Total Bilirubin Level

The maximum diameter of the extrahepatic bile duct was significantly greater in the CDDB and CIDB groups than in the control group ($p < 0.01$). It was also significantly greater in the CDDB group than in the CIDB group ($p < 0.01$). These differences

were readily observed in the 2-week study (Table 9.3, Figures 9.3 and 9.4). There was no jaundice in the 2-week study, but in the 16-week study the total bilirubin level was significantly higher in the CDDB group than in the control and CIDB groups (Table 9.3).

Table 9.3 Diameter of the extrahepatic bile duct and levels of serum total bilirubin

	2-Week study			16-Week study		
Groups	No. of hamsters	Diameter (mm)	Total bilirubin	No. of hamsters	Diameter (mm)	Total bilirubin
Control	10	0.2 ± 0.1	0.37 ± 0.24	20	0.9 ± 0.1	0.28 ± 0.05
CDDB	10	3.6 ± 0.7*	0.35 ± 0.25	22	4.9 ± 0.5*	3.02 ± 3.35*
CIDB	7	0.5 ± 0.1*,**	0.30 ± 0.07	23	1.9 ± 0.3*,**	0.92 ± 0.71**

Expressed as mean ± SE.
CDDB, cholecystoduodenostomy with dissection of the distal end of the common duct; CICD, cholecystoileostomy with dissection of the distal end of the common duct.
*$p < 0.01$ vs. Control.
**$p < 0.01$ vs CDDB. (modified from [38], with permission)

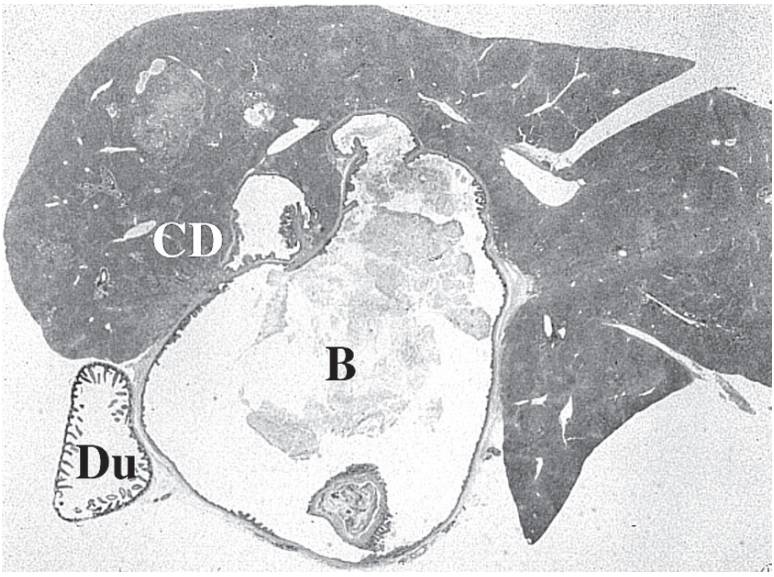

Fig. 9.3 Histologic sections of the biliary tract from a hamster subjected to CDDB in the 16-week study (H&E stain). Marked dilatation of the extrahepatic bile duct can be seen. B, bile duct; CD, cholecystoduodenostomy; Du, duodenum (modified from [38], with permission)

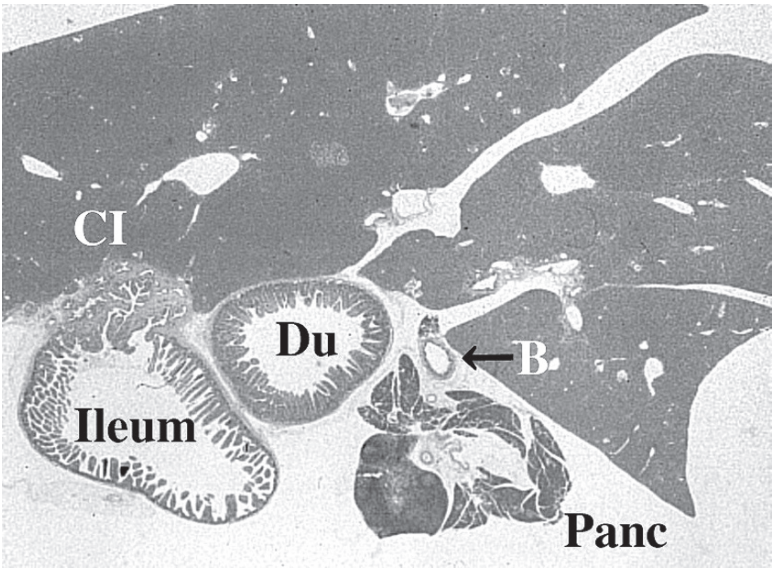

Fig. 9.4 Histologic sections of the biliary tract from a hamster subjected to CIDB in the 16-week study (H&E). Mild dilatation of the extrahepatic bile duct can be seen. B, bile duct; CI, cholecystoileostomy; Du, duodenum; Panc, pancreas (modified from [38], with permission)

9.11 Bioassay of CCK

In the 2-week study, plasma CCK levels were significantly higher in the CIDB group ($p < 0.05$), and significantly lower in the CDDB group ($p < 0.01$) than in the control group. However, the CCK level did not change in any group in the 16-week study (Table 9.4)

9.12 Carcinoma in the Biliary System and the Pancreas

No carcinoma was observed in any groups in the 2-week study. Table 9.5 summarizes the incidence of carcinoma in the intra- and extrahepatic bile ducts, gallbladder, and pancreas in the 16-week study. The incidence of intrahepatic bile duct carcinoma incidence was higher in the CDDB and CIDB groups than in the control group ($p < 0.05$ and $p < 0.01$, respectively) and significantly more tumor-bearing animals were found in the CIDB group than in the CDDB group ($p < 0.05$). A significant increase in the incidence of carcinoma was also noted in both the extrahepatic bile duct and the gallbladder in the CDDB group ($p < 0.05$ and 0.01, respectively, vs. the control group). No significant difference was noted in the

Table 9.4 Fasting bioassay of plasma CCK

	2-Week study		16-Week study	
Groups	No. of Hamsters	Plasma CCK (pM)	No. of hamsters	Plasma CCK (pM)
Control	10	6.4 ± 0.6	20	6.9 ± 0.5
CDDB	10	2.6 ± 0.3*	22	9.7 ± 3.1
CIDB	7	8.7 ± 0.9**.***	23	6.3 ± 2.0

Expressed by mean ± SE.
CDDB, cholecystoduodenostomy with dissection of the distal end of the common duct.
CICD, cholecystoileostomy with dissection of the distal end of the common duct.
*$p < 0.01$ vs. Control.
**$p < 0.05$ vs. Control.
***$p < 0.01$ vs. CDDB. (modified from [38], with permission)

Table 9.5 Incidences of carcinoma induced in the biliary system and pancreas of the hamster (16-week Group)

		No. of hamsters with carcinoma			
Groups	No. of hamsters	Intrahepatic bile duct	Extrahepatic bile duct	Gallbladder	Pancreas
Control	20	1(5)	0	0	10(50)
CDDB	22	8(36)*	6(27)*	10(46)**	16(72)
CIDB	23	17(74)**.***	2(9)	3(13)	12(52)

Numbers in parentheses are percentages.
CDDB, cholecystoduodenostomy with dissection of the distal end of the common duct; CICD, cholecystoileostomy with dissection of the distal end of the common duct.
*$p < 0.05$ vs. Control.
**$p < 0.01$ vs. Control.
***$p < 0.05$ vs. CDDB. (modified from [38], with permission)

incidence of pancreatic carcinoma. Histologically, the intrahepatic bile duct lesions were tubular adenocarcinoma, the extrahepatic bile duct and gallbladder tumors were papillary adenocarcinoma, and the pancreatic tumors were ductular adenocarcinoma.

9.13 PCNA Labeling Indices

The pattern of labeling is shown in Figures 9.5–9.7 and the LI of the biliary epithelium and pancreatic ductal epithelia are summarized in Table 9.6. Significant increases were found in the LI of the intrahepatic bile duct in the CIDB group ($p < 0.01$ vs. control and CDDB groups) and in the LI of the extrahepatic bile duct and gallbladder in the CDDB group ($p < 0.01$ vs. control and CIDB groups). There was no significant difference in the LI of the pancreatic ductal epithelium among the three groups.

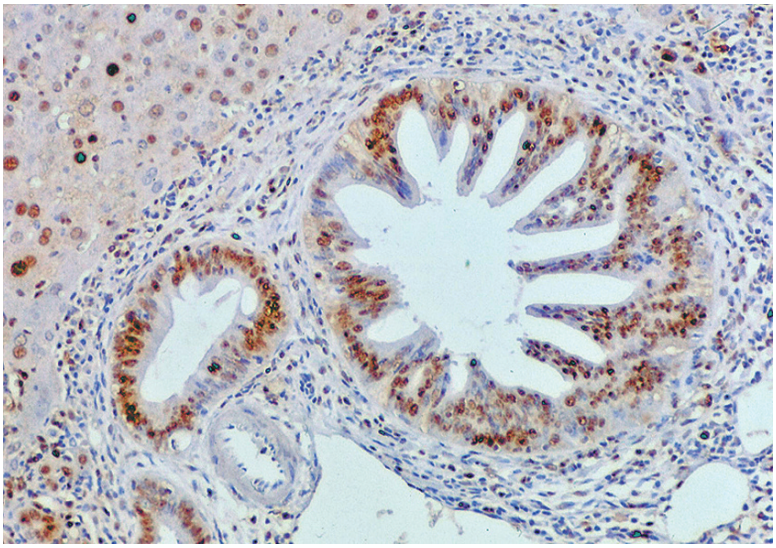

Fig. 9.5 Accelerated cell proliferation in biliary epithelium stained with anti-PCNA/horseradish peroxidase. Note the labeling of most epithelial cells in the intrahepatic bile duct of a hamster from the CIDB group (×200) ([38], with permission)

Table 9.6 Proliferating cell nuclear antigen labelling indices (%)

Groups	No. of hamsters	Intrahepatic bile duct epithelium	Extrahepatic bile duct epithelium	Gallbladder epithelium	Pancreatic duct epithelium
Control	10	7.4 ± 2.8	0.3 ± 0.1	0.4 ± 0.3	0.2 ± 0.1
CDDB	10	11.4 ± 1.9	26.0 ± 1.5***	33.8 ± 2.3***	2.5 ± 1.0
CIDB	10	29.7 ± 4.4*,**	0.9 ± 0.5**	6.3 ± 0.8**,****	4.8 ± 2.8

Expressed as mean ± SE.
CDDB, cholecystoduodenostomy with dissection of the distal end of the common duct; CICD, cholecystoileostomy with dissection of the distal end of the common duct.
$^{*}p < 0.01$ vs. Control.
$^{**}p < 0.01$ vs. CDDB.
$^{***}p < 0.01$ vs. Control.
$^{****}p < 0.05$ vs. Control. (modified from [38], with permission)

9.14 Comments

The fact that patients with PBM are prone to gallbladder and extrahepatic bile duct carcinomas, but not generally to intrahepatic bile duct carcinomas suggests that the mechanisms of carcinogenesis of the biliary tree are different [27–29]. Biliary carcinoma was significantly enhanced by BOP in the CDDB hamster model [8]. In this model, the maximum diameter of the extrahepatic bile duct was significantly greater than that in controls. Moreover, the extrahepatic bile duct was significantly more dilated

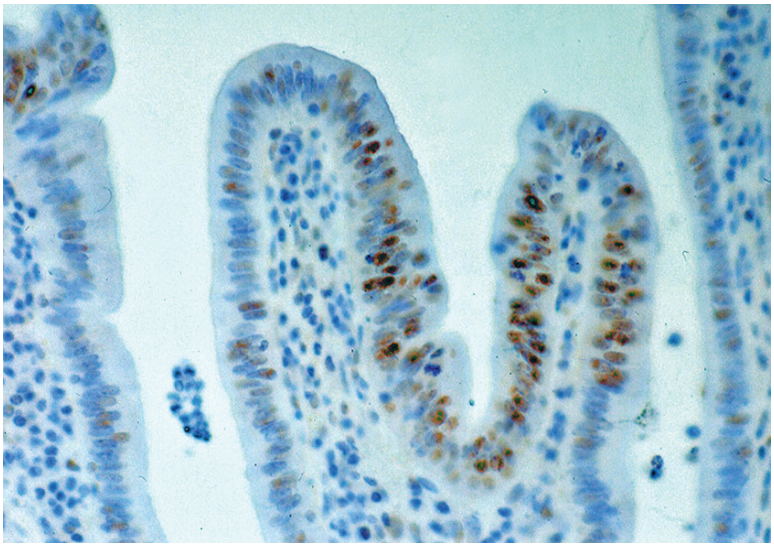

Fig. 9.6 PCNA staining of the gallbladder in a hamster from the CDDB group, showing labeling of many nuclei (×400)

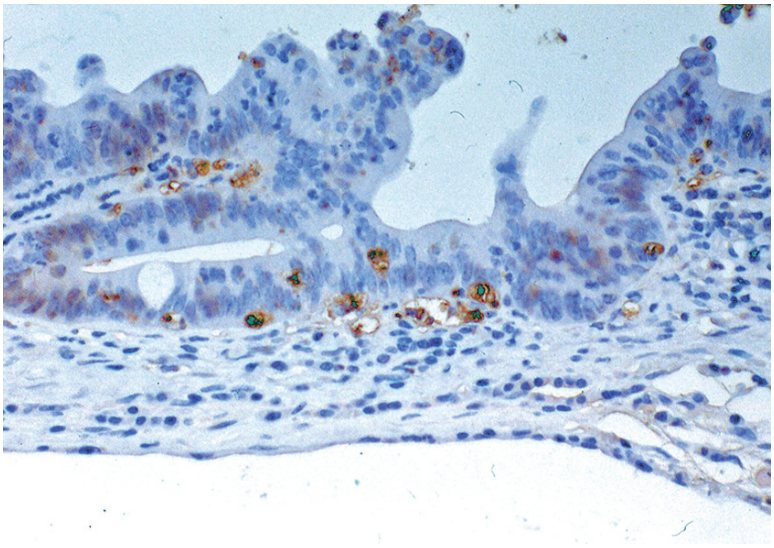

Fig. 9.7 PCNA staining of the extrahepatic bile duct in a hamster from the CDDB group with labeling of many cells, especially at the base of the epithelium (×400)

in the CIDB group than that in the control group, but less than in the CDDB group. This is analogous with the human situation, when patients who have PBM without choledochal dilatation are most prone to the development of gallbladder cancer [31]. Accordingly, the CDDB group, resembling PBM with choledochal dilatation, had a significantly higher incidence of biliary carcinoma than the control group. On the other hand, the CIDB group, resembling patients without choledochal dilatation, had no significant increase in extrahepatic bile duct and gallbladder carcinogenesis, compared with the control group. These results suggest that resection of the extrahepatic bile duct in PBM patients with choledochal dilatation and prophylactic cholecystectomy in PBM patients without choledochal dilatation may be therapeutic [31].

The biliary tract was more dilated after CDDB than after CIDB. The fact that significant dilatation of the extrahepatic bile duct without jaundice was observed in the CDDB group of the 2-week study suggests that a factor in the refluxed duodenal juice rather than stenosis caused by bilioenterostomy, was responsible for the choledochal dilatation.

We found that exogenous CCK octapeptide promoted the carcinogenicity of the intrahepatic bile duct carcinoma, and that loxiglumide (CCK receptor antagonist) inhibited its effect in the CDDB + BOP hamster model [7]. In rats and humans, the drainage of pancreatic juice and bile from the duodenum and jejunum is known to stimulate endogenous CCK release from CCK-secreting cells [32,33]. In the CIDB group, which had pancreaticobiliary drainage, fasting CCK bioactivity was elevated significantly in the 2-week study, but not in the 16-week study. This finding is consistent with the possibility that endogenous CCK-secreting cells in the fasting state are exhausted over 4 weeks of endogenous stimulation [34]. In the postprandial state, the plasma CCK levels in the CIDB group were higher than in the control and CDDB groups [34]. The lower CCK levels in the 2-week CDDB group could be attributed to the continuous flow of pancreatic juice and bile through the cholecystoduodenostomy into the duodenum. Moreover, the high but not significant CCK levels in the CDDB group in the 16-week study could have been due to impairment of pancreaticobiliary flow by the gallbladder cancer and extrahepatic bile duct carcinoma, as evidenced by the development of jaundice.

In the 16-week study, intrahepatic bile duct carcinoma was observed mainly in the CIDB group with stimulated release of endogenous CCK in pancreaticobiliary juice from the first part of small intestine. The oversecretion of endogenous CCK in BOP-treated hamsters, and the administration of pharmacological doses of exogenous CCK seem to induce intrahepatic bile duct carcinoma [30]. On the other hand, carcinoma of the extrahepatic bile duct and the gallbladder were significantly higher in the CDDB group, in which the common bile duct was dilated even in the 2-week study. Therefore, it seems that the factors promoting choledochal dilatation in hamsters also promote carcinoma of the gallbladder and the extrahepatic bile duct, as in humans with PBM [27–29].

The non-tumorous epithelium of the intrahepatic bile duct in the CIDB group and the non-neoplastic epithelium of the extrahepatic bile duct and the gallbladder in the CDDB group were mainly labeled with PCNA, which labels the intranuclear protein engaged in the cell cycle essential for cellular DNA synthesis [35,36].

The acceleration of DNA synthesis in the intrahepatic bile duct epithelium by endogenous CCK release or by inflammation induced by the reflux of duodenal juice could provoke BOP carcinogenesis in the intrahepatic bile duct in the CIDB or CDDB group [18,19]. Gallbladder carcinoma and extrahepatic bile duct carcinoma rarely develop from BOP in hamsters with a long common duct. Consequently, it could be assumed that the mixture of pancreatic juice, bile, and refluxed duodenal juice is essential for inflammation of the common bile duct. None of the procedures affected the incidence of pancreatic cancer, possibly because of the lower LI of the pancreatic ductal cells. Pancreatic carcinoma in hamsters is believed to be activated by BOP without the presence of pancreatitis [37].

In conclusion, the present study suggests that the reflux of intestinal and pancreatic juice into the bile duct plays an important role in BOP carcinogenesis of the gallbladder and extrahepatic bile duct and this event also amplifies the dilatation of the biliary duct.

C. Bile Acids and Their Absorbents

9.15 Summary

The effects of tauroursodeoxycholate (TUDC) and cholestyramine resin (CR) on biliary carcinogenesis were investigated in the hamster model. Syrian hamsters were subjected to cholecystoduodenostomy with dissection of the extrahepatic bile duct on the distal end of the common duct (CDDB). The hamsters were randomly divided into the following three groups: a control group, a TUDC group, and a CR group. Pancreaticobiliary cancer was induced by *N*-nitrosobis(2-oxopropyl)amine in all animals. The experiment was terminated in week 16 and the number of neoplastic lesions was counted microscopically. In the TUDC group, intrahepatic biliary carcinogenesis was more accelerated than in the control group, but no promoting effect was seen in the pancreas, gallbladder, or extrahepatic bile duct. In the CR group, both intrahepatic biliary and gallbladder carcinogenesis were more suppressed than in the control and TUDC groups. Thus, TUDC enhanced intrahepatic bile duct carcinogenesis, whereas CR inhibited both intrahepatic bile duct and gallbladder carcinoma. This indicates that bile acids induce biliary carcinoma in the hamster model.

9.16 Introduction

The etiology of biliary cancer is obscure. Hamsters subjected to bilioenterostomy with *N*-nitrosobis(2-oxopropyl)amine (BOP), which is a model of choledochal cyst with an anomalous pancreaticobiliary maljunction, have a high incidence of bile duct carcinoma, similar to that in humans [8]. Moreover, our studies have demonstrated

that the exogenous administration of cholecystokinin (CCK) and the endogenous stimulation of CCK induced by bilioenterostomy accelerate intrahepatic biliary carcinogenesis in hamsters [30,38].

The absence or shortage of bile acids in the upper part of the small intestine is known to stimulate endogenous CCK secretion [39]. In fact, some bile acids are suggested to be cytotoxic and carcinogenic to the biliary epithelium [40,41]. However, ursodeoxycholic acid and chenodeoxycholic acid are used in the treatment of patients with cholestasis caused by primary biliary cirrhosis or primary sclerosing cholangitis, to increase bile flow.

In this study, the effects of oral tauroursodeoxycholate (TUDC), a taurine conjugate of ursodeoxycholate, and cholestyramine resin (CR), a non-absorbable bile salt binding resin, on biliary carcinogenesis were evaluated in the hamster model.

9.17 Experimental Protocol

Non-inbred 7-week-old female Syrian golden hamsters (SLC, Inc., Shizuoka, Japan) were used. The animals were housed individually in plastic cages on sawdust bedding in an air-conditioned room with an alternate 12 h light and dark cycle, at 24 ± 2 °C with 50 ± 20% humidity. They were fed a CE-2 pelleted diet (fat 4.4% and protein 24.8%, Clea Japan, Inc., Tokyo, Japan). Animals were checked daily and weighed weekly during the experiment. BOP and CR were purchased from Nakarai Tesque (Kyoto, Japan) and Sigma Chemical Co. (St. Louis, MO), respectively. TUDC was donated by Tokyo Tanabe Co. Ltd. (Tokyo, Japan).

A cholecystoduodenostomy with dissection of the extrahepatic bile duct at the distal end of the common duct (CDDB) was performed on 90 animals under sodium pentobarbital anesthesia administered intraperitoneally at a dose of 50 mg/kg body weight. Of the total 90 hamsters, 73 tolerated the procedures up until postoperative day 7, and 17 died early of biliary peritonitis. The surviving animals were divided into three groups as follows: 27 hamsters were given water (control group); 23 were given water containing 1% (w/w) TUDC (TUDC group); and 23 were given water containing 4% (w/w) CR (CR group). Animals had free access to the water throughout the experimental period. The animals were given BOP in 0.9% saline at a dose of 10 mg/kg body weight, subcutaneously, weekly for 9 weeks. All animals were killed in postoperative week 16.

After the hamsters were fasted overnight, they were killed by exsanguination, and the liver, duodenum, biliary system, and pancreas were removed. The pancreas was spread out on a piece of paper to ensure a maximal transectional area for subsequent sectioning. A portion of the liver, an area of the anastomosis including the duodenum, the common bile duct, and the duodenal segment of the pancreas were embedded en bloc and cut in step sections (five sections per animal). Histological sections were stained with haematoxylin and eosin, and examined by light microscopy. The grade of pancreatitis and cholangitis was assessed by the degree of inflammatory cell infiltration and fibrosis, and scored as follows: severe, 3; moderate, 2; and mild to none; 1 (see Chapter 7). Pancreaticobiliary neoplastic lesions

were counted by anatomic location in representative sections. A pathologist without any knowledge of the case blindly examined all histological specimens.

Blood samples, collected in ice-chilled tubes containing heparin were left in an ice-bath until centrifugation (3,000 rpm) at 4 °C for 10 min. Total bilirubin levels were measured by the Bilirubin B II-Test (Wako, Osaka, Japan) and bilirubinemia was diagnosed when levels exceeded 3 mg/dl. Total bile acids in plasma were measured using Enzabile 2 (Nycomed Pharmacia, Oslo, Norway). The remaining plasma was stored at −80 °C until CCK was extracted and concentrated on Sep Pac C18 cartridges (Waters Assoc., Milford, MA). Plasma CCK levels were measured by bioassay using dispersed acini, as described elsewhere [12].

The incidence of tumor production and bilirubinemia was analyzed statistically using the chi-square test with continuity correction. Student's *t* test was also used to compare total bile acids and plasma CCK bioactivity.

9.18 Survival Rate in Each Group

All animals survived for at least 13 weeks of the experiment, but then some died of the pancreaticobiliary tumor. During weeks 15 and 16, significantly lower survival rates were observed in the TUDC group (58% and 38%, respectively) than in the control (100% and 100%, respectively) and CR groups (95% and 90%, respectively; $p < 0.01$, Figure 9.8).

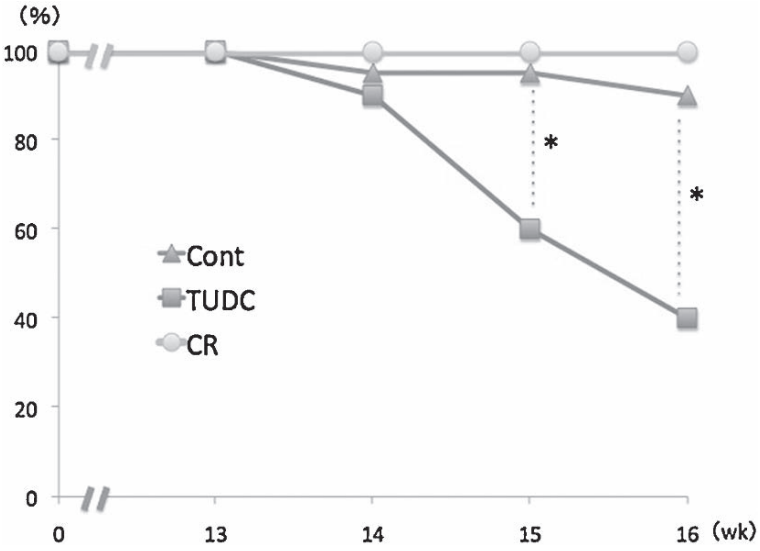

Fig. 9.8 Survival curve of the BOP-treated hamsters after cholecystoduodenostomy with dissection of the extrahepatic bile duct at the distal end of the common duct below the opening of the pancreatic duct. The survival rate of the TUDC group was low after 15 weeks of the experiment ($^{*}p < 0.01$). Cont, control group; CR, cholestyramine resin group; TUDC, tauroursodeoxycholate group (modified from [51], with permission)

9.19 Bilirubinemia, Total Bile Acids, and CCK

The TUDC group had a significantly higher rate of jaundice than the control and CR groups (83% vs. 19% and 9%, respectively; $p < 0.01$). Total bile acids were also significantly higher in the TUDC group than in the control and CR groups ($p < 0.01$, Figure 9.9). Figure 9.10 shows a significant decrease in plasma CCK levels in the TUDC group compared with the control ($p < 0.05$).

9.20 Carcinoma in the Biliary System and the Pancreas

The incidence of intrahepatic bile duct carcinoma was significantly higher in the TUDC group than in the control group ($p < 0.01$), but significantly lower in the CR group than in the control and TUDC groups ($p < 0.01$; Table 9.7). No significant difference in the incidence of carcinoma was noted in either the extrahepatic bile duct or the pancreas (Tables 9.8. and 9.9). However, the incidence of gallbladder carcinoma was lower in the CR group than in the control and TUDC groups ($p < 0.01$). Moreover, the mean number of pancreatic carcinomas in the tumor-bearing animals in the CR group was significantly lower than in the control and TUDC groups ($p < 0.01$). Histologically, most of the lesions in the intrahepatic bile duct and pancreas were tubular adenocarcinoma (Tables 9.7. and 9.9).

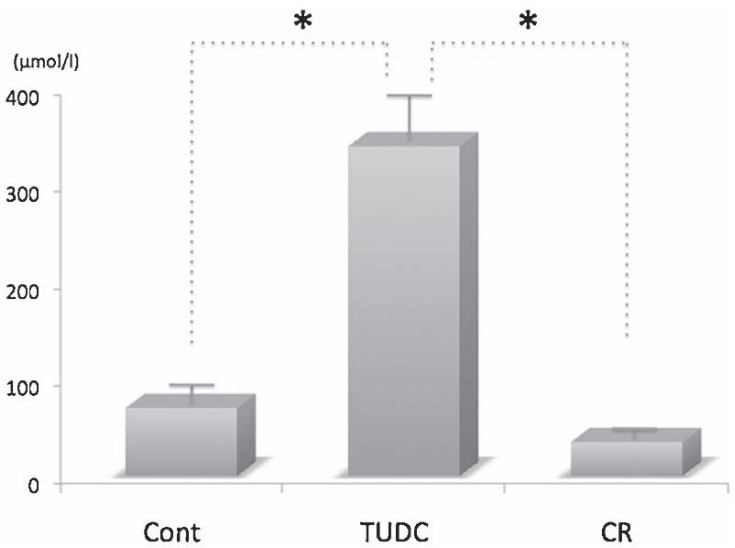

Fig. 9.9 Serum total bile acid levels in the three groups after 16 weeks of the experiment. Cont, control group (66.8 μmol/l); TUDC, tauroursodeoxycholate group (348.0 μmol/l); CR, cholestyramine resin group (25.4 μmol/l), respectively ($^{*}p < 0.01$) (modified from [51], with permission)

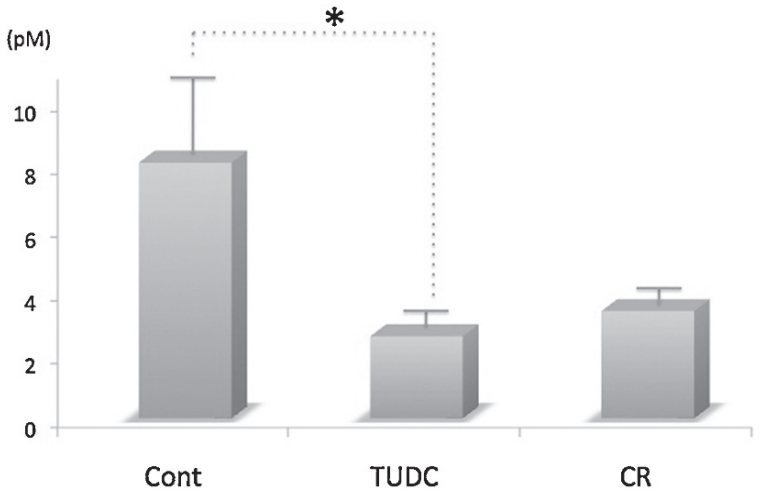

Fig. 9.10 Plasma cholecystokinin levels in the three groups after 16 weeks of the experiment. Cont, control group (8.14 pM); TUDC, tauroursodeoxycholate group (2.66 pM); CR, cholestyramine resin group (3.63 pM), respectively ($^{*}p < 0.05$) (modified from [51], with permission)

Table 9.7 Carcinoma of the intrahepatic bile duct

Group	No. of hamsters	No. with carcinoma (%)	No. of carcinoma (No. per TBA)	Histology		
				Tubular	Papillary	Others
Control	27	15(56)	52(3.5)	46	1	5[a]
TUDC	23	22(96)*	182(8.3)*	181	0	1[b]
CR	23	1(4)*,**	1(1)**	1	0	0

TBA, tumor bearing animal; TUDC, tauroursodeoxycholate; CR, cholestyramine resin.
$^{*}p < 0.01$ compared to Control.
$^{**}p < 0.01$ compared to TUDC.
[a]Schirrus:3, mucinous:1, cystadenocarcinoma:1.
[b]Mucinous:1. (modified from [51], with permission)

Table 9.8 Carcinomas of the extrahepatic bile duct and of the gallbladder

Group	No. of hamsters	No. with carcinoma (%)	
		Extrahepatic bile duct	Gallbladder
Control	27	4(15)	11(41)
TUDC	23	0	6(26)
CR	23	1(4)	0*,**

TUDC, tauroursodeoxycholate, CR, cholestyramine resin.
$^{*}p < 0.01$ compared to Control.
$^{**}p < 0.05$ compared to TUDC. (modified from [51], with permission)

Table 9.9 Carcinoma of the pancreas

Group	No. of hamsters	No. with carcinoma (%)	No. of carcinoma (No.per TBA)	Histology		
				Tubular	Papillary	Others
Control	27	21(78)	51(2.4)	41	6	4[a]
TUDC	23	20(87)	49(2.5)	44	1	4[b]
CR	23	12(52)	15(1.3)[*,**]	15	0	0

TBA, tumor bearing animal; TUDC, tauroursodeoxycholate; CR: cholestyramine resin.
[*] $p < 0.01$ compared to Control
[**] $p < 0.01$ compared to TUDC
[a]Papillary-cystic:2, cystadenocarcinoma:2.
[b]Papillary-cystic:4. (modified from [51], with permission)

9.21 Grades of Cholangitis and Pancreatitis

Figures 9.11 and 9.12 show the grades of cholangitis and pancreatitis. The grade of cholangitis in the TUDC group was significantly higher than those in the control and CR groups ($p < 0.01$), whereas the grade of pancreatitis was significantly lower in the CR group than in the control and TUDC groups ($p < 0.01$).

9.22 Comments

In postoperative week 16, the incidence of intrahepatic bile duct carcinoma in the CDDB model was higher than in the sham-operated controls (see Chapter 5). When pancreaticobiliary juice drained into the ileum instead of the duodenum in this hamster bilioenterostomy model, the absence of protease activity in the upper small intestine stimulated endogenous CCK release, inducing intrahepatic bile duct carcinogenesis [38]. CCK is also thought to accelerate intrahepatic bile duct carcinoma in humans and hamsters [30]. Interestingly, CCK release in the CR group was lower than that in the control group, when the animals were killed, which raises the question about whether exogenous bile acid intake or endogenous bile acid shortage inhibits biliary carcinogenesis. Before the experiment was terminated, we expected that TUDC would inhibit intrahepatic carcinogenesis as well as CCK release, and that CR would maximize both these effects. We thought that the CCK releasing cells were exhausted by long-term CR stimulation, but boosted with food intake stimulation [34]. Contrary to our hypothesis, this experiment showed that TUDC promoted intrahepatic bile duct carcinoma in this hamster model. More than half of the animals in the TUDC group had died of intrahepatic bile duct carcinoma with jaundice by week 16. Conversely, CR inhibited both intrahepatic and pancreatic carcinogenesis, and the survival rate of the CR group at the end of the experiment was the same as that of the control group.

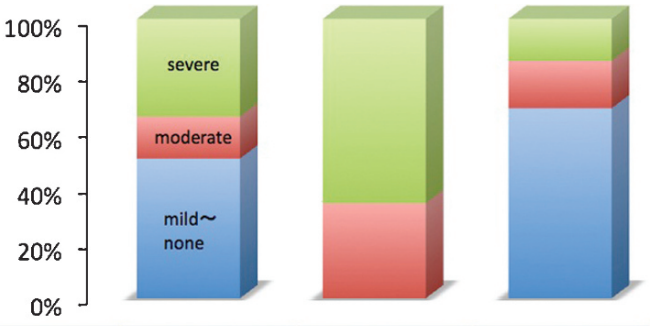

	Cont	TUDC*	CR
Mean	1.9	2.7	1.4
SE	0.2	0.1	0.2

*;p<0.01 compared to Cont and CR

Fig. 9.11 Grades of cholangitis in the three groups after 16 weeks of the experiment (*$p < 0.01$ vs. Cont and CR). Cont, control group; TUDC, tauroursodeoxycholate group; CR, cholestyramine resin group (modified from [51], with permission)

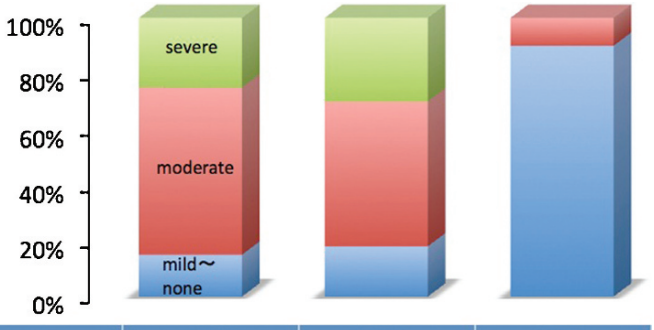

	Cont	TUDC	CR*
Mean	2.1	2.1	1.1
SE	0.1	0.2	0.1

*;p<0.01 compared to Cont and TUDC

Fig. 9.12 Pancreatitis scores in the three groups after 16 weeks of the experiment (*$p < 0.01$ vs. Cont and TUDC). Cont, control group; TUDC, tauroursodeoxycholate group; CR, cholestyramine resin group (modified from [51], with permission)

TUDC is a taurine conjugated ursodeoxycholate, commonly used in the treatment of cholestasis [42]. TUDC has also been reported to have a cytoprotective effect against hepatocytes [43–45]. The oral administration of TUDC inhibits endogenous CCK levels under pancreaticobiliary extracorporeal drainage [46]. Furthermore, some bile acids have been reported to induce experimental biliary carcinogenesis [40]. It was thought that TUDC would induce intrahepatic biliary carcinogenesis by an unknown mechanism. CR conjugates with bile acids *in vivo*, then carries them out

of the body, disrupting the enterohepatic circuit of bile acids [47]. Therefore, CR is used in the treatment of patients with familial hyperlipemia to reduce serum cholesterol levels. It was thought that CR would affect pancreaticobiliary carcinogenesis by reducing the endogenous bile acids.

Cholangitis is suspected to be a precancerous lesion predisposing to the later development of intrahepatic bile duct carcinoma [48]. In both parasitic and idiopathic hepatolithiasis, intrahepatic bile duct carcinoma arises after long-term inflammation [49,50]. It is unclear whether cholangitis or bile duct carcinoma comes first in this hamster model. As CR could have inhibited inflammation in the intrahepatic bile duct by absorbing bile acids, we suspected that bile acids played a major role in the inflammation process, which resulted in carcinogenesis of the intrahepatic bile duct. Conversely, CR decreased the incidence of pancreatitis, whereas TUDC had no effect. These data suggest that CR stops the process of cholangitis and pancreatitis by absorbing endogenous bile acids, thereby preventing intrahepatic biliary and pancreatic carcinogenesis.

In conclusion, TUDC induced intrahepatic bile duct carcinoma, probably by injuring the biliary epithelium in the process of cholangitis, whereas CR inhibited cholangitis and pancreatitis, thus reducing intrahepatic carcinoma, gallbladder carcinoma, and pancreatic carcinoma. The direct cytotoxicity of TUDC on the epithelium was thought to play a greater role in biliary carcinogenesis than the endogenous CCK pathway.

References

1. Tsunoda T, Eto T, Koga M, Tomioka T, Motoshima K, Yamaguchi T, Izawa K, Tsuchiya R. Early carcinoma of the extrahepatic bile duct. Jpn J Surg 1989 19(6):691–698.
2. Lamote J, Willems G. DNA synthesis, cell proliferation index in normal and abnormal gallbladder epithelium. Microsc Res Tech 1997 38:609–615.
3. Barrowman JA. The tropic action of gastro-intestinal hormones. Digestion 1975 12(2):92–104.
4. Lamote J, Putz P, Willems G. Effect of cholecystokinin-octapeptide, caerulein, and pentagastrin on epithelial cell proliferation in the murine gallbladder. Gastroenterology 1982 83(2):371–377.
5. Douglas BR, Woutersen RA, Jansen JB, de Jong AJ, Rovati LC, Lamers CB. Influence of cholecystokinin antagonist on the effects of cholecystokinin and bombesin on azaserine-induced lesions in rat pancreas. Gastroenterology 1989 96(2 Pt 1):462–469.
6. Douglas BR, Woutersen RA, Jansen JB, de Jong AJ, Rovati LC, Lamers CB. Modulation by CR-1409 (lorglumide), a cholecystokinin receptor antagonist, of trypsin inhibitor-enhanced growth of azaserine-induced putative preneoplastic lesions in rat pancreas. Cancer Res 1989 49(9):2438–2441.
7. Evers BM, Gomez G, Townsend CM Jr, Rajaraman S, Thompson JC. Endogenous cholecystokinin regulates growth of human cholangiocarcinoma. Ann Surg 1989 210(3):317–322.
8. Tajima Y, Eto T, Tsunoda T, Tomioka T, Inoue K, Fukahori T, Kanematsu T. Induction of extrahepatic biliary carcinoma by *N*-nitrosobis(2-oxopropyl)amine in hamsters received cholecystoduodenostomy with dissection of the common duct. Jpn J Cancer Res 1994 85:780–788.
9. Solomon TE, Petersen H, Elashoff J, Grossman MI. Interaction of caerulein and secretin on pancreatic size and composition in rat. Am J Physiol 1978 235(6):E714–19.
10. Setnikar I, Bani M, Cereda R, Chisté R, Makovec F, Pacini MA, Revel L. Anticholecystokinin activities of loxiglumide. Arzneimittelforschung 1987 37(10):1168–1171.
11. Liddle RA, Goldfine ID, Williams JA. Bioassay of plasma cholecystokinin in rats: effects of food, trypsin inhibitor, and alcohol. Gastroenterology 1984 87(3):542–549.

12. Otsuki M, Okabayashi Y, Nakamura T, Fujii M, Tani S, Fujisawa T, Koide M, Baba S. Bioassay of plasma cholecystokinin in rat and human: inhibition of protein synthesis prevents the decrease in the sensitivity and responsiveness of isolated rat pancreatic acini to CCK-8. Pancreas 1989 4:447–451.
13. Douglas BR, Woutersen RA, Jansen JBMJ, Rovati LC, Lamers CBHW. Study into the role of cholecystokinin in bombesin-stimulated pancreatic growth in rats and hamsters. Eur J Pharmacol 1989 161:209–214.
14. Meijers M, van Garderen-Hoetmer A, Lamers CBHW, Rovati LC, Jansen JBMJ, Woutersen RA. Role of cholecystokinin in the development of BOP-induced pancreatic lesions in hamsters. Carcinogenesis 1990 11:2223–2226.
15. Chu M, Rehfeld JF, Borch K. Chronic endogenous hypercholecystokininemia promotes pancreatic carcinogenesis in the hamster. Carcinogenesis 1997 18:315–320.
16. Meijers M, van Garderen-Hoetmer A, Lamers CBHW, Rovati LC, Jansen JBMJ, Woutersen RA. Effect of bombesin on the development of *N*-nitrosobis(2-oxopropyl)amine-induced pancreatic lesions in hamsters. Cancer Lett 1991 59:45–50.
17. Pour PM, Lawson T, Helgeson S, Dennelly T, Stepan K. Effect of cholecystokinin on pancreatic carcinogenesis in the hamster model. Carcinogenesis 1988 9:597–601.
18. Scarpelli DG, Rao MS, Subbarao V. Augmentation of carcino-geniesis by *N*-nitrosobis (2-oxopropyl)amine administered during S phase of the cell cycle in regenerating hamster pancreas. Cancer Res 1983 43:611–616.
19. Flanigan DP. Biliary cysts. Ann Surg 1975 182:635–643.
20. Tsuchiya R, Harada N, Ito T, Furukawa M, Yoshihiro I, Kusano T, Uchimura M. Malignant tumors in choledochal cysts. Ann Surg 1977 186:22–28.
21. Tada M, Omata M, Ohto M. High incidence of *ras* gene mutation in intrahepatic cholangiocarcinoma. Cancer 1992 69:1115–1118.
22. Schwarzendrube J, Niederau M, Luthen R, Niederau C. Effects of cholecystokinin-receptor blockade on pancreatic and biliary function in healthy volunteers. Gastroenterology 1991 100:1683–1690.
23. Malesci A, de Fazio C, Festorazzi S, Bonato C, Valentini A, Tacconi M, Rovati L, Setnikar I. Effect of loxiglumide on gallbladder contractile response to caerulein and food in humans. Gastroenterology 1990 98:1307–1310.
24. Konturek JW, Konturek SJ, Kurek A, Bogdal J, Oleksy J, Rovati L. CCK receptor antagonism by loxiglumide and gallbladder contractions in response to cholecystokinin, sham feeding and ordinary feeding in man. Gut 1989 30:1136–1142.
25. Nio Y, Tsubono M, Morimoto H, Kawabata K, Masai Y, Hayashi H, Manabe T, Imamura M, Fukumoto M. Loxiglumide (CR-1505), a cholecystokinin antagonist, specifically inhibits the growth of human pancreatic cancer lines xenografted into nude mice. Cancer 1993 72:3599–3606.
26. Japanese Pancreaticobiliary Maljunction Meeting. Diagnostic criteria of pancreaticobiliary maljunction. J Hepatobiliary Pancreat Surg 1994 1:219–221
27. Miyazaki M, Takada T, Miyakawa S, Tsukada K, Nagino M, Kondo S, Furuse J, Saito H, Tsuyuguchi T, Chijiiwa K, Kimura F, Yoshitomi H, Nozawa S, Yoshida M, Wada K, Amano H, Miura F. Risk factors for biliary tract and ampullary carcinomas and prophylactic surgery for these factors. J Hepatobiliary Pancreat Surg 2008 15:15–24.
28. Sai JK, Suyama M, Kubokawa Y, Nobukawa B. Gallbladder carcinoma associated with pancreatobiliary reflux. World J Gastroenterol 2006 12:6527–6530.
29. Kimura K, Ohto M, Saisho H, Unozawa T, Tsuchiya Y, Morita M, Ebara M, Matsutani S, Okuda K. Association of gallbladder carcinoma and anomalous pancreaticobiliary ductal union. Gastroenterology 1985 89:1258–1265.
30. Ikematsu Y, Tomioka T, Tajima Y, Tsnoda T, Kanematsu T. Enhancement of biliary carcinogenesis in hamsters by cholecystokinin. Word J Surg 1995 19(6):847–851.
31. Kamisawa T, Tu Y, Kuwata G, Egawa N, Nakajima H, Tsuruta K, Okamoto A, Matsukawa M. Biliary carcinoma risk in patients with pancreaticobiliary maljunction and the degree of extrahepatic bile duct dilatation. Hepatogastroenterology 2006 53:816–818.

32. Koop I, Dorn S, Koop H, Witzleb S, Beglinger C, Schafmayer A, Arnold R. Dissociation of cholecystokinin and pancreaticobiliary response to intraduodenal bile acid and cholestyramine in humans. Dig Dis Sci 1991 36:1625–1632.
33. Davies HA, Wheeler MH, Psaila J, Rhodes J, Newcombe RG, Jones JM, Procter D, Adrian TE, Bloom SR. Bile exclusion from the duodenum. Its effect on gastric and pancreatic function in the dog. Dig Dis Sci 1985 30:954–960.
34. Koop I, Fellgiebel A, Koop H, Schafmayer A, Arnold R. Effect of cholestyramine on plasma cholecystokinin and pancreatic polypeptide levels, and exocrine pancreatic secretion. Eur J Clin Invest 1988 18:517–523.
35. Mathews MB, Bernstein RM, Franza BR, Garrels JI. Identity of the proliferating cell nuclear antigen and cyclin. Nature 1984 309:374–376.
36. Bravo R, Frank R, Blundell PA, MacDonald BH. Cyclin/PCNA is the auxiliary protein of DNA polymerase delta. Nature 1987 326:515–517.
37. Pour P, Takahashi M, Donnelly T, Stepan K. Modification of pancreatic carcinogenesis in the hamster model. IX. Effect of pancreatitis. J Natl Cancer Inst 1983 71:607–613.
38. Ikematsu Y, Tomioka T, Yamanaka S, Tajima Y, Tsunoda T, Kanematsu T. Bilioenterostomy enhances biliary carcinogenesis in hamsters. Carcinogenesis 1996 17:1505–1509.
39. Koop I. Regulation of CCK Release by Bile Acids: CCK Antagonists in Gastroenterology. Springer-Verlag: Berlin Heidelberg. 1991, pp. 152–158.
40. Kinami Y, Ashida Y, Gotoda H, Seto K, Kojima Y, Takashima S. Promoting effects of bile acid load on the occurrence of cholangiocarcinoma induced by diisopropanol-nitrosamine in hamsters. Oncology 1993 50:46–51.
41. Park JY, Park BK, Ko JS, Bang S, Song SY, Chung JB. Bile acid analysis in biliary tract cancer. Yonsei Med J 2006 47:817–825.
42. Caglieris S, Giannini E, Dardano G, Mondello L, Valente U, Testa R. Tauroursodeoxycholic acid administration as adjuvant therapy in cirrhotic patients on transplantation waiting lists. Hepatogastroenterology 2000 47:1045–1047.
43. Schoemaker MH, Gommans WM, Conde de la Rosa L, Homan M, Klok P, Trautwein C, van Goor H, Poelstra K, Haisma HJ, Jansen PL, Moshage H. Resistance of rat hepatocytes against bile acid-induced apoptosis in cholestatic liver injury is due to nuclear factor-kappa B activation. J Hepatol 2003 39:153–161.
44. Schoemaker MH, Conde de la Rosa L, Buist-Homan M, Vrenken TE, Havinga R, Poelstra K, Haisma HJ, Jansen PL, Moshage H. Tauroursodeoxycholic acid protects rat hepatocytes from bile acid-induced apoptosis via activation of survival pathways. Hepatology 2004 39:1563–1573.
45. Tsukahara K, Kanai S, Ohta M, Kitani K. Taurine conjugate of ursodeoxycholate plays a major role in the hepatoprotective effect against cholestasis induced by taurochenodeoxycholate in rats. Liver 1993 13:262–269.
46. Miyasaka K, Funakoshi A, Shikado F, Kitani K. Stimulatory and inhibitory effects of bile salts on rat pancreatic secretion. Gastroenterology 1992 102:598–604.
47. Poley JR. Fat digestion and absorption in lipase and bile acid deficiency. In: Rommel K, Goebell HD, eds. Lipid Absorption: Biochemical and Clinical Aspects. MTP Press: Lancaster. 1976, pp. 151–202.
48. Chu KM, Lo CM, Liu CL, Fan ST. Malignancy associated with hepatolithiasis. Hepatogastroenterology. 1997 44:352–357.
49. Ohshima H, Bandaleetova TY, Brouet I, Bartsch H, Kirby G, Ogunbiyi F, Vatanasapt V, Pipitgool V. Increased nitrosamine and nitrate biosynthesis mediated by nitric oxide synthase induced in hamster infected with liver fluke (Opisthorchis viverrini). Carcinogenesis 1994 15:271–275.
50. Zhou YM, Yin ZF, Yang JM, Li B, Shao WY, Xu F, Wang YL, Li DQ. Risk factors for intrahepatic cholangiocarcinoma: a case-control study in China. World J Gastroenterol 2008 14:632–635.
51. Ikematsu Y, Tomioka T, Kitajima T, Inoue K, Tajima Y, Kanematsu T. Tauroursodeoxycholate and cholestyramine enhance biliary carcinogenesis in hamsters. World J Surg. 2000 24:22–26.

Chapter 10
Chemoprevention of Biliary Carcinogenesis

Noritsugu Tsuneoka, Tamotsu Kuroki, Tomoo Kitajima, Kenzo Fukuda, Shinya Onizuka, Yoshitsugu Tajima, and Takashi Kanematsu

A. Cyclooxygenase-2-specific Inhibitor

10.1 Summary

This study was conducted to find out if etodolac, a cyclooxgenase-2 (COX-2)-specific inhibitor, could prevent chemically induced biliary carcinogenesis in bilioenterostomized hamsters. Syrian golden hamsters were subjected to choledochojejunostomy and then given subcutaneous injections of *N*-nitrosobis (2-oxopropyl)amine (BOP) 10 mg/kg body weight every 2 weeks. BOP was started 4 weeks after surgery, and continued for 18 weeks. The animals were simultaneously given etodolac 10 mg/kg body weight in 0.5% methylcellulose solution orally three times per week (etodolac group). The control hamsters were administered methylcellulose solution alone. The hamsters were killed 22 weeks after surgery, and the biliary carcinomas were examined histologically. The presence and degree of cholangitis and the cell kinetic status of the biliary epithelium were also evaluated with special reference to biliary carcinogenesis. Intrahepatic bile duct carcinomas developed in 15 (88%) of 17 hamsters in the control group, but in only 6 (33%) of 18 hamsters in the etodolac group ($P < 0.01$). The incidence and number of developing biliary carcinomas correlated well with the degree of cholangitis, and severe cholangitis was evident in the controls. The cell kinetic study demonstrated that the proliferating cell nuclear antigen-labeling index of the biliary epithelium was 9.67% in the control group and 5.14% in the etodolac group ($P < 0.05$). The mean levels of prostaglandin E2 (PGE2) products in the liver tissue were 14.14 ± 3.31 pg/total protein (TP) mg in the control group, and 7.46 ± 2.34 pg/TP mg in the etodolac group ($P < 0.05$). These findings indicated that etodolac inhibited the occurrence of severe cholangitis and the acceleration of biliary epithelial cell kinetics after bilioenterostomy, thereby preventing BOP-induced biliary carcinogenesis in hamsters. In conclusion, the COX-2-specific inhibitor, etodolac, could be used to prevent not only reflux cholangitis, but also biliary carcinoma after bilioenterostomy.

Y. Tajima et al. (eds.), *Hepatobiliary and Pancreatic Carcinogenesis in the Hamster*,
DOI: 10.1007/978-4-431-87773-8_10, © Springer 2009

10.2 Introduction

Bilioenterostomy is commonly performed in hepatobiliary pancreatic surgery; however, it is often complicated by reflux cholangitis [1–3], biliary stones [3,4], and liver abscess [2]. Recent clinical studies have shown that biliary carcinomas can occur as a delayed complication of bilioenterostomy for benign diseases [5–7] In Chapters 7 and 8, we showed that persistent reflux cholangitis after bilioenterostomy accelerated biliary carcinogenesis by activating biliary epithelial cell kinetics in hamsters [8,9].

Non-steroidal anti-inflammatory drugs (NSAIDs) are known to have anticarcinogenic effects on chemically induced or genetic mutational carcinogenesis [10–15]. Numerous epidemiological studies have provided evidence that NSAIDs reduce the incidence of colorectal cancer in humans [16–22]. On the other hand, cyclooxgenase-2 (COX-2), one of the major target molecules of NSAIDs, was recently found to be over-expressed in inflamed biliary epithelium and biliary neoplasms in humans [23,24]. In this study, we investigated whether etodolac, a COX-2-specific inhibitor, could prevent biliary carcinogenesis in bilioenterostomized hamsters [25].

10.3 Experimental Protocol

Seven-week-old female Syrian golden hamsters (SLC, Shizuoka, Japan) were housed, one per plastic cage, on sawdust bedding. They were kept at 24 ± 2 °C in 50 ± 20% humidity with a 12-h light/12-h dark cycle. They were fed a CE-2 pelleted diet (Clea Japan, Tokyo, Japan), and provided drinking water ad libitum. The animals were checked daily and weighed weekly throughout the experiments.

Choledochojejunostomy using a Roux-en Y procedure was performed in all hamsters. The scheme of the completed surgical procedure of the choledochojejunostomy is illustrated in Figure 10.1 The details of the surgical techniques are described in Chapter 5.

All hamsters were given subcutaneous (sc) injections of a chemical carcinogen, *N*-nitrosobis(2-oxopropyl)amine (BOP) (Nakarai Tesque, Kyoto, Japan), 10 mg/kg body weight in 0.9% saline, every 2 weeks [26,27]. BOP was started 4 weeks after surgery, and continued for 18 weeks [8,27]. The animals were randomly divided into two groups according to the different regimens. Twenty hamsters were given oral etodolac (Nippon Shinyaku, Kyoto, Japan), 10 mg/kg body weight [28] in 10 ml/kg body weight of 0.5% methylcellulose solution (Shin-Etsu Chemical, Tokyo, Japan) [29], three times per week, starting 4 weeks after surgery and continuing for 18 weeks (etodolac group). The control group consisted of 20 hamsters given the same dose of methylcellulose solution alone.

All hamsters were killed in postoperative week 22 and the maximum diameter of the extrahepatic bile duct was measured. Blood samples from the vena cava were collected in ice-chilled tubes containing heparin, centrifuged (3,000 rpm) for

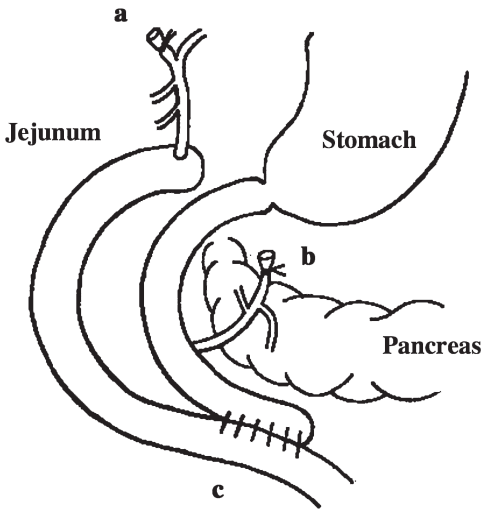

Fig. 10.1 Operating schema of choledochojejunostomy with the Roux-en-Y procedure in a hamster. The jejunal limb was 4 cm long. (a) The gallbladder was removed. (b) The common bile duct was transected at the distal end. (c) Side-to-side intestinal anastomosis was done 7 cm from the pyloric ring ([25], with permission)

10 min, and then serum samples were collected in new ice-chilled tubes. The serum levels of total bilirubin (T-Bil), alkaline phosphatase (ALP), glutamic-oxaloacetic transaminase (GOT), and glutamic-pyruvic transaminase (GPT) were measured.

The liver, biliary system and pancreas were removed en bloc. After fixation in 10% neutral formalin, the specimens were cut into five blocks, so that four sections contained the liver and one section contained the hepatic duct, and embedded in paraffin. The histological sections were stained with hematoxylin and eosin (H&E) and examined by a pathologist who was blinded to the treatment allocation of the sections. The number of histologically verified adenomas and carcinomas was counted. Carcinoma was diagnosed on the basis of disruption of epithelial cell polarity and evidence of invasion.

To evaluate the relationship between cholangitis and biliary carcinogenesis, the grade of cholangitis was scored in accordance with the infiltration of inflammatory cells and the fibrous change of Glison as follows: grade 0, no cholangitis; grade 1, mild invasion of inflammatory cells around the bile duct without fibrous change of Glison; grade 2, severe invasion of inflammatory cells around the bile duct and/or fibrous change of Glison; and grade 3, abscess formation in the liver (see Chapter 7).

Proliferating cell nuclear antigen (PCNA) was used as a marker of biliary epithelial cell kinetics. Tissue sections were cut at 4-mm, mounted on glass slides coated with 5-aminoprophyltriethoxy saline, and dewaxed in xylene. The sections were treated with microwave heating for 5 min in phosphate-buffered saline at 500 W. After blocking endogenous peroxidase, the sections were incubated with mouse monoclonal antibodies against PCNA (clone-PC 10; DAKO, Kyoto, Japan) at a dilution of

1:100. The cell nuclei were counterstained with hematoxylin. The proportion of labeled nuclei (labeling index; LI) was calculated by counting the labeled nuclei in >1,000 non-neoplastic epithelial cells of the intrahepatic bile ducts [30].

Prostaglandin E2 (PGE2) production in the liver tissue was used as a marker of inflammation and COXs activity. The right lateral lobe of the liver was removed, immediately frozen in liquid nitrogen, and stored at −80 °C in a sterile 1.5 ml Eppendorf tube until analysis. The frozen tissue was homogenized in saline containing 10 mg/l indomethacin, and ethanol was added to achieve the final proportion of 20%. After centrifugation, the supernatant was removed and agitated in octadecylsilyl silica (ODS) suspension to adsorb PGE2. Protein and lipids were eliminated from the ODS carrier by washing with ethanol, hydrochloric acid, and petroleum ether in turn. Then, PGE2 was eluted from the ODS carrier by adding acetic ether, and it was measured by a radioimmunoassay (RIA) technique using a prostaglandin E2 [125I] RIA kit (Perkin Elmer Life Sciences, Boston, MA). To define normal levels of PGE2 production in the liver tissue and PCNA-LI of the biliary epithelium, twelve 29-week-old hamsters that had received no treatment were also investigated.

The side effects of etodolac, such as gastrointestinal mucosal injury, liver and renal dysfunction, and eosinophilic pneumonia, may have adverse effects on the vital state. Accordingly, the animals were checked daily and weighed weekly throughout the experimental period. The incidence of tumor development and the grade of cholangitis were analyzed using the χ^2 exact test. The Mann–Whitney test was also used for statistical analyses of the diameter of the extrahepatic bile duct, the number of tumors per animal, serum laboratory data, and PCNA-LI and PGE2 production. Differences of $P < 0.05$ were considered significant.

10.4 Morphological and Biochemical Changes

Table 10.1 summarizes the morphological and biochemical changes in the hepatobiliary system of the hamsters. There were 17 hamsters in the control group and 18 hamsters in the etodolac group. Three hamsters from the control group and two from the etodolac group died of liver abscess and/or obstructive jaundice before the end of the experiment. The average diameter of the extrahepatic bile duct was 2.8 ± 1.9 mm in the control group and 1.9 ± 1.3 mm in the etodolac group, without a significant difference between the groups. However, the serum levels of T.Bil, GOT, and ALP were significantly higher in the control group than in the etodolac group ($P < 0.05$).

10.5 Occurrence of Biliary Tumors

Biliary adenomas and carcinomas were observed in the hamsters from both groups (Table 10.2). The rates of adenoma were 88% and 61% in the control and etodolac groups, respectively, without a significant difference. However, numerous biliary

Table 10.1 Morphological and biochemical changes in the hepatobiliary system of hamsters after bilioenterostomy

Groups	No. of hamsters	Average diameter of the EHBD (mm)[a]	Serum levels[a]			
			T.Bil (mg/l)	ALP (IU/l)	GOT(IU/l)	GPT(IU/l)
Control	17	2.8 ± 1.9	1.9 ± 1.8	249.5 ± 278.1	187.2 ± 136.6	95.1 ± 47.5
Etodolac	18	1.9 ± 1.3	1.4 ± 2.8*	128.6 ± 93.7*	109.5 ± 75.9*	91.2 ± 65.0

EHBD, extrahepatic bile duct; T.Bil, total bilirubin; ALP, alkaline phosphatase; GOT, glutamic-oxaloacetic transaminase; GPT, glutamic-pyruvic transaminase.
[a]Mean ± SD.
*Significantly different from control group ($P < 0.05$). (modified from [25], with permission)

Table 10.2 The incidence and number of intrahepatic bile duct carcinomas developed in hamsters after bilioenterostomy

Groups	No. of hamsters	No. (%) of hamsters with		Average no. of tumors per animal[a]	
		Adenoma	Carcinoma	Adenoma	Carcinoma
Control	17	15(88)	15(88)	5.1 ± 4.1	11.4 ± 12.4
Etodolac	18	11(61)	6(33)*	2.1 ± 2.4*	1.8 ± 3.5*

*Significantly different from control group ($P < 0.01$).
[a]Mean ± SD. (modified from [25], with permission)

adenomas developed in the control group, and the average number of adenomas per animal was significantly higher in the control group than in the etodolac group ($P < 0.01$). Intrahepatic bile duct carcinoma developed in 15 (88%) of the 17 control hamsters, and the average number of carcinomas per animal was 11.4. Conversely, only 6 (33%) of the 18 etodolac hamsters had intrahepatic bile duct carcinoma, and the average number of carcinomas per animal was 1.8. Both the incidence of carcinoma and the average number of carcinomas per animal were significantly lower in the etodolac group than in the control group ($P < 0.01$).

10.6 Cholangitis, Biliary Epithelial Cell Kinetics, PGE2 Production, and Biliary Carcinogenesis

Cholangitis was recognized in all hamsters in the control group and 89% of the hamsters in the etodolac group (Table 10.3). Severe cholangitis was frequently observed in the control hamsters, which had a significantly higher average cholangitis score ($P < 0.05$). The PCNA-LI of the biliary epithelium was 9.67 ± 5.90% in the control group, which was significantly higher than that in the etodolac group ($P < 0.05$). Moreover, the PCNA-LI of the biliary epithelium in

Table 10.3 The occurrence of cholangitis and changes in biliary epithelial cell kinetics and PGE2 products in hamsters after bilioenterostomy

			Average of		
Groups	No. of hamsters	No.(%) of hamsters with cholangitis	Cholangitis score[a]	PCNA-LI (%)[a]	PGE2 products (pg/TP mg)[a]
Control	17	17(100)	2.08 ± 0.97	9.67 ± 5.90	14.14 ± 3.31
Etodolac	18	16(89)	1.28 ± 0.89*	5.14 ± 4.55*	7.46 ± 2.34*

PCNA-LI, proliferating cell nuclear antigen labeling index; PGE2, prostagrandine E2.
*Significantly different from control group ($P < 0.05$).
[a]Mean ± SD (modified from [25], with permission)

the hamsters that received no treatment was 2.4 ± 1.5%. The mean level of PGE2 products in the liver tissue was 14.14 ± 3.31 pg/TP mg in the control group, which was significantly higher than the 7.46 ± 2.34 pg/total protein (TP) mg in the etodolac group ($P < 0.05$). In hamsters that received no treatment, it was 1.5 ± 0.1 pg/TP mg, which was significantly different from the control and etodolac groups ($P < 0.05$).

Figure 10.2 shows the correlation between the cholangitis score and biliary carcinogenesis. Highly scored cholangitis of grade 2 or 3 was observed in 59% of the hamsters in the control group, and 22% of the hamsters in the etodolac group. Biliary carcinomas were observed frequently in each grade of cholangitis in the control group, whereas in the etodolac group the incidence of biliary carcinoma decreased with the degree of cholangitis, and carcinomas were observed in only 2 of the 14 hamsters with cholangitis of grade 0 or 1.

10.7 Transition of Body Weight

Figure 10.3 shows the transition curves of the body weight of hamsters during the experiment. Until week 15 of the study, the average body weight of the hamsters in both groups increased similarly. Thereafter, the body weight of the hamsters in the etodolac group increased continuously, whereas that in the control group decreased gradually.

10.8 Comments

Patients with intrahepatic or extrahepatic biliary carcinomas, which are resistant to traditional cytotoxic chemo- and radio-therapeutic approaches, have a dismal outcome even if the tumor is resected. Thus, cancer chemoprevention is hoped to be effective in the management of biliary carcinoma. Numerous studies have proved

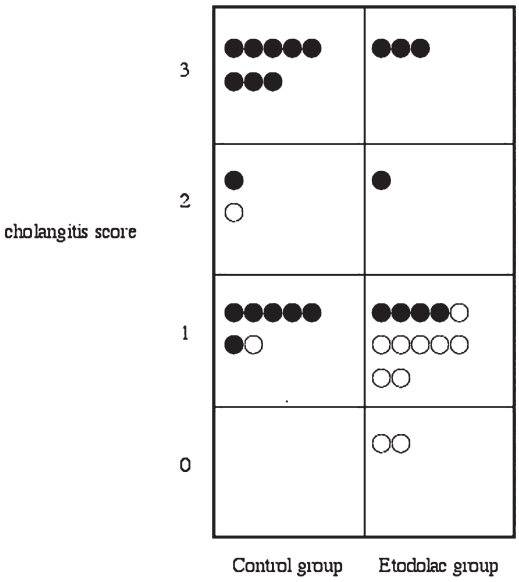

Fig. 10.2 Correlation between cholangitis score and biliary carcinogenesis in hamsters after bilioenterostomy. Black circle, hamster with carcinoma; closed circle, hamster without carcinoma ([25], with permission)

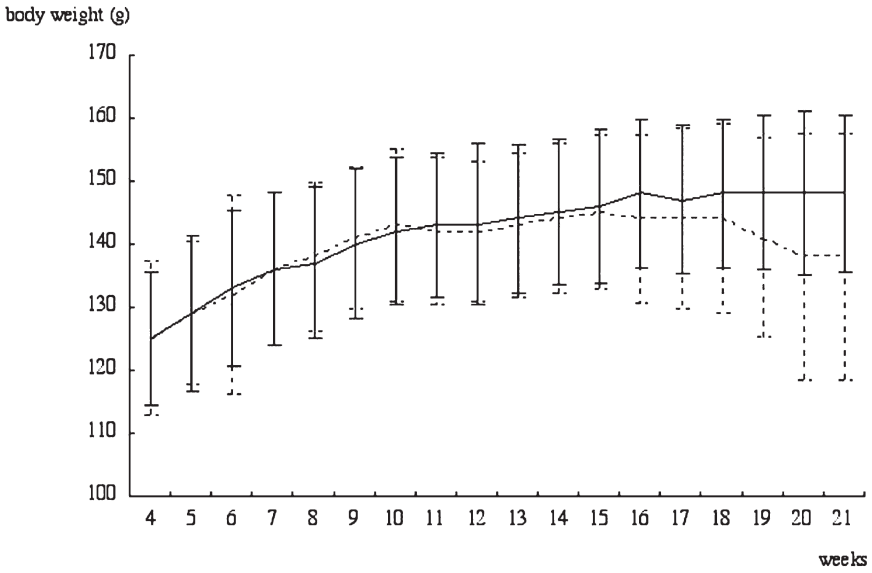

Fig. 10.3 Transition curve of the average body weight of hamsters after bilioenterostomy. Solid line, etodolac group; dashed line, control group. The bars represent the standard error ([25], with permission)

that NSAIDs reduce the incidence of several kinds of cancer [31–33]. We obtained evidence that persistent cholangitis after bilioenterostomy accelerated the development of biliary carcinoma in hamsters, and that severe cholangitis was associated with a higher incidence of biliary carcinoma through an increase in the proliferative activity of the biliary epithelium[8,9]. Therefore, we speculated that NSAIDs could reduce biliary carcinogenesis by inhibiting biliary inflammation.

The present study clearly demonstrated the preventative effect of etodolac on BOP-induced biliary carcinogenesis in hamsters undergoing bilioenterostomy. To the best of our knowledge, this is the first successful *in vivo* study on the chemoprevention of biliary carcinogenesis by a COX-2-specific inhibitor. Although etodolac failed to inhibit reflux cholangitis, it reduced the severity of cholangitis. Moreover, etodolac down-regulated the cell kinetic activity of the biliary epithelium. These findings suggest that although reflux cholangitis was inevitably induced after choledochojejunostomy, the aggravation of cholangitis was attenuated by etodolac. The inhibitory effects of etodolac on inflammation and inflammation-activated biliary epithelial cell kinetics may participate in the tumor-preventing mechanisms in our hamster model [34].

It is well known that COXs mediate the rate-limiting step of prostaglandin, including PGE2 and biosynthesis in the arachidonic acid cascade, and that PGE2 is a reliable biomarker of COXs activity [35]. On the other hand, PGE2 is upregulated in inflammatory sites through upregulated COXs activity. Recent *in vitro* studies have shown that COX-2 and COX-2-mediated prostanoids, including PGE2, are strongly related to cancer development and progression through their anti-apoptotic effects [35], the enhancement of angiogenesis, or the suppression of cell-to-cell adhesive activity [36–38]. In the present study, PGE2 products in the liver tissue were significantly decreased in the etodolac group. Although the tissue of interest is the epithelium of the intrahepatic bile duct, it is likely that the changes seen in the liver would be similar to those occurring in the bile duct epithelium. Considering our findings and the evidence reported, the inhibition of COXs activity, especially COX-2, is considered to be another possible mechanism of the chemopreventive effect of etodolac on biliary carcinogenesis in bilioenterostomized hamsters.

The toxicity and efficacy of NSAIDs are mediated through the inhibition of COX-mediated prostaglandin synthesis [39]. Because of the non-selective inhibitory effects of conventional NSAIDs on COX-1 and COX-2, with their many side-effects, including gastrointestinal bleeding, their clinical use is limited. However, etodolac mainly inhibits COX-2, and its adverse effects on the gastrointestinal tract occur less frequently [40]. The body weight of hamsters in our etodolac group was well maintained throughout the experiment, unlike that of the hamsters in the control group. These findings suggest that etodolac had no critical adverse effects. Thus, the long-term administration of etodolac might be feasible and convenient for cancer prevention.

In conclusion, etodolac inhibited BOP-induced biliary carcinogenesis in hamsters subjected to choledochojejunostomy. Suppression of the proliferative activity of biliary epithelial cells and the reduction of PGE2 products in the liver, in association

with the attenuation of persistent cholangitis by etodolac, were considered possible mechanisms of cancer prevention in this hamster model. We also obtained evidence supporting the benefits of etodolac in the management of reflux cholangitis. Clinical trials will be necessary to assess the utility of specific COX-2 inhibitors, not only to prevent biliary carcinogenesis, but also to treat reflux cholangitis in patients undergoing bilioenterostomy.

B. Hochu-ekki-to (TJ-41)

10.9 Summary

Recent clinical studies have revealed that biliary carcinomas can develop after bilioenterostomy. The present study was designed to evaluate whether hochu-ekki-to (TJ-41), a Japanese herbal drug, could prevent chemically induced biliary carcinomas in bilioenterostomized hamsters. Syrian golden hamsters were subjected to choledochojejunostomy and then given subcutaneous injections of *N*-nitrosobis (2-oxopropyl)amine (BOP), 10 mg/kg, every 2 weeks from 4 weeks after surgery. The animals were simultaneously given oral TJ-41, 1,000 mg/kg, in water every day (TJ-41 group). The control hamsters were given only water. The hamsters were killed 22 weeks after surgery, and the development of biliary carcinomas, the presence and degree of cholangitis, and the cell kinetic status of the biliary epithelium were evaluated histologically. Intrahepatic bile duct carcinomas developed in 15 (88%) of the 17 hamsters in the control group and in only 8 (47%) of the 17 hamsters in the TJ-41 group ($P < 0.05$). The degree of cholangitis was not different in the two groups; however, the proliferating cell nuclear antigen labeling index (PCNA-LI) of the biliary epithelium was significantly lower in the TJ-41 group (6.46%) than in the controls (9.67%) ($P < 0.05$). These findings indicate that TJ-41 inhibited the biliary epithelial cell kinetics after bilioenterostomy, thereby preventing carcinogenesis. Thus, TJ-41 has a preventive effect on chemically induced carcinoma of the biliary tract after bilioenterostomy.

10.10 Introduction

Hochu-ekki-to (TJ-41), a Japanese herbal drug, is known to reduce the severity of side effects such as leukopenia and intestinal damage, resulting from radiation or chemotherapy for malignant tumors [41,42]. Moreover, TJ-41 has recently been reported to activate macrophages and natural killer (NK) cells [43–45]; to inhibit experimental liver metastasis [46]; and to exert an anti-neoplastic effect on several malignancies, including skin cancer, hepatoma, ovarian cancer, and uterine cancer [47–50]. In this study, we investigated if TJ-41 could prevent biliary carcinogenesis in bilioenterostomized hamsters.

10.11 Experimental Protocol

Seven-week-old female Syrian golden hamsters (SLC, Inc., Shizuoka, Japan) were housed, one per plastic cage, on sawdust bedding. They were kept at 24 ± 2 °C in 50 ± 20% humidity with a 12-h light/12-h dark cycle, and fed a CE-2 pelleted diet (Clea Japan, Inc., Tokyo, Japan), and provided drinking water *ad libitum*. The animals were checked daily and weighed every 2 weeks throughout the experiments.

All hamsters were subjected to choledochojejunostomy using a Roux-en-Y procedure as described in Chapter 5 (Figure 10.1). The hamsters were given subcutaneous injections of a chemical carcinogen, *N*-nitrosobis(2-oxopropyl)amine (BOP) (Nakarai Tesque, Kyoto, Japan), 10 mg/kg body weight, every 2 weeks. BOP was started 4 weeks after surgery and continued for 18 weeks. The animals were randomly divided into two groups according to the different regimens. Twenty hamsters were given oral TJ-41 (Tsumura Co., Ltd., Tokyo, Japan) 1,000 mg/kg body weight, in water, daily, starting from 4 weeks after surgery and continuing for 18 weeks (TJ-41 group). TJ-41 was added to the water that the hamsters drank *ad-libitum*. In the control group, twenty hamsters were provided with just water. All hamsters were killed in postoperative week 22.

The maximum diameter of the extrahepatic bile duct was measured. Blood samples from the vena cava were collected in ice-chilled tubes containing heparin, and centrifuged at 3,000 rpm for 10 min; then serum samples were collected in new ice-chilled tubes. The serum levels of total bilirubin (T-Bil), alkaline phosphatase (ALP), aspartate aminotransferase (AST), and alanine aminotransferase (ALT) were measured.

The liver, biliary system, and pancreas were removed *en bloc*. After fixation in 10% neutral formalin, the specimens were cut into five blocks so that four sections contained the liver and one section contained the hepatic duct. They were then embedded in paraffin. The histological sections were stained with hematoxylin and eosin (H&E) and examined by a pathologist blinded to the treatment allocation of the sections. The number of histologically verified carcinomas was counted. Carcinoma was diagnosed on the basis of the WHO classification of tumors of the hamster [51].

To evaluate the relationship between cholangitis and biliary carcinogenesis, we scored the grade of cholangitis in accordance with the infiltration of inflammatory cells and the fibrous change of Glison as follows: grade 0, no cholangitis; grade 1, mild invasion of inflammatory cells around the bile duct without fibrous change of Glison; grade 2, severe invasion of inflammatory cells around the bile duct and/or fibrous change of Glison; and grade 3, abscess formation in the liver (see Chapter 7).

Proliferating cell nuclear antigen (PCNA) was used as a marker of biliary epithelial cell kinetics. Tissue sections were cut at 4 μm, mounted on glass slides coated with 5-aminoprophyltriethoxy saline, and dewaxed in xylene. The sections were treated with microwave heating for 5 min in phosphate-buffered saline (PBS) at 500 W. After the blocking of endogenous peroxidase, the sections were incubated with mouse monoclonal antibodies against PCNA (clone-PC 10; DAKO, Kyoto, Japan) at a dilution of 1:100. The cell nuclei were counterstained with hematoxylin. The proportion of labeled nuclei (labeling index, LI) was calculated

Table 10.4 Morphological and biochemical changes in the hepatobiliary system of hamsters after bilioenterostomy

Groups	No. of hamsters	Average diameter of the EHBD (mm)[a]	Serum levels[a]			
			T.Bil (mg/l)	ALP (IU/l)	AST(IU/l)	ALT(IU/l)
Control	17	2.8 ± 1.9	1.9 ± 1.8	249.5 ± 278.1	187.2 ± 136.6	95.1 ± 47.5
TJ-41	17	3.3 ± 2.7	1.3 ± 1.3	95.2 ± 44.5*	109.5 ± 75.9*	78.6 ± 47.0

EHBD, extrahepatic bile duct; T.Bil, total bilirubin; ALP, alkaline phosphatase; AST, aspartate aminotransferase; ALT, alanine aminotransferase.
*Significantly different from control group ($P < 0.05$).
[a] Mean ± SD. (modified from [61], with permission)

by counting the labeled nuclei in >1,000 non-neoplastic epithelial cells of the intrahepatic bile ducts.

The possible side effects of TJ-41, such as pseudo aldosteronism, liver dysfunction, and myopathy, may affect the vital state of hamsters. Accordingly, the animals were checked daily and weighed every 2 weeks throughout the experiments. The incidence of carcinomas and the grade of cholangitis were analyzed using the χ^2 exact test. The Mann–Whitney U test was used for statistical analyses of the diameter of the extrahepatic bile duct, the number of tumors per animal, serum laboratory data, and PCNA-LI. Differences of $P < 0.05$ were considered significant.

10.12 Morphological and Biochemical Changes

The morphological and biochemical changes in the hepatobiliary system of hamsters are summarized in Table 10.4. The total number of hamsters examined in the control and TJ-41 groups was 17, because three hamsters from each group died of liver abscess and/or obstructive jaundice before they were killed. There was no significant difference in the average diameter of the extrahepatic bile duct between the groups. However, the serum levels of AST and ALP were significantly higher in the control group than in the TJ-41 group ($P < 0.05$).

10.13 Development of Biliary Carcinomas

Figure 10.4 shows H&E staining of typical intrahepatic bile duct cancer that developed in the hamster. Biliary carcinomas developed in both groups (Table 10.5). However, in the control group, intrahepatic bile duct carcinoma developed in 88% of the hamsters, and the average number of carcinomas per animal was 11.4, whereas in the TJ-41 group, intrahepatic bile duct carcinoma developed in only 47% of the hamsters, and the average number of carcinomas per animal was 3.9.

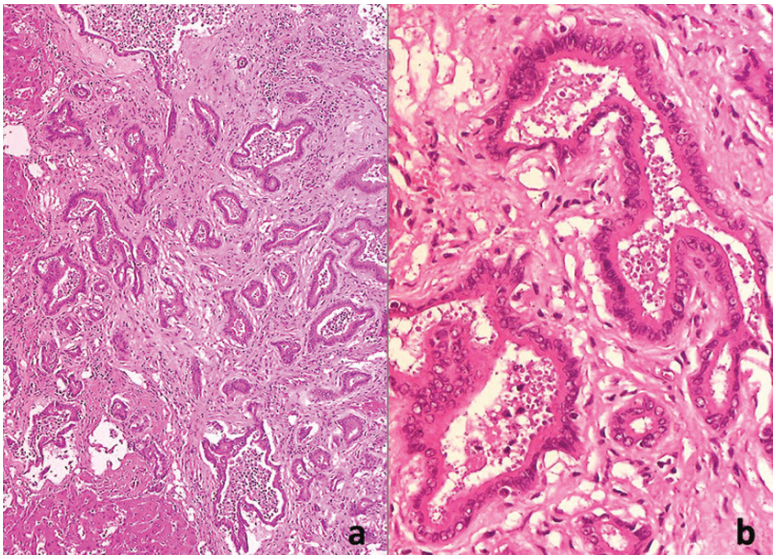

Fig. 10.4 H&E staining of the typical intrahepatic bile duct cancer that developed in a hamster (a, H&E, ×50; b, H&E, ×100) ([61], with permission)

Table 10.5 Incidence and number of intrahepatic bile duct carcinomas in hamsters after bilioenterostomy

Groups	No. of hamsters	No.(%) of hamsters with carcinoma	No. of carcinomas developed	Average no. of carcinomas per animal[a]
Control	17	15 (88)	193	11.4 ± 12.4
TJ-41	17	8 (47)*	67	3.9 ± 5.8*

*Significantly different from control group ($P < 0.05$).
[a]Mean ± SD. (modified from [61], with permission)

Both the incidence of carcinoma and the average number of carcinomas per animal were significantly lower in the TJ-41 group than in the control group ($P < 0.05$).

10.14 Cholangitis, Biliary Epithelial Cell Kinetics, and Biliary Carcinogenesis

Cholangitis was recognized in all hamsters in the control group and in 82% of the hamsters in the TJ-41 group (Table 10.6). There was no significant difference in the degree of cholangitis between the two groups ($P = 0.06$). Figure 10.5 shows PCNA

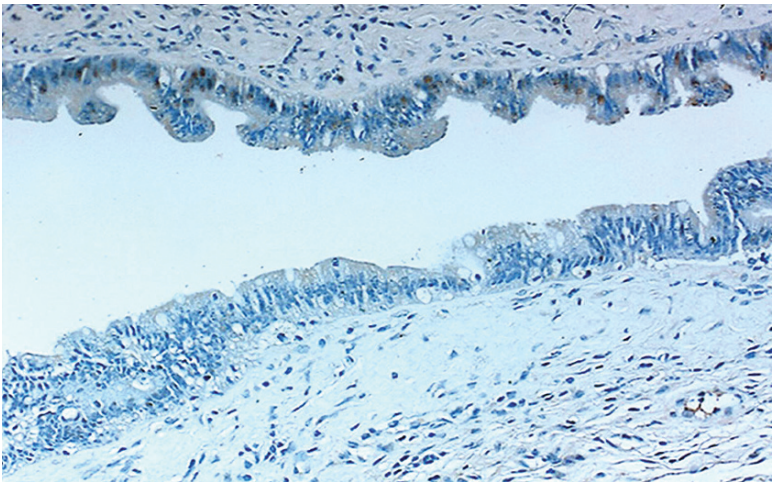

Fig. 10.5 PCNA staining of non-neoplastic epithelial cells of the intrahepatic bile ducts (×50) (modified from [61], with permission)

Table 10.6 The occurrence of cholangitis and changes in biliary epithelial cell kinetics and PGE2 products in hamsters after bilioenterostomy

Groups	No. of hamsters	No. (%) of hamsters with cholangitis	Average of cholangitis score[a]	PCNA-LI (%)[a]
Control	17	17(100)	2.06 ± 0.23	9.67 ± 5.90
TJ-41	17	14(82)	1.47 ± 0.24	6.46 ± 4.82*

PCNA-LI, proliferating cell nuclear antigen labeling index.
*Significantly different from control group ($P < 0.05$).
[a]Mean ± SD. (modified from [61], with permission)

staining of the biliary epithelium. PCNA-LI of the biliary epithelium in the control group was significantly higher than that of the TJ-41 group ($P < 0.05$).

10.15 Change of Body Weight

Figure 10.6 shows the transition curves of body weight in each group during the experiment. In the control group, the average body weight of the hamsters increased up until the 15th week of the study and gradually decreased thereafter, whereas in the TJ-41 group, the body weight of the hamsters continued to increase throughout the study.

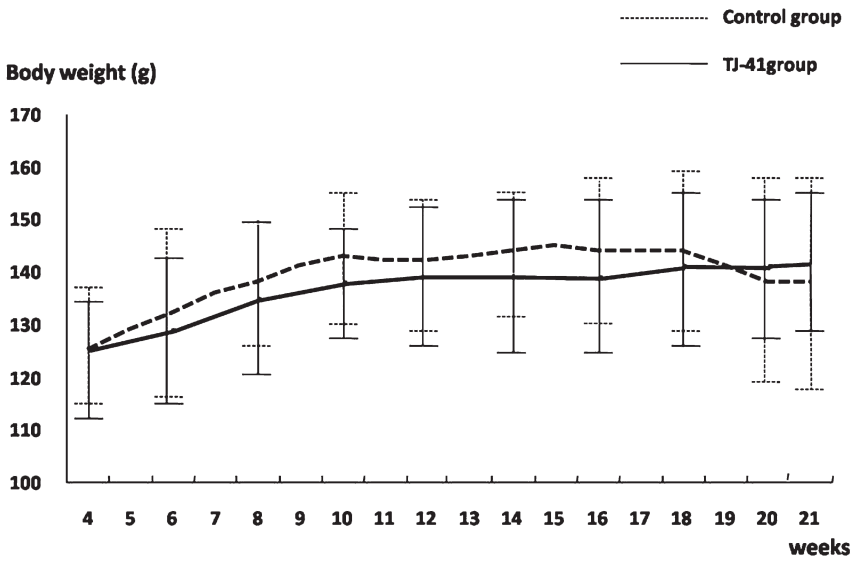

Fig. 10.6 Transition curve of the average body weight of hamsters after bilioenterostomy. Solid line, TJ-41 group; dashed line, control group. The bars represent the standard error ([61], with permission)

10.16 Comments

Despite recent advances in diagnostic modalities and surgical techniques, the clinical course of patients with carcinoma of the biliary tract remains dismal, even after curative resection. Both intra- and extrahepatic biliary carcinomas are resistant to traditional cytotoxic chemo- and radiotherapy. Thus, cancer chemoprevention holds promise as a new approach in the management of biliary carcinoma.

Chronic infection and inflammation involving the biliary tree, such as mechanical irritation by cholelithiasis [52] chronic intrahepatic cholangitis with hepatolithiasis [53], bile stasis and bacterial infection [54], and primary sclerosing cholangitis (PSC) [55–57], are risk factors for the development of biliary carcinoma. Our previous studies provided evidence that persistent cholangitis after bilioenterostomy in hamsters accelerates the development of biliary carcinoma through an increase in the proliferative activity of the biliary epithelium in accordance with the severity of cholangitis [8,9]. We also found that etodolac, a COX-2-specific inhibitor, reduces both the occurrence of severe cholangitis and the acceleration of biliary epithelial cell kinetics after bilioenterostomy in hamsters, thereby preventing BOP-induced biliary carcinogenesis. Recent studies have proved that TJ-41 inhibits the development of several kinds of cancer [47–50] and the activity of inflammatory cytokines [58–60]. Therefore, we evaluated the chemopreventative effect of TJ-41 on biliary carcinogenesis in bilioenterostomized hamsters.

The results of the present study clearly demonstrated the preventative effect of TJ-41 on BOP-induced biliary carcinogenesis in hamsters undergoing bilioenterostomy; however, TJ-41 did not inhibit the development of reflux cholangitis. Moreover, TJ-41 downregulated the cell kinetic activity of the biliary epithelium. Several recent studies have found that TJ-41 has several cancer-preventing mechanisms; namely, the activation of NK cells/T-cells [47], a blocking effect on the cell cycle [48], and inhibition of the expression of c-jun, tumor necrosis factor (TNF)-alpha, and estrogen receptor (ER)-alpha/beta [50]. Although the inhibitory effect of TJ-41 on biliary epithelial cell kinetics may help prevent biliary carcinoma in our hamster model with persistent reflux cholangitis, further studies should be carried out to clarify the cancer-preventing mechanism of TJ-41.

The occasional side-effects of TJ-41 include hypercalcemia, liver dysfunction, allergy, and digestive dysfunction, although their incidences are very low. In the present study, the body weight of hamsters in the TJ-41 group was well maintained throughout the experiment, in contrast to the hamsters in the control group. This may be attributed to the suppression of developing biliary carcinoma in the TJ-41 group and suggests that TJ-41 had no critical adverse effects. The Japanese herbal drug TJ-41 is much less expensive than conventional anticancer drugs; thus, its long-term administration could be feasible for cancer prevention.

In conclusion, TJ-41 inhibited BOP-induced biliary carcinogenesis in hamsters subjected to choledochojejunostomy. Suppression of the proliferative activity of the biliary epithelial cells was considered to be the possible mechanism of cancer prevention in this hamster model. However, clinical trials should be performed to assess the utility of TJ-41 in the prevention of biliary carcinogenesis in patients undergoing biliary reconstruction with bilioenterostomy.

References

1. Tocchi A., Costa G., Lepre L., Liotta G., Mazzoni G., Sita A. The long-term outcome of hepaticojejunostomy in the treatment of benign bile duct strictures. Ann. Surg. 1996 224:162–167.
2. Rothlin M.A., Lopfe M., Schlumpf R., Largiader F. Long-term results of hepaticojejunostomy for benign lesions of the bile ducts. Am. J. Surg. 1998 175:22–26.
3. Saing H., Han H., Chan K.L., Lam W., Chan F.L., Cheng W., Tam P.K. Early and late results of excision of choledochal cysts. J. Pediatr. Surg. 1997 32:1563–1566.
4. Uno K., Tsuchida Y., Kawarazaki H., Ohmiya H., Honna T.J. Development of intrahepatic cholelithiasis long after primary excision of choledochal cysts. Am. Coll. Surg. 1996 183:583–588.
5. Coyle K.A., Bradley E.L III. Cholangiocarcinoma developing after simple excision of type II choledochal cyst. South. Med. J. 1992 85:540–544.
6. Watanabe Y., Toki A., Todani T. Bile duct cancer developed after cyst excision for choledochal cyst. J. Hep. Bil. Pancr. Surg. 1999 6:207–212.
7. Strong R.W. Late bile duct cancer complicating biliary-enteric anastomosis for benign disease. Am. J. Surg. 1999 177:472–474.
8. Kitajima T., Tajima Y., Onizuka S., Matsuzaki S., Matsuo K., Kanematsu T. Linkage of persistent cholangitis after bilioenterostomy with biliary carcinogenesis in hamsters. J. Exp. Clin. Cancer Res. 2000 19:453–458.

9. Kitajima T., Tajima Y., Matsuzaki S., Kuroki T., Fukuda K., Kanematsu T. Acceleration of spontaneous biliary carcinogenesis in hamsters by bilioenterostomy. Carcinogenesis 2003 24:133–137.
10. Pollard M., Luckert P.H. Treatment of chemically-induced intestinal cancer with indomethacin. Proc. Soc. Exp. Biol. Med. 1981 167:161–164.
11. Pollard M., Luckert P.H. Effect of indomethacin on intestinal tumor induced in rats by the acetate derivative of dimethylnitrosamine. Science 1981 214:558–559.
12. Reddy B.S., Rao C.V., Rivenson A., Kelloff G. Inhibitory effect of aspirin on azoxymethane-induced colon carcinogenesis in F344 rats. Carcinogenesis 1993 14:1493–1497.
13. Mahmoud N., Boolbol S., Dannenberg A., Mestre J., Bilinski R., Martucci C., Newmark H., Chadburn A., Bertagnolli M. The sulfide metabolite of sulindac prevents tumors and restores enterocyte apoptosis in a murine model of familial adenomatous polyposis. Carcinogenesis 1998 19:87–91.
14. Chiu C., McEntee M., Whelan J. Sulindac causes rapid regression of preexisting tumors in Min/+ mice independent of prostaglandin biosynthesis. Cancer Res. 1997 57:4267–4273.
15. Oshima M., Dinchuk J., Kargman S., Oshima H., Hancock B., Kwong E., Trzaskos J., Evans J., Taketo M. Suppression of intestinal polyposis in Apc716 knockout mice by inhibition of cyclooxygenase 2 (COX-2). Cell 1996 87:803–809.
16. Logan R.F.A., Little J., Hawtin P.G., Hardcastle J.D. Effect of aspirin and nonsteroidal anti-inflammatory drugs on colorectal adenomas: case-control study of subjects participating in the Nottingham faecal occult blood screening programme. Br. Med. J. 1993 307:285–289.
17. Kune G., Kune S., Watson L. Colorectal cancer risk, chronic illnesses, operations, and medications: case control results from the Melbourne colorectal cancer study. Cancer Res. 1988 48:4399–4404.
18. Thun M.J., Namboodiri M.M., Heath C.W. Jr. Aspirin use and reduced risk of fatal colon cancer. N. Engl. J. Med. 1991 328:1593–1596.
19. Giovannucci E., Egan K., Hunter D., Stampfer M., Colditz G., Willett W., Speizer F. Aspirin and the risk of colorectal cancer in women. N. Engl. J. Med. 1995 333:609–614.
20. Winde G., Gumbinger H., Osswald H., Kemper F., Bunte H. The NSAID sulindac reverses rectal adenomas in colectomized patients with familial adenomatous polyposis: clinical results of a dose-finding study on rectal sulindac administration. Int. J. Colorectal Dis. 1993 8:13–17.
21. Winde G., Schmid K., Brandt B., Muller O., Osswald H. Clinical and genomic influence of sulindac and rectal mucosa in familial adenomatous polyposis. Dis. Colon Rectum 1997 40:1156–1168.
22. Matsuhashi N., Nakajima A., Fukushima Y., Yazaki Y., Oka T. Effects of sulindac on sporadic colorectal adenomatous polyps. Gut 1997 40:344–349.
23. Hayashi N., Yamamoto H., Hiraoka N., Dono K., Ito Y., Okami J., Kondo M., Nagano H., Umeshita K., Sakon M., Matsuura N., Nakamori S., Monden M. Differential expression of cyclooxgenase-2 (COX-2) in human bile duct epithelial cells and bile duct neoplasm. Hepatology 2001 34:638–650.
24. Chariyalertsak S., Sirikulchayanonta V., Mayer D., Kopp-Schneider A., Fürstenberger G., Marks F., Müller-Decker K. Aberrant cyclooxgenase isozyme expression in human intrahepatic cholangiocarcinoma. Gut 2001 48:80–86.
25. Tsuneoka N., Tajima Y., Kitazato A., Fukuda K., Kitajima T., Kuroki T., Onizuka S., Kanematsu T. Chemopreventative effect of a cyclooxygenase-2-specific inhibitor (etodolac) on chemically induced biliary carcinogenesis in hamsters. Carcinogenesis 2005 26:465–469.
26. Pour P., Althoff J., Kruger F.W., Mohr U. A potent pancreatic carcinogen in Syrian hamsters: *N*-nitrosobis(2-oxopropyl)amine. J. Natl. Cancer Inst. 1977 58:1449–1453.
27. Tajima Y., Eto T., Tsunoda T., Tomioka T., Inoue K., Fukahori T., Kanematsu T. Induction of extrahepatic biliary carcinoma by *N*-nitrosobis(2-oxopropyl)amine in hamsters given cholecystoduodenostomy with dissection of the common duct. Jpn. J. Cancer Res. 1994 85(8):780–788.

28. Kishimoto Y., Tanaka N., Jinnai T., Morisawa T., Shiota G., Kawasaki H., Hasegawa T. Sulindac and a cyclooxgenase-2 inhibitor, etodolac, increase APC mRNA in the colon of rats treated with azoxymethane. Gut 2000 47:812–819.
29. Inoue K., Fujisawa H., Sasaki Y., Nishimura T., Nishimura I., Inoue Y., Yokota M., Masuda T., Ueda F., Shibata Y. Pharmacological properties of the new non-steroidal anti-inflammatory agent etodolac. Arzneimittelforschung 1991 41:228–235.
30. Fukuda K., Kuroki T., Tajima Y., Tsuneoka N., Kitajima T., Matsuzaki S., Furui J., Kanematsu T. Comparative analysis of Helicobacter DNAs and biliary pathology in patients with and without hepatobiliary cancer. Carcinogenesis 2002 23:1927–1931.
31. Zhigng L., Yutaka S., Atsushi K., Fumiaki S., Masato M., Izumi K., Tao H., Yongzeng D., Junichi K., Masayuki I. Suppression of N-nitrosomethyl- benzylamine (NMBA)-induced esophageal tumorigenesis in F344 rats by JTE-522, a selective COX-2 inhibitor. Carcinogenesis 2001 22:547–551.
32. Hu P.J., Yu J., Zeng Z.R., Leung W.K., Lin H.L., Tang B.D., Bai A.H., Sung J.J. Chemoprevention of gastric cancer by celecoxib in rats. Gut 2004 53:195–200.
33. Furukawa F., Nishikawa A., Lee I.S., Kanki K., Umemura T., Okazaki K., Kawamori T., Wakabayashi K., Hirose M. A cyclooxygenase-2 inhibitor, nimesulide, inhibits postinitiation phase of *N*-nitrosobis(2-oxopropyl)amine-induced pancreatic carcinogenesis in hamsters. Int. J. Cancer 2003 104:269–273.
34. Ogura Y., Matsuda S., Ito M., Niimi R., Sumitomo M., Kawarada Y. Chemoprevention of biliary carcinogenesis in Syrian hamsters by the novel carboxamide IS-741 after initiation with *N*-nitrosobis(2-oxopropyl)amine (BOP). Carcinogenesis 2000 21:1469–1475.
35. Yunjie S., Xi M.T., Elizabeth Half M., Tien K., Frank A.S. Cyclooxygenase-2 overexpression reduces apoptotic susceptibility by inhibiting the cytochrome c-dependent apoptotic pathway in human colon cancer cells. Cancer Res. 2002 62:6323–6328.
36. Michael K.J., Hongtao W., Brigitta M.P., Ellis L., Rabiha M.I., James S., Andrzej S.T. Inhibition of angiogenesis by nonsteroidal anti-inflammatory drugs: insight into mechanism and implications for cancer growth and ulcer healing. Nat. Med. 1999 5:1418–1424.
37. Tsujii M., Kawano S., Tsuji S., Sawaoka H., Hori M., Dubois R.N. Cyclooxygenase regulates angiogenesis induced by colon cancer cells. Cell 1988 93:705–716.
38. Tsuchida A., Nagakawa Y., Kasuya K., Itoi T., Endo M., Ozawa T., Aoki T., Koyanagi Y. Immunohistochemical analysis of cyclooxygenase-2 and vascular endothelial growth factor in pancreaticobiliary maljunction. Oncol. Rep. 2003 2:339–343.
39. Vane J.R. Inhibition of prostaglandin synthesis as a mechanism of action for aspirin-like drugs. Nat. New Biol. 1971 231:232–235.
40. Warner T.D., Giuliano F., Vojnovic I., Bukasa A., Mitchell J.A., Vane J.R. Nonsteroid drug selectivities for cyclo-oxygenase-1 rather than cyclo-oxygenase-2 are associated with human gastrointestional toxicity: A full in vitro analysis. Proc. Natl. Acad. Sci. U. S. A. 1999 96:7563–7568.
41. Kim S.H., Lee S.E., Oh H., Kim S.R., Yee S.T., Yu Y.B., Byun M.W., Jo S.K. The radioprotective effects of bu-zhong-yi-qi-tang: a prescription of traditional Chinese medicine. Am. J. Chin. Med. 2002 30:127–137.
42. Kaneko M., Kawakita T., Kumazawa Y., Takimoto H., Nomoto K., Yoshikawa T. Accelerated recovery from cyclophosphamide-induced leukopenia in mice administered a Japanese ethical herbal drug, Hochu-ekki-to. Immunopharmacology 1999 44:223–231.
43. Cho J.M., Sato N., Kikuchi K. Prophylactic anti-tumor effect of Hochu-ekki-to (TJ41) by enhancing natural killer cell activity. In Vivo 1991 5:389–391.
44. Ohnishi Y., Fujii H., Hayakawa Y., Sakukawa R., Yamaura T., Sakamoto T., Tsukada K., Fujimaki M., Nunome S., Komatsu Y., Saiki I. Oral administration of a kampo (Japanese herbal) medicine Juzen-taiho-to inhibits liver metastasis of colon 26-L5 carcinoma cells. Jpn. J. Cancer Res. 1998 9:206–213.
45. Utsuyama M., Seidlar H., Kitagawa M., Hirokawa K. Immunological restoration and antitumor effect by Japanese herbal medicine in aged mice. Mech. Ageing Dev. 2001 122:341–352.

46. Onishi Y., Yamaura T., Tauchi K., Sakamoto T., Tsukada K., Nunome S., Komatsu Y., Saiki I. Expression of the anti-metastatic effect induced by Juzen-taiho-to is based on the content of Shimotsu-to constituents. Biol. Pharm. Bull. 1998 21:761–765.
47. Harada M., Seta K., Ito O., Tamada K., Li T., Terao H., Takenoyama M., Kimura G., Nomoto K. Concomitant immunity against tumor development is enhanced by the oral administration of a Kampo medicine, Hochu-ekki-to (TJ-41: Bu-Zhong-Yi-Qi-Tang). Immunopharmacol. Immunotoxicol. 1995 17:687–703.
48. Kao S.T., Yeh C.C., Hsieh C.C., Yang M.D., Lee M.R., Liu H.S., Lin J.G. The Chinese medicine Bu-Zhong-Yi-Qi-Tang inhibited proliferation of hepatoma cell lines by inducing apoptosis via G0/G1 arrest. Life Sci. 2001 69:1485–1496.
49. Zhu K., Fukasawa I., Furuno M., Inaba F., Yamazaki T., Kamemori T., Kousaka N., Ota Y., Hayashi M., Maehama T., Inaba N. Inhibitory effects of herbal drugs on the growth of human ovarian cancer cell lines through the induction of apoptosis. Gynecol. Oncol. 2005 97:405–409.
50. Onogi K., Niwa K., Tang L., Yun W., Mori H., Tamaya T. Inhibitory effects of Hochu-ekki-to on endometrial carcinogenesis induced by N-methyl-N- nitrosourea and 17beta-estradiol in mice. Oncol. Rep. 2006 16:1343–1348.
51. Moore M.A., Thamavit W., Bannasch P. Tumours of the liver. In Pathology of tumours in laboratory animals, V.S. Turusov and U. Mohr, eds., Vol. 3, Tumours of the hamster, 2/e. Lyon: International Agency for Research on Cancer, 1996, pp. 79–108.
52. Ohta T., Nagakawa T., Ueda N., Nakamura T., Akiyama T., Ueno K., Miyazaki I. Mucosal dysplasia of the liver and the intraductal variant of peripheral cholangiocarcinoma in hepatolithiasis. Cancer 1991 68:2217–2223.
53. Falchuk K.R., Lesser P.B., Galdabini J.J., Isselbacher KJ. Cholangiocarcinoma as related to chronic intrahepatic cholangitis and hepatolithiasis. Case report and review of the literature. Am. J. Gastroenterol. 1976 66:57–61.
54. Chijiiwa K., Ichimiya H., Kuroki S., Koga A., Nakamura F. Late development of cholangiocarcinoma after the treatment of hepatolithiasis. Surg. Gynecol. 1993 177:279–282.
55. Holzinger F., Z'graggen K., Büchler M.W. Mechanisms of biliary carcinogenesis: a pathogenetic multi-stage cascade towards cholangiocarcinoma. Ann. Oncol. 1999 10:122–126.
56. Chapman R.W. Risk factors for biliary tract carcinogenesis. Ann. Oncol. 1999 10:308–311.
57. Taniai M., Higuchi H., Burgart L.J., Gores G.J. p16INK4a promoter mutations are frequent in primary sclerosing cholangitis (PSC) and PSC-associated cholangiocarcinoma. Gastroenterology 2002 123:1090–1098.
58. Mori K., Kido T., Daikuhara H., Sakakibara I., Sakata T., Shimizu K., Amagaya S., Sasaki H., Komatsu Y. Effect of hochu-ekki-to (TJ-41), a Japanese herbal medicine, on the survival of mice infected with influenza virus. Antivir. Res. 1999 44:103–111.
59. Hai le X., Kogure T., Niizawa A., Fujinaga H., Sakakibara I., Shimada Y., Watanabe H., Terasawa K. Suppressive effect of hochu-ekki-to on collagen induced arthritis in DBA1J mice. J. Rheumatol. 2002 29:1601–1608.
60. Furuya Y., Akashi T., Fuse H. Effect of Bu-zhong-yi-qi-tang on seminal plasma cytokine levels in patients with idiopathic male infertility. Arch. Androl. 2004 50:11–14.
61. Tsuneoka N., Tajima Y., Kitasato A., Fukuda K., Kitajima T., Adachi T., Mishima T., Kuroki T., Onizuka S., Kanematsu T. Chemopreventative effect of hochu-ekki-to (TJ41) on chemically induced biliary carcinogenesis in hamsters. J Surg Res. 2008 Feb 1. [Epub ahead of print]

Chapter 11
Hamster Model of an Intraductal Papillary Mucinous Neoplasm (IPMN) of the Pancreas

Tomohiko Adachi, Yoshitsugu Tajima, Amane Kitasato, Noritsugu Tsuneoka, Ryuji Tsutsumi, Tamotsu Kuroki, and Takashi Kanematsu

11.1 Summary

The reflux of pancreatic juice into the biliary tract is a well-known risk factor for the development of biliary carcinoma. In this study, we investigated the role of bile-reflux into the pancreatic ducts in pancreatic carcinogenesis, especially in the development of carcinoma in the main pancreatic duct, in hamsters. Syrian hamsters were subjected to one of three surgical procedures: cholecystoduodenostomy with dissection of the extrahepatic bile duct on the distal end of the common duct (Model A); cholecystoduodenostomy with dissection of the common bile duct (Model B); or simple laparotomy (Model C). Four weeks after the surgery, the animals received weekly subcutaneous injections of *N*-nitrosobis(2-oxopropyl) amine (BOP), for 9 weeks. They were killed for pathological investigation 16 weeks after the initial BOP injection. Pancreatic carcinomas developed in 95%, 88%, and 90% of the Model A (n = 22), Model B (n = 24), and Model C (n = 21) hamsters, respectively. The induced pancreatic tumors were classified into four histological types: papillary; tubular; cystic adenocarcinoma; and intraductal carcinoma of the main pancreatic duct, consisting of intraductal papillary carcinoma (IPC) and intraductal tubular carcinoma (ITC). The number and incidence of IPCs induced in the Model A hamsters were 24 lesions and 77%, which were significantly higher than those in the Model B (7 lesions and 29%) and C hamsters (7 lesions and 33%) ($P < 0.01$). Bile-reflux into the pancreatic ducts was seen only in the Model A hamsters, after an indocyanine green injection via the portal vein. Proliferative cell nuclear antigen labeling indices of the epithelial cells in the main pancreatic duct, with no BOP treatment, were 3.8%, 0.8%, and 1.1% in Models A (n = 10), B (n = 10), and C (n = 10), respectively. These differences were significant ($P < 0.01$). Our findings suggest that bile-reflux into the pancreatic ducts is a significant factor predisposing to the development of IPC of the pancreas through the acceleration of epithelial cell kinetics of the main pancreatic duct.

Y. Tajima et al. (eds.), *Hepatobiliary and Pancreatic Carcinogenesis in the Hamster*,
DOI: 10.1007/978-4-431-87773-8_11, © Springer 2009

11.2 Introduction

Pancreaticobiliary maljunction (PBM), a congenital anomaly involving the union of the pancreatic and bile ducts, which are located outside the duodenal wall [1,2], is now recognized as a high-risk for the development of biliary carcinoma [3–5]. In this disorder, pancreatic juice flows into the biliary tracts because the pressure in the pancreatic ducts is higher than in the biliary tree. Thus, proteolytic pancreatic enzymes and phospholipase A2 activated in the biliary tree subsequently stimulate the biliary epithelial cells, leading to biliary carcinogenesis [6,7]. Two-way regurgitation, created by the reflux of bile up the pancreatic ducts, can occur in this anomaly [8–10] because the sphincter of Oddie does not functionally affect the anomalous union. Consequently, various pathological conditions are induced even in the pancreas.

Acute and chronic pancreatitis, hyperamylasemia, and pancreatic carcinoma are reported to be the most important pancreatic disorders associated with PBM [9–12]. Recent clinical studies have found an intraductal papillary mucinous neoplasm (IPMN) in the main or large pancreatic ducts of patients with PBM. To our knowledge, at least 16 cases of pancreas carcinoma in patients with PBM have been reported [6,13–23], and 5 (31%) of these tumors were confirmed histologically to be intraductal papillary mucinous carcinoma (IPMC). Because IPMC accounts for only about 3% of all pancreas carcinomas [24,25], this clinical evidence suggests a strong relationship between IPMC and PBM, supporting the hypothesis that bile-reflux into the pancreatic ducts may be a risk factor for the development of IPMC.

We established a hamster model mimicking PBM [26], in which biliary carcinomas were frequently induced with chemicals, and the developmental process and morphobiological characteristics of the induced carcinomas were evaluated (see Chapters 5 and 6). In this study, we investigated the significance of bile-reflux into the pancreatic ducts in pancreatic carcinogenesis in hamsters, focusing on the development of carcinoma in the main pancreatic duct.

11.3 Experimental Protocol

We used 109 seven-week-old female Syrian golden hamsters (Shizuoka Laboratory Animal Center, Shizuoka, Japan) with an average weight of 100 g at the initiation of the experiments. The animals were housed one per cage with sawdust bedding under standard laboratory conditions in the Laboratory Animal Center for Biochemical Research at Nagasaki University Graduate School of Biomedical Sciences. They were given a standard pellet diet and allowed water *ad libitum* during the experiment.

With the intention of manipulating the bile flow into the pancreatic ductal system, we prepared three surgical modifications (Figure 11.1). Following the intraperitoneal administration of sodium pentobarbital, 50 mg/kg body weight, the hamsters were subjected to cholecystoduodenostomy with dissection of the extrahepatic bile duct at the distal end of the common duct (CDDB procedure), so that bile would

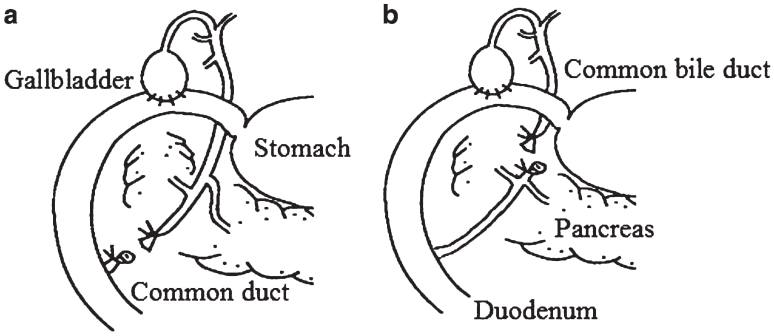

Fig. 11.1 Surgical procedures in the hamsters. (a) Model A: cholecystoduodenostomy with dissection of the extrahepatic bile duct in the distal end of the common duct. (b) Model B: cholecystoduodenostomy with dissection of the common bile duct ([33], with permission)

regurgitate into the pancreatic ducts (Model A). The animals were also subjected to cholecystoduodenostomy with dissection of the common bile duct, interrupting the connection between the pancreatic and biliary tracts (Model B). In this model, the bile never refluxed into the pancreatic ducts. Sham-operated controls were subjected to a simple laparotomy (Model C).

Bile-reflux into the pancreatic ducts was evaluated after an injection of Indocyanine green (ICG; Diagnogreen Inj. Daiichi Pharmaceutical Co., Ltd., Tokyo, Japan) via the portal vein. Four hamsters each from Models A, B, and C were subjected to relaparotomy 12 weeks after surgery and given a slow bolus injection of 1 ml of ICG (2.5 mg/mL) via the portal vein for 1 min. The stream of ICG into the pancreaticobiliary ductal system was observed macroscopically 30 min after the pigment injection.

To investigate the effect of bile-reflux into the pancreatic ducts on pancreatic carcinogenesis, the hamsters received weekly subcutaneous injections of *N*-nitrosobis(2-oxopropyl)amine (BOP; Nakarai Chemical Co., Kyoto, Japan) at a dose of 10 mg/kg body weight for 9 consecutive weeks. The BOP administration was begun 4 weeks after surgery. The animals were killed for pathological investigation 16 weeks after the initial administration of BOP. The pancreas was removed en bloc with the attached duodenum and fixed in 10% buffered formalin. The formalin-fixed tissue was then embedded in paraffin and processed routinely for hematoxylin and eosin staining. The numbers of hamsters examined were 22, 24, and 21 from Models A, B, and C, respectively. The lesions induced in the pancreas were classified according to the WHO classification of tumors of the hamster [27].

Proliferating cell nuclear antigen (PCNA) was used to evaluate the epithelial cell kinetic activity of the main pancreatic duct. Pancreatic tissue sections from 10 hamsters each without BOP treatment from Models A, B, and C were cut at 4 μm, mounted on glass slides coated with 5-aminoprophyltriethoxy saline, and dewaxed in xylene. The sections were treated with microwave heating for 5 min in PBS at 500 W. After blocking endogenous peroxidase, the sections were incubated with

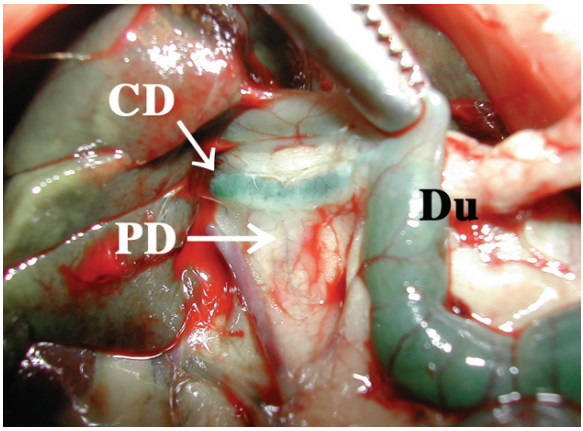

Fig. 11.2 Bile-reflux into the pancreatic ductal system in a Model A hamster. The common duct (CD) and the main pancreatic duct (PD) were stained green 20 min after the injection of ICG via the portal vein. Du, duodenum

mouse monoclonal antibodies against PCNA (clone-PC 10; DAKO, Kyoto, Japan) at a dilution of 1:100. The cell nuclei were counterstained with hematoxylin. The proportion of labeled nuclei (labeling index, LI) was calculated by counting the labeled nuclei in >1,000 epithelial cells of the main pancreatic duct. Cell kinetic studies of the pancreatic tumors induced by BOP were also done.

The Mann–Whitney *U* and Kruskal–Wallis tests were used for statistical analyses. Differences of $P < 0.05$ were considered significant.

11.4 Bile-Reflux Studies

Bile-reflux into the pancreatic ducts was clearly evident in the Model A hamsters. The main pancreatic ducts in all Model A hamsters were dyed green throughout, 30 min after the injection of ICG via the portal vein (Figures 11.2 and 11.3a). In contrast, no Model B or C hamsters showed pancreatic ductal staining with ICG (Figure 11.3b).

11.5 Carcinogenic Studies

The incidence, number, and histological findings of the pancreatic carcinomas induced in the BOP-treated hamsters are summarized in Table 11.1. Pancreatic carcinomas developed in 95%, 88%, and 90% of the hamsters in Models A, B, and C, respectively. The induced pancreatic tumors were classified grossly into four types

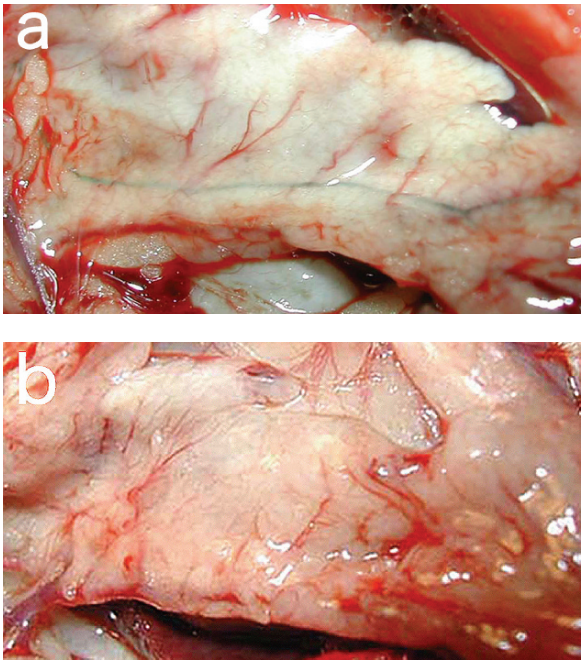

Fig. 11.3 Bile-reflux into the pancreatic ductal system. (a) In the Model A hamsters, the main pancreatic duct throughout the head and tail was stained green 30 min after the injection of ICG via the portal vein. (b) In the Model B hamsters, there was no pancreatic ductal staining with ICG (modified from [33], with permission)

histologically: papillary (Figures 11.4 and 11.5); tubular (Figures 11.6 and 11.7); or cystic adenocarcinoma (Figures 11.8 and 11.9); or intraductal carcinoma arising in the main pancreatic duct (Figures 11.10 and 11.11). The intraductal carcinoma comprised intraductal papillary carcinoma (IPC) (Figure 11.12) and intraductal tubular carcinoma (ITC) (Figures 11.13 and 11.14). Most of the induced pancreatic carcinomas were tubular adenocarcinomas, and there were no significant differences in the number or incidence of papillary, tubular, or cystic adenocarcinomas among the groups. However, in Model A, numerous IPCs were seen in the main pancreatic duct. The number and incidence of IPCs induced in the Model A hamsters were significantly higher than in Models B and C, respectively ($P < 0.01$).

IPCs developed mainly in the main pancreatic duct of the head of the pancreas in Models B and C. In contrast, the IPCs in Model A arose from the entire main pancreatic duct. Although some IPCs were recognized in the first-order pancreatic branches, these lesions were not counted in this study since they could not be distinguished from the IPCs originating in the main pancreatic duct. IPCs were usually confined within the mucosal layer of the duct with a papillary configuration,

Table 11.1 Incidence and pathological findings of carcinomas of the pancreas induced in hamsters

Models	No. of hamsters examined	No.(%) of hamsters with carcinoma	No. of carcinomas induced						Incidence (%) of hamsters with IPC	Location of IPC in the pancreas	
			Total	Pap	Tub	Cyst	IPC	ITC		Head	Body/ tail
A	22	21(95)	66*	3	33	4	24**	2	77**	11	13
B	24	21(88)	51	4	36	4	7	0	29	5	2
C	21	19(90)	42	5	29	1	7	0	33	6	1

Pap, papillary adenocarcinoma; Tub, tubular adenocarcinoma; Cyst, cystic adenocarcinoma; IPC, intraductal papillary carcinoma; ITC, intraductal tubular carcinoma.

*Significantly different from Model C ($P<0.05$).

**Significantly different from Model B and C ($P<0.01$). (modified from [33], with permission)

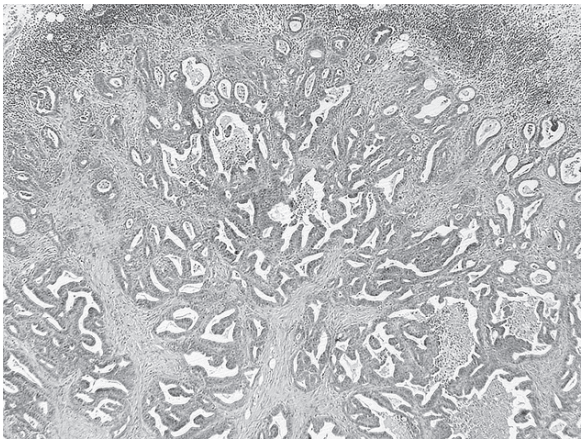

Fig. 11.4 Papillary adenocarcinoma of the pancreas (H&E, ×40)

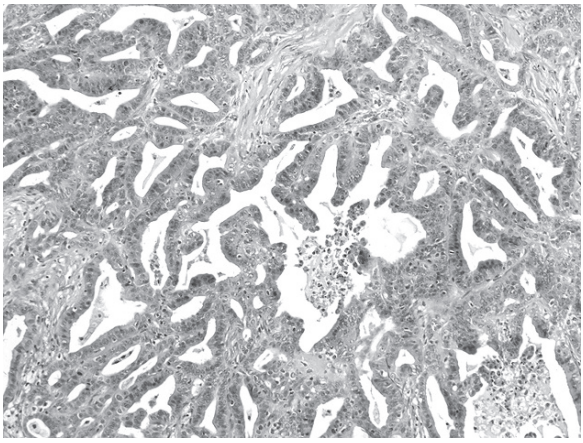

Fig. 11.5 Magnification of the papillary adenocarcinoma (H&E, ×120)

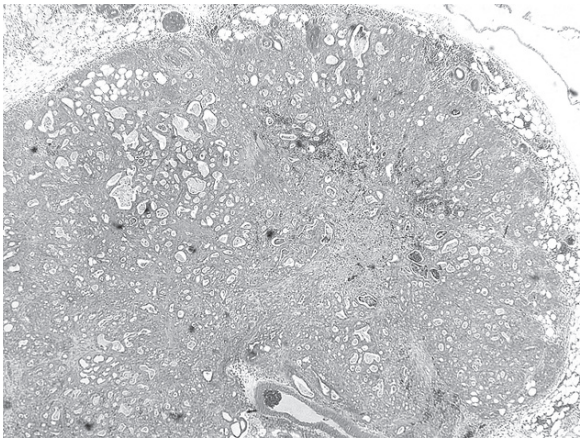

Fig. 11.6 Tubular adenocarcinoma of the pancreas (H&E, ×40)

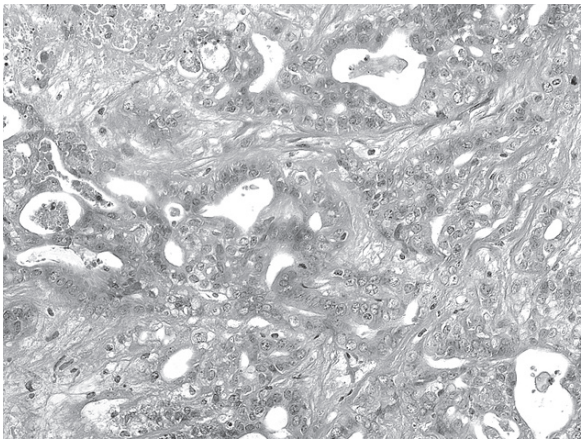

Fig. 11.7 Magnification of the tubular adenocarcinoma (H&E, ×200)

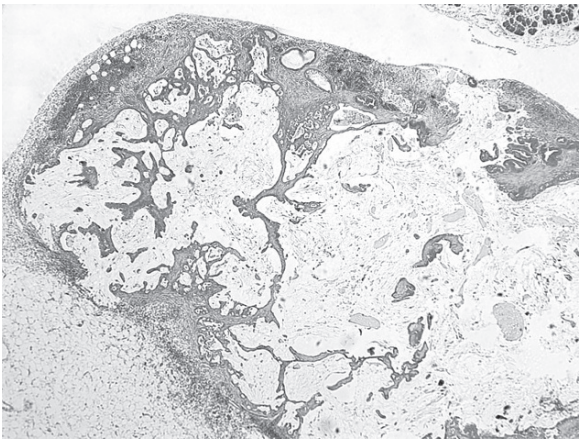

Fig. 11.8 Cystic adenocarcinoma of the pancreas (H&E, ×20)

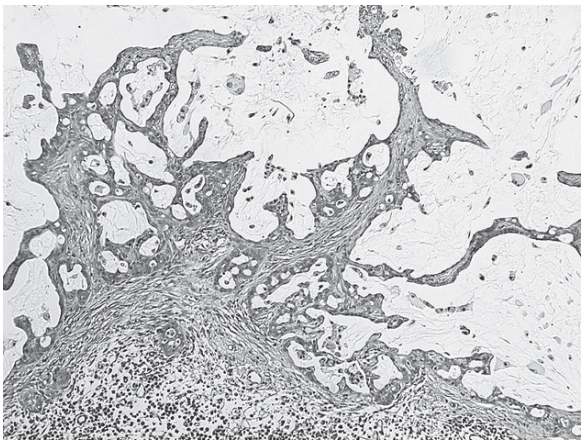

Fig. 11.9 Magnification of the cystic adenocarcinoma (H&E, ×120)

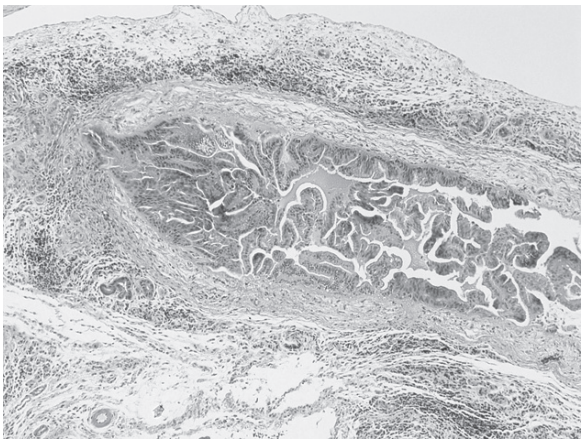

Fig. 11.10 Intraductal papillary carcinoma of the main pancreatic duct (H&E, ×80)

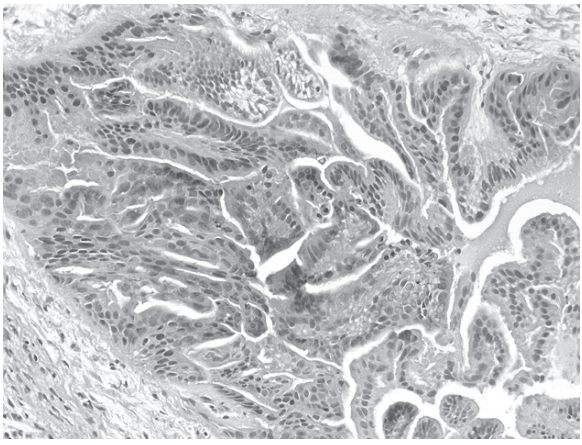

Fig. 11.11 Magnification of the intraductal papillary carcinoma (H&E, ×200)

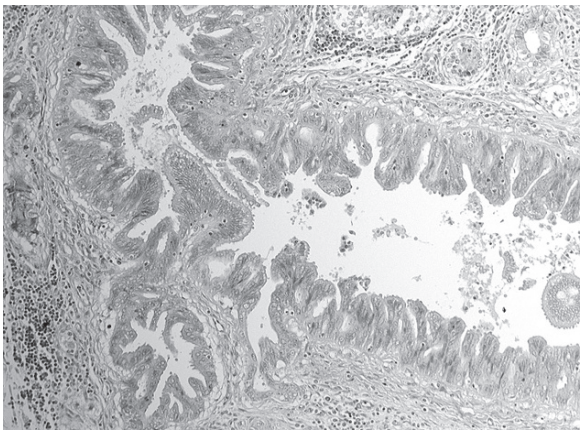

Fig. 11.12 Intraductal papillary carcinoma (IPC) of the main pancreatic duct. The tumor was growing into the lumen of the main pancreatic duct with marked papillary projections (H&E, ×120) (modified from [33], with permission)

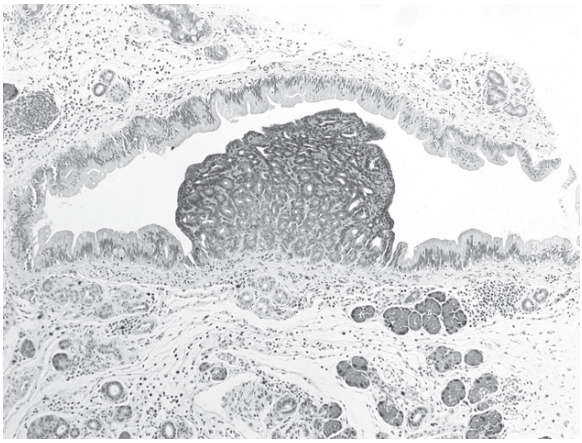

Fig. 11.13 Intraductal tubular carcinoma (ITC) of the main pancreatic duct. The tumor showed a polypoid growth (H&E, ×100) (modified from [33], with permission)

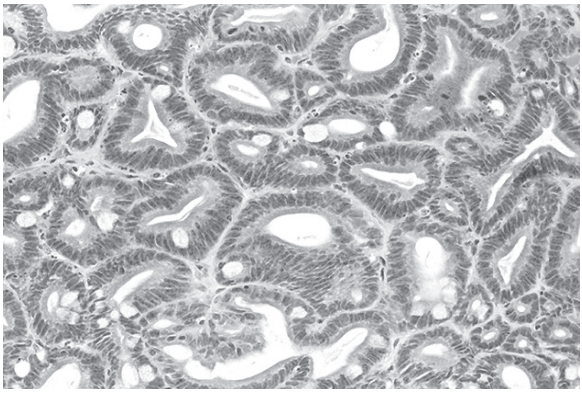

Fig. 11.14 Magnification of the intraductal tubular carcinoma (H&E, ×200)

and abundant intraductal mucin-hypersecretion was not observed in the main pancreatic duct of hamsters with IPCs. Some IPCs showed an accumulation of mucin in the main pancreatic duct (Figure 11.15) or invasion into the pancreatic parenchyma (Figures 11.16).

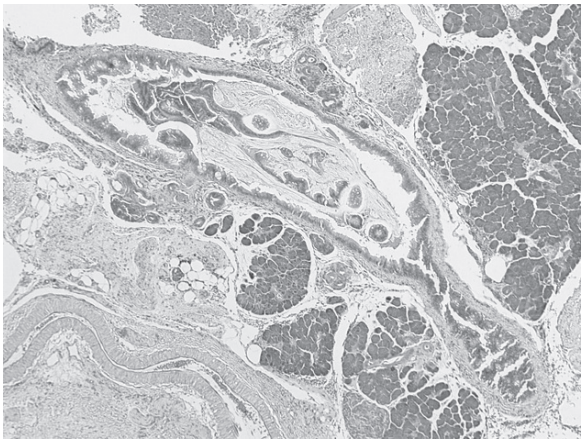

Fig. 11.15 Intraductal papillary carcinoma of the main pancreatic duct with mucin production (H&E, ×60)

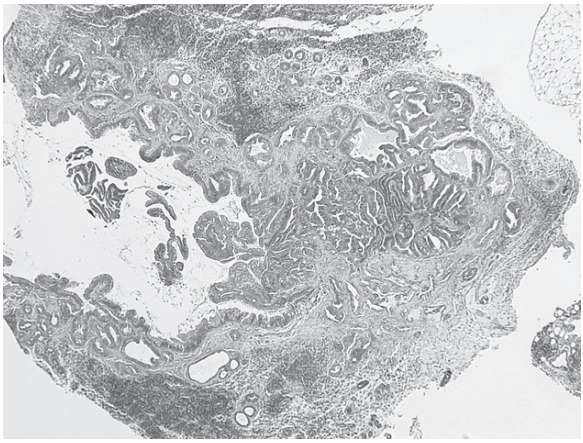

Fig. 11.16 Intraductal papillary carcinoma of the main pancreatic duct with parenchymal invasion (H&E, ×40)

11.6 Cell Kinetic Studies

The PCNA-LIs of epithelial cells of the main pancreatic duct in hamsters without BOP treatment were 3.8%, 0.8%, and 1.1% in Models A, B, and C, respectively (Table 11.2). The PCNA-LI was significantly higher in the Model A hamsters than in the Model B or C hamsters ($P < 0.01$). The PCNA-LIs of cancer cells differed among the histological types of tumors. The cell kinetic activity of IPCs was lower than those of the papillary and tubular adenocarcinomas; with a PCNA-LI of 37.5% ($P < 0.01$).

11.7 Comments

The tumorigenicity of pancreatic juice in the biliary tree has been proven clinically and experimentally [6,28], but the carcinogenic ability of the bile to induce pancreatic carcinoma has not been evaluated. In the present study, we prepared three different hamster models to control the bile flow; however, only the main pancreatic ducts in the Model A hamsters were clearly dyed green after the injection of ICG via the portal vein. ICG, a water soluble tricarbocyanine dye, is metabolized in the liver through uptake across the sinusoidal plasma membrane and then excreted into the bile [29,30]. Thus, the pancreatic ductal staining with ICG indicated

Table 11.2 Cell kinetic activity of epithelial cells of the main pancreatic duct in hamsters without *N*-nitrosobis(2-oxopropyl)amine (BOP)-treatment and induced pancreas carcinomas by BOP

Lesions	No. of lesions examined	Average of PCNA-LI (%)[a]
Pancreatic ductal epithelium		
Model A without BOP treatment	10	3.8 ± 1.1[*]
Model B without BOP treatment	10	0.8 ± 0.6
Model C without BOP treatment	10	1.1 ± 0.5
Pancreas carcinomas		
Papillary adenocarcinoma	12	55.6 ± 8.7[**]
Tubular adenocarcinoma	32	59.2 ± 9.1 [***]
Cystic adenocarcinoma	9	33.2 ± 9.8
IPC	18	37.5 ± 9.2

PCNA-LI, proliferating cell nuclear antigen labeling index; IPC, intraductal papillary carcinoma.

[*]Significantly different from Model B and C ($P<0.01$).

[**]Significantly different from cystic adenocarcinoma and IPC ($P<0.01$).

[***]Significantly different from cystic adenocarcinoma and IPC ($P<0.01$).

[a]Mean ± SD. (modified from [33], with permission)

that the bile flowed into the pancreatic ducts of the Model A hamsters. Moreover, significantly more IPCs developed in the main pancreatic duct in the Model A hamsters than in the other hamsters. BOP usually induces pancreatic carcinomas originating from the small pancreatic ducts or ductules in hamsters; that is, papillary, tubular, or cystic adenocarcinoma. In this study, the occurrence rates of these ordinary pancreas carcinomas were similar in the three groups, but the occurrence rates of IPCs were different. Furthermore, in the Model A hamsters, IPCs developed entirely in the main pancreatic duct. These findings support our hypothesis that bile reflux into the pancreatic ductal system is associated with the development of IPMC in the main pancreatic duct.

Proliferating cells are generally more susceptible to the tumorigenic effects of various carcinogens. Our cell kinetic studies using a PCNA-staining technique demonstrated remarkably elevated cell kinetic activity of the epithelial cells in the main pancreatic duct in the Model A hamsters. This suggests that IPCs develop through activated pancreatic ductal cells with high proliferating activity after being exposed to bile. In the PBM patients, bile regurgitates into the pancreatic ducts under conditions such as contraction of the gallbladder after meals, bile stasis in the choledochal cyst, the occurrence of cholangitis, and increased strain of the sphincter muscle of the papilla of Vater [6,21]. In these situations, the refluxing bile would have a carcinogenic effect on the pancreatic ducts. The bacterium infection of the bile may also affect the pancreatic ductal system in patients with PBM [12]. Although a bacterial study of bile and pancreatic juice was not done in our series, it is known that β-glucuronidase originating from bacteria in infectious bile causes breakdown of the protective barrier of the pancreatic ductal epithelium [9,31]. Further studies on bile as a pancreatic carcinogen are needed.

Because the IPCs induced in our hamster model had a low level of cell kinetic activity and were restricted to within the mucosal layer of the main pancreatic duct, they were of a lower-grade malignancy than papillary or tubular carcinoma of the pancreas. Oncologically, there are many similarities between the IPCs in our hamster model and IPMCs in humans: the tumors originate from the main or large pancreatic ducts; they show the histological pattern of papillary adenocarcinoma; they show intraductal papillary growth; and they are of low-grade malignancy. Therefore, our hamster model should be useful for investigating the etiology, pathogenesis, and biological behavior of IPMCs of the pancreas. However, the IPCs in our hamster models showed a low tendency to produce mucin in the main pancreatic duct, whereas abundant intraductal mucin-production is characteristic of IPMC in humans. The properties of the pancreatic ductal cells of hamsters to secrete mucin vary in the literature [27,32], and changes in mucinhypersecretion during pancreatic carcinogenesis should be investigated.

We concluded that bile-reflux into the pancreatic ducts activates the epithelial cell kinetics of the main pancreatic duct, resulting in the development of IPC in hamsters. Thus, the development not only of biliary carcinoma, but also of pancreatic carcinoma, especially IPMC, should be kept in mind when treating patients with PBM.

References

1. Irwin ST, Morison JE. Congenital cyst of the common bile duct containing stones and undergoing cancerous change. Br J Surg 1944 32:319.
2. Matsumoto Y, Fujii H, Itakura J, Matsuda M, Nobukawa B, Suda K. Recent advances in pancreaticobiliary maljunction. J Hepatobiliary Pancreat Surg 2002 9:45–54.
3. Miyazaki M, Takada T, Miyakawa S, Tsukada K, Nagino M, Kondo S, Furuse J, Saito H, Tsuyuguchi T, Chijiiwa K, Kimura F, Yoshitomi H, Nozawa S, Yoshida M, Wada K, Amano H, Miura F. Risk factors for biliary tract and ampullary carcinomas and prophylactic surgery for these factors. J Hepatobiliary Pancreat Surg 2008 15:15–24.
4. Sugiyama M, Atomi Y. Anomalous pancreaticobiliary junction without congenital chledochal cyst. Br J Surg 1998 85:911.
5. Kimura Y, Nishikawa N, Okita K, Furuhata T, Mizuguchi T, Nobuoka T, Nishimori H, Zenbutsu H, Satoh M, Katsuramaki T, Hirata K. Biliary tract malignancy and chronic inflammation from the perspective of pancreaticobiliary maljunction. Oncology 2005 69(Suppl 1):41.
6. Sugiyama M, Abe N, Tokuhara M, Masaki T, Mori T, Atomi Y. Pancreatic carcinoma associated with anomalous pancreaticobiliary junction. Hepatogastroenterology 2001 48:1767–1769.
7. Shimada K, Yanagisawa J, Nakayama F. Increased lysophosphatidylcholine and pancreatic enzyme content in bile of patients with anomalous pancreaticobiliary ductal junction. Hepatology 1991 13:438.
8. Itokawa F, Itoi T, Nakamura K, Sofuni A, Kakimi K, Moriyasu F, Tsuchida A, Aoki T. Assessment of occult pancreatobiliary reflux in patients with pancreaticobiliary disease by ERCP. J Gastroenterol 2004 39:988.
9. Kamisawa T, Matsukawa M, Amemiya K, Tu Y, Egawa N, Okamoto A, Aizawa S. Pancreatitis associated with pancreaticobiliary maljunction. Hepatogastroenterology 2003 50:1665.
10. Kamisawa T, Tu Y, Nakajima H, Egawa N, Tsuruta K, Okamoto A, Matsukawa M. Acute pancreatitis and a long common channel. Abdom Imaging. 2007 32:365–369.
11. Nakamura T, Okada A, Higaki J, Tojo H, Okamoto M. Pancreaticobiliary maljunction-associated pancreatitis: an experimental study on the activation of pancreatic phospholipase A2. World J Surg 1996 20:543.
12. Arendt T, Nizze H, Mönig H, Kloehn S, Stüber E, Fölsch UR. Biliary pancreatic reflux-induced acute pancreatitis—myth or possibility? Eur J Gastroenterol Hepatol 1999 11:329.
13. Dexter D. Choledochal cyst with carcinoma of the intrahepatic bile ducts and pancreatic ducts. Br J Cancer 1957 11:18.
14. Kelly TR, Schlueter TM. Choledochal cyst with coexistent carcinoma of the pancreas. Am Surg 1964 30:209.
15. Binks JB, Pauline GJ. Choledochal cyst and carcinoma of the pancreas in a boy of fifteen years. Aust N Z J Surg 1970 40:42.
16. Wood CB, Baum M. Carcinoma of the head of the pancreas in a young woman with a choledochal cyst. Br J Clin Pract 1975 29: 160.
17. Deeg JH, Rominger JM, Shah AN. Choledochal cyst and pancreatic carcinoma demonstrated simultaneously by endoscopic retrograde cholangiopancreaticography. South Med J 1980 73:1678.
18. Morohoshi T, Kunimura T, Kanda M, Takahashi H, Yagi H, Shimizu K, Nakayoshi A, Asanuma K. Multiple carcinomata associated with anomalous arrangement of the biliary and pancreatic duct system. A report of two cases with a literature survey. Acta Pathol Jpn 1990 40:755.
19. Ueda N, Nagakawa T, Ohta T, Kayahara M, Ueno K, Konishi I, Izumi R, Miyazaki I. Synchronous cancer of the biliary tract and pancreas associated with anomalous arrangement of the pancreaticobiliary ductal system. J Clin Gastroenterol 1992 15:136.
20. Silas DN. Association of a choledochocele and pancreatic carcinoma. Gastrointest Endosc 1994 40:94.

21. Kuga H, Yamaguchi K, Shimizu S, Yokohata K, Chijiiwa K, Tanaka M. Carcinoma of the pancreas associated with anomalous junction of pancreaticobiliary tracts: report of two cases and review of the literature. J Hepatobiliary Pancreat Surg 1998 5:113.
22. Hünerbein M, Ghadimi BM, Benhidjeb T, Schlag PM. A rare malformation of the pancreaticobiliary junction long common channel choledochal cyst and pancreas divisum in a patient with pancreatic cancer. Hepatogastroenterology 1999 46:1647.
23. Eriguchi N, Aoyagi S, Okuda K, Hara M, Fukuda S, Tamae T, Kanazawa N, Jimi A. Carcinoma arising in the pancreas 17 years after primary excision of a choledochal cysts: report of a case. Surg Today 2001 31:534.
24. McDonald JM, Williard W, Mais D, Beitler A. The incidence of intraductal papillary mucinous tumors of the pancreas. Curr Surg 2000 57:610.
25. Adsay NV, Conlon KC, Zee SY, Brennan MF, Klimstra DS. Intraductal papillarymucinous neoplasms of the pancreas: an analysis of in situ and invasive carcinomas in 28 patients. Cancer 2002 94:62.
26. Tajima Y, Eto T, Tsunoda T, Tomioka T, Inoue K, Fukahori T, Kanematsu T. Induction of extrahepatic biliary carcinoma by *N*-nitrosobis(2-oxopropyl)amine in hamsters given cholecystoduodenostomy with dissection of the common duct. Jpn J Cancer Res 1994 85:780.
27. Pour PM, Tomioka T. Tumours of the pancreas. IARC Sci Publ 1996 126:149.
28. Ogura Y, Matsuda S, Usui M, Hanamura N, Kawarada Y. Effect of pancreatic juice reflux into biliary tract on *N*-nitrosobis(2-oxopropyl)amine (BOP)-induced biliary carcinogenesis in Syrian hamsters. Dig Dis Sci 1999 44:79.
29. Hsieh CB, Chen CJ, Chen TW, Yu JC, Shen KL, Chang TM, Liu YC. Accuracy of indocyanine green pulse spectrophotometry clearance test for liver function prediction in transplanted patients. World J Gastroenterol 2004 10:2394.
30. Wheeler HO, Cranston WI, Meltzer JI. Hepatic uptake and biliary excretion of indocyanine green in the dog. Proc Soc Exp Biol Med 1958 99:11.
31. Suda K, Miyano T, Suzuki F, Matsumoto M, Yamashiro Y, Tokumaru T, Oyama T, Matsumoto Y. Clinicopathologic and experimental studies on cases of abnormal pancreaticocholedochoductal junction. Acta Pathol Jpn 1987 37:1549.
32. Tsutsumi M, Konishi Y. Precancerous conditions for pancreatic cancer. J Hepatobiliary Pancreat Surg 2000 7:575.
33. Adachi T, Tajima Y, Kuroki T, Mishima T, Kitasato A, Fukuda K, Tsutsumi R, Kanematsu T. Bile-reflux into the pancreatic ducts is associated with the development of intraductal papillary carcinoma in hamsters. J Surg Res 2006 136:106–11.

Chapter 12
Chemoprevention of Pancreatic Carcinogenesis

Tomohiko Adachi, Yoshitsugu Tajima, Tamotsu Kuroki, Takehiro Mishima, Amane Kitasato, Noritsugu Tsuneoka, and Takashi Kanematsu

12.1 Summary

The present study was designed to establish if Etodolac, a selective cyclooxygenase-2 inhibitor, prevents chemically induced intraductal papillary carcinoma (IPC) in the main pancreatic duct of hamsters. Hamsters were subjected to cholecystoduodenostomy with dissection of the distal end of the common duct. Four weeks after surgery, the surviving hamsters were given subcutaneous injections of *N*-nitrosobis(2-oxopropyl)amine (BOP) 10 mg/kg body weight, every 2 weeks, four times. The animals were divided into three groups based on the simultaneous oral intake of a CE-2 pelleted diet, which contained 0% (group CE, n = 30), 0.01% (group ET, n = 21), or 0.04% Etodolac (group ET4, n = 25), respectively. Hamsters were killed for pathological examination 36 weeks after the operation. The incidence of induced pancreatic carcinoma was 93%, 81%, and 72% in groups CE, ET, and ET4, respectively. The pancreatic carcinomas were classified into four histological types: tubular, papillary, and cystic adenocarcinoma, and IPC. The incidence of IPC and the number of IPCs per animal were significantly lower in groups ET4 (36% and 0.48) and ET (48% and 0.62) than in group CE (67% and 1.30). The proliferating cell nuclear antigen labeling indices in the noncancerous epithelial cells of the main pancreatic duct were 2.8% and 6.8% in groups ET4 and ET, respectively; being significantly lower than that in group CE (10.8%). In conclusion, Etodolac inhibited BOP-induced IPC in hamsters. The suppression of epithelial cell proliferation of the main pancreatic duct was considered a possible mechanism of cancer prevention in this hamster model.

12.2 Introduction

Intraductal papillary mucinous neoplasm (IPMN) of the pancreas, first described in 1982 by Ohashi et al. [1], is a well-established clinical and pathological entity characterized by the papillary proliferation of neoplastic epithelium with mucin-hypersecretion [2]. The recorded incidence of this unusual pancreatic disease has been increasing with advances in diagnostic imaging modalities. The more common

Y. Tajima et al. (eds.), *Hepatobiliary and Pancreatic Carcinogenesis in the Hamster*,
DOI: 10.1007/978-4-431-87773-8_12, © Springer 2009

pancreatic ductal carcinoma originates from the pancreatic ductules, whereas IPMN arises from the main pancreatic duct or its major branches [1,3], and is classified grossly into two types: main-duct IPMN and branch-duct IPMN [4]. IPMNs show a wide spectrum of histological differentiation, ranging from benign to malignant with the hyperplasia–adenoma–carcinoma sequence [5–7], and can often be multifocal. Therefore, the appropriate management for IPMN remains unclear. Some patients with IPMN require aggressive surgery such as total pancreatectomy, whereas others can be managed with limited pancreatic resections or careful observation without surgery. The advantage of a surgical approach must be balanced against the risks and the impaired postoperative quality of life with pancreatic endocrine and exocrine deficiency, especially for elderly patients. Therefore, a potent chemopreventive agent would be beneficial in the management of patients with IPMN.

Nonsteroidal anti-inflammatory drugs, including selective cyclooxygenase-2 (COX-2) inhibitors, have been used as chemopreventive drugs against several carcinomas [8,9]. However, Kokawa et al. [5] recently reported the incidence of COX-2 expression in intraductal papillary mucinous adenoma (IPMA) and carcinoma (IPMC) of the pancreas to be 58% and 70%, respectively. Studies have found that the incidence of COX-2 expression increases with progression of the adenoma–carcinoma sequence in IPMNs [6,7]. This suggests that the suppression of COX-2 expression may prevent the development and progression of IPMN. In the present study, we investigated the effects of Etodolac, a selective COX-2 inhibitor, on the prevention of IPMNs of the pancreas in a hamster model of intraductal papillary carcinoma (IPC) induced in the main pancreatic duct or its major branches [10]. We used Syrian hamsters as the animal model because the anatomical structure of their pancreaticobiliary ductal system, bile acid composition, and pancreatic juice components in this species are similar to those of humans [11,12].

12.3 Experimental Protocol

Seventy-six 7-week-old female Syrian golden hamsters (Shizuoka Laboratory Animal Center, Shizuoka, Japan) were used. The average weight of the hamsters at the start of the experiments was 100 g. Animals were housed one per cage with sawdust bedding under standard laboratory conditions in the Laboratory Animal Center for Biochemical Research at Nagasaki University Graduate School of Biomedical Sciences.

Following the intraperitoneal administration of sodium pentobarbital, 50 mg/kg body weight, hamsters were subjected to cholecystoduodenostomy with dissection of the distal end of the common duct, to make the bile regurgitate into the pancreatic ducts and activate the epithelial cell kinetics of the main pancreatic duct [10].

All hamsters were given four biweekly subcutaneous injections of *N*-nitrosobis(2-oxopropyl)amine (BOP) (Nakarai Chemical Co., Kyoto, Japan), 10 mg/kg body weight, from 4 weeks after surgery. The animals were divided into three groups

based on the simultaneous oral intake of a CE-2 pelleted diet (Clea Japan, Tokyo, Japan), which contained 0% (group CE), 0.01% (group ET), or 0.04% Etodolac (group ET4), respectively. The dosage of 0.01% Etodolac in the CE-2 pelleted diet was worked out by calculating the amount of food ingested daily by the hamsters in relation to the clinical daily-dose of Etodolac in humans. Each animal's body weight and the amount of food they ingested was checked weekly throughout the experiment. Hamsters were killed for pathological investigation 36 weeks after surgery. Pancreatic tissue samples were taken from the distal part of the splenic lobe of the pancreas, then frozen immediately in liquid nitrogen, and stored at −80 °C in a sterile 1.5 ml Eppendolf tube for analysis of prostaglandin products. The residual pancreas was embedded in paraffin and processed routinely for hematoxylin and eosin staining; then examined by a pathologist who was blinded to the treatment allocation of the study. To investigate the adverse effects of Etodolac such as gastric ulceration and myocardial injury, the stomach and the heart were examined macroscopically and microscopically. Tumor lesions induced in the pancreas were classified according to the WHO classification of tumors of the hamster [13].

To evaluate the suppressive effects of Etodolac on COX-2 activity, we measured the prostaglandin E2 (PGE2) products in the pancreatic tissues. Frozen tissue obtained from the splenic lobe of the pancreas was homogenized in saline containing 10 mg/l indomethacin, and ethanol was added to achieve the final proportion of 20%. After centrifugation, the supernatant was removed and agitated in octadecylsilyl silica (FUJIGEL HANBAI Co. Ltd., Tokyo, Japan) suspension to absorb PGE2. Deproteinization and delipidization were performed, and prostaglandins were eluted by ethyl acetate. The dried residue containing prostaglandins was dissolved in eluent 1 (acetonitrile: chloroform: acetic acid, 10:90:0.5) and applied to a silica open minicolumn Bond Elut Si (Varian, Inc. Scientific Instruments, CA). The column was washed with 10 ml of eluent 1, after which PGE2 was eluted, first with 5 ml of eluent 2 (acetonitrile: chloroform: acetic acid, 20:80:0.5) and then with 5 ml of eluent 3 (acetonitrile: chloroform: acetic acid, 50:50:0.5). We assayed PGE2 by a radioimmunoassay technique using a [^{125}I] Prostaglandin E2 RIA kit NEK-020 (PerkinElmer Life and Analytical Sciences, Inc., MA).

Proliferating cell nuclear antigen (PCNA) was used to evaluate the epithelial cell kinetic activity of the main pancreatic duct. Pancreatic tissue sections obtained from all hamsters were cut at 4 μm, then mounted on glass slides coated with 5-aminoprophyltriethoxy saline, and dewaxed in xylene. The sections were treated with microwave heating for 5 min in phosphate-buffered saline at 500 W. After blocking endogenous peroxidase, the sections were incubated with mouse monoclonal antibodies against PCNA (clone-PC 10; DAKO, Kyoto, Japan) at a dilution of 1:100. The cell nuclei were counterstained with hematoxylin and the proportion of labeled nuclei (labeling index, LI) was calculated by counting the labeled nuclei in >1,000 normal epithelial cells of the main pancreatic duct. We examined 19, 16, and 26 regions of normal epithelium in the main pancreatic duct in groups CE, ET, and ET4, respectively.

The Mann–Whitney *U*-test was used for statistical analysis. Differences of $p < 0.05$ were considered to be significant.

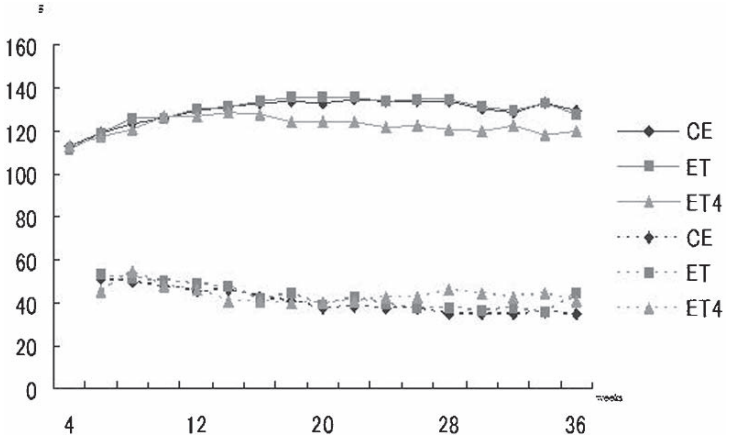

Fig. 12.1 Transition curves of the average body weight of, and the amount of food ingested by hamsters in each group during the experiment. Solid line, average body weight of hamsters; dashed line, average amount of food ingested (modified from [33], with permission)

12.4 Transition of Body Weight and Amount of Food Ingested

There were 30, 21, and 25 hamsters in groups CE, ET, and ET4, respectively. The differences in these numbers was mainly due to operative death within 4 weeks after surgery. The transition curves of the average body weight and food ingested in each group are shown in Figure 12.1. There were no significant differences in body weight or food ingestion among the groups in any period. Moreover, there was no macroscopic or microscopic evidence of gastric ulcer or myocardial injury in any group.

12.5 Dosage of Etodolac

The dose of Etodolac given to the hamsters, based on their food intake, was 36 to 53 mg/kg body weight/week in group ET and 160 to 192 mg/kg body weight/week in group ET4, respectively (Figure 12.2). In group ET, the dose of Etodolac was within the human clinical range of 28 to 56 mg/kg body weight/week.

12.6 Prostaglandin Products

The mean PGE2 production in the pancreatic tissue was 19.7 ± 13.3 (mean ± SD), 15.4 ± 13.3, and 10.2 ± 7.8 pg/wet weight mg in groups CE, ET, and ET4, respectively, with production decreasing in proportion to the mixing dose of Etodolac, with a significant difference between groups CE and ET4 ($p < 0.01$) (Figure 12.3).

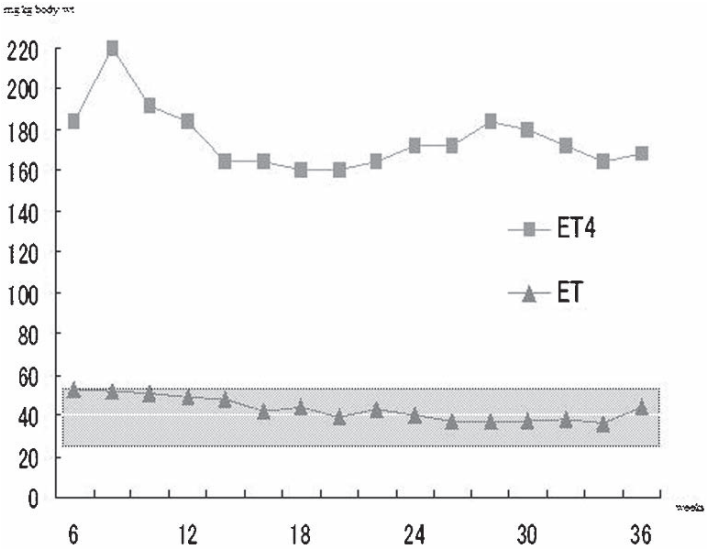

Fig. 12.2 The weekly dose of Etodolac given to hamsters in groups ET and ET4 was based on the amount of food containing Etodolac that they ingested. The gray area shows the range of the clinical dosage of Etodolac. In group ET, the doses of Etodolac given were within human clinical dosage levels throughout the experiment (modified from [33], with permission)

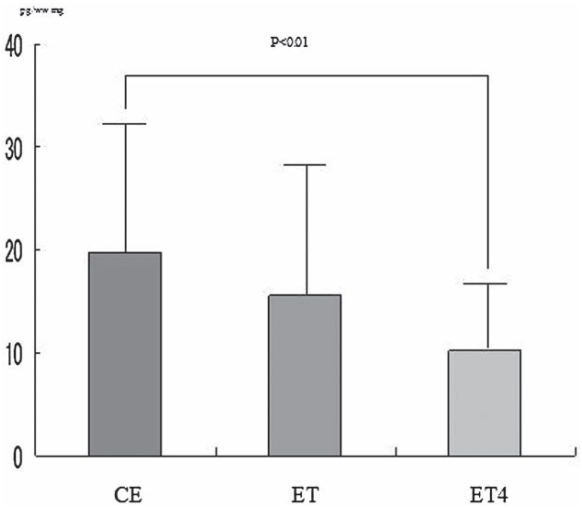

Fig. 12.3 The mean PGE2 production per wet weight of pancreatic tissue in each group. PGE2 production in the pancreatic tissue decreased in proportion to the mixing dosage of Etodolac (modified from [33], with permission)

12.7 Carcinogenic Studies

The incidence, number, and histological findings of pancreatic carcinomas induced in hamsters are summarized in Table 12.1. Pancreatic carcinomas developed in 93%, 81%, and 72% of hamsters in groups CE, ET, and ET4, respectively. The difference between groups CE and ET4 was significant ($p < 0.05$). The induced pancreatic tumors were classified grossly into four types histologically: tubular, papillary, and cystic adenocarcinoma, and IPC arising in the main pancreatic duct. Although some IPCs were recognized in the first-order pancreatic branches, these lesions were not counted in this study because they could not be distinguished from IPC originating in the main pancreatic duct. Most of the induced pancreatic carcinomas in each group were tubular adenocarcinoma; however, numerous IPCs were recognized in the main pancreatic duct in the group CE hamsters (Figure 12.4). The incidences of IPC were 67%, 48%, and 36% in groups CE, ET, and ET4, respectively, and were significantly lower in group ET4 ($p < 0.05$) than in group CE. The number of IPCs per animal was 1.30, 0.62, and 0.48 in groups CE, ET, and ET4, respectively, being significantly lower in groups ET ($p < 0.05$) and ET4 ($p < 0.01$) than in group CE. Neither the incidence nor the number of tubular adenocarcinomas was affected by Etodolac treatment.

12.8 Cell Kinetic Studies

The PCNA-LIs of the normal epithelial cells of the main pancreatic duct were 10.8 ± 4.9% (mean ± SD), 6.8 ± 3.8%, and 2.8 ± 2.5% in groups CE, ET, and ET4, respectively. The differences among the groups were significant (Figure 12.5).

12.9 Comments

Recent clinical investigations have revealed COX-2 expression in cancers of the colon, lung, stomach, and esophagus [14–17]. The over-expression of COX-2 inhibits the apoptosis of cancer cells [18], prolonging the survival of DNA-damaged cells, increasing metastatic potential [19]. and promoting angiogenesis [20]. Therefore, selective COX-2 inhibitors have been proposed as appropriate chemopreventive drugs against cancer. In fact, the chemopreventive effects of selective COX-2 inhibitors have been demonstrated in pancreatic cancer cell lines [21,22] and animal models [23,24], with COX-2 expression involved in the development and progression of invasive ductal carcinoma of the pancreas [25–27]. However, the usefulness of chemoprevention against pancreatic cancer is controversial [28]. According to the results of a recent clinical study of the simultaneous use of gemcitabine and the selective COX-2 inhibitor celecoxib by El-Rayes et al. [29], a

Table 12.1 Pathological findings of carcinomas of the pancreas induced in hamsters

Groups	No. of hamsters examined	No. of hamsters with carcinoma	Incidence of carcinoma (%)					No. of carcinomas induced per animal (mean ± SD)				
			Total	Tub	Pap	Cyst	IPC	Total	Tub	Pap	Cyst	IPC
CE	30	28	93	60	37	33	67	3.00 ± 1.94	0.83 ± 0.87	0.43 ± 0.68	0.43 ± 0.73	1.30 ± 1.24
ET	21	17	81	62	14	5*	48	1.76 ± 1.31*	0.95 ± 1.07	0.14 ± 0.36	0.05 ± 0.22	0.62 ± 0.80*
ET4	25	18	72*	48	4**	16	36*	1.28 ± 1.13**	0.52 ± 0.65	0.04 ± 0.20**	0.16 ± 0.37	0.48 ± 0.77**

Tub, tubular adenocarcinoma; Pap, papillary adenocarcinoma; Cyst, cystic adenocarcinoma; IPC, intraductal papillary carcinoma.
*Significantly different from group CE ($P < 0.05$).
**Significantly different from group CE ($P < 0.01$). (modified from [33], with permission)

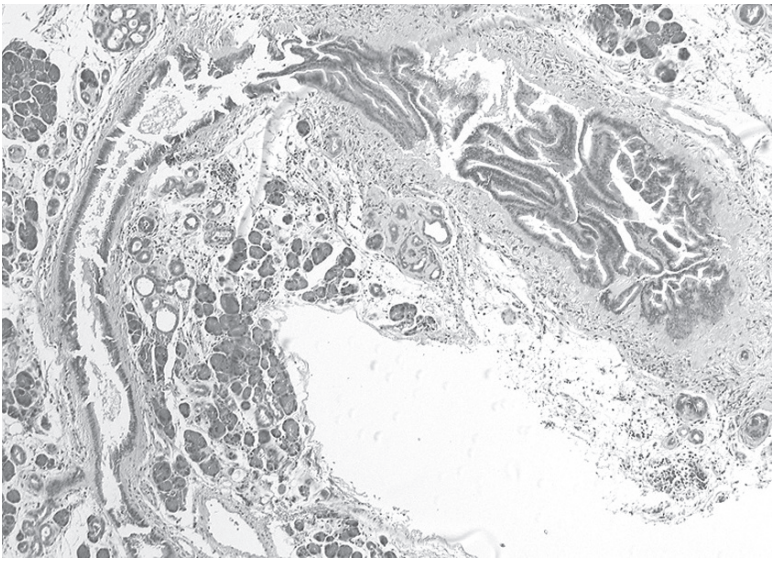

Fig. 12.4 Representative case of induced IPC of the main pancreatic duct in hamsters. The IPC shows marked papillary proliferation growing into the lumen of the main pancreatic duct (H&E ×150) (modified from [33], with permission)

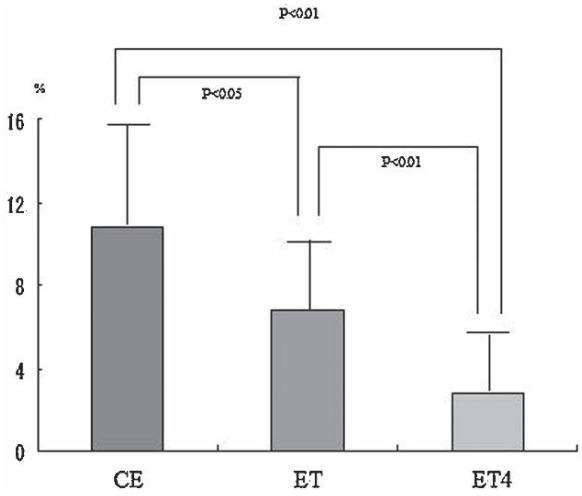

Fig. 12.5 PCNA-LIs of normal epithelial cells in the main pancreatic duct of hamsters from each group. PCNA-LIs were significantly suppressed in accordance with the mixing dosage of Etodolac (modified from [33], with permission)

selective COX-2 inhibitor alone might be insufficient to reverse chemoresistance in pancreatic cancer. Conversely, Crowell et al. [25] stressed the importance of COX-2 activation in the early stages of human pancreatic carcinogenesis; in PanIN1 and PanIN2 lesions. The importance of COX-2 expression in the early stage of polyp formation in the intestine has also been reported [30]. Because

IPMNs of the pancreas follow the hyperplasia–adenoma–carcinoma sequence [5–7] and are less aggressive than pancreatic ductal carcinoma [31], a selective COX-2 inhibitor might be a potential drug for the prevention of IPMNs.

In the present study, oral Etodolac had no chemopreventive effect on the development of BOP-induced tubular adenocarcinoma of the pancreas, which is the ordinary type of human pancreatic cancer. However, Etodolac inhibited the development of IPCs in the main pancreatic duct even in the group ET hamsters given Etodolac at a dosage equal to the human clinical dosage. To our knowledge, this is the first successful *in vivo* study on the chemoprevention of IPCs of the pancreas by a selective COX-2 inhibitor. Both the PGE2 production in the pancreatic tissue and the PCNA-LIs in the noncancerous epithelial cells of the main pancreatic duct were suppressed in proportion to the Etodolac dose in this study.

It is known that COX mediates the late limiting step of prostaglandin biosynthesis in the arachidonic acid cascade and that PGE2 is a reliable biomarker of COX activity [25,32]. These results indicate that suppression of epithelial cell proliferation of the main pancreatic duct by giving Etodolac to reduce PGE2 production in the pancreas is a possible mechanism of cancer prevention in our hamster model.

IPCs induced in the main pancreatic duct of our hamster model produced a smaller amount of mucin than IPMNs in humans. However, there were many similarities between IPCs and IPMNs from an oncological perspective: the tumor developed from the main or large pancreatic ducts, there was intraductal papillary growth with a histological pattern of papillary proliferation of tumor cells, and the malignancy was low-grade [10,31]. Furthermore, no adverse effects of Etodolac on the stomach or heart were seen in any hamster, even those in the ET groups, although cardiovascular morbidity remains a clinical concern with the long-term use of selective COX-2 inhibitors. These findings may support the safe use of Etodolac to prevent the development of IPMNs in humans. In particular, branch duct IPMNs without clinico-radiological indicators of possible malignancy in younger patients and IPMNs in elderly patients with a high surgical risk are good subjects for cancer chemoprevention. For multifocal branch duct IPMNs, surgical removal of the prominent lesions and monitoring the remaining lesions in the remnant pancreas with chemoprevention by selective COX-2 inhibitors may be a reasonable treatment.

In conclusion, the present study demonstrated the chemopreventive effects of Etodolac on BOP-induced IPC of the main pancreatic duct in hamsters. Because human IPMNs have many characteristic features suited for cancer chemoprevention, the administration of selective COX-2 inhibitors may be effective to control IPMNs or to prevent their recurrence after surgery.

References

1. Hruban R.H., Takaori K., Klimstra D.S., Adsay N.V., Albores-Saavedra J., Biankin A.V., Biankin S.A., Compton C., Fukushima N., Furukawa T., Goggins M., Kato Y., Kloppel G., Longnecker D.S., Luttges J., Maitra A., Offerhaus G.J., Shimizu M., Yonezawa S. An illustrated consensus on the classification of pancreatic intraepithelial neoplasia and intraductal papillary mucinous neoplasms. Am. J. Surg. Pathol., 2004 28: 977–987.

2. Ohhashi K., Murakami Y., Maruyama M., Takekoshi T., Ohta H., Ohhashi I., Takagi K., Kato Y. Four cases of mucous secreting pancreatic cancer. Prog. Dig. Endosc., 1982 20: 348–351.
3. Kloppel G., Luttges J. WHO-classification 2000: Exocrine pancreatic tumors. Verh. Dtsch. Ges. Pathol., 2001 85:219–228.
4. Tanaka M., Chari S., Adsay V., Fernandez-del Castillo C., Falconi M., Shimizu M., Yamaguchi K., Yamao K., Matsuno S. International Association of Pancreatology. International consensus guidelines for management of intraductal papillary mucinous neoplasms and mucinous cystic neoplasms of the pancreas. Pancreatology 2006 6:17–32.
5. Kokawa A., Kondo H., Gotoda T., Ono H., Saito D., Nakadaira S., Kosuge T., Yoshida S. Increased expression of cyclooxygenase-2 in human pancreatic neoplasms and potential for chemoprevention by cyclooxygenase inhibitors. Cancer 2001 91:333–338.
6. Niijima M., Yamaguchi T., Ishihara T., Hara T., Kato K., Kondo F., Saisho H. Immunohistochemical analysis and in situ hybridization of cyclooxygenase-2 expression in intraductal papillary-mucinous tumors of the pancreas. Cancer 2002 94:1565–1573.
7. Aoki T., Nagakawa Y., Tsuchida A., Kasuya K., Kitamura K., Inoue K., Ozawa T., Koyanagi Y., Itoi T. Expression of cyclooxygenase-2 and vascular endothelial growth factor in pancreatic tumors. Oncol. Rep. 2002 9:761–765.
8. Hu P.J., Yu J., Zeng Z.R., Leung W.K., Lin H.L., Tang B.D., Bai A.H., Sung J.J. Chemoprevention of gastric cancer by celecoxib in rats. Gut 2004 53:195–200.
9. Ricchi P., Zarrilli R., Di Palma A., Acquaviva A.M. Nonsteroidal anti-inflammatory drugs in colorectal cancer: from prevention to therapy. Br. J. Cancer 2003 88:803–807.
10. Adachi T., Tajima Y., Kuroki T., Mishima T., Kitasato A., Fukuda K., Tsutsumi R., Kanematsu T. Bile-reflux into the pancreatic ducts is associated with the development of intraductal papillary carcinoma in hamsters. J. Surg. Res. 2006 136:106–111.
11. Takahashi M., Pour P., Althoff J., Donnelly T. The pancreas of the Syrian hamster (Mesocricetus auratua). Lab. Anim. Sci. 1977 27: 336.
12. Rinderknecht H., Maset R., Collias K., Carmack C. Pancreatic secretory profiles of protein, digestive, and lysosomal enzymes in Syrian golden hamster. Effect of secretin and cholecystokinin. Dig. Dis. Sci. 1983 28: 518.
13. Pour PM. Tomioka T. Tumours of the pancreas. IARC. Sci. Publ. 1996 126: 149.
14. Eberhart C.E., Coffey R.J., Radhika A., Giardiello F.M., Ferrenbach S., DuBois R.N. Up-regulation of cyclooxygenase 2 gene expression in human colorectal adenomas and adenocarcinomas. Gastroenterology 1994 107:1183–1188.
15. Ristimaki A., Honkanen N., Jankala H., Sipponen P., Harkonen M. Expression of cyclooxygenase-2 in human gastric carcinoma. Cancer Res. 1997 57:1276–1280.
16. Zimmermann K.C., Sarbia M., Weber A.A., Borchard F., Gabbert H.E., Schror K. Cyclooxygenase-2 expression in human esophageal carcinoma. Cancer Res. 1999 59:198–204.
17. Patel S., Chiplunkar S. Role of cyclooxygenase-2 in tumor progression and immune regulation in lung cancer. Indian J. Biochem. Biophys. 2007 44:419–428.
18. Tsujii M., DuBois RN. Alterations in cellular adhesion and apoptosis in epithelial cells overexpressing prostaglandin endoperoxide synthase 2. Cell 1995 83:493–501.
19. Tsujii M., Kawano S., DuBois RN. Cyclooxygenase-2 expression in human colon cancer cells increases metastatic potential. Proc. Natl. Acad. Sci. U. S. A. 1997 94:3336–3340.
20. Tsujii M., Kawano S., Tsuji S., Sawaoka H., Hori M., DuBois R.N. Cyclooxygenase regulates angiogenesis induced by colon cancer cells. Cell 1998 93:705–716.
21. Molina M.A., Sitja-Arnau M., Lemoine M.G., Frazier M.L., Sinicrope F.A. Increased cyclooxygenase-2 expression in human pancreatic carcinomas and cell lines: growth inhibition by nonsteroidal anti-inflammatory drugs. Cancer Res. 1999 59:4356–4362.
22. El-Rayes B.F., Ali S., Sarkar F.H., Philip P.A. Cyclooxygenase-2-dependent and -independent effects of celecoxib in pancreatic cancer cell lines. Mol. Cancer Ther. 2004 23:1421–1426.
23. Furukawa F., Nishikawa A., Lee I.S., Kanki K., Umemura T., Okazaki K., Kawamori T., Wakabayashi K., Hirose M. A cyclooxygenase-2 inhibitor, nimesulide, inhibits postinitiation

phase of *N*-nitrosobis(2-oxopropyl)amine-induced pancreatic carcinogenesis in hamsters. Int. J. Cancer 2003 104:269–273.
24. Schuller H.M., Zhang L., Weddle D.L., Castonguay A., Walker K., Miller M.S. The cyclooxygenase inhibitor ibuprofen and the FLAP inhibitor MK886 inhibit pancreatic carcinogenesis induced in hamsters by transplacental exposure to ethanol and the tobacco carcinogen NNK. J. Cancer Res. Clin. Oncol. 2002 128:525–532.
25. Crowell P.L., Schmidt C.M., Yip-Schneider M.T., Savage J.J., Hertzler D.A. 2nd, Cummings W.O. Cyclooxygenase-2 expression in hamster and human pancreatic neoplasia. Neoplasia 2006 8:437–445.
26. Matsubayashi H., Infante J.R., Winter J., Klein A.P., Schulick R., Hruban R., Visvanathan K., Goggins M. Tumor COX-2 expression and prognosis of patients with resectable pancreatic cancer. Cancer Biol. Ther. 2007 6:1569–1575.
27. Yip-Schneider M.T., Barnard D.S., Billings S.D., Cheng L., Heilman D.K., Lin A., Marshall S.J., Crowell P.L., Marshall M.S., Sweeney C.J. Cyclooxygenase-2 expression in human pancreatic adenocarcinomas. Carcinogenesis 2000 21:139–146.
28. Larsson S.C., Giovannucci E., Bergkvist L., Wolk A. Aspirin and nonsteroidal anti-inflammatory drug use and risk of pancreatic cancer: a meta-analysis. Cancer Epidemiol. Biomarkers Prev. 2006 15:2561–2564.
29. El-Rayes B.F., Zalupski M.M., Shields A.F., Ferris A.M., Vaishampayan U., Heilbrun L.K., Venkatramanamoorthy R., Adsay V., Philip P.A. A phase II study of celecoxib, gemcitabine, and cisplatin in advanced pancreatic cancer. Invest. New Drugs 2005 23:583–590.
30. Oshima M., Dinchuk J.E., Kargman S.L., Oshima H., Hancock B., Kwong E., Trzaskos J.M., Evans J.F., Taketo M.M. Suppression of intestinal polyposis in Apc delta716 knockout mice by inhibition of cyclooxygenase 2 (COX-2). Cell 1996 87:803–809.
31. Maire F., Hammel P., Terris B., Paye F., Scoazec J.Y., Cellier C., Barthet M., O'Toole D., Rufat P., Partensky C., Cuillerier E., Lévy P., Belghiti J., Ruszniewski P. Prognosis of malignant intraductal papillary mucinous tumours of the pancreas after surgical resection. Comparison with pancreatic ductal adenocarcinoma. Gut 2002 51:717–722.
32. Sun Y., Tang X.M., Half E., Kuo M.T., Sinicrope F.A. Cyclooxygenase-2 overexpression reduces apoptotic susceptibility by inhibiting the cytochrome c-dependent apoptotic pathway in human colon cancer cells. Cancer Res. 2002 62:6323–6328.
33. Adachi T, Tajima Y, Kuroki T, Mishima T, Kitasato A, Tsuneoka N, Kanematsu T. Chemopreventive effects of a selective cyclooxygenase-2 inhibitor (etodolac) on chemically induced intraductal papillary carcinoma of the pancreas in hamsters. Carcinogenesis 2008 29:830–833.

Chapter 13
Establishment of Transplantable Biliary Cancer Lines

Tomohiro Fukahori, Keiji Inoue, Tsutomu Tomioka, Yoshitsugu Tajima, Tsukasa Tsunoda, and Takashi Kanematsu

A. Cancer Line from Gallbladder Carcinoma

13.1 Summary

A transplantable cancer line from the gallbladder was established in Syrian golden hamsters. The primary tumor of the gallbladder was induced by a subcutaneous injection of *N*-nitrosobis(2-oxopropyl)amine (BOP) in hamsters after cholecystoduodenostomy with dissection of the common duct. The tumor was inoculated into the cavity of the gallbladder and subcutaneous tissue and was transplantable, with an uptake rate of 100%. Histologically, the primary induced gallbladder tumor was well-differentiated papillary adenocarcinoma and the principal structure of all allograft tumors was of poorly differentiated ductal adenocarcinoma. These tumors expressed blood group-related antigens, including A, H, and P-glycoproteins. To our knowledge, this is the first report of carcinoma of the gallbladder transplantable in a laboratory animal.

13.2 Introduction

Carcinoma of the gallbladder is a therapeutic challenge. To improve the results of various treatments, *in vivo* or *in vitro* models of this malignant neoplastic disease are needed for related studies. For this study, we induced gallbladder carcinomas by *N*-nitrosobis(2-oxopropyl)amine (BOP) in Syrian golden hamsters after dissection of the common duct and cholecystoduodenostomy [1]. The tumor was inoculated into the gallbladder and subcutaneous tissues of inbred recipient hamsters [2]. The tumor has remained transplantable for 20 generations. Thus, we describe the characteristics of this transplantable carcinoma of the gallbladder.

Y. Tajima et al. (eds.), *Hepatobiliary and Pancreatic Carcinogenesis in the Hamster*,
DOI: 10.1007/978-4-431-87773-8_13, © Springer 2009

13.3 Experimental Protocol

Syrian golden hamsters obtained from Shizuoka Laboratory Animal Center (Shizuoka Japan) at the age of 4–12 weeks were housed singly in plastic cages on sawdust bedding. They were kept under standard laboratory conditions at a temperature 22 °C in relative humidity 40 ± 5% with a 12 h light/12 h dark cycle. They were given CE-2 pelleted food (Japan Clea, Tokyo, Japan) and water *ad libitum*.

The tumor was derived from a gallbladder cancer induced by *N*-nitrosobis (2-oxopropyl)amine (BOP) injection into the subcutaneous tissue of Syrian golden hamsters after cholecystoduodenostomy and dissection of the common duct [1]. Following anesthetization with pentobarbital 50 mg/kg body weight, i.p., the tumor in the primary gallbladder carcinoma was resected, washed in Hanks' solution, and minced with scissors into approximately 2 mm pieces. These pieces were inoculated subcutaneously into the bilateral dorsum using a 14-gauge needle. By 3 weeks later, the tumor had grown to approximately 2 cm in diameter (Figure 13.1), and was serially transplanted in the same manner. The tumor in the 10th generation was used for the present investigation. For intra-gallbladder transplantation, the minced pieces were inserted into the cavity of the gallbladder, through a 2 mm incision. Following insertion, the incised wound was closed with a continuous suture of 7-0 nylon. Subcutaneous transplantation of the tumor was carried out simultaneously. The hamsters were killed and the whole liver, gallbladder, and subcutaneous tumors were removed, fixed in 10% formalin, embedded in paraffin, serially sectioned, and stained with hematoxylin and eosin (H&E).

The length and width of the subcutaneously transplanted tumors were measured on post-inoculation days 7, 14 and 21. Five hamsters were each given two inoculations. Intra-gallbladder transplantation was done in 15 hamsters. Five hamsters were killed on days 14 and 21, and the tumor size was measured. We did not perform the measurements on day 28 because the hamsters began to die. The tumor volume in cubic centimeters was calculated by the following formula: Tumor volume = $a^2 \times b/2$ (cm^3), where "a" is the short diameter (cm) and "b" is the long diameter (cm).

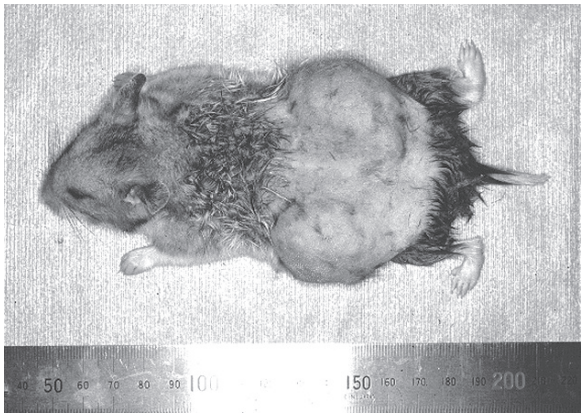

Fig. 13.1 The subcutaneously transplantable gallbladder carcinoma 3 weeks after inoculation of the tumor into the bilateral dorsum of a hamster

DNA patterns were examined by flow cytometry. Specimens taken from the subcutaneous tumor were placed in phosphate buffer solution. The tumor tissue was sliced and cut into smaller pieces of about 0.5 mm^3 using a scalpel and forceps. After passing the tumor tissue through wire mesh gauze, a single cell suspension was obtained. An equal volume of 1% RNAase was added and DNA was stained with propidium iodide 50 µg/ml in Tris-EDTA buffer. The stained solution was examined using a flow cytometer (FACS can, Becton & Dickinson, Mountain View, CA).

The transplanted gallbladder tumors were examined with scanning electron microscopy (SEM). After repeated washing in a 0.1 M sodium cacodylate buffer (pH 7.4), the tissues were fixed in 2% buffered glutaraldehyde with 10% formalin, then postfixed in 2% buffered osmium tetroxide. After dehydration through a graded series of ethanol, the tumors were dried by the critical point method and gold spattered. Tissues for SEM were examined under a JSM-35CLaB6 (Japan Electron Optics Laboratory (JEOL), Tokyo, Japan) with 15 kV accelerating voltage. The remaining tissues were examined histologically.

Tissues for transmission electron microscopy (TEM) were prepared in a similar manner, up to the postfixation by buffered 2% osmium tetroxide. After dehydration through a graded series of ethanol, the tissues were embedded in Epon. Ultra-thin sections (60–80 µm) were stained on the grid with 2% uranyl acetate and 0.4% lead citrate, and then examined under a JEM-1200EX (JOEL, Tokyo, Japan) with 60–80 kV accelerating voltage.

Commercially available monoclonal antibodies (MAb) against the synthetic trisaccharide of blood group A, B, and H determinants (DAKO Japan), CA 19-9 (Toray-Fuji Bionics, Tokyo, Japan), carcinoembryonic antigen (CEA; DAKO Japan), and P-glycoprotain (P-glyco-CHEK-c219, Centcore, Malvern, PA) were used. The concentration of each MAb was 40 µg/ml. Immunohistochemical staining was done using a Vectastain Avidin Biotin peroxidase Complex (ABC) kit (Vector Laboratories, Burlingame, CA) [3]. The gallbladder tumors were resected and fixed in 10% formalin for 1–2 days. The tissues were dehydrated as usual for paraffin embedding and 4 µm thick serial sections were stained. The reactivity with each of the antibodies was determined on an arbitrary scoring system. For each tumor, the number of positively stained cells was estimated as follows: 0% (–); up to 5% (1+); between 5% and 30% (2+); between 30% and 70% (3+); and between 70% and 100% (4+). The pattern of cellular staining was categorized as glycocalyx (luminal), diffuse (granular), cytoplasmic, and Golgi [4].

13.4 Tumorigenicity and Growth Characteristics

The uptake rate of the tumors inoculated into the gallbladder and subcutaneous tissue was 100%. The growth curves of the transplanted tumors are shown in Figure 13.2. Allografts in the cavity of the gallbladder grew rapidly and were clearly visible 7 days after inoculation. By 3 weeks, the mean volume of the tumors had reached 1.3 cm^3, and from 4 weeks, the hamsters began to die of progression of the carcinoma. Growth of the

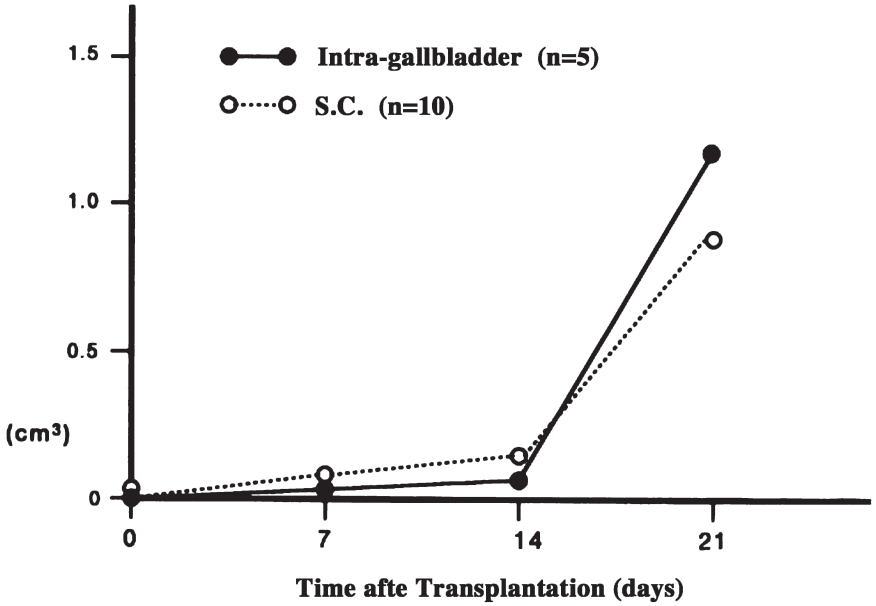

Fig. 13.2 Growth curves of the intra-gallbladder and subcutaneous transplants. The intra-gallbladder tumors adhere to the mucosa of the gallbladder for longer, but expand faster than the subcutaneous tumors (modified from [2], with permission)

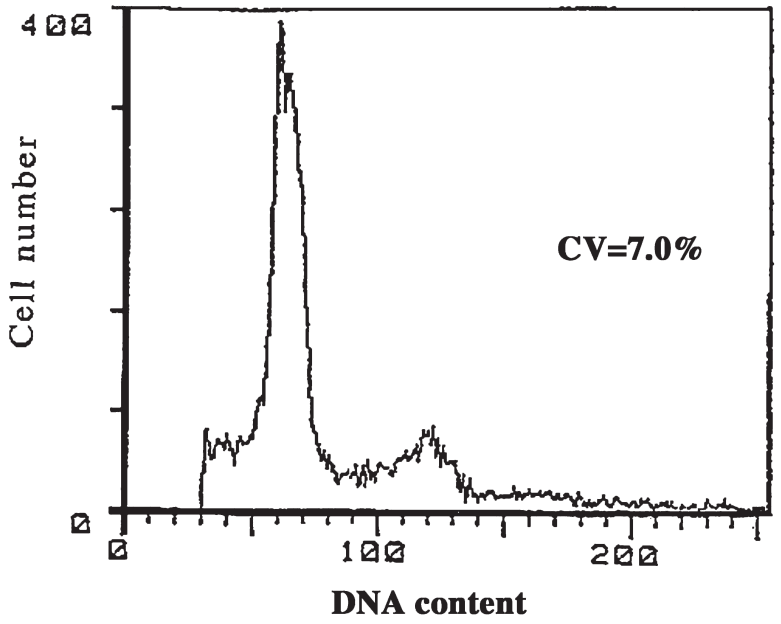

Fig. 13.3 Histogram of the DNA aneuploidy pattern (modified from [2], with permission)

subcutaneous allografts was slower than that of the intra-gallbladder transplants at 21 days. The hamsters in this group were still alive even after 8 weeks. By 10 weeks, the tumor had grown to about 4.5 cm in greatest diameter, with ulceration of the skin.

All the intra-gallbladder transplants invaded the liver, and a few metastasized to the regional lymph nodes and peritoneum. Metastases to the axillary lymph nodes and para-aortic lymph nodes were evident in the subcutaneous group more than 8 weeks after the implant. Lung metastasis was occasionally evident, but there were no metastases to the liver or other organs.

13.5 DNA Analysis

The DNA histogram is shown in Figure 13.3. The pattern of this tumor was DNA aneuploidy; hence, the malignant potential was high.

13.6 Morphology

The primary tumor was soft, white, and localized in the gallbladder. Histologically, it was well-differentiated adenocarcinoma with a papillary structure (Figures 13.4 and 13.5). The macroscopic appearance of the intra-gallbladder transplants was firm, round or lobulated, yellowish-white and solid (Figure 13.6) when small, and

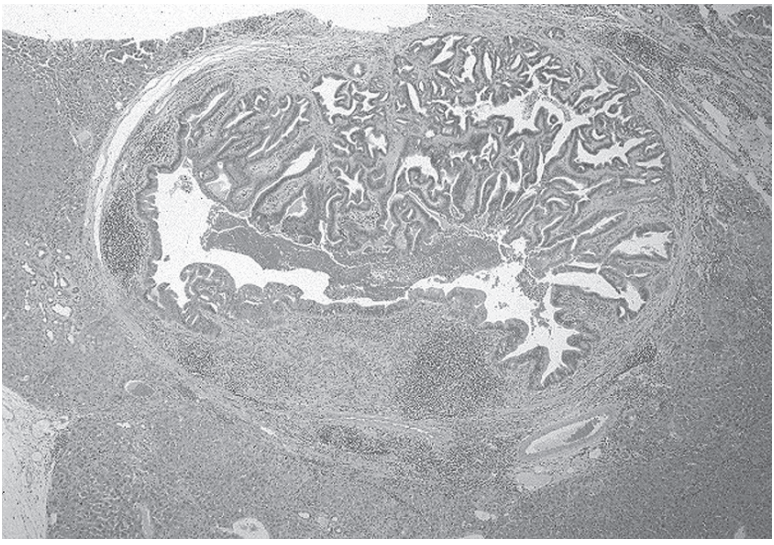

Fig. 13.4 A section of the primary tumor in the gallbladder. Well-differentiated adenocarcinoma with a papillary structure was seen. The tumor was localized in the gallbladder and the wall of the gallbladder, which was thickened and fibrotic, but not invaded (H&E, ×35) (modified from [2], with permission)

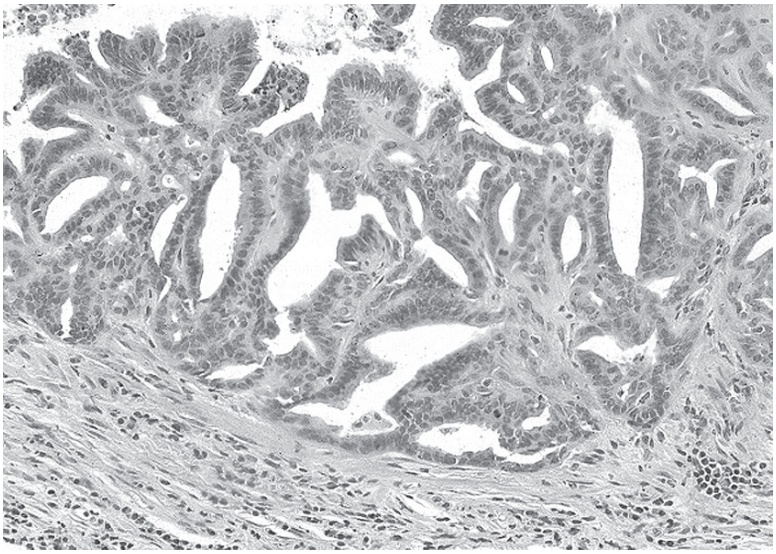

Fig. 13.5 Magnified view of the primary gallbladder carcinoma. The papillary structures are lined with tall columnar cells with little nuclear pleomorphism (H&E, ×200) (modified from [2], with permission)

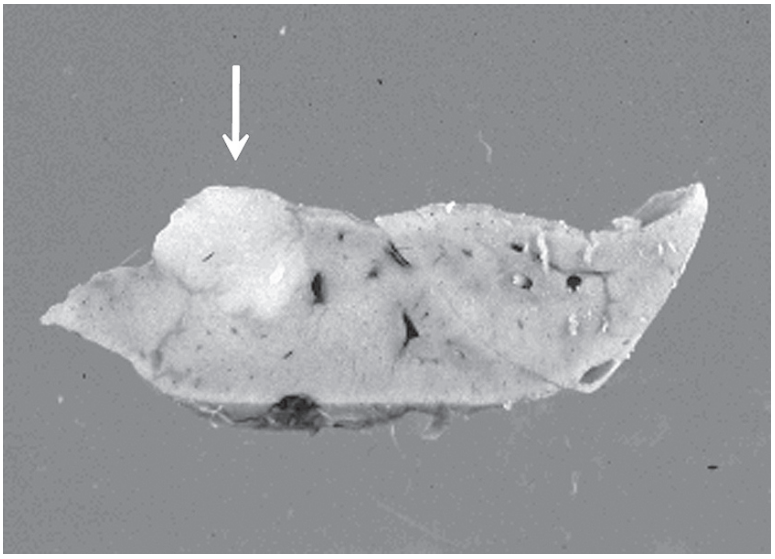

Fig. 13.6 Macroscopic appearance of the intra-gallbladder transplants

yellow and soft with central necrosis when larger than 1.5 cm. The subcutaneous transplants were usually well circumscribed, elastic, and yellowish-white, with central necrosis in tumors larger than 0.5 cm, which was earlier than the intra-gallbladder transplants. Many of the subcutaneous tumors greater than 2 cm in diameter penetrated the skin.

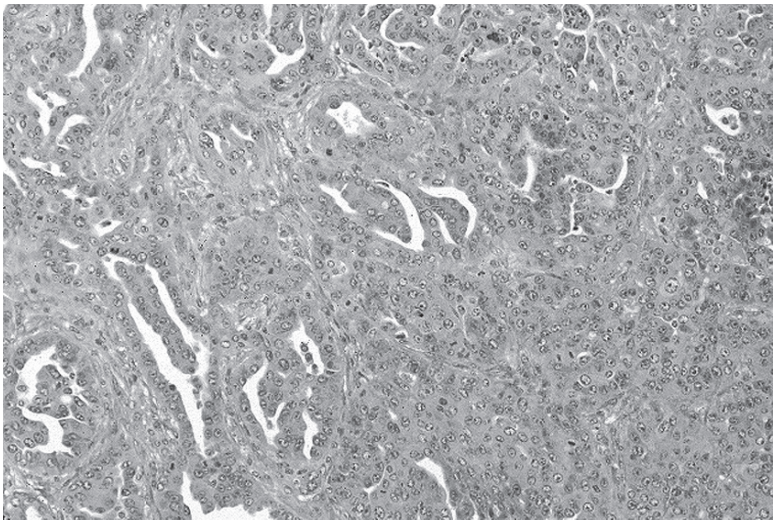

Fig. 13.7 Histological appearance of an intra-gallbladder transplanted tumor. Poorly differentiated adenocarcinoma with an irregular arrangement and few gland formations was seen (H&E, ×100)

Histologically, the principal structure of all the transplanted tumors was poorly differentiated ductal adenocarcinoma (Figure 13.7), in contrast to the primary induced gallbladder cancer, which was well-differentiated papillary adenocarcinoma. Intra-gallbladder transplants rapidly invaded the liver and the gallbladder retained its shape, even in the late stage. The tumor sometimes showed uplift into the lumen of the gallbladder (Figure 13.8). Subcutaneous tumors larger than 0.5 cm had central necrosis and bleeding, which occurred earlier than in the intra-gallbladder.

13.7 Electron Microscopic Findings

13.7.1 Scanning Electron Microscopy (SEM)

In cross sections, the tumors showed medullary proliferation separated by stroma of varying width and there were gland formations. The cells varied in size and shape. The gland was lined by columnar cells. The cell surface was covered by microvilli of varying density and length (Figure 13.9).

13.7.2 Transmission Electron Microscopy (TEM)

The cells had the usual cuboidal shape, but the nuclei were irregular or ovoid with multiple indentations, and contained a coarse marginal chromatin and one or two

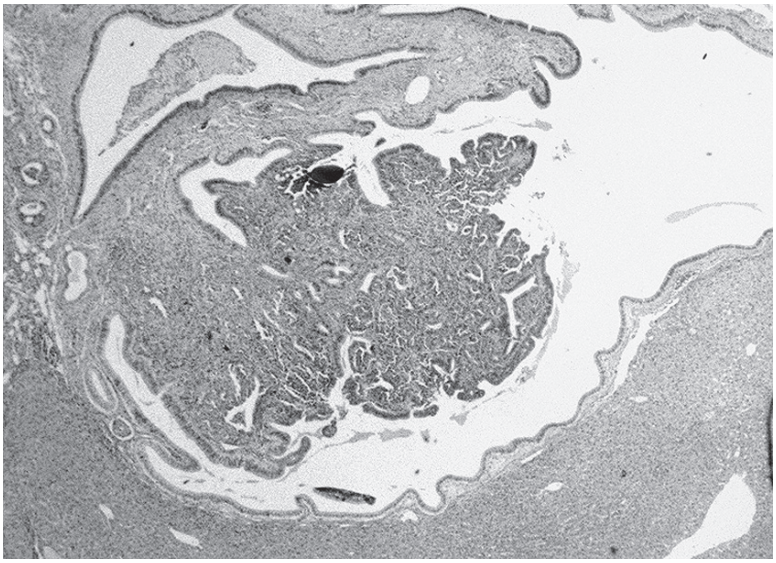

Fig. 13.8 Tumor transplants in the gallbladder. A 2 mm solid tumor arose in the lumen of the gallbladder (H&E, ×35) (modified from [2], with permission)

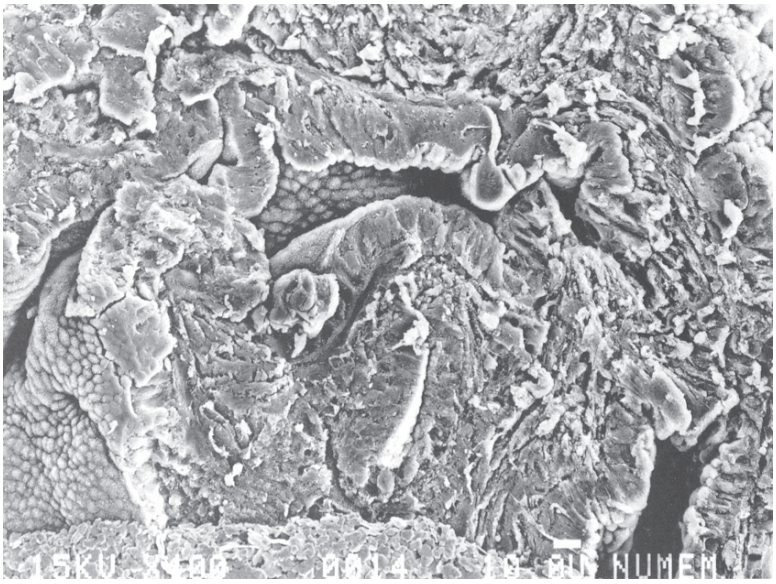

Fig. 13.9 Electron microscopic appearance of an intra-gallbladder transplanted tumor. Small glands consisted of columnar cells with short microvilli on the surface (SEM, ×1,000) ([2], with permission)

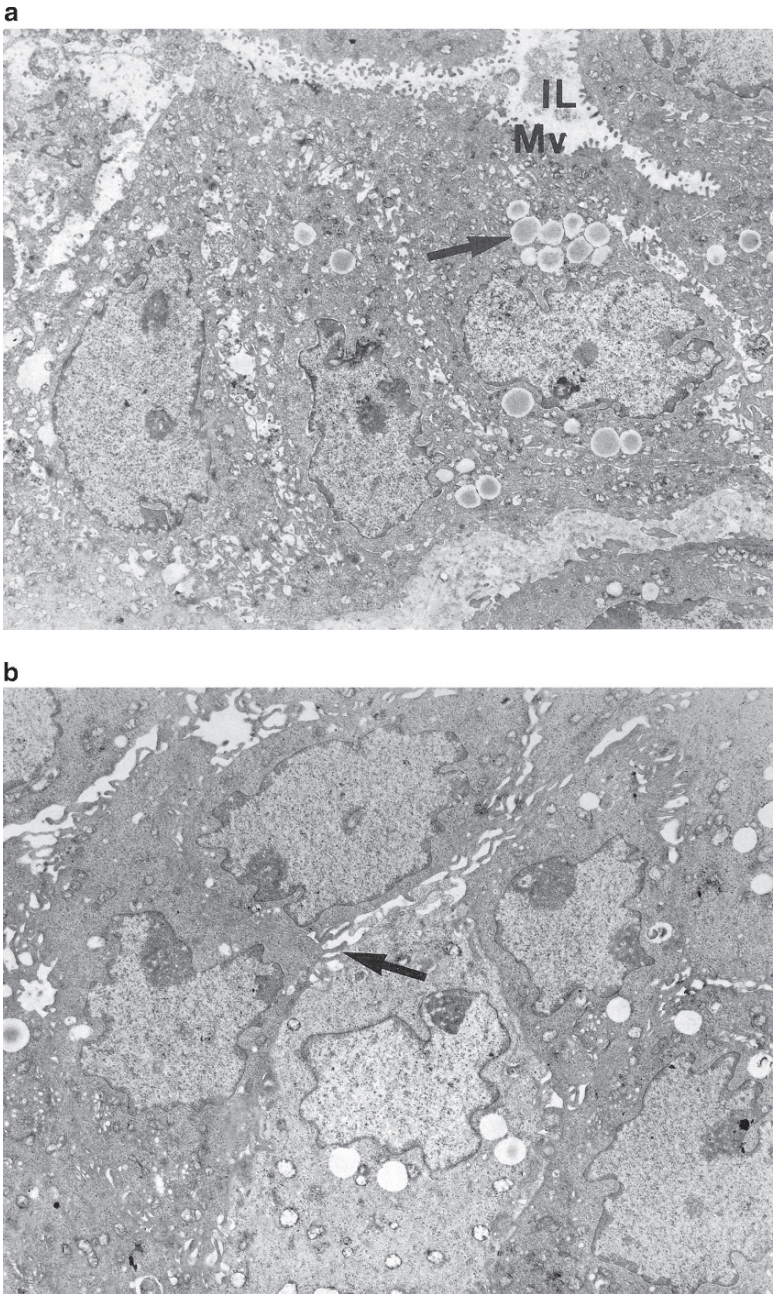

Fig. 13.10 Ultrastructure of the tumor. **(a)** Tumor transplants with intercellular lumen (IL). Well-differentiated microvilli (MV), which were short and blunt, emerged into the gland lumen. The irregular nuclei had multiple indentations. Secretory granules were evident (*arrow*) (TEM, ×2,000). **(b)** The cells were connected by slender cytoplasmic processes (*arrow*) (TEM, ×3,000) ([2], with permission)

nucleoli. Microvilli, most of which were short and blunt, emerged from the apical surface and projected into the gland lumen. These nuclear atypia and immature structures corresponded with the malignant behavior of this tumor. Mucin vacuoles were present in the cytoplasm. The cells were connected by cytoplasmic processes (Figure 13.10).

13.8 Expression of Antigens

The immunohistochemical findings are summarized in Table 13.1. The cells of both allografts expressed Blood Group Related Antigens (BGR-Ags) A and H, and P-glycoproteins. MAb-A and H showed both diffuse and glycocalyx patterns (Figure 13.11), whereas reactivity of the MAb-P-glycoprotein was of a Golgi pattern (Figure 13.12). Negative reactivity was found with antibodies against B, CA19-9 and CEA. Similar patterns were found in the metastases of the tumors.

13.9 Comments

Advances in biomedical research depend on the availability of appropriate experimental animal models. We succeeded in inducing gallbladder carcinoma at a high frequency in Syrian golden hamsters, by administering BOP, then performing cholecystoduodenostomy and dissection of common duct [1]. To our knowledge, this is the first available model of common carcinoma: many experiments have produced adenomas, but none have produced carcinoma with certainty [5–7]. The administration of BOP has resulted in carcinoma of the pancreas and intrahepatic bile duct carcinoma, but rarely carcinoma of the gallbladder [8].

From the malignant tumors grown by Tajima, we established a transplantable carcinoma. A distinctive feature of this transplantable tumor was its potential to be transplanted into the gallbladder in inbred hamsters. This characteristic makes feasible studies on the mechanism of invasion into the liver and of metastasis to regional lymph nodes and other organs. Although the available human gallbladder carcinoma cell lines are useful for examining the characteristics of the cells [9–13], they do not enable us

Table 13.1 Expression of antigens in gallbladder carcinoma of the hamster

Antibody	Staining score	Pattern of cellular staining
CEA	(−)	(−)
CA19-9	(−)	(−)
BGR-Ag		
A	(4+)	Glycocalyx and diffuse cytoplasmic
B	(−)	(−)
H	(2+)	Glycocalyx and diffuse cytoplasmic
P-glycoprotein	(4+)	Golgi

BGR-Ag, blood group related antigen; CEA, carcinoembryonic antigen.
Staining score: 0% (−); 0–5% (+); 5–30% (2+); 30–70% (3+); 70–100% (4+).
(modified from [2], with permission)

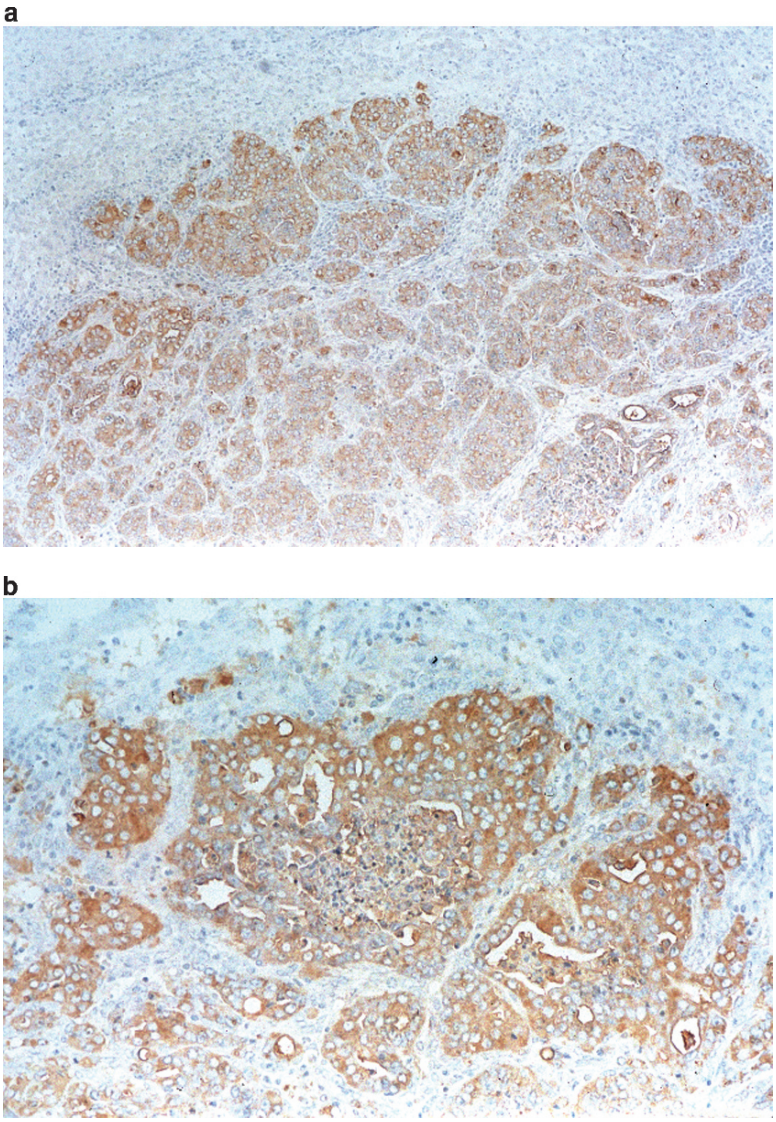

Fig. 13.11 Expression of A-antigen of the intra-gallbladder transplants in the liver (lower half). **(a)** The reactive area was limited to the tumor (ABC method, ×100). **(b)** The reactivity of MAb-A was mainly of a diffuse cytoplasmic pattern (ABC method, ×400) (modified from [2], with permission)

to examine the behavior of cells in the gallbladder *in vivo*. With our model, the node of progression of the tumor and its response to drugs can be closely followed.

Morphologically, this tumor closely resembles poorly differentiated adenocarcinoma of the gallbladder in humans: a small-cell type characterized by the proliferation of small round cells that grow in nodules, single rows, solid sheets, nests, cords, or

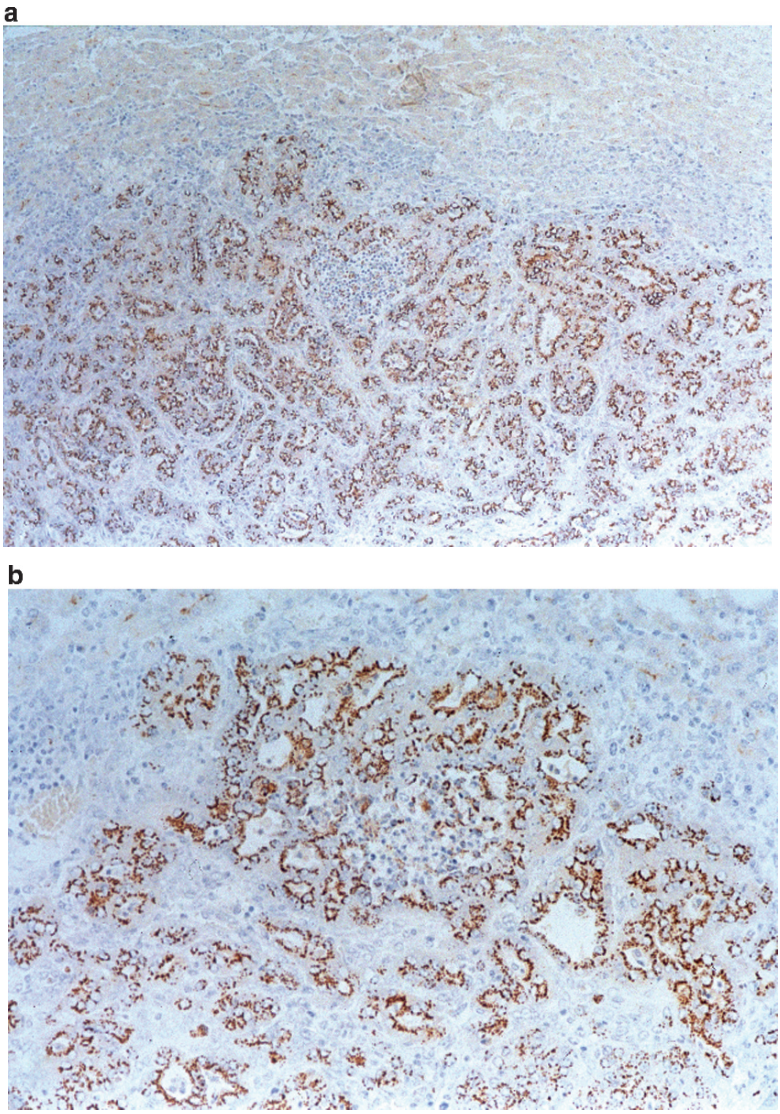

Fig. 13.12 Expression of the P-glycoprotein. (**a**) The upper part was normal liver tissue. The reactivity in the neoplastic portion, like A-antigen (ABC method, ×100). (**b**) Strong reactivity of a Golgi pattern was seen in the tumor area (ABC method, ×400)

trabeculae. The individual cells contain round or ovoid vesicular hyperchromatic nuclei with prominent nucleoli and the stroma shows variable fibrosis. Vascular invasion and extensive necrosis are consistent features.

These transplantable gallbladder and subcutaneous tumors expressed the BGR-Ags A type. There are reports of tumor markers such as the carbohydrate antigens containing BGR-Ags and CA19-9 in humans. Immunohistochemical testing of carcinomas revealed positivity for BGR-Ags in the lung [14], stomach [15,16],

colon [17], pancreas [18], breast [17], urinary bladder [19,20], and ovaries [17]. These BGR-Ags, which are not seen in normal tissue, provide useful information about the mechanism of carcinogenesis and aid in detecting the malignancy as tumor markers. We reported findings of a BGR-Ag positive pancreatic carcinoma cell line induced by BOP in hamsters [4]. BGR-Ags seem to be tumor-associated antigens in the pancreas, liver, and bile duct of Syrian golden hamsters. P-glycoprotein is a cell surface membrane protein related to multidrug resistance [21,22]. This protein was localized only in the tumor, whereas BGR-Ags were present in the tumors and also in the hyperplastic bile duct epithelium. P-glycoprotein is more sensitive for detecting the extension of the tumor.

This transplantable tumor should prove to be an important addition to the laboratory armamentarium for studying the nature of gallbladder carcinoma. This model can also be used to examine the mechanisms of intra-bile duct lymphatic, and perineural spread, and possible therapeutics.

In summary, we developed a transplantable gallbladder carcinoma in Syrian golden hamsters. The tumor was derived from the model of the anomalous arrangement of the pancreatico-biliary ductal system, with the administration of BOP. This tumor is available for the study of gallbladder carcinoma in the laboratory animal.

B. Cancer Line from Intrahepatic Bile Duct Carcinoma

13.10 Summary

A subcutaneously transplantable cancer line from the intrahepatic bile duct (IHBD) induced by *N*-nitrosobis(2-oxopropyl)amine was established in Syrian golden hamsters. The doubling time of this tumor was 2.6 days when 2×10^5 tumor cells were inoculated subcutaneously, with an uptake rate of 100%. Tumor growth was significantly faster in the male hamsters, but neither estrogen nor androgen receptors were detected in the tumor. The primary and all allograft tumors were tubular adenocarcinomas with fibrosis and a scirrhous pattern resembling human peripheral IHBD carcinoma. Transmission electron microscopy showed irregular glands covered with numerous microvilli. Blood group-related antigens including A, B and H were positive. P-glycoprotein, which is an indicator of multidrug resistance, was also positive. Carcinoembryonic antigen and CA19-9 as general tumor markers of the biliary tract were negative. The DNA pattern of this transplantable carcinoma was diploid. From this transplantable cancer line, we established new cell lines in culture; namely, NUF-BD-4 and NUF-BD-9. The doubling times of these cell lines were calculated as 16 and 23 h, respectively. Scanning electron microscopic findings showed an irregular cell membrane covered in numerous microvilli. In NUF-BD-4, the blood group-related A-antigen was positive. Subcutaneous inoculation of both cell lines resulted in tumor growth in hamsters. This newly established animal model of a transplantable IHBD cancer line and cell lines can be used to investigate the mechanisms of the synthesis and secretion of tumor-associated antigens and to study potential therapeutic agents.

13.11 Introduction

The management of patients with intrahepatic bile duct (IHBD) carcinoma is fraught with difficulties. The major concerns are finding ways of early detection, routes of tumor spread, and effective treatment approaches. We induced primary IHBD carcinoma in Syrian golden hamsters after cholecystoduodenostomy with dissection of the distal common duct and the administration of *N*-nitrosobis(2-oxopropyl)amine (BOP). BOP is well recognized as a potent pancreatic carcinogen in hamsters, which also induces bile duct carcinoma [1,23]. The tumors induced in the IHBD were morphologically similar to those found in humans. We succeeded in transplanting this IHBD tumor into the subcutaneous tissue of hamsters [24]. Moreover, from this transplantable cancer line, we established new cell lines in culture. The biological and morphological characteristics of the cancer line and cell lines are described herein.

13.12 Experimental Protocol

13.12.1 Establishment of the Cancer Line

Eighty Syrian golden hamsters of both sexes were supplied by the Shizuoka Laboratory Animal Center Co. Ltd. (Shizuoka, Japan). The hamsters were over 6 weeks of age and non-inbred. They were housed in plastic cages on sawdust bedding and given a CE2 pelleted diet (Japan Clea Inc., Tokyo, Japan) and water *ad libitum*. The standard laboratory conditions at the Laboratory Animal Center for Biochemical Research, Nagasaki University School of Medicine were as follows: temperature, 22 °C; relative humidity, 40 ± 5%; 12 h light/12 h dark cycle.

Histologically diagnosed IHBD cancer was induced by the subcutaneous injection of BOP into hamsters. The primary tumor shown in Figure 13.13 contained glands with a small lumen and produced mucin in a uniform pattern. The glandular epithelium was composed of small cuboidal cells with round nuclei. Some tumors had predominantly small cells with scanty cytoplasm, but abundant sclerosis. The tumors were removed after anesthetization of the animals with intra peritoneal sodium pentobarbital, 50 mg/kg body weight. Tumor specimens were rinsed in sterile saline and transferred to a sterile plastic Petri dish to which Hanks' solution was added. Using a sterile scalpel, scissors and forceps, tumor tissues were minced, sliced, and cut into 0.5 mm^3 pieces. Some cells were tested for viability, using the trypan blue dye exclusion method. Viable tumor cells were inoculated subcutaneously into the dorsum of anesthetized hamsters and histological confirmation of the tumors that developed was recorded.

Viable 2×10^5 (0.2 ml, 10^6/ml) tumor cells were injected into the subcutaneous tissue of 10 recipient female hamsters and a growth curve was estimated by measuring the longest and shortest diameters of the tumors on days 7, 11, 14, 18, and 21 after inoculation. Measurements were taken after the animals were anesthetized with

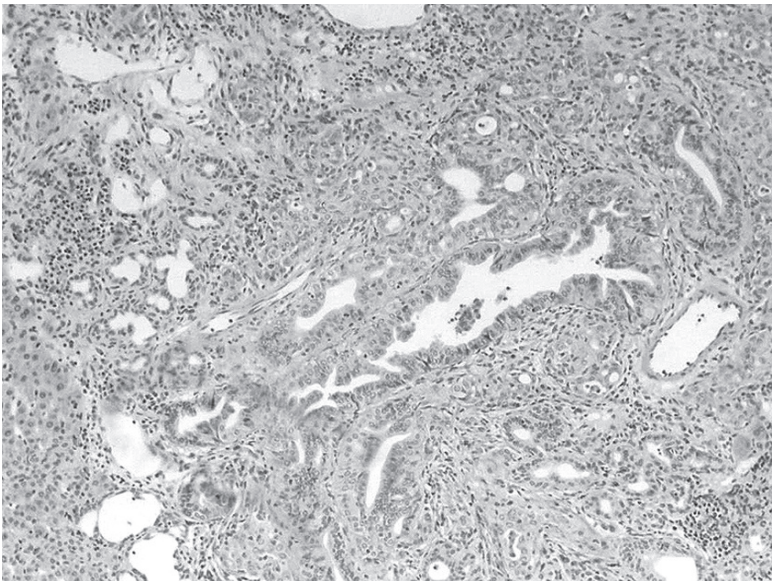

Fig. 13.13 Histologic appearance of a primary IHBD tumor with well-differentiated adenocarcinoma. The glands had a small lumen and epithelium was composed of small cuboidal cells with round nuclei (H&E, ×100) (modified from [24], with permission)

ether, and the estimated tumor weight was calculated using the method of Ovejera et al. [25]: tumor weight = $a^2 \times b/2$ (g), where "a" is the shortest diameter (cm) and "b" is the longest diameter (cm).

To evaluate the effects of the sex of animal on growth, viable 1×10^5 (0.1 ml, 10^6/ml) tumor cells were injected into the subcutaneous tissue of five 8-week-old male and five 8-week-old female hamsters. Tumor size was measured on days 7, 14, and 21 after inoculation. Samples to test for estrogen receptors were collected from females and samples to test for androgen receptors were collected from males. The resected specimens were placed immediately in a dry-ice box and receptors were examined by radioimmunoassay.

We used the 10th generation subcutaneous tumors for histological examination. Pieces of each tumor were fixed in 10% formalin and embedded in paraffin, using standard techniques. Each 4-μm section was stained with hematoxylin and eosin. For transmission electron microscopy (TEM) and scanning electron microscopy (SEM), tumor tissues were fixed in 2% buffered glutaraldehyde with 10% formalin. After fixation, these tissues were sliced about 1 mm thick. After repeated washing in phosphate buffer solution (PBS), samples were fixed in 2% osmium tetroxide, and dehydrated in an ascending series of ethanol. Samples for TEM were embedded in Epon, sliced into ultra-thin sections (60–80 nm), stained on the grid with 2% uranyl acetate and 0.4% lead citrate, and observed using a JEM-1200EX (Japan Electron Optics Laboratory, Tokyo, Japan) with 60–80 kV accelerating voltage. After dehydration, samples for SEM were dried by the critical point method and

spattered with gold. Observation was done using a JSM-35CLaB6 (Japan Electron Laboratory) with 15 kV accelerating voltage.

For immunohistochemical analysis, we used monoclonal antibodies (MAb) against the synthetic trisaccharide of blood groups A, B, and H determinants (Dick, Tokyo, Japan). CEA (Dick), CA19-9 (Toray-Fuji Bionics, Tokyo, Japan) and P-glycoprotein (P-glcoCHEK-c219, Cent core, Malvern, PA) were examined using the avidin-biotin peroxides complex (ABC) immunohistochemical method, with a Vectastain ABC kit (Vector Laboratories Buringame, CA). The concentration of each MAb was 40 µg/ml. Samples for examination were obtained from the subcutaneous tumors. The staining score was based on the number of positive staining cells, and samples were categorized into one of the following: 0% (–); <5% (1+); 5–30% (2+); 30–70% (3+); and >70% (4+). The pattern of cellular staining was categorized as glycocalyx (luminal), diffuse (granular), cytoplasmic, or Golgi patterns [26].

Specimens taken from the subcutaneous tumors were placed in PBS for DNA analysis. Tumor tissues were sliced into 0.5 mm^3 pieces, using a sterilized scalpel, scissors, and forceps. After the addition of PBS, the preparation was passed through wire mesh. An equal volume of 1% ribonucleic acidase was added and DNA was stained with propidium iodide in TRIS-EDTA buffer (50 µg/ml). The attained solution was analyzed using a flow cytometer (FACScan, Becton and Dickinson, Mountain View, CA). Comparisons between the mean tumor weights of male and female hamsters were made using Student's *t* test.

13.12.2 Establishment of Cancer Cell Lines

The transplanted subcutaneous tumors were removed after intraperitoneal anesthetization of the animals with sodium pentobarbital, 50 mg/kg body weight. Tumor specimens were rinsed in sterile saline and transferred to a sterile plastic Petri dish, to which Hanks' solution was added. Tumor tissues were minced using a sterile scalpel, scissors, and forceps and transferred through wire mesh gauze into RPMI-1640 (Nissui Pharmaceutical Co., Ltd., Tokyo) culture medium supplemented with 10% fetal bovine serum (GIBCO, New York). The cultures were incubated at 37 °C in a humidified 5% CO_2/95% air atmosphere. The tissue debris was removed the next day and the culture medium was replaced. The culture dish was examined for the growth of inoculated cells under a phase-contrast microscope twice a week. When the culture cells were confluent, subculture was done as follows: The culture medium was replaced by 1 ml of 0.25% trypsin phosphate buffer solution (PBS) and incubated for 15 min at 37 °C in an atmosphere with 5% CO_2. We added 2 ml culture medium to stop the action of trypsin. After centrifugation at 1,000 rpm for 5 min, the supernate was decanted, and the cell pellet was resuspended in the culture medium and transferred into six well-dishes. When cells formed colonies, a drop of 0.25% trypsin was added to a single colony and incubated for 15 min. Separated cells were transferred into the culture dishes. When the cells formed colonies again, the same colonial cloning was done. After this procedure, the cells separated by

trypsin were transferred into the 96 well-dishes with culture medium at final concentration of one cell/dish for pure cell cloning. The culture dish was examined for growth of inoculated cells under a phase-contrast microscope twice a week. When the culture cells were confluent, the culture medium was replaced with 100 ml 0.25% trypsin and incubated for 15 min at 37 °C in an atmosphere with 5% CO_2. Separated cells were transferred into the culture dishes and incubated. When the culture dishes were confluent, subculture was repeated.

We subcultured $10^4 \times$ 20th generation viable tumor cells in 12 well-dishes. Cell numbers were counted every 24 h for up to 120 h. The viable cell count was estimated using the trypan blue dye exclusion method. Next, $10^4 \times$ 40th generation viable tumor cells in 0.2 ml were subcultured on sterile glass slides in the laboratory dish for 24 h. The specimens on the glass slides were fixed in alcohol, and stained with hematoxylin and eosin. Stained cells were examined under light microscopy.

Samples for examination were obtained by the same procedure as for light microscopy. We used MAbs against the synthetic trisaccharide of blood groups A, B and H determinants and an Avidin Biotin peroxides Complex immunohistochemical method, with a Vectastain ABC kit. The concentration of each MAb was 40 mg/ml.

Viable tumor cells (NUF-BD-4, 20th generation) were subcultured on sterile glass slides in a laboratory dish for 24 h for electron microscopy. The specimens on the glass slides were fixed in 2% buffered glutaraldehyde with 10% formalin. After washing in PBS, the samples were fixed in 2% osmium tetroxide. After dehydration, the samples were dried and observed using JSM-35CLaB6 with 15 kV accelerating voltage. Next, 10^5 viable tumor cells (0.2 ml, 5×10^5/ml, NUF-BD-9) were inoculated subcutaneously into the dorsum of eight anesthetized female hamsters. Histological confirmation of the developed tumor was recorded. The growth curve was estimated by measuring the long and short diameters of the tumors on days 7, 11, 14, 18, and 21 after inoculation. Measurements were done after the animals were anesthetized with ether and the estimated tumor weight was calculated using the method of Ovejera et al. [25].

13.13 Growth Curve of Cancer Line

Serial changes in tumor weight are illustrated in Figure 13.14. The mean tumor weights were approximately 1.5 and 3.0 g on days 14 and 18 after inoculation and the doubling time was calculated as 2.6 days. Cystic change in the tumor was evident on day 14. The uptake rate was 100%. There were no metastatic lesions.

13.14 Influence of the Sex of the Animal on Tumor Growth

The tumor weights on day 21 after inoculation in the male and female hamsters were significantly different ($p < 0.05$), as shown in Figure 13.15. The doubling time was 2.8 days in both sexes. Based on this evidence, we searched for receptors for estrogen and androgen in the tumor tissue, but all findings were negative.

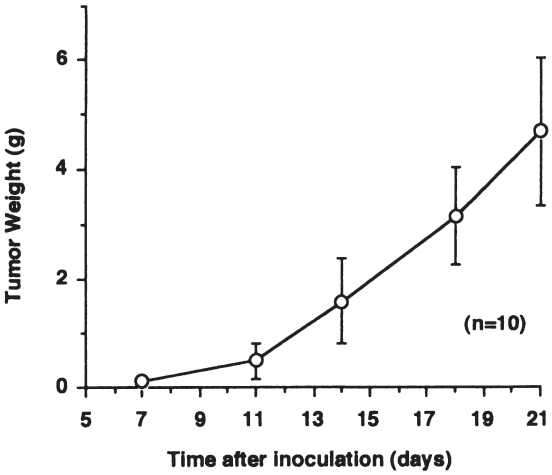

Fig. 13.14 Growth curve (*in vivo* cancer line) when 2 × 10^5 (n = 10) tumor cells were inoculated into the subcutaneous tissue of the hamsters. Tumor weight was calculated using the following method. Tumor weight = (short diameter)^2 × (long diameter)/2 ([24], with permission)

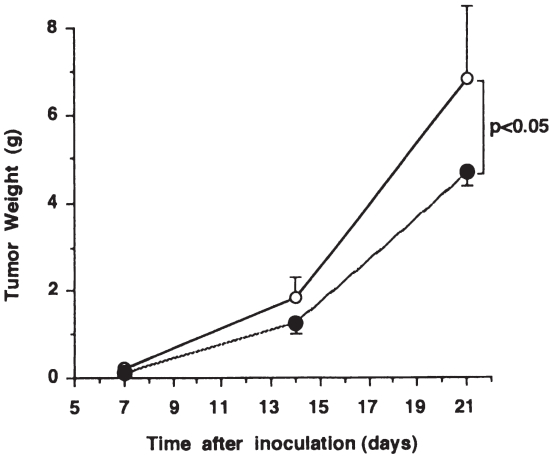

Fig. 13.15 Influence of the animal's sex on tumor growth: 10^5 tumor cells were inoculated subcutaneously into male (o, n = 5) and female (•, n = 5) hamsters. On day 21 after inoculation, there was a significant difference in tumor weight between the sexes ($p < 0.05$)

13.15 Histological Findings of the Cancer Line

Small transplanted subcutaneous tumors were firm and round, but when they grew rapidly, progressive cystic change was seen. The cut surface of the tumor was yellowish-white. The primary was a well-differentiated adenocarcinoma, but 10th generation tumors were moderately or poorly differentiated (Figure 13.16). We evaluated the tumor histologically up to the 20th generation: the main structure of all tumors was tubular adenocarcinoma, which had not changed from the primary lesion.

13.16 Immunohistochemical Findings of the Cancer Line

The expression of antigens is listed in Table 13.2. Both A-antigen and the antibody against P-glycoprotein were stained strongly, but a different pattern was observed

between MAbs A and P-glycoprotein. Staining of MAb A was diffuse and of a glycocalyx pattern (Figure 13.17), whereas the pattern of MAb P-glycoprotein was Golgi (Figure 13.18). Both MAbs B and H showed a moderate staining score. Antibodies against CEA and CA19-9 were negative.

13.17 Electron Microscopy of the Cancer Line

On TEM, the tumor cells were composed of an irregular glandular structure with numerous microvilli. Different-sized lysosome granules were seen near the lumen. Cells were connected by primitive junctions in a scirrhous area. The nuclei were

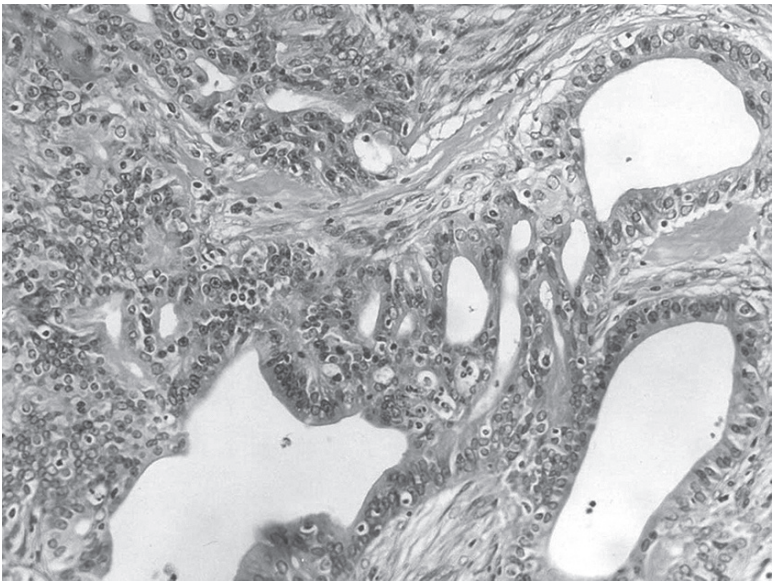

Fig. 13.16 Histological appearance of a 4th generation subcutaneous tumor of moderately differentiated adenocarcinoma. Various sized glands and abundant fibrosis were seen (H&E, ×200)

Table 13.2 Expression of antigens in subcutaneous allografts (avidin biotin peroxidase complex method)

Antigens	Staining score
A-antigen	(4+)
B-antigen	(2+)
H-antigen	(1+)
P-glycoprotein	(4+)
CEA	(−)
CA 19-9	(−)

CEA, carcinoembryonic antigen.
Staining score on the basis of the number of cells showing: (−), 0%; (1+), <5%; (2+), 5–30%; (3+), 30–70%; (4+), >70%. ([24], with permission)

almost oval but some were irregularly shaped and notches were present. The marginal chromatin was coarse and a few nucleoli were seen (Figure 13.19). SEM revealed that the lumen of the glands was lined with a single layer of tumor cells and that

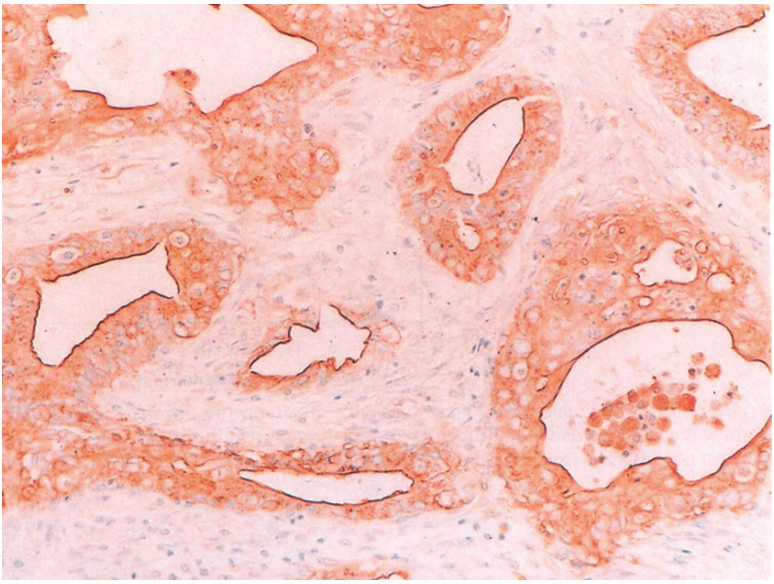

Fig. 13.17 Expression of A-antigen in the transplanted tumor. Tumor cells show diffuse and glycocalyx patterns (ABC method, ×200) ([24], with permission)

Fig. 13.18 Expression of antibody against P-glycoprotein in the transplanted tumor. Gland-forming tumor cells showed Golgi patterns (ABC method, ×200) ([24], with permission)

the glands were irregularly shaped. These findings corresponded to the histological findings in gland formation. These tumor cells had a columnar epithelium and the cell boundaries were clearly distinguished. Cell surfaces were slightly rounded and covered with numerous microvilli.

13.18 DNA Analysis of the Cancer Line

A DNA histogram is shown in Figure 13.20. The DNA pattern was diploidy and the coefficient of variation (CV) was 3.9%.

13.19 Subculture of Cell Lines

Using colonial and pure cell cloning methods, we established two cell lines from the 4th and 9th generation subcutaneous tumors, which we named "NUF-BD-4" and "NUF-BD-9", respectively. Their phase-contrast microscopic findings are shown in Figure 13.21. Polygonal cells grew in a single layer and their margin was irregularly shaped like a feeler. The NUF-BD-4 cells were sharper and smaller than the NUF-BD-9 cells. The doubling times of NUF-BD-4 and NUF-BD-9 were calculated to be 16 and 23 h, respectively.

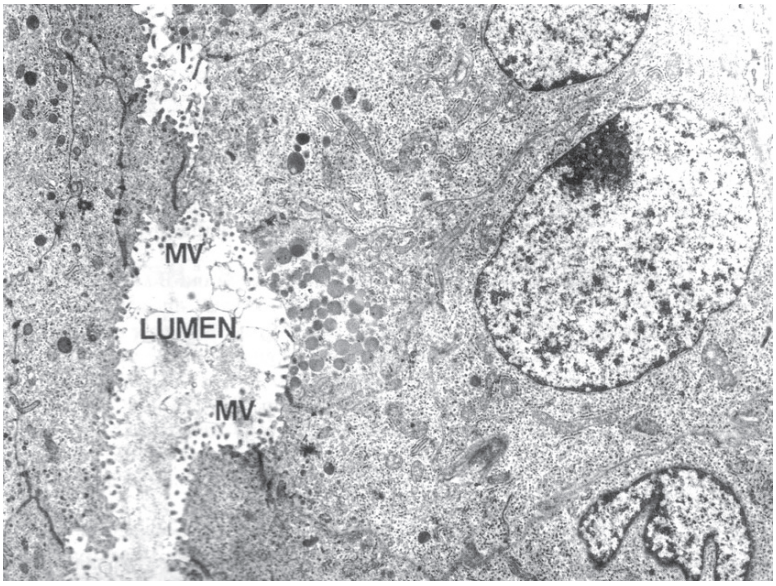

Fig. 13.19 Transmission electron microscopic examination revealed an irregular gland with well-developed microvilli (MV). The nuclei were almost oval, but notches were sometimes present (TEM, ×5,000) ([24], with permission)

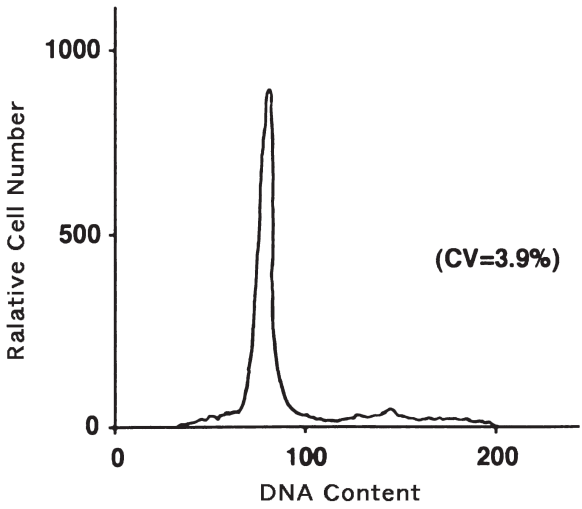

Fig. 13.20 DNA histogram, showing a single and a diploidy pattern. The coefficient of variation (CV) was 3.9% ([24], with permission)

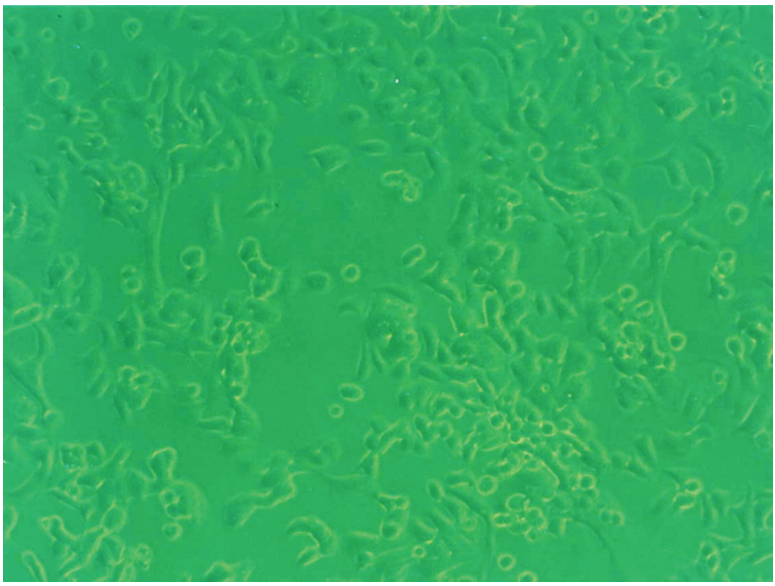

Fig. 13.21 Phase-contrast microscopical findings of NUF-BD-4 grown on a cell culture dish (×250)

13.20 Light Microscopic Findings of the Cell Lines

The cell form was similar to the phase-contrast microscopic findings. Polygonal cells grew in a single layer and their margin was irregularly shaped like a feeler. The nuclei had abundant chromatin (Figure 13.22). This finding suggested that these cells were derived from a malignant tumor and had malignant potential.

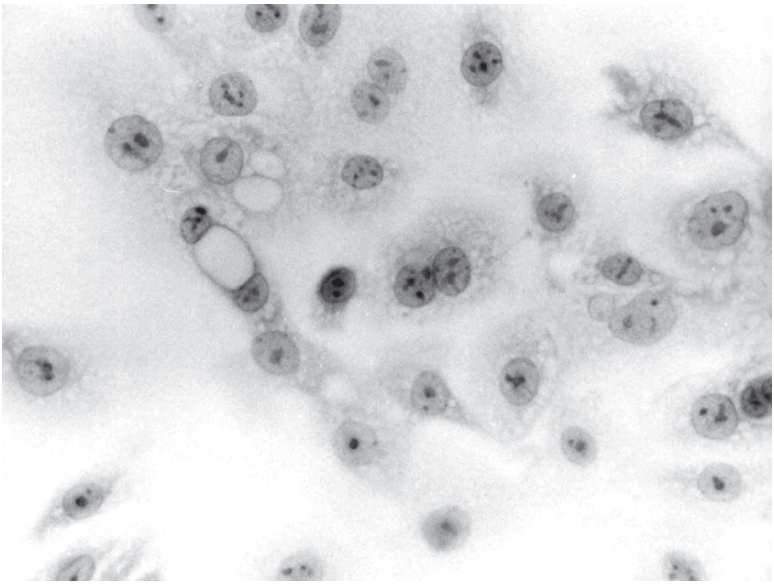

Fig. 13.22 Light microscopic findings of NUF-BD-4 grown on a prepared slide (×200)

13.21 Immunohistochemical Findings of the Cell Lines

The A-antigen in NUF-BD-4 was highly expressed (Figure 13.23), but other antigens were not stained. The *in vivo* subcutaneous cancer line A-antigen was also highly stained. Both B and H antigens were moderately stained.

13.22 Electron Microscopical Findings of the Cell Lines

The cell margin of the NUF-BD-4 line was irregularly shaped like a feeler (Figure 13.24). This finding was similar to the phase-contrast microscopic findings. Cell surfaces were covered with numerous microvilli. The *in vivo* subcutaneous cancer line cell surfaces were also covered with numerous microvilli.

13.23 Transplantation into the Hamster

Both cell lines were transplantable into hamsters. When the NUF-BD-9 cells were inoculated subcutaneously, the mean tumor weights were approximately 1.8 and 4.5 g on days 14 and 21 after inoculation. The uptake rate was 100% (8/8). There were no metastatic lesions. Histopathologically, the subcutaneously transplanted tumors were poorly differentiated tubular adenocarcinoma (Figure 13.25).

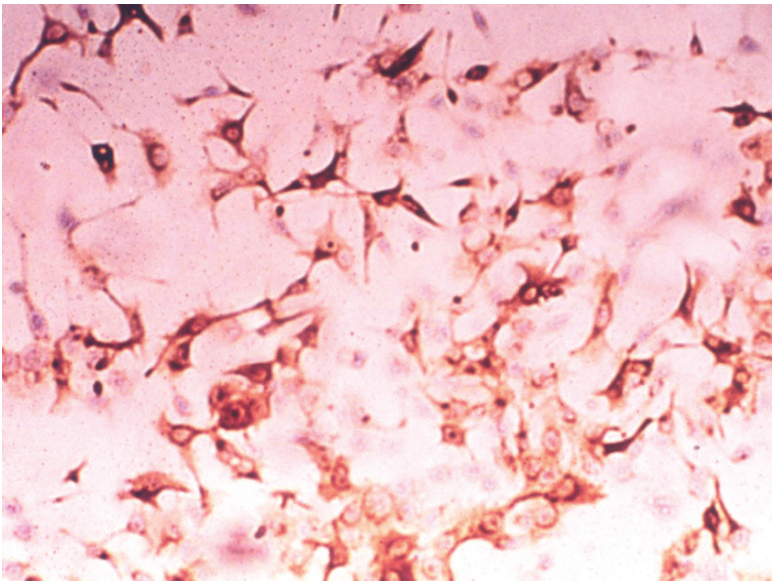

Fig. 13.23 Expression of A-antigen in the NUF-BD-4. All cells stained positively (ABC method, ×400)

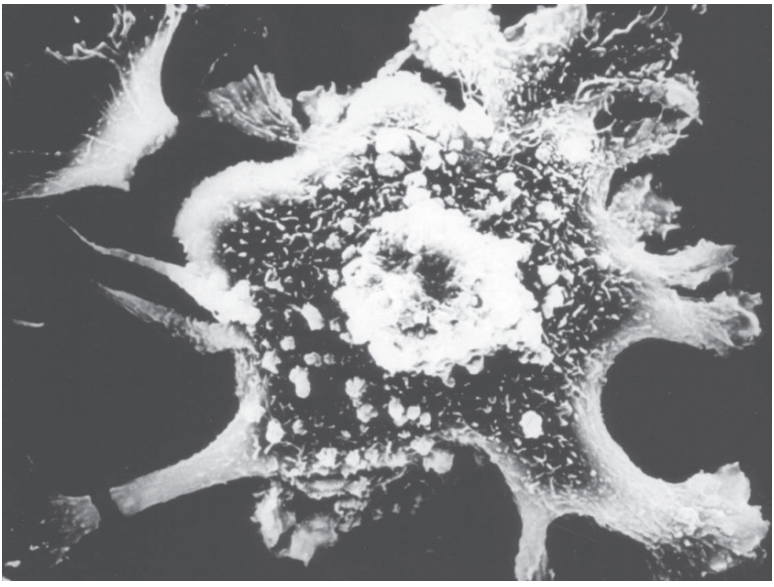

Fig. 13.24 Electron microscopic appearance of the NUF-BD-4 showing numerous microvilli on the cell surface (×2,000)

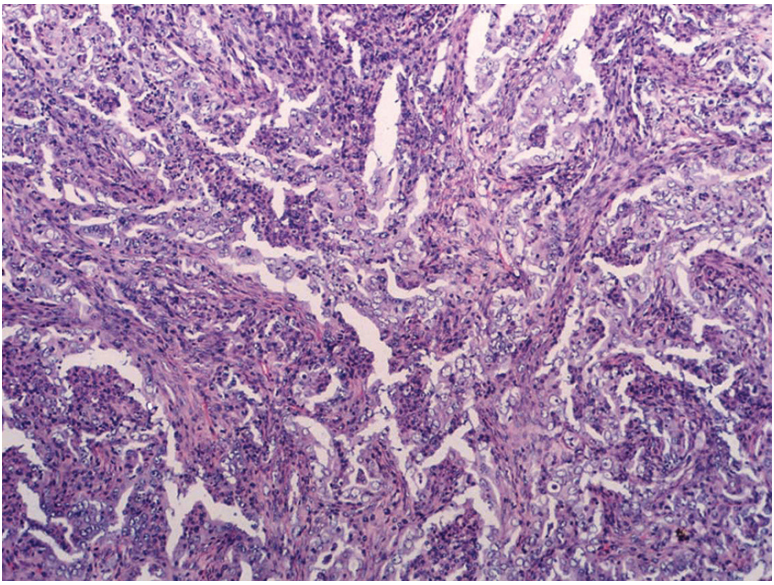

Fig. 13.25 Histological appearance of a tumor subcutaneously transplanted in a hamster, showing poorly differentiated tubular adenocarcinoma (H&E, ×200)

13.24 Comments

Recent advances in basic pathophysiology and developments in novel diagnostic modalities have improved the management of hepatobiliary and pancreatic malignant disease; however, the prognosis of IHBD carcinoma remains poor. Thus, an animal model would be a useful tool to assess sensitivity to anti-cancer drugs and to elucidate events related to tumor extension and metastasis.

In our experiments using this hamster model, the induced primary IHBD tumor was located within a portal area and was tubular adenocarcinoma with a fibrous, scirrhous pattern. Subcutaneous inoculation of the IHBD carcinoma cells produced locally growing tumors in all the recipient hamsters, with an uptake rate of 100%. Histologically, all allografts also showed tubular adenocarcinoma with a fibrous, scirrhous pattern. These findings are consistent with those of the peripheral type of human IHBD carcinoma, the most common histological pattern of which is small glandular adenocarcinoma with abundant sclerosis [27].

In experimental pancreatic carcinoma in hamsters, the A-antigen and pancreatic tumor antigen are considered to be effective tumor markers [28]. In our experimental IHBD cancer line and cell line (NUF-BD-4), the A-antigen was strongly stained. The so-called blood group-related antigens are a family of cell surface carbohydrate structures [29]. There are many reports of these antigens as tumor markers [30,31] and positive reactions were observed in human carcinoma of the stomach [32], colon [17], pancreas [33], lung[34], and urinary tract [19]. These antigens are also

tumor markers in neoplastic lesions in Syrian golden hamsters [35]. The A-antigen discriminates between benign and malignant lesions much better than other antigens [4]. Our experimental IHBD carcinoma model may thus be useful for diagnostic studies on blood group-related antigens.

The staining score of P-glycoprotein in this transplantable carcinoma was high. P-glycoprotein is a product of the *mdr*-1 gene and is considered to be a drug pump that carries anti-tumor agents out of the cell [36,37]. Therefore, this antigen plays an important role in multidrug resistance and our model will be useful for studies on the effects of drug therapy.

MAb c219 is not completely characterized as a MAb against P-glycoprotein, as it also reacts with the *mdr*-3 gene product [38]. This *mdr*-3 gene is not well understood and the importance of this finding is uncertain. Both A-antigen and P-glycoprotein were strongly stained. We used MAb c219 as a MAb P-glycoprotein, and c219 cross-reacts with the blood type A substance [39]. However, MAb A and MAb c219 showed different staining patterns: diffuse for MAb A with a glycocalyx pattern, whereas MAb c219 had a Golgi pattern. The c219 probably reacts to MAb P-glycoprotein.

The doubling time of IHBD carcinoma from days 7 to 21 was identical at 2.8 days in both sexes, but on day 21 after inoculation there was a significant difference between the tumor weights in the males and females ($p < 0.05$). These findings suggest that inoculated cells have a latent phase, which is shorter in males. A similar sexual difference was seen in an azaserine-induced rat pancreatic carcinoma model [40–42]. Tumor growth was faster in intact than in castrated males [40]. In our IHBD carcinoma model, neither estrogen nor androgen receptors were detected. Similarly, no such receptor was detected in drug-induced pancreatic carcinoma in rats [43].

Our cell lines were able to be transplanted into hamsters. These cell lines thus enable us to plan experimental studies, not only *in vitro* but also *in vivo*. Because hamsters have normal immunological responses, our hamster model may be useful for researching cancer immunology.

In conclusion, the present newly established transplantable IHBD cancer line and cell lines, which will aid in elucidating the mechanisms involved in the synthesis and secretion of tumor-associate antigens, and will help to evaluate possible related therapeutics.

References

1. Tajima Y, Eto T, Tsunoda T, Tomioka T, Inoue K, Fukahori T, Kanematsu T. Induction of extrahepatic biliary carcinoma by *N*-nitrosobis(2-oxopropyl)amine in hamsters given cholecystoduodenostomy with dissection of the common duct. Jpn J Cancer Res 1994 85(8):780–788.
2. Inoue K, Tomioka T, Tajima Y, Fukahori T, Eto T, Tsunoda T, Kanematsu T. Characterization of an established transplantable adenocarcinoma of the gallbladder in Syrian golden hamster. J Surg Oncol. 1994 56(4):269–276.
3. Hsu SM, Raine L, Fanger H. Use of avidin-biotin-peroxidase complex (ABC) in immunoperoxidase techniques: a comparison between ABC and unlabeled antibody (PAP) procedures. J Histochem Cytochem 1981 29(4):577–580.

4. Tomioka T, Fujii H, Egami H, Takiyama Y, Pour PM. Correlation between morphology and blood group-related antigen expression in pancreatic tumors induced in Syrian hamsters. Carcinogenesis 1991 12(3):441–447.
5. Petrov NN, Krotkina NA. Experimental carcinoma of the gallbladder: supplementary data. Ann Surg 1947 125(2):241–248.
6. Desforges G, Desforges J, Robbins SL. Carcinoma of the gallbladder: an attempt at experimental production. Cancer 1950 3(6):1088–1096.
7. Kowalewski K, Todd EF. Carcinoma of the gallbladder induced in hamsters by insertion of cholesterol pellets and feeding dimethylnitrosamine. Proc Soc Exp Biol Med 1971 136(2):482–486.
8. Pour P, Althoff J, Krüger FW, Mohr U. A potent pancreatic carcinogen in Syrian hamsters: *N*-nitrosobis(2-oxopropyl)amine J Natl Cancer Inst 1977 58(5):1449–1453.
9. Koyama S, Yoshioka T, Mizushima A, Kawakita I, Yamagata S, Fukutomi H, Sakita T, Kondo I, Kikuchi M. Establishment of a cell line (G-415) from a human gallbladder carcinoma. Gann 1980 71(4):574–575.
10. Morgan RT, Woods LK, Moore GE, McGavran L, Quinn LA, Semple TU. A human gallbladder adenocarcinoma cell line. In Vitro 1981 17(6):503–510.
11. Egami H, Sakamoto K, Yoshimura R, Kikuchi H, Akagi M. Establishment of a cell line of gallbladder carcinoma (GBK-1) producing human colony stimulating factor. Jpn J Cancer Res 1986 77(2):168–176.
12. Koyama S, Mukai R, Fukao K, Arimura H, Iwasaki Y, Osuga T. Monoclonal antibody against human gallbladder carcinoma-associated antigen. Cancer Res 1987 47(17):4667–4673.
13. Johzaki H, Iwasaki H, Nishida T, Isayama T, Kikuchi M. A human gallbladder adenocarcinoma cell line. Cancer 1989 64(11):2262–2268.
14. Huang LC, Brockhaus M, Magnani JL, Cuttitta F, Rosen S, Minna JD, Ginsburg V. Many monoclonal antibodies with an apparent specificity for certain lung cancers are directed against a sugar sequence found in lacto-N-fucopentaose III. Arch Biochem Biophys 1983 220(1):318–320.
15. Magnani JL, Nilsson B, Brockhaus M, Zopf D, Steplewski Z, Koprowski H, Ginsburg V. A monoclonal antibody-defined antigen associated with gastrointestinal cancer is a ganglioside containing sialylated lacto-N-fucopentaose II. J Biol Chem 1982 257(23):14365–14369.
16. Lee HS, Choe G, Kim WH, Kim HH, Song J, Park KU. Expression of Lewis antigens and their precursors in gastric mucosa: relationship with Helicobacter pylori infection and gastric carcinogenesis. J Pathol 2006 209(1): 88094.
17. Sakamoto J, Furukawa K, Cordon-Cardo C, Yin BW, Rettig WJ, Oettgen HF, Old LJ, Lloyd KO. Expression of Lewisa, Lewisb, X, and Y blood group antigens in human colonic tumors and normal tissue and in human tumor-derived cell lines. Cancer Res 1986 46(3):1553–1561.
18. Itzkowitz SH, Yuan M, Ferrell LD, Ratcliffe RM, Chung YS, Satake K, Umeyama K, Jones RT, Kim YS. Cancer-associated alterations of blood group antigen expression in the human pancreas. J Natl Cancer Inst 1987 79(3):425–434.
19. Kay HE, Wallace DM. A and B antigens of tumors arising from urinary epithelium. J Natl Cancer Inst 1961 26:1349–1365.
20. Feizi T. Carbohydrate antigens in human cancer. Cancer Surv 1985 4(1):245–269.
21. Weinstein RS, Kuszak JR, Kluskens LF, Coon JS. P-glycoproteins in pathology: the multidrug resistance gene family in humans. Hum Pathol 1990 21(1):34–48.
22. Higgins CF. Multiple molecular mechanisms for multidrug resistance transporters. Nature 2007 446:749–757.
23. Pour P, Donnelly T. Effect of cholecystoduodenostomy and choledochostomy in pancreatic carcinogenesis. Cancer Res 1978 38(7):2048–2051.
24. Fukahori T, Tomioka T, Inoue K, Tajima Y, Tsunoda T, Kanematsu T. Establishment of a transplantable carcinoma arising from the intrahepatic bile duct in Syrian golden hamsters. Virchows Arch A Pathol Anat Histopathol 1993 422(3):233–238.
25. Ovejera AA, Houchens DP, Barker AD. Chemotherapy of human tumor xenografts in genetically athymic mice. Ann Clin Lab Sci 1978 8(1):50–56.

26. Egami H, Takiyama Y, Martin C, William HH, Parviz MP. Establishment of hamster pancreatic ductal carcinoma cell line (PC-1) producing blood group-related antigens. Carcinogenesis 1989 10: 861–869.
27. Roy CC. Colour atlas of histopathology. Liver, Gallbladder and Pancreas. Igaku-Shoin, Tokyo, p 22, 1979.
28. Matsuzaki M, Katsuragi M, Obara T, Ura H, Ito S, Tsutsumi M, Konishi Y. Pancreatic tumor antigen in transplantable adenocarcinoma induced by N-bis (2-hydroxypropyl) nitrosamine in hamsters. Pancreas 1987 2:545–550.
29. John SC, Ronald SW. Blood group-related antigens as markers of malignant potential and heterogeneity in human carcinomas. Hum Pathol 1986 17:1089–1106.
30. Kenneth OL. Blood group antigens as markers for normal differentiation and malignant changes in human tissues. Am J Clin Pathol 1987 87:129–139.
31. Ten F. Carbohydrate antigens in human cancer. Cancer Surv 1985 4:245–269.
32. John LM, Bo N, Manfred B, David Z, Zenon S, Hilary K, Victor G. A monoclonal antibody-defined antigen associated with gastrointestinal cancer is a ganglioside containing sialylated lact-N-fucopentaose 2. J Biol Chem 1982 257:14365–14369.
33. Steven HI, Mei Y, Linda DF, Murray R, Yong-Suk C, Satake K, Umeyama K, Raymond TJ, Young SK. Cancer associated alterations of blood group antigen expression in the human pancreas. J Natl Cancer Inst 1987 79:425–434.
34. Laura CH, Manfred B, John LM, Frank C, Steven R, John DM, Victor G. Many monoclonal antibodies with unapparent specificity for certain lung cancers are directed against a sugar sequence found in lacto-N-fucopentaose 3. Archives Biochem Biophys 1983 220:318–320.
35. Egami H, Tomioka T, Margaret T, David K, Parviz MP. Development of intrapancreatic transplantable model of pancreatic duct adenocarcinoma in Syrian golden hamsters. Am J Pathol 1991 138:557–561.
36. Joshura E, Bart B. Tumor resistance to chemotherapy associated with expression of the multidrug resistance phenotype. Cancer Bull 1989 41:41–44.
37. Ronald SW, Jerome RK, Larry FK, John SC. The multidrug resistance gene family in humans. Hum Pathol 1990 21:34–48.
38. Schinkel AH, Roelofs EM, Borst P. Characterization of the human MDR3 P-glycoprotein and its recognition by P-glycoprotein-specific monoclonal antibodies. Cancer Res 1991 51(10):2628–2635.
39. Finstad CL, Yin BW, Gordon CM, Federici MG, Welt S, Lloyd KO. Some monoclonal antibody reagents (C219 and JSB-1) to P-glycoprotein contain antibodies to blood group A carbohydrate determinants: a problem of quality control for immunohistochemical analysis. J Histochem Cytochem 1991 39(12):1603–1610.
40. Daniel SL, Sumi C. Effects of sex steroid hormones on pancreatic cancer in the rat. Int J Pancreatol 1990 6:159–165.
41. Pour MP. Experimental pancreatic cancer. Am J Surg Pathol 1989 13(Suppl 1):96–103.
42. Sumi C, Daniel SL, Roebuck BD, Brinck-Johmsen T. Inhibitory effects of estrogen and castration on the early stage of pancreatic carcinogenesis in Fischer rats treated with azaserine. Cancer Res 1989 49:2332–2336.
43. Lhost EF, Roebuck BD, Stern JE, Longnecker DS. Effects of orchiectomy and testosterone on the early stages of azaserine-induced pancreatic carcinogenesis in the rat. Pancreas 1987 2:38–43.

Chapter 14
Establishment of Biliary Epithelial Cell Lines from the Hamster

Takayuki Asakawa, Amane Kitasato, Tsutomu Tomioka, Tamotsu Kuroki, Ryuji Tsutsumi, Yoshitsugu Tajima, and Takashi Kanematsu

A. Isolation, Culture and Transplantation of Biliary Epithelial Cells

14.1 Summary

We describe a method for the simultaneous culturing of biliary epithelial cells (BECs) from the gallbladder (GB), extrahepatic bile duct (EBD), and intrahepatic bile duct (IBD) of hamsters. The GB, EBD and IBD were excised from the biliary tree after collagenase perfusion of the liver. These biliary segments were minced into fragments, which were embedded in collagen gel and cultured in Dulbeccos Modified Eagle Medium/HamF12 Medium containing 10% fetal bovine serum. The various cells subsequently spread from the fragments and formed cellular sheets. After the fragments and flattened cells were removed under phase-contrast microscopy, the sheets remaining were found to be composed of cuboidal cells. These cuboidal cells expressed gamma glutamyl transpeptidase and cytokeratin 7, which are known to be specific markers of BECs. Ultrastructurally, there were many microvilli on the luminal surface and junctional complex and interdigitation was identifiable on the lateral surfaces. BEC cultures were subcultured by digestion with collagenase and dispase and then dissociated by subsequent digestion in trypsin and ethylenediaminetetraacetic acid. They were maintained in collagen gel for up to 8 weeks. After several passages, the BECs in the culture eventually grew and showed vacuoles in the cytoplasm. They demonstrated irreversible growth arrest at 9 weeks. The BECs tended to form cystic structures when they were transplanted with collagen gel into the interscapular fat pads of the syngeneic hamsters.

14.2 Introduction

Biliary epithelial cells (BECs) have phenotypes, structures and possible functional heterogeneity varying within the different regions of the biliary tree [1,2]. Pathologically, certain anatomical levels of the biliary tree are preferentially affected. For example, in

Y. Tajima et al. (eds.), *Hepatobiliary and Pancreatic Carcinogenesis in the Hamster*,
DOI: 10.1007/978-4-431-87773-8_14, © Springer 2009

primary biliary cirrhosis, intrahepatic small bile ducts are damaged selectively, whereas the extrahepatic and intrahepatic large bile ducts are preferentially involved in primary sclerosing cholangitis [3]. Such anatomical preferences in the disease processes may be related to the functions and antigenicity of BECs and their microenvironments at the individual anatomical level. Until now, BECs have been isolated independently and cultured successfully from different parts of the biliary tract in humans [4,5] and rodents [6–9]. Several investigators have reported the importance of establishing long-term cultures using collagen gel as the substrate for adherence[6,7,9]. Recently, the isolation and cultivation of pure BECs using an explant of the biliary tree on collagen gel was reported [6,9]. All of these methods involve the isolation of BECs from a certain anatomical segment of the biliary tree or the isolation of certain pathologically proliferated BECs.

Syrian Golden Hamsters have been used to study the pancreas because the anatomical structure of their pancreaticobiliary ductal system is similar to that of humans [10]. Moreover, both the bile acid composition and pancreatic juice component in this species closely resemble those in humans [11,12]. We previously reported the Syrian golden hamster as a useful animal for investigating biliary carcinogenesis [13–18]. To our knowledge, no previous studies have been published on the successful culturing of biliary epithelial cells from the hamster.

We describe a direct method for the simultaneous isolation of intrahepatic, extrahepatic, and gallbladder BECs, followed by their cultivation and transplantation in normal hamsters.

14.3 Experimental Protocol

Female Syrian golden hamsters aged 5–6 weeks were used. The livers were perfused in situ with 100 ml Ca^{2+}- and Mg^{2+}-free phosphate-buffered saline (CMF-PBS) containing 10 mmol/l HEPES (pH 7.4), 1 mmol/l ethylene glucol-bis (E-aminoethylether) *N, N, N′,N′*-tetraacetic acid (EGTA) via the inferior vena cava for 10 min at 37 °C. The vein was clamped above the diaphragm, and the perfusate was allowed to drain through the portal vein, followed by perfusion with 100 ml Hanks' balanced salt solution containing 50 mmol/l HEPES, 0.02% soybean trypsin inhibitor (Sigma Chemical Co., St. Louis, MO) and 0.04% collagenase (Wako Chemical Co., Tokyo) for 10 min at 37 °C (Figure 14.1). Then, the liver, gallbladder and extrahepatic bile duct were removed. After the capsule of the liver was removed with a comb and brush, the biliary tree (Figure 14.2) was dissociated with scissors and separated into the intrahepatic bile duct (IBD), extrahepatic bile duct (EBD) and the gallbladder (GB) in CMF-PBS containing EGTA 0.1 mmol/l. These fragments were then incubated in culture medium composed of Dulbecco's modified Eagle medium (DMEM, Nissui Pharmaceutical Co., Tokyo)/HamF12 medium (HamF12, Nissui, Tokyo) containing 10% fetal bovine serum (GIBCO, Grand Island, NY) for 12 h at 37 °C in an incubator (5% CO_2).

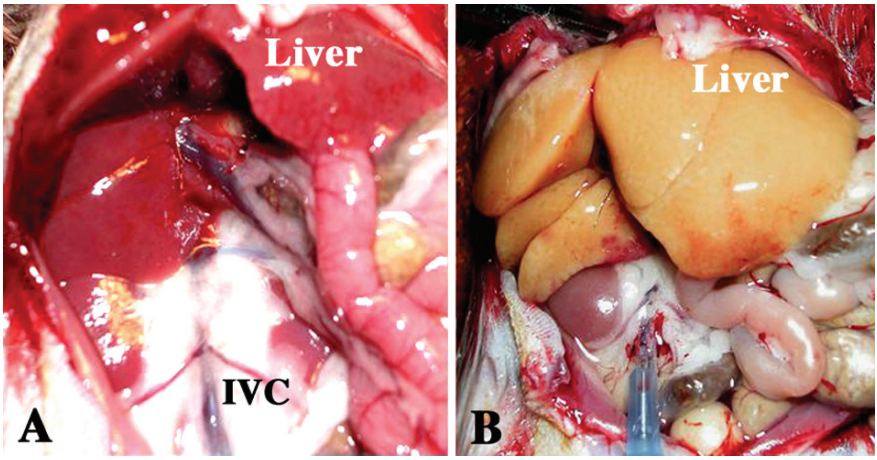

Fig. 14.1 Perfusion of the liver. (a) The inferior vena cava (IVC) is completely exposed. (b) Appearance of the liver after the completion of liver perfusion

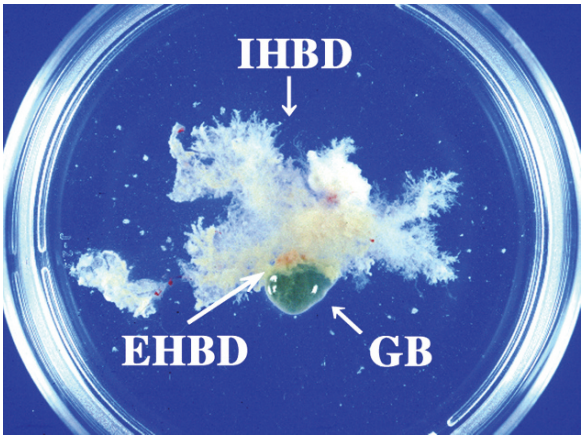

Fig. 14.2 Biliary tree of the hamster. GB, gallbladder; IHBD, intrahepatic bile duct; EHBD, extrahepatic bile duct

A collagen gel plate was made by coating 60-mm petri dishes with 2 ml of an ice-cold mixture of collagen solution, 0.3% acid solution collagen (Cellmatrix Type I-A, Nittazeratin, Osaka), 10 × Ham F12, and 0.8 N NaOH (8:1:1). The fragments of the biliary tree were embedded in the collagen gels. After incubation for 20–30 min at 37 °C, collagen gels were overlaid with 5 ml of culture medium. After 7–10 days in culture, the fragments and nonepithelial cells were collected under a phase-contrast microscope using a Pasteur pipette. The remnant culture cells were released from

the collagen gel by digestion for 40–50 min with 0.1% (wt/vol) collagenase and 10 U/ml dispase (Gohdo Shusei, Chiba, Japan) in Hanks' solution, and collected by centrifugation at 1,000 rpm for 5 min. After a single wash through CMF-PBS by centrifugation at 1,000 rpm for 5 min, the culture cells were dissociated in CMF-PBS containing 0.05% trypsin and 0.02% ethylenediaminetetraacetic acid (EDTA, Wako Chemical Co., Tokyo).

After incubation for 5 min at 37 °C, the digestion was discontinued by addition of the culture medium. These cuboidal cells were washed twice in CMF-PBS, then resuspended at 1×10^5 cells/ml in the culture medium, and 5 ml of the cell suspension was plated on a plastic dish, a collagen-coated dish, and on top of 2 ml collagen gels in 60-mm petri dishes. These culture cells were maintained at 37 °C in an incubator, and the culture medium was changed every 3 days. At 80% confluence, the culture cells were released from the collagen gel by digestion with collagenase and dispase, and they were then dissociated by subsequent digestion in 0.05% trypsin and 0.02% EDTA.

Morphological examination of the culture cells, including histochemical and immunohistochemical study as well as an ultrastructural examination, was done at every passage. The monolayer culture cells on top of the collagen gel were fixed in 10% buffered formalin. The cells on the collagen gel were then embedded in paraffin using standard techniques. Each 5-μm section of a paraffin block was stained with hematoxylin and eosin (H&E), periodic acid–Schiff (PAS) and mucicarmine stains.

The cells cultured on collagen gel were fixed with paraformaldehyde for 3 h at 4 °C, then embedded in Optimal Cutting Temperature (OCT) compounds (Miles, Elkhart, USA), and fixed at −80 °C. Each 5-μm section of the OCT compound block was used for the immunohistochemical staining of cytokeratin 7 (Progen Biotechnik, Heidelberg, Germany) and the cytochemical demonstration of gamma glutamyl transpeptidase (GGT), as described by Rutenburg et al. [19] Immunocytochemical staining was done using a Vectastain avidin–biotin peroxidase complex kit (Vector Laboratories, Burlingame, CA).

To examine the ultrastructure of the cultured cells, the cells cultured on collagen gel were washed with 0.1 M cacodylate buffer and fixed with 2% glutaraldehyde in 0.1 M cacodylate buffer, pH 7.4 at 37 °C for 30 min. The cells were post-fixed in 1% osmium tetroxide at 4 °C for 30 min. These fixed cells were dehydrated in ascending series of ethanol, and then embedded in Epon mixture and polymerized at 60 °C for 12 h. Thin sections were stained with uranyl acetate and lead tartrate, and examined with JEM-1200EX (Japan Electron Optics Laboratory, Tokyo) operated at 60–80 kV accelerating voltage.

The cells were grown on collagen gel-coated 13-mm glass coverslips. They were washed, fixed, and dehydrated by the same method for TEM and critical point drying necessary to prepare the cells for scanning electron microscopy. Each specimen was coated with gold–palladium and examined under a JSM-35CLaB6 (Japan Electron Optics Laboratory, Tokyo) with a 15-kV accelerating voltage.

To examine the growth pattern of these cells *in vivo*, the cultured cells were inoculated into the fat pads of syngeneic hamsters. When 90% confluence of the culture cells on 0.3 ml collagen gel/well was achieved (24-well plates, Falcon, Lincoln Park, NJ), the culture cells were rinsed twice with CMF-PBS. The culture

cells on collagen gel in wells were inoculated into the intrascapular fat pads of 6–7-week-old female Syrian golden hamsters. After 3–4 weeks, the hamsters were killed and then the area of cell inoculation in the fat pad was fixed in 10% buffered formalin. After appropriate processing, the fat pad tissue after transplantation was examined with H&E, PAS, mucicarmine, cytokeratin 7 and GGT stains.

14.4 Culture of Biliary Epithelial Cells

Varying numbers of cells spread from the fragment (Figure 14.3). The distinction of epithelial cells from such nonepithelial cells as fibroblasts and endothelial cells was easy with a phase-contrast microscope. The epithelial cells spread faster than the nonepithelial cells. The peripheral parts of the sheet were composed exclusively of cuboidal cells (Figure 14.4), whereas the central parts were composed of epithelial cells and mesenchymal cells. The central region was released from collagen gel with a Pasture pipette. On the other hand, the subcultured cells formed cuboidal cells, but few flattened cells were seen.

The rate of successful isolation of epithelial cells depended on whether they had been taken from the gallbladder, the extrahepatic duct, or the intrahepatic duct (Table 14.1). The composition of the substratum was also important for the growth, morphology, and survival of cuboidal cells in culture. When a subculture cell suspension was plated on plastic, air-dried collagen, or collagen gel, cuboidal cells attached and formed colonies with similar efficiencies. However, after 5–7 days of culture, the cells growing on plastic or air-dried collagen-coated dishes started to

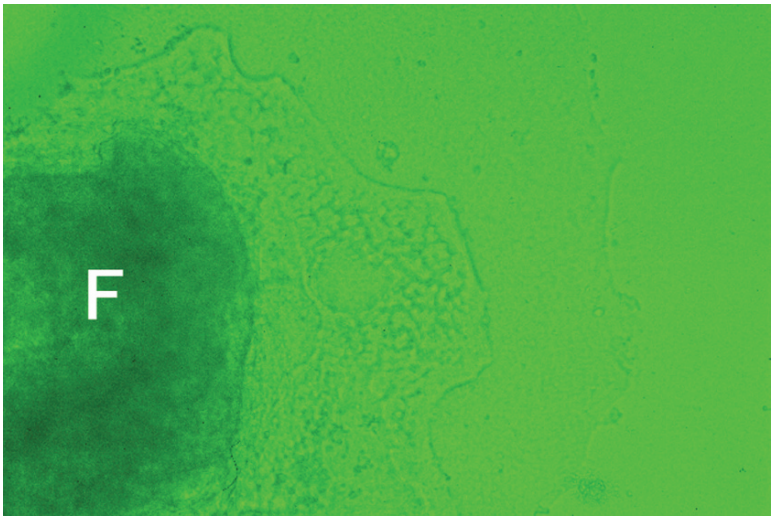

Fig. 14.3 A fragment (F) embedded in collagen gel and cultured for 7 days. Varying numbers of cells spread from the fragment on the collagen gel (phase-contrast microscope, ×60) (modified from [35], with permission)

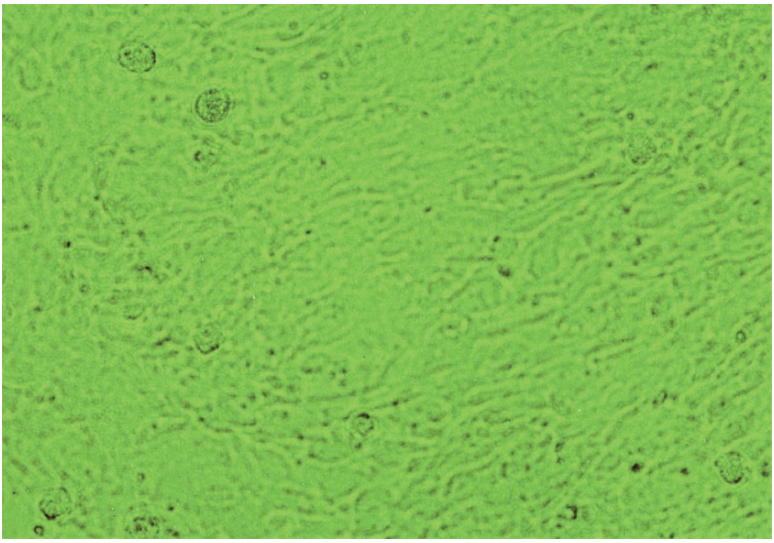

Fig. 14.4 The peripheral area in Figure 14.2 is formed of cuboidal cells (phase-contrast microscope, ×200) ([35], with permission)

Table 14.1 The successful cultivation rate of biliary epithelial cells (BECs) from fragments differed depending on whether they were from extrahepatic bile duct, intrahepatic bile duct or gall bladdeer of seven hamsters (modified from [35], with permission)

Original site	No. of fragments	No. of isolations	Rate of isolation and cultivation (%)
Intrahepatic bile duct	52	17	33
Extrahepatic bile duct	21	16	76
Gallbladder	30	28	93

become detached from the dish. In contrast, under identical conditions cuboidal cells remained on top of the collagen gel, preserving epithelial cell morphology and eventually formed a confluent monolayer by 8 weeks. Thus, collagen gel rather than plastic dishes or collagen-coated dishes appeared to be most suitable for the growth and attachment of these culture cells. At 8 or 9 weeks, the culture cells became detached from the collagen gel.

14.5 Characteristics of Biliary Epithelial Cells

Light microscopy revealed that the primary cultured peripheral region was composed of cuboidal cells on collagen gel (Figure 14.5). By 8 weeks after primary culture, these cuboidal cells were positive for PAS and mucicarmine staining. In the subculture, the culture cells showed histochemical staining reaction for GGT activity. The cytoplasm of the cultured cells reacted intensely with anticytokeratin 7 (Figure 14.6).

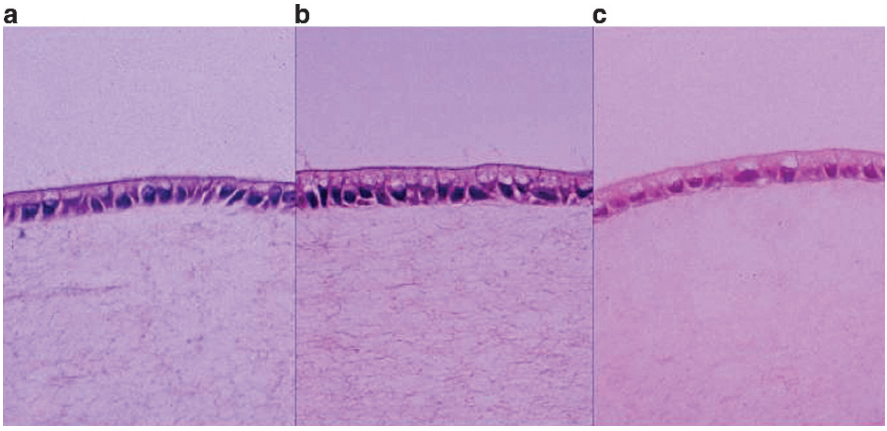

Fig. 14.5 Biliary epithelial cells cultured on collagen gel after subculture. The culture cells formed a monolayer and were cuboidal or columnar cells (a) (H&E, ×200). These cells were positive for PAS staining (b, ×200) and mucicarmine staining (c, ×200)

Fig. 14.6 The cultured biliary epithelial layer was positive for cytokeratin 7 (ABC method, ×400) (modified from [35], with permission)

14.6 Transmission Electron Microscopy

Ultrastructurally, the cultured cells on collagen gel were covered with short stubby microvilli on the luminal surface and contained a golgi apparatus, abundant mitochondria and rough endoplasmic reticulum in the cytoplasm. Junctional complexes such as desmosomes, tight junctions and interdigitations were formed between the

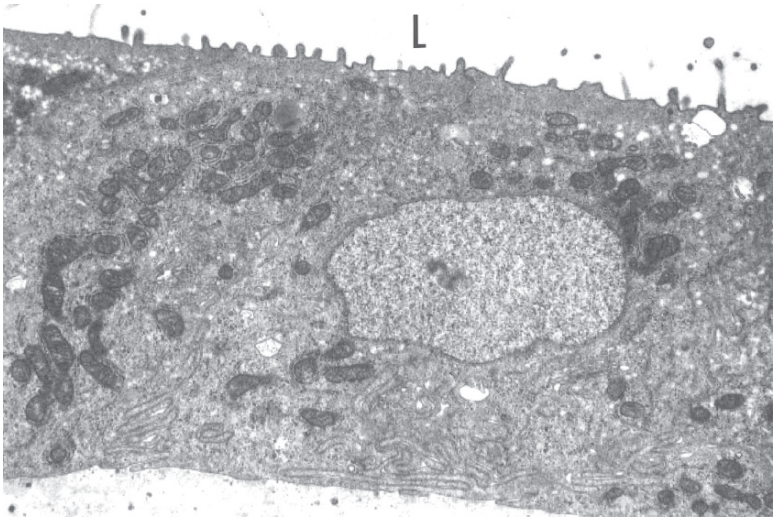

Fig. 14.7 Transmission electron microscopy of cultured cells on collagen gel after two passages. The monolayers of the biliary epithelial cells were composed of polarized cells from the lateral membrane with well defined junctional complexes and luminal membrane (L) covered with numerous short microvilli. The basement membrane of the biliary epithelial cells lacked microvilli and showed evidence of basal lamina (×4,000) ([35], with permission)

intercellular spaces. The nuclei were located either centrally or basally (Figure 14.7). By 8–9 weeks after primary culture the culture cells had attached to the collagen gel and maintained a junctional complex but demonstrated multiple vacuoles in the cytoplasm.

14.7 Scanning Electron Microscopy

SEM studies also revealed a regular lining of cells growing in one plane. No duct or gland-like structures were noted. The surface topography of the cultured cells at confluence was uniform and cell–cell junctions were identified. The apical membranes were polygonal and covered with numerous microvilli (Figure 14.8). These features were very similar to those of normal BECs.

14.8 Transplantation of BECs

Transplanting culture cells into the interscapular fat pads of a syngeneic recipient hamster resulted in cystic growth. Normal BECs gave rise to cystic structures supported by a connective tissue stroma from 3 to 4 weeks after inoculation into the

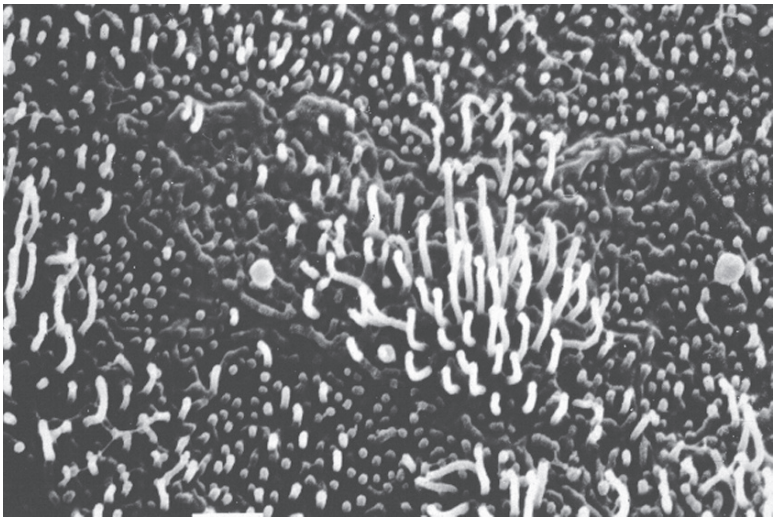

Fig. 14.8 Scanning electron microscopy of cultured cells on collagen gel after two passages. Numerous microvilli were seen on the apical membrane of the biliary epithelial cells (×3,000)

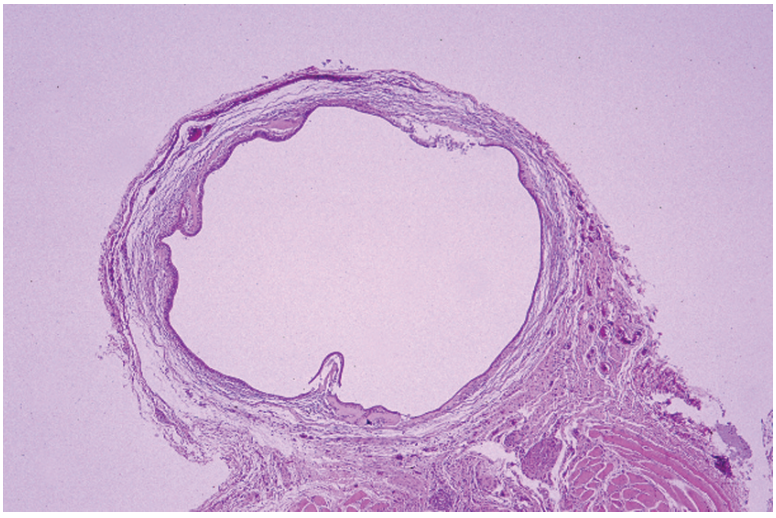

Fig. 14.9 Inoculation of cultured cells on collagen gel after two passages into the interscapular fat pads of syngeneic recipient hamsters. The cystic structure was formed 3 weeks after the inoculation of biliary epithelial cells (H&E, ×40)

fat pads (Figures 14.9 and 14.10). After transplantation, these cells were positive for PAS, mucicarmine, cytokeratin 7, and GGT (Figure 14.11). The successful inoculation rate of BECs is shown in Table 14.2.

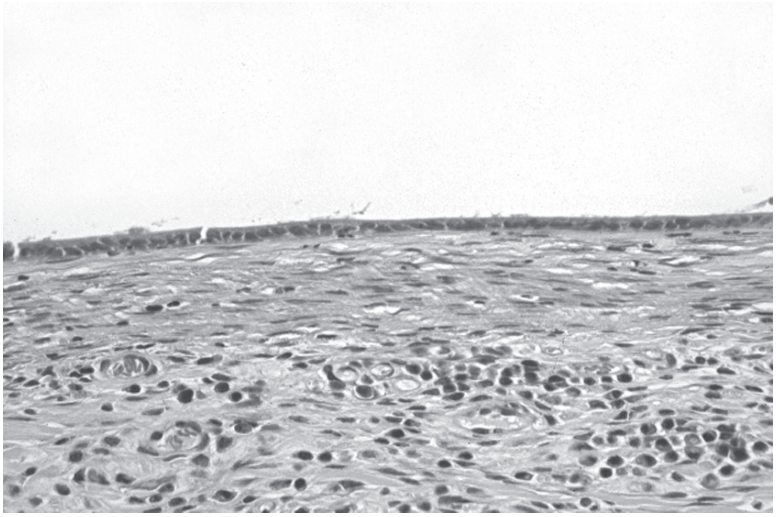

Fig. 14.10 A higher magnification of the cystic structures shows cuboidal or low columnar epithelial cells around the luminal surface (H&E, ×200) ([35], with permission)

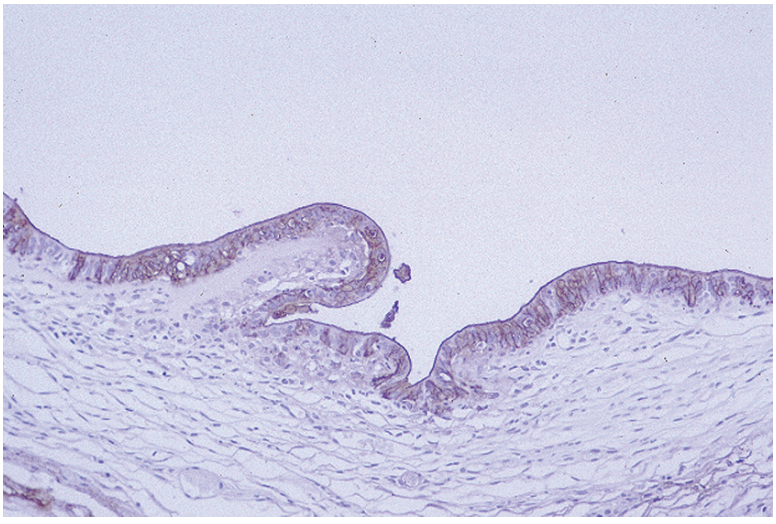

Fig. 14.11 The cells cultured on collagen gel were positive for cytokeratin 7 (ABC method, ×200)

14.9 Comments

We described a method for the simultaneous isolation, culture, and transplantation of BECs from the IBD, EBD, and GB in the normal hamster. Syrian golden hamsters have been used for experimental models of the pancreas to study pancreatic

Table 14.2 The successful transplantation rate of biliary epithelial cells (BECs) from seven hamsters was no different from the original site. The BECs on collagen gel were obtained after two passages and inoculated into the interscapular fat pads of hamster (modified from [35], with permission)

Original of BECs	No. of inoculated wells	Cystic formation	Successful inoculation rate (%)
Intrahepatic bile duct	13	11	85
Extrahepatic bile duct	15	13	87
Gallbladder	21	18	86

carcinogenesis [20–22] and for cultivation of the pancreatic duct [23]. Although we reported the hamster as a useful tool for studying biliary carcinoma, until now there has not been a report on the culture of normal BECs from the hamster.

The isolation of BECs has been used widely for isopyknic centrifugation, Percoll density gradient sedimentation, centrifugal elutriation, and antibody sorting [24]. These isolation methods require both surgical and pharmacological treatments to obtain higher yields of isolated BECs. The isolated cells are subsequently cultured on extracellular matrix materials; however, the culturing of some normal and neoplastic epithelial cells on specific extracellular matrix materials greatly affects their organization and differentiation [7,9]. Yang et al. [9] reported that the extracellular matrix plays an important role in the maintenance of cell shape, proliferation, and differentiation in the epithelial cells. The extracellular matrix was found to influence the morphology and differentiation of several types of normal cells in culture [7,9,23]. Thus, collagen gel has recently been used for the isolation of BECs [6,9].

In our studies, the fragment was embedded in collagen gel, BECs were grown on collagen gel, and fibroblasts were seen in the collagen gel beneath the monolayer of BECs. The isolation using collagen resulted in different growth patterns and rates. Furthermore, contaminant cells seen occasionally in the BEC suspension were fibroblasts, which grew beneath the BEC monolayers on collagen gel, forming an environment similar to that in the bile duct *in vivo*. However, they never interposed cultured BECs on collagen gel or broke any monolayers. Thus, the collagen gel was used to isolate the epithelial cells from normal hamster liver and culture the epithelial cells.

The different rates of successful cultivation of BECs depending on anatomical origin may be due to the presence of mechanical and enzymatic damage during preparation of the biliary tree. In addition, more nonepithelial cells were observed around the IBD than around either the EBD or the GB. BECs can proliferate in culture, and their morphology, including ultrastructural and histochemical findings, can be maintained for up to 8 weeks, or longer. No differences were observed in the morphological findings, culture period, or transplantation in the anatomical origin. Several reports have described using a primary culture as an *in vitro* model for studying carcinogenesis [21,25]. Thus, the period of cultivation is considered sufficient for studying carcinogenesis *in vitro*.

This method is useful for analyzing the influence of BECs at different anatomical levels by immunologic or chemical treatment. Moreover, when BECs on collagen gel were inoculated into the interscapular fat pads of hamsters, they formed cystic structures with a luminal membrane of monolayer cells. These morphological findings

are characteristic of normal BECs *in vivo*. This transplantation method can be used for pathological analysis of the cultured cells.

Our results suggest the possibility of establishing an *in vitro* transplantation model with these cells to study biliary carcinogenesis and the regulation of cell functions, proliferation, and modulation in various parts of the biliary tree under controlled experimental conditions.

B. Inflammatory Cytokines and Biliary Carcinogenesis

14.10 Summary

Chronic inflammation and the associated oxidative stress are well-known risk factors for the development of carcinoma in many digestive organs. However, the cellular mechanism of biliary carcinogenesis in response to inflammation remains unclear. This study investigated the link between chronic biliary inflammation and biliary carcinogenesis using gallbladder epithelial cells and inflammatory cytokines. Gallbladder epithelial cells were isolated from hamsters and cultured with a mixture of inflammatory cytokines including interleukin-1β, interferon-γ, and tumor necrosis factor-α. We evaluated inducible nitric oxide synthase (iNOS) expression, nitric oxide (NO) generation, and DNA damage. NO generation was increased significantly after cytokine stimulation, and it was suppressed by an iNOS inhibitor. iNOS mRNA expression was demonstrated in the gallbladder epithelial cells during exposure to inflammatory cytokines. Furthermore, NO-dependent DNA damage, as estimated by the comet assay, was significantly increased by cytokines, and it was decreased to control levels by an iNOS inhibitor. In conclusion, cytokine stimulation induced iNOS expression and NO generation in normal hamster gallbladder epithelial cells, which was sufficient to cause DNA damage. These results indicate that NO-mediated genotoxicity induced by inflammatory cytokines through the activation of iNOS may be involved in the process of biliary carcinogenesis in response to chronic inflammation of the biliary tree.

14.11 Introduction

It is well known that chronic local inflammation increases the risk of cancer in several organs, including the colon, lung, pancreas, and esophagus [26,27]. Similarly, biliary carcinoma develops under chronic inflammatory conditions of the biliary epithelium in the setting of gallstone disease, congenital choledochal cyst, pancreaticobiliary maljunction, or primary sclerosing cholangitis [28,29]. Recent reports have also described secondary biliary carcinomas in patients with persistent reflux cholangitis after bilioenterostomy, transduodenal sphincteroplasty, or endoscopic

sphincterotomy for both benign and malignant diseases of the liver, bile duct, and pancreas [30–32]. However, the molecular mechanisms of biliary carcinogenesis as a consequence of chronic biliary inflammation remain unclear. We reported previously that persistent reflux cholangitis after bilioenterostomy accelerates biliary carcinogenesis through the activation of biliary epithelial cell kinetics in hamsters [17,33,34]. We also found that severe cholangitis was associated with a high occurrence of biliary carcinoma in hamsters, but as in humans, the molecular mechanisms remain obscure. Meanwhile, we have established a method for culturing biliary epithelial cells from the hamster using a collagen gel technique [35].

Chemically reactive oxidants, radicals, and electrophilic mediators, such as hydrogen peroxide and oxyradicals, nitric oxide, malondialdehyde, 4-hydroxynonenal, or eicosanoids, are produced during inflammation, and these chemical mediators are known to induce a variety of biological reactions [27]. Much recent attention has been focused on nitric oxide (NO) as an endogenous mutagen, an angiogenesis factor, and an inhibitor of apoptosis [36]. NO is a free radical synthesized from L-arginine by the nitric oxide synthase (NOS) family. Three isoforms of the NOS family have been isolated: neuronal NOS (nNOS), endothelial NOS (eNOS), and inducible NOS (iNOS) [37,38]. Although nNOS and eNOS are present constitutively, iNOS is induced in inflamed tissues and generates larger amounts of NO than of nNOS and eNOS [37–39]. Cytokine or lipopolysaccharide stimulation, or both, induce iNOS expression in macrophages, hepatocytes, and many other cell types including certain epithelial cells [40–43]. Moreover, it is thought that iNOS expression and the generation of NO in inflamed tissues might induce the malignant transformation of epithelial cells because NO can promote mutagenic changes in DNA through DNA oxidization and protein nitrosylation [44,45].

In this study, we investigated the role of iNOS activation, NO generation, and DNA damage as the link between chronic inflammation and biliary carcinogenesis, using normal hamster gallbladder epithelial cells cultured with inflammatory cytokines.

14.12 Experimental Protocol

Five-week-old female Syrian golden hamsters were used. Biliary epithelial cells were isolated from the biliary tree of hamsters [11] as described above. After laparotomy, the inferior vena cava was paracentesed with a 22G needle, and the liver was perfused in situ with 100 ml Ca^{2+}- and Mg^{2+}- free phosphate-buffered saline (CMF-PBS) containing 10 mmol/l 2-[4-(2-Hydroxyethyl)-1-piperazinyl] ethanesulfonic acid (HEPES) at pH7.4, and 1 mmol/l ethylene glucol-bis (E-aminoethylether) *N, N, N′, N′*-tetraacetic acid (EGTA) for 10 min at 37 °C. The vena cava was clamped above the diaphragm, and the perfusing solution was drained via the incised portal vein, followed by perfusion with 100 ml Hanks' balanced salt solution (GIBCO, Grand Island, NY) containing 50 mmol/l HEPES and 0.04% collagenase (Nittazeratin, Osaka, Japan) for 10 min at 37 °C. After perfusion with the collagenase solution, the liver, gallbladder, and extrahepatic bile duct were removed en bloc, and the biliary

tree was isolated. The biliary tree was separated into the intrahepatic and extrahepatic bile ducts and the gallbladder in CMF-PBS containing 0.1 mmol/l EGTA.

The biliary fragments were minced and embedded on collagen gel plated (Collagen Gel Culture kit; Nittazeratin, Osaka, Japan) 60-mm petri dishes with 2 ml of an ice-cold mixture of collagen solution composed of 0.3% acid solution collagen (Cellmatrix Type I-A), 10 × HamF12, and 0.8 N NaOH at 8:1:1 dilution. After incubation at 37 °C with 5% CO_2 and 95% humidity for 20–30 min, the collagen gels were overlaid with 5 ml of culture medium composed of Dulbecco's modified Eagle medium/HamF12 medium (DMEM/HamF12, GIBCO) and 10% fetal bovine serum (GIBCO). After incubating the biliary fragments for 7–10 days, the biliary epithelial cells spread superficially on the surface of the gel to form cellular sheets toward the peripheral region, whereas the mesenchymal cells progressed toward the inside of the gel. Thus, the biliary epithelial cells were isolated from the peripheral region of the cellular sheets (Figure 14.12).

We used gallbladder epithelial cells isolated from hamsters because of their higher cellular activity than other biliary epithelial cells. Resuspended gallbladder epithelial cells (1×10^5 cells/ml) were plated on collagen-coated plates, then incubated for 24 h and prepared for three different experimental protocols: incubation with culture medium alone (control group); incubation with a cytokine mixture known to increase iNOS expression in other cell types [42,46], which consisted of human recombinant interleukin (IL) 1-β (0.5 ng/ml), interferon (IFN)-γ (5 ng/ml), and tumor necrosis factor (TNF)-α (250 ng/ml) (CM group); or incubation with the same cytokine mixture and an iNOS inhibitor L-N(G)-monomethyl arginine (L-NMMA, 0.03 mM) (CM + L-NMMA group). These human recombinant cytokines and L-NMMA were obtained from the Sigma Chemical Co. (St. Louis, MO). Gallbladder epithelial cells from each group were incubated at 37 °C for 24 h, and then processed for the following analyses:

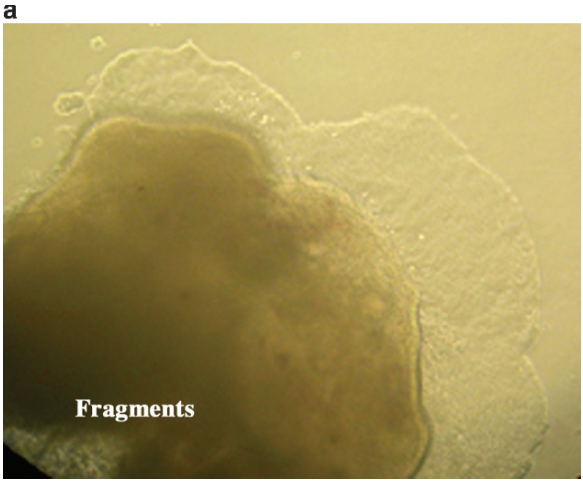

Fig. 14.12 Isolation of hamster biliary epithelial cells. (a): Phase contrast microscopy revealed very few hamster gallbladder epithelial cells growing on the collagen gels 24 h after culture (×100). (modified from [63], with permission)

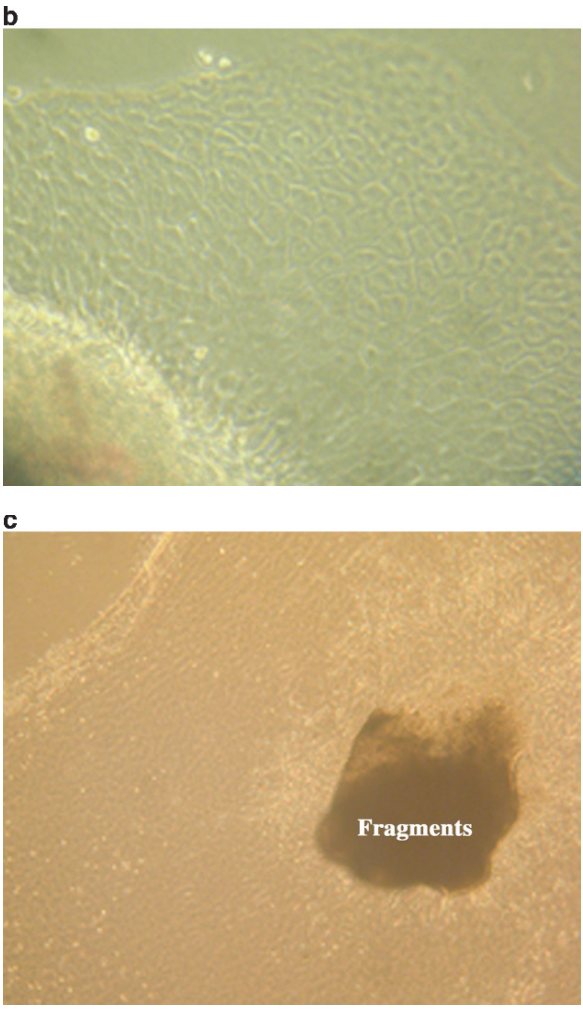

Fig. 14.12 (continued) (b) High magnification of the hamster gallbladder epithelial cells showed cuboidal cells around the biliary fragments (×400). (c) Phase contrast microscopy showed widely extended gallbladder epithelial cells on the surface of the gel 7 days after culture (×40) (modified from [63], with permission)

To calculate the amount of NO produced by the gallbladder epithelial cells, nitrite (NO_2^-) and nitrate (NO_3^-) levels were measured in the culture media by high performance liquid chromatography with a NOx analyzer (ENO-10; Eicom, Kyoto) [47]. iNOS mRNA was amplified by using a nested RT-PCR method [48]. The sequences of primers (Invitrogen Life Technologies, Carlsbad, CA) used in this study are shown in Table 14.3 [48–50].

Total RNA was extracted from the gallbladder epithelial cells using an RNA extraction kit (ISOGEN; Nippon Gene, Tokyo). Reverse transcription and PCR amplification were performed with an RNA PCR kit Ver.3.0 (Takara Shuzo, Tokyo, Japan). After reverse transcription, the first amplification was performed using

Table 14.3 Oligonucleotide primers used for RT-PCR (modified from [63], with permission)

Primers	Sequences	References
NOS-590F	GGYTGGTACATGRGCACYGAGATYGG	Cox et al. [49]
NOS-893R	AAGGCRCARAASTGDGGRTA	Cox et al. [49]
NOS40F	GCAGGATGGGAAACTGAGGCCCAG	Ramirez-Emiliano et al. [48]
NOS40R	TGAACAAGGCAGCCAGGTCCCGG	Ramirez-Emiliano et al. [48]
GAPDHF	TCCCTCAAGATTGTCAGCAA	Liu et al. [50]
GAPDHR	AGATCCACAACGGATACATT	Liu et al. [50]

1 μM of the cDNA, together with the PCR primers NOS-590F and NOS-893R. The PCR conditions consisted of one cycle of denaturing for 2 min at 95 °C, followed by a touch-down protocol consisting of 18 cycles for 15 s at 95 °C, 30s at 60 °C minus 1 °C per cycle, and for 1 min at 72 °C; then 25 cycles for 15 s at 95 °C, for 30 s at 42 °C, for 1 min at 72 °C, and a final extension for 10 min at 72 °C [48]. Next, 1 μl of the cDNA from this amplification was reamplified using the PCR primers specific for iNOS (NOS40F and NOS40R) [48]. The PCR conditions were initial denaturation for 2 min at 95 °C, followed by a touch-down protocol consisting of 13 cycles for 15 s at 95 °C, for 30 s at 70 °C minus 1 °C per cycle, for 1 min at 72 °C, then 30 cycles for 15 s at 95 °C, for 30 s at 57 °C, for 1 min at 72 °C, and a final extension for 10 min at 72 °C [48]. As a control, amplification of mRNA for glyceraldehyde-3-phosphate dehydrogenase (GAPDH) was performed [48,50], and the PCR conditions were the same as those described for the first nested PCR amplification. The amplification products were resolved by electrophoresis in 3% (wt/vol) agarose gels containing 0.1 μg/ml ethidium bromide and photographed under UV trans-illumination.

The comet assay was performed as described previously [51,52]. The gallbladder epithelial cells in each group were resuspended at 1×10^5 cells/ml in ice cold CMF-PBS and combined with molten LMAgarose (Trevigen, Gaitherburg, MD) at a ratio of 1:10 (v/v). The sample was immediately pipetted onto a frosted microscope slide (CometSlide; Trevigen, Gaitherburg, MD). The slides were placed flat at 4 °C in the dark for 10 min, immersed in prechilled Lysis Solution (Trevigen, Gaitherburg, MD), and left at 4 °C for 30 min to remove cellular proteins, leaving DNA as nucleoids. The slides were then immersed in an alkaline solution (pH > 13, 0.3 M NaOH and 0.001 M EDTA) for 30 min to denature the DNA and hydrolyze the sites of damage. The samples were electrophoresed for 10 min and stained with SYBR green I (Trevigen, Gaitherburg, MD) according to the manufacture's instructions. At least 75 cells on each slide, randomly selected with fluorescence microscopy, were analyzed using National Institutes of Health image (Netscape Navigator) with the comet analysis macro (comet 1.4 macro) [53].

NO_2^- + NO_3^- levels and the proportion of DNA damage are expressed as mean values ± S.E. For statistical analysis, non-repeated measure ANOVA was used to

compare the groups, followed by Bonferroni correction for paired comparison. Significance was established at $p < 0.05$.

14.13 Generation of NO_2^- and NO_3^-

The amount of NO measured by high performance liquid chromatography in each group is shown in Figure 14.13. The concentration of $NO_2^- + NO_3^-$ in the media was 10.35 ± 0.47 μM in the control group (n = 26), 11.06 ± 0.18 μM in the CM group (n = 26), and 10.46 ± 0.18 μM in the CM + L-NMMA group (n = 27). The NO generation was significantly higher in the CM group than in the control group ($p < 0.001$). The NO generation in the CM + L-NMMA group was similar to that in the control group, and significantly lower than that in the CM group ($p < 0.001$).

14.14 RT-PCR

The results of RT-PCR/touch down amplification of iNOS mRNA in the gallbladder epithelial cells are shown in Figure 14.14. The CM cells expressed iNOS mRNA (183 bp), but the control cells did not.

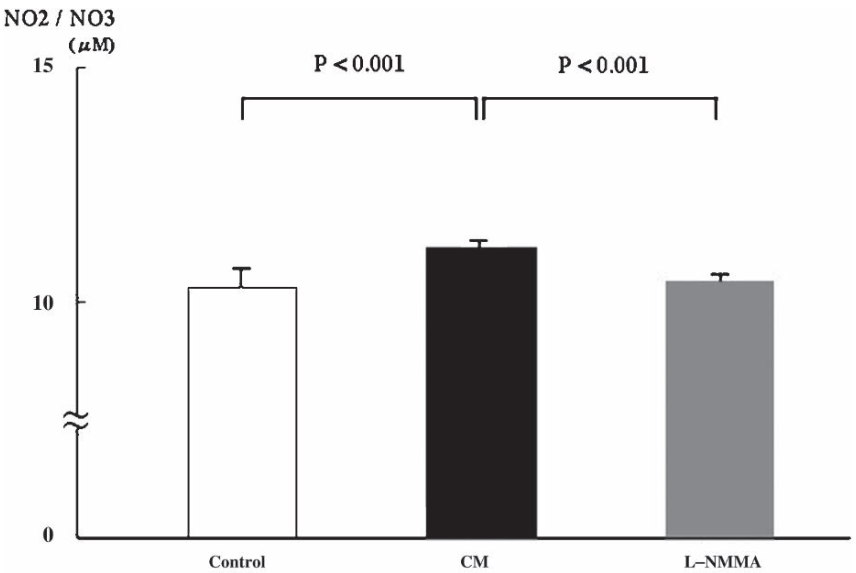

Fig. 14.13 High performance liquid chromatography showed significantly higher $NO_2^- + NO_3^-$ levels in the CM group than in the control and CM + L-NMMA groups, which had similar NO generation ([63], with permission)

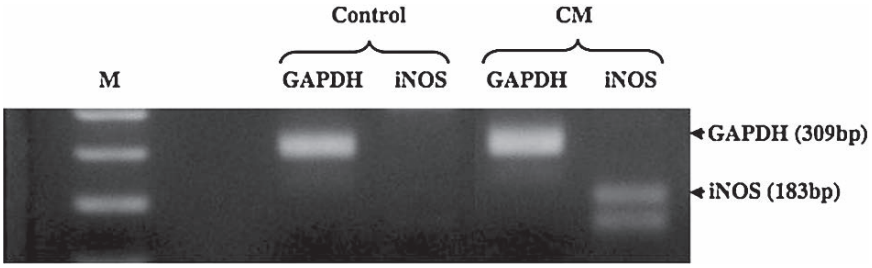

Fig. 14.14 iNOS mRNA expression in the gallbladder epithelial cells. The CM group expressed iNOS mRNA, but the control group did not express iNOS ([63], with permission)

14.15 Comet Assay

Representative fluorescent micrograph images evaluated by single cell gel electrophoresis using the comet assay are shown in Figure 14.15a In contrast to the intact spherical nuclei observed in the control group, the cells treated with cytokine mixture demonstrated a comet tail indicative of DNA damage. The CM + L-NMMA group cells also had intact spherical nuclei. The ratio of DNA exhibiting comet tails, evaluated by an NIH image, was 2.14 ± 0.59% in the control group, 5.14 ± 0.69% in the CM group, and 1.70 ± 0.62% in the CM + L-NMMA group (Figure 14.15b). The level of DNA damage in the CM group was significantly higher than that in the control group ($p < 0.001$), but decreased to the control level by the addition of L-NMMA.

14.16 Comments

The induction of iNOS expression and NO production has been found in a variety of precancerous or cancerous lesions, in which NO is produced in proportion to the degree of malignancy [54–56]. Recently, Jaiswal et al. [51,57] reported that human cholangiocarcinomas showed intensive immunohistochemical staining for iNOS and that cholangiocarcinoma cell lines stimulated by inflammatory cytokines and cholangiocyte cell lines transfected with iNOS produced large amounts of NO caused by iNOS expression, resulting in oxidative DNA damage and inhibition of the excision DNA repair process. In the present study, we used primary epithelial cells isolated from the gallbladder because they allowed us to evaluate the involvement of iNOS and NO in biliary carcinogenesis, especially when biliary carcinoma was induced in response to chronic inflammation.

Following stimulation with a mixture of the inflammatory cytokines, IL-1β, IFN-γ, and TNF-α, the NO generation increased significantly in the gallbladder epithelial cells. The production of NO in the presence of inflammatory cytokines was also completely suppressed by the addition of an iNOS inhibitor, L-NMMA.

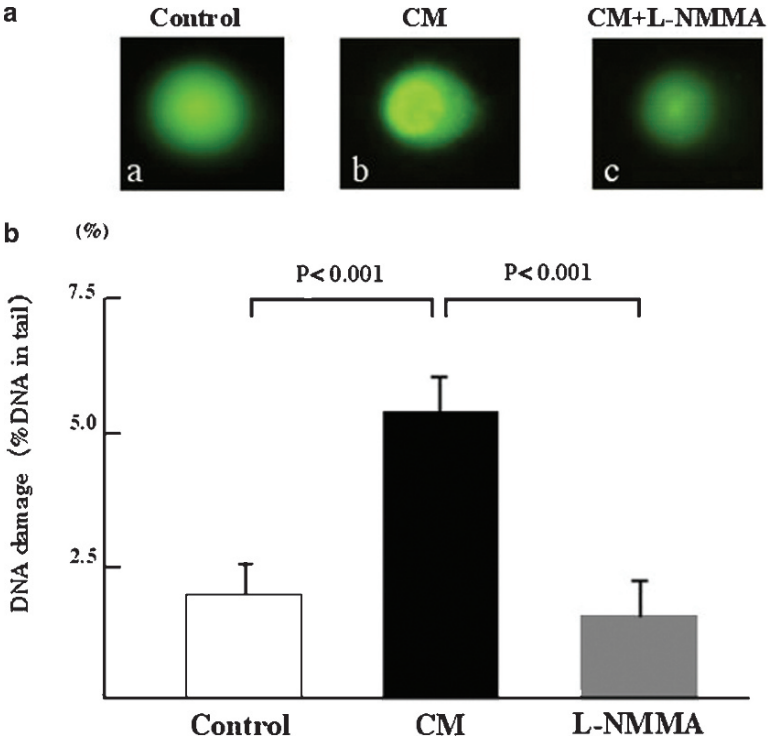

Fig. 14.15 NO-dependent DNA damage evaluated by the comet assay. (a) Fluorescence microscopy showing the apparent comet tail in the gallbladder cells stimulated by the cytokine mixture, and cells with intact spherical nuclei in the control and CM + L-NMMA groups. (b) Analysis of the proportion of DNA that migrated to comet tails using an NIH image revealed a significantly higher level of DNA damage in the CM group than in the control group, which decreased to the control level after the addition of L-NMMA ([63], with permission)

Expression of iNOS mRNA in the gallbladder epithelial cells was strong in the presence of cytokine-stimulation using nested RT-PCR, but not in the absence of stimulatory cytokines. These findings suggest that inflammatory cytokines promote iNOS expression and NO generation in normal epithelial cells in the hamster gallbladder.

NO has the ability to oxidize DNA directly, causing mutagenic changes [44,45]. NO also contributes to intracellular communication, inhibits apoptosis, and enhances vascular dilatation, permeability, and neovascularization[58,59]; however, DNA damage may be an essential and initial component in the malignant transformation of a variety of epithelial cells. The DNA damage in an individual cell can be detected using the highly sensitive comet assay [51,52,57]. In this assay, damaged single- and double-stranded DNA within the nucleus are allowed to migrate toward the anode, by an alkaline hydrolysis process, during electrophoresis, resulting in the appearance of a “comet tail”. In our study, the comet assay showed clearly that the proportion of DNA moving to the comet tail, indicating DNA damage, was significantly higher in

the cytokine mixture group than in the control group, and that the increased DNA damage was completely inhibited by L-NMMA. These data indicate that inflammatory cytokines stimulate iNOS-mediated DNA damage in normal gallbladder epithelial cells. Almost all DNA oxidative breaks can be excised by multiple excision DNA repair processes before mutations occur [60], but DNA damage can lead to p53-mediated cell growth arrest and apoptosis, and the accumulation of p53 protein can repress the transcription of iNOS [61]. A recent study also found that the tumor suppressant organization of normal p53 protein is inhibited in the presence of large amounts of NO in inflamed tissues [62]. In consideration of these facts, our findings suggest that the NO-mediated oxidative DNA damage produced by inflammatory cytokines through iNOS expression is involved in an initiation process linking chronic biliary inflammation to malignant transformation.

The inflammatory cytokines released in inflamed tissues trigger the release of iNOS, resulting in increased NO production. Our findings show that iNOS-mediated NO production induces DNA damage in normal biliary epithelial cells. Persistent biliary inflammation and the accumulation of NO-mediated genotoxicity may initiate the malignant transformation of epithelial cells lining the biliary tree. Our hamster models of *in vivo* and *in vitro* tumorigenesis will contribute to a better understanding of the mechanisms of inflammation-related biliary carcinogenesis.

References

1. Elsing C., Kassner A., Hubner C., Buhl H., Stremmel W. Absorptive and secretory mechanisms in biliary epithelial cells. J Hepatol 1996 24:121–127.
2. Nakanuma Y., Sasaki M. Expression of blood group-related antigens in the intrahepatic biliary tree and hepatocytes in normal livers and various hepatobiliary diseases. Hepatology 1989 10:174–178.
3. Nakanuma Y., Ohta G. Histometric and serial section observations of the intrahepatic bile ducts in primary biliary cirrhosis. Gastroenterology 1979 76:1326–1332.
4. Auth M.K., Keitzer R.A., Scholz M., Blaheta R.A., Hottenrott E.C., Herrmann G., Encke A., Markus B. Establishment and immunological characterization of the cultured human gallbladder epithelial cells. Hepatology 1993 18:546–555.
5. Strain A.J., Wallace L., Joplin R., Daikuhara Y., Ishii T., Kelly D.A., Neuberger J.M. Characterization of biliary epithelial cells isolated from needle biopsies of human liver in the presence of hepatocyte growth factor. Am J Pathol 1995 146:537–545.
6. Katayanagi K., Kono N., Nakanuma Y. Isolation, culture and characterization of biliary epithelial cells from different anatomical levels of the intrahepatic and extrahepatic biliary tree from a mouse. Liver 1998 18:90–98.
7. Mathis G.A., Walla S.A., Sirica A.E. Biochemical characteristics of hyperplastic rats bile ductular epithelial cells cultured “on top” and “inside” different extracellular matrix substitutes. Cancer Res 1988 48:6145–6153.
8. Paradis K., Sharp H.L. In vitro duct-like structure formation after isolation of the bile ductular cells from murine model. J Lab Clin Med 1989 113:689–694.
9. Yang L., Faris R.A., Hixson D.C. Long-term culture and characteristics of normal rat liver bile duct epithelial cells. Gastroenterology 1993 104:840–852.
10. Takahashi M., Pour P., Althoff J., Donnelly T. The panceras of the Syrian hamster (Mesocricetus auratus). 1 Anatomical study. Lab Anim Sci 1977 27: 336–342.

11. Peralman B.J., Bonorris G.G., Philips M.J., Chung A., Vimadalal S., Marks J.W., Schoenfield L.J. Cholesterol gallstone formation and prevention by chenodeoxycholic and ursodeoxycholic acids. A new hamster model. Gastroenterology 1979 77:634–641.
12. Rinderknecht H., Maset R., Collias K., Carmack C. Panceratic secretory profiles of protein, digestive, and lysosomal enzymes in Syrian golden hamster. Effect of secretin and cholecystokinin. Dig Dis Sci 1983 28:518–525.
13. Fukahori T., Tomioka T., Inoue K., Tajima Y., Tsunoda T., Kanematsu T. Establishment of a transplantable carcinoma arising from the intrahepatic bile duct in Syrian golden hamster. Virchows Arch A Pathol Anat 1993 422:233–238.
14. Ikematsu Y., Tomioka T., Tajima Y., Tsunoda T., Kanematsu T. Enhancement of biliary carcinogenesis in hamsters by cholecystokinin. World J Surg 1995 19:847–851.
15. Ikematsu Y., Tomioka T., Yamanaka S., Tajima Y., Tsunoda T., Kanematsu T. Bilioenterostomy enhances biliary carcinogenesis in hamsters. Carcinogenesis 1996 17:1505–1509.
16. Inoue K., Tomioka T., Tajima Y., Fukahori T., Eto T., Tsunoda T., Kanematsu T. Characterization of an established transplantable adenocarcinoma of the gallbladder in Syrian golden hamster. J Surg Oncol 1994 56:269–276.
17. Tajima Y., Eto T., Tsunoda T., Tomioka T., Inoue K., Fukahori T., Kanematsu T. Induction of extrahepatic biliary carcinoma by *N*-nitrosobis(2-oxopropyl)amine in hamsters given cholecystoduodenostomy with dissection of the common duct. Jpn J Cancer Res 1994 85:780–788.
18. Yamanaka S., Tomioka T., Tajima Y., Okada K., Shiku H., Kanematsu T. K-ras gene mutations in intrahepatic bile duct tumors of Syrian golden hamsters. J Surg Oncol 1997 66:97–103.
19. Rutenburg A.M., Kim H., Fishbein J.W., Hander J.S., Wasserkrug H.L., Seligman A.M. Histochemical and ultrastructural demonstration of E-glutamyl transpeptidase activity. J Histochem Cytochem 1969 17:517–526
20. Hall P.A., Lemoine N.R. Models of pancreatic cancer. Cancer Surv 1993 16:135–155.
21. Mangold K.A., Hubchak S., Mangino M.M., Laconi S., Scarpelli D.G. In vitro carcinogenesis of hamster pancreatic duct cells: cellular and molecular alterations. Carcinogenesis 1994 15(9):1979–1984.
22. Takeuchi Y., Takahashi M., Sakano K., Mutoh M., Niho N., Yamamoto M., Sato H., Sugimura T., Wakabayashi K. Suppression of *N*-nitrosobis(2-oxopropyl)amine-induced pancreatic carcinogenesis in hamsters by pioglitazone, a ligand of peroxisome proliferatior-activated receptor gamma. Carcinogenesis 2007 28(8):1692–1696.
23. Hubchak S., Mangino M.M., Reddy M.K., Scarpelli D.G. Characterization of differentiated Syrian golden hamster pancreatic duct cells maintained in extended monolayer culture. In Vitro Cell Dev Biol 1990 26(9):889–897.
24. Sirica A.E., Mathis G.A., Sano N., Elmore L.W. Isolation, culture, and transplantation of intrahepatic biliary epithelial cells and oval cells. Pathobiology 1990 58(1):44–64.
25. De Lü M., Miyazaki K., Yoshitomi S., Nakayama F. DNA repair synthesis in primary culture of bovine bile duct epithelial cells induced by chemical agents in relation to bile duct cancer. Mutat Res 1988 194(1):73–79.
26. Ohshima H., Bartsh H. Chronic infections and inflammatory process as cancer risk factors: possible role of nitric oxide in carcinogenesis. Mutat Res 1994 305:253–264.
27. Fitzpatrick F.A. Inflammation, carcinogenesis and cancer. Int Immunopharmacol 2001 1:1651–1667.
28. Baumann R., Uettwiller H., Duclos B., Jouin H., Kerschen A., Adloff M., Weill J.P. Congenital cystic dilatation of the common bile duct, anomaly of the biliopancreatic junction and cancer of the bile ducts. Gastroenterol Clin Biol 1987 11:849–855.
29. Fujii H., Yang Y., Tang R., Kunitomo K., Itakura J., Mogaki M., Matsuda M., Suda K., Nobukawa B., Matsumoto Y. Epithelial cell proliferation activity of the biliary ductal system with congenital biliary malformations. J Hepatobiliary Pancr Surg 1999 6:294–302.
30. Tocchi A., Mazzoni G., Liotta G., Lepre L., Cassini D., Miccini M. Late development of bile duct cancer in patients who had biliary-enteric drainage for benign disease: a follow up study of more than 1,000 patients. Ann Surg. 2001 234:210–214.

31. Hakamada K., Sasaki M., Endoh M., Itoh T., Morita T., Konn M. Late development of bile duct cancer after sphincteroplasty: a ten- to twenty-two-year follow up study. Surgery 1997 121:488–492.
32. Tanaka M., Takahata S., Konomi H., Matsunaga H., Yokohata K., Takeda T., Utsunomia N., Ikeda S. Long-term consequence of endoscopic sphincterotomy for bile duct stones. Gastrointest Endosc 1998 48:465–469.
33. Kitajima T., Tajima Y., Onizuka S., Matsuzaki S., Matsuo K., Kanematsu T. Linkage of persistent cholangitis after bilioenterostomy with biliary carcinogenesis in hamsters. J Exp Clin Cancer Res 2000 19:453–458.
34. Kitajima T., Tajima Y., Matsuzaki S., Kuroki T., Fukuda K., Kanematsu T. Acceleration of spontaneous biliary carcinogenesis in hamsters by bilioenterostomy. Carcinogenesis 2003 24:133–137.
35. Asakawa T., Tomioka T., Kanematu T. A method for culturing and transplanting biliary epithelial cell from Syrian golden hamster. Virchows Arch 2000 436:140–146.
36. Facchetti F., Vermi W., Fiorentini S., Chilosi M., Caruso A., Duse M., Notarangelo L.D., Badolato R. Expression of inducible nitric oxide synthase in human granulomas and histiocytic reactions. Am J Pathol 1999 154:145–152.
37. Geller D.A., Billiar T.R. Molecular biology of nitric oxide synthases. Cancer Metastasis Rev 1998 17:7–23.
38. Marletta M. Nitric oxide synthase: aspects concerning structure and catalysis. Cell 1994 78:927–930.
39. Michel T., Feron O. Perspective series: Nitric oxide and nitric oxide synthases. J Clin Invest 1997 100:2146–2152.
40. Mannick J.B., Asano K., Izumi K., Kieff E., Stamler J.S. Nitric oxide produced by human B lymphocytes inhibits apoptosis and Epstein-Barr virus reactivation. Cell 1994 79:1137–1146.
41. Hoffman R.A., Zhang G.S., Nussler N.C., Gleixner S.L., Ford H.R., Simmons R.L., Watkins S.C. Constitutive expression of inducible nitric oxide synthase in the mouse ileal mucosa. Am J Phys 1997 35:G383–G392.
42. Geller D.A., Nussler A.K., Di Silvio M.A., Lowenstein C.J., Shapiro R., Wang S.C., Simmons R.L., Billiar T.R. Cytokines, endotoxin and glicocorticoids regulate the expression of inducible nitric oxide synthase in hepatocytes. Proc Natl Acad Sci U S A 1992 90:522–526.
43. Geller D.A., Di Silvio M., Nussler A.K., Wang S.C., Shapiro R.A., Simmons M.D., Billiar T.R. Nitric oxide synthase expression is induced in hepatocytes in vivo during hepatic inflammation. J Surg Res 1993 55:427–432.
44. Tamir S., Burney S., Tannenbaum S.R. DNA damage by nitric oxide. Chem Res Toxicol 1996 9(5):821–827.
45. Lachances S., Chan J.S. Nitric oxide co-operates with hydrogen peroxide in inducing DNA fragmentation and cell lysis in murine lymphoma cells. Biochem J 1997 321:897–901.
46. Nussler A.K., Geller D.A., Aweetland M.A., Di Silvio M., Billiar T.R., Madariaga J.B., Simmons R.L., Lancaster J.R. Induction of nitric oxide synthesis and its reactions in cultured human and rat hepatocytes stimulated with cytokines plus lipopolysaccharides. Biochem Biophys Res Commun 1993 194:820–835.
47. Archer S. Measurement of nitric oxide in biological models. FASEB J 1993 7:349–360.
48. Ramirez-Emiliano J., Gonzalez-Hernandes A., Arias-Negrete S. Expression of inducible nitric oxide synthase mRNA and nitric oxide production during the development of liver abscess in hamster inoculated with Entamoeba histolytica. Curr Microbiol 2005 50:299–308.
49. Cox R., Mariano T., Heck D., Laskin J., Stegeman J. Nitric oxide synthase sequences in the marine fish Stenotomus chrysops and the sea urchin Arbacia punctulata, and phylogenetic analysis of nitric oxide synthase calmodulin-binding domains. Comp Biochem Physiol B Biochem Mol Biol 2001 130:479–49.
50. Liu S., Adcock I., Old R., Barnes P., Evans T. Lipopolysaccharide treatment *in vivo* induces widespread tissue expression of inducible nitric oxide synthase mRNA. Biochem Biophys Res Commun 1993 196:1208–1213.

51. Jaiswal M., LaRusso N.F., Burgart L.J., Gores G.J. Inflammatory cytokines induce DNA damage and inhibit DNA repair in cholangiocarcinoma cells by nitric oxide-dependent mechanism. Cancer Res 2000 60:184–190.
52. Duthie S.J., McMillian P. Uracil misincorporation in human DNA detected using single cell gel electrophoresis. Carcinogenesis 1997 18:1709–1714.
53. Helma C., Uhl M. A public domain image-analysis program for the single-cell gel-electrophoresis (comet) assay. Mutat Res 2000 466:9–15.
54. Szabo C., Oshima H. DNA damage induced by peroxynitrite: subsequent biological effects. Nitric Oxide Biol Chem 1997 1:373–385.
55. Ambs S., Bennett W.P., Merriam W.G., Ogunfusika M.O., Oser S.M., Harrington A.M., Shields P.G., Felly-Bosco E., Hussain S.P., Harris C.C. Relationship between *p53* mutations and inducible nitric oxide synthase expression in human colorectal cancer. J Natl Cancer Inst 1999 91:86–88.
56. Murakami A., Ohigashi H. Targeting NOX, INOS and COX-2 in inflammatory cells: chemoprevention using food phytochemicals. Int J Cancer 2007 121(11):2357–2363.
57. Jaiswal M., LaRusso N.F., Shapiro R.A., Billiar T.R., Gores G.J. Nitric oxide-mediated inhibition of DNA repair potentiates oxidative DNA damage in cholangiocytes. Gastroenterology 2001 120:190–199.
58. Perez-Sala D., Rebollo A. Novel aspects of Ras proteins biology: regulation and implications. Cell Death Differ 1999 6:722–728.
59. Garcia-Cardena G., Folkman J. Is there a role for nitric oxide in tumor angiogenesis? J Natl Cancer Inst 1998 90:560–561.
60. Wood R.D., Mitchell M., Sgouros J., Lindahl T. Human DNA repair genes. Science 2001 291(5507):1284–1289.
61. Ambs S., Hussain P., Harris C.C. Interactive effects of nitric oxide and the *p53* tumor suppressor gene in carcinogenesis and tumor progression. FASEB J 1997 11:443–448.
62. Calmels S., Hainaut P., Oshima H. Nitric oxide induces conformational and functional modifications of wild-type p53 tumor suppressor protein. Cancer Res 1997 57:3365–3369.
63. Kitasato A, Tajima Y, Kuroki T, Tsutsumi R, Adachi T, Mishima T, Kanematsu T. Inflammatory cytokines promote inducible nitric oxide synthase-mediated DNA damage in hamster gallbladder epithelial cells. World J Gastroenterol 2007 13(47):6379–84.

Index